# ASPECTS OF INFLATION IN STRING THEORY

Daniel Baumann

A Dissertation

Presented to the Faculty

of Princeton University

in Candidacy for the Degree

of Doctor of Philosophy

Recommended for Acceptance

by the Department of Physics

Advisor: Paul Steinhardt

June 2008

ABSTRACT. In this thesis we make small steps towards the ambitious goal of a microphysical understanding of the inflationary era in the early universe. We identify three key questions that require a proper understanding of the ultraviolet limit of the theory: i) the delicate flatness of the inflaton potential, ii) the possibility of observable gravitational waves and iii) a large non-Gaussianity of the primordial density fluctuations. We study these fundamental aspects of inflation in the context of string theory.

$V(\phi)$: In the first half of the thesis, we give the first fully explicit derivation of the potential for warped D-brane inflation. The analysis exposes the eta-problem, relates effective parameters in the inflaton Lagrangian to microscopic string theory input, and illustrates important correlations between the parameters of the potential. We show that compactification constraints significantly limit the possibility of obtaining inflationary solutions in these scenarios.

$r$: All inflationary models that predict an observable gravitational wave signal require that the inflaton field evolves over a super-Planckian range. In the second half of the thesis, we derive a microscopic bound on the maximal inflaton field variation for D-brane models. The bound arises from the compact nature of the extra dimensions and puts a strong upper limit on the gravitational wave signal.

$f_{\rm NL}$: Finally, we explain that our limit on the field range also significantly constrains the parameter space of Dirac-Born-Infeld inflation. In this case the bound strongly restricts the possibility of a large non-Gaussianity in the primordial fluctuations.

*For Anna/Mama*

# Contents

Acknowledgments viii

Chapter 1. Introduction 2
1. Prelude 2
2. From String Compactification to the Low Energy Lagrangian 3
3. Compactification Effects in D-brane Inflation 5
4. String Theory and Primordial Gravitational Waves 7
5. Outline of the Thesis 8

**Part 1. Review of String Cosmology** 12

Chapter 2. Aspects of Modern Cosmology 14
1. A Brief History of the Universe 15
2. Status of Observational Cosmology 22
3. Dark Energy 32
4. Inflation 34

Chapter 3. Elements of String Compactifications 46
1. The Moduli-Stabilization Problem 46
2. Flux Compactification 47
3. De Sitter Vacua in String Theory 49
4. Klebanov-Strassler Geometry 51

Chapter 4. Inflation in String Theory 54
1. UV Challenges/Opportunities 55
2. Warped D-brane Inflation 57
3. Models of String Inflation 63
4. Inflation from Explicit String Compactifications 68

**Part 2. The Inflaton Potential** 70

Chapter 5. On D3-brane Potentials in Compact Spaces 71
1. Introduction 71
2. D3-branes and Volume Stabilization 75
3. Warped Volumes and the Superpotential 79
4. D3-brane Backreaction 82

5. Backreaction in Warped Conifold Geometries 86
6. Compactification Effects 93
7. Implications and Conclusion 99

Chapter 6. Compactification Obstacles to D-brane Inflation 102
1. Introduction 102
2. The Compactification 104
3. Towards Fine-Tuned Inflation 105
4. Microscopic Constraints 109
5. Conclusions 109

Chapter 7. Towards an Explicit Model of D-brane Inflation 111
1. Introduction 111
2. D3-brane Potential in Warped Backgrounds 116
3. Case Study: Kuperstein Embedding 123
4. Search for an Inflationary Trajectory 129
5. Comments on Other Embeddings 140
6. Discussion 146
7. Conclusions 149

**Part 3. String Theory and Gravitational Waves** 154

Chapter 8. A Microscopic Limit on Gravitational Waves 156
1. Introduction 156
2. The Lyth Bound 157
3. Constraint on Field Variation in Compact Spaces 160
4. Implications for Slow-Roll Brane Inflation 164
5. Implications for DBI Inflation 166
6. Conclusions 173
7. Epilogue 176

Chapter 9. Comments on Field Ranges in String Theory 180
1. String Moduli and the Lyth Bound 180
2. Branes 181
3. Axions 189
4. Volume Modulus 190
5. Implications 192

**Part 4. Conclusions** 193

Chapter 10. Inflationary UV Challenges/Opportunities 194
1. The Inflaton Potential 194
2. Gravitational Waves 196
3. Non-Gaussianity 196

Chapter 11. Epilogue 199

**Appendix** 201

Appendix A. Primordial Fluctuations from Inflation 203

Appendix B. Green's Functions on Conical Geometries 212

Appendix C. Computation of Backreaction in the Singular Conifold 216

Appendix D. Computation of Backreaction in $Y^{p,q}$ Cones 224

Appendix E. The F-term Potential 231

Appendix F. Dimensional Reduction 235

Appendix G. Stability in the Angular Directions 244

Appendix H. Stabilization of the Volume 256

Appendix J. Collection of Useful Results 261

Bibliography 268

## Acknowledgments

I cannot thank *Liam McAllister* enough for his contributions to this thesis and to my understanding of physics in general. Most of all, I owe Liam thanks for helping me to regain my passion for theoretical physics. Liam came to Princeton as a post-doc when I was halfway through my PhD. Progress was slow and I had the canonical depression which grad students feel at that time. Liam reminded me why theoretical physics is fun. We discussed physics almost every day – on the blackboard, on the phone or via email. Liam's infinite patience continues to amaze me and his research style has become my inspiration. But, above all, Liam has become a great friend.

I am deeply indebted to my advisor, *Paul Steinhardt*, for his guidance and support. Paul's imagination, passion for science and professionalism are an inspiration for me. I am grateful for his advice not just on technical aspects, but also on personal questions on life in science more generally. Finally, I thank Paul for encouraging my passion for teaching. Paul is an exceptional teacher and co-teaching "physics for poets" with him was one of my highlights at Princeton.

I am most grateful to *Igor Klebanov* who has in many ways acted like a second advisor to me. Igor was closely involved in most of the research in this thesis and has been very generous with his time and technical knowledge. I admire Igor's dedication and careful consideration of computational details (*i.e.* factors of 2 and $\pi$).

Thanks to my scientific hero, *Juan Maldacena*, for sharing his insights with me and for inspiring some of the problems in this thesis.

Thanks to *David Spergel* for sharing his vast knowledge of astrophysics with me.

Thanks to *Anatoly Dymarsky* for computing the uncomputable (see Appendix D).

Modern theoretical physics is largely a collaborative effort. This dissertation would not have been possible without the input and guidance of my outstanding collaborators. The results presented here have been obtained together with Liam McAllister, Igor Klebanov, Anatoly Dymarsky, Juan Maldacena, Arvind Murugan and Paul Steinhardt. I also feel very privileged to have worked with Asantha Cooray, Brett Friedman, Dragan Huterer, Kiyotomo Ichiki, Shamit Kachru, Marc Kamionkowski, Hiranya Peiris, Keitaro Takahashi, Neil Turok, Devdeep Sarkar, Paolo Serra, and Kris Sigurdson.

For stimulating discussions about physics I wish to thank: Niayesh Afshordi, Nima Arkani-Hamed, Daniel Babich, Raphael Bousso, Latham Boyle, Cliff Burgess, Jim Cline, Joe Conlon, Jo Dunkley, Richard Easther, Alan Guth, Petr Horava, Mark Jackson, Shamit Kachru, Renata Kallosh, Marc Kamionkowski, Justin Khoury, Eiichiro Komatsu, Louis Leblond, Eugene Lim, Andrei Linde, Lyman Page, Enrico Pajer, Hiranya Peiris, Uros Seljak, Leonardo Senatore, Sarah Shandera, Gary Shiu, Eva Silverstein, Tristan Smith, Michael Strauss, Wati Taylor, Max Tegmark, Andrew Tolley, Fernando Quevedo, Bret Underwood, Daniel Wesley, Herman Verlinde, and Matias Zaldarriaga.

Parts of the research described in this thesis were conducted during visits to the Perimeter Institute and the theory groups at Harvard, MIT, Berkeley, Caltech, Stanford, Austin and Cornell. I thank these institutions for their kind hospitality and for providing stimulating research environments.

Thanks to my friends in Jadwin Hall for "sharing the pain", especially Mihail Amarie, Latham Boyle, Jo Dunkley, Joel Erickson, Justin Khoury, Katie Mack, Arvind Murugan, Andrew Tolley, Amol Upadhye, and Daaan Wesley.

I am grateful to Laurel Lerner and Angela Glenn for helping me out on many administrative emergencies.

I wish to express special thanks to the people who have enriched my personal life at Princeton, especially my roommates David Hsieh, Mikael Rechtsman, Yuri Corrigan, and Grunde Jomaas – You have been great! Finally, thanks to Zhi Cheng for her emotional support.

Going back in time, there have been many people who supported my academic career:

First, I wish to thank to my father, *Fritz Baumann*, (who knows little about physics, but much about everything else) for supporting my earliest interests in science. Recognizing my curiosity about physics, my father gave me two inspiring popular science books ('The Dancing Wu Li Masters' and 'A Brief History of Time') and a video documentary on Richard Feynman. After these experiences I started studying physics. I will always be grateful to my father for his vision and support.

I had two remarkable high school teachers: *Rolf Becken* and *Rainer Gaitzsch*. I thank them for not laughing at me when I wanted to learn relativity and quantum mechanics. Thanks also to my fellow high school student, *Ferdl Kümmeth*, for many discussions on physics and mathematics.

At Cambridge I received generous support from the following teachers: *Anthony Challinor*, *Richard Hills*, *Neil Turok*, *Bill Saslaw*, as well as *Yen Lee* and *Bernard Leong*. Special thanks to Bernard for teaching me general relativity, for introducing me to LaTeX and Mathematica, and for supporting my first research as an undergraduate.

As a summer student at Caltech I was supervised by *Asantha Cooray* and *Marc Kamionkowski*. I have valued their friendship and support ever since. I am very grateful for Asantha's faith in me.

Finally, thanks to all the friends I have neglected over the past five years for their understanding:

- my friends in Jamaica: Rebecca, David, Ronnie and the Dougalls
- my friends in Germany: especially Markus Twardowitz, David Fassbender, Molly Donohue and Urs Wien
- my family in Canada: Uncle Andrew, Aunt Marie, and my cousins Asha, Candice and Leah
- my family in Germany: my late Aunt Annerl, my Uncle Heinz and my cousin Klaus
- and my family in Jamaica: especially my late grand-parents, Ivan and Monica Arscott. I wish I had the chance to explain this thesis to Grand-dad Ivan.

Der grösste Dank gebürt meiner Familie – meinen Eltern, *Anna* und *Fritz* Baumann, meinem Bruder, *Julian* Baumann, und meiner *Oma*, Anna Baumann. Worte sind nicht genug um auszudrücken wie viel mir meine Familie bedeutet. Ich habe sie sehr vermisst in den letzten Jahren.

Julian, Ich bin sehr stolz auf Dich.

Fritz, Danke für die herzlichen Versuche meine Arbeit zu verstehen.

Anna, Ich schulde Dir alles.

Princeton, June 2008 Daniel Baumann

"I'm astounded by people who want to 'know' the Universe when it's hard enough to find your way around Chinatown."

*Woody Allen*

CHAPTER 1

# Introduction

## 1. Prelude

The classical Big Bang theory is incomplete. In particular, it fails to explain why the universe is so smooth on scales that according to the Big Bang picture have never been in causal contact. Cosmological inflation solves this 'horizon problem' in an elegantly simple way [83]. By hypothesizing an early period of accelerated expansion the puzzle is solved. In addition, quantum mechanical fluctuations during inflation are stretched to cosmic scales. Inflation therefore explains both the large-scale homogeneity of the universe as well as the small primordial fluctuations that are the seeds for large-scale structure.

However, a period of prolonged inflation requires that the early universe was dominated by a form of energy whose density stays nearly constant as the universe expands. This is unlike any physical phenomenon we have ever probed in terrestrial experiments. The energy densities we are familiar with all dilute with expansion. We are therefore led to ask: What is the physics of inflation? Can inflation be embedded in a theory of fundamental physics?

Cosmic inflation is thought to have occurred at extremely high energies ($\sim 10^{15}$ GeV), far out of reach of terrestrial particle accelerators ($\sim 10^3$ GeV). Given that the inflationary proposal requires a huge extrapolation of the known laws of physics, it is not surprising that the physics governing this phase of rapid expansion is still very uncertain. In the absence of a complete theory, a standard practice has been a

phenomenological approach where an effective potential $V(\phi)$ is postulated. Here $\phi$ is an order parameter used to describe the change in the inflationary energy during inflation. The requirement of slow evolution of the energy density puts constraints on the shape of $V(\phi)$. Ultimately, however, $V(\phi)$ should be derived from a fundamental theory. Since string theory is the leading candidate for a UV-completion of the Standard Model that consistently unifies gauge and gravitational interactions, it is natural to search in string theory for a realization of the inflationary paradigm. One of the main results of this thesis is an explicit derivation of $V(\phi)$ for a specific model of inflation in string theory.

## 2. From String Compactification to the Low Energy Lagrangian

In this thesis we will be mainly concerned with describing low energy physics from a top down approach. Our philosophy is illustrated in Figure 1.

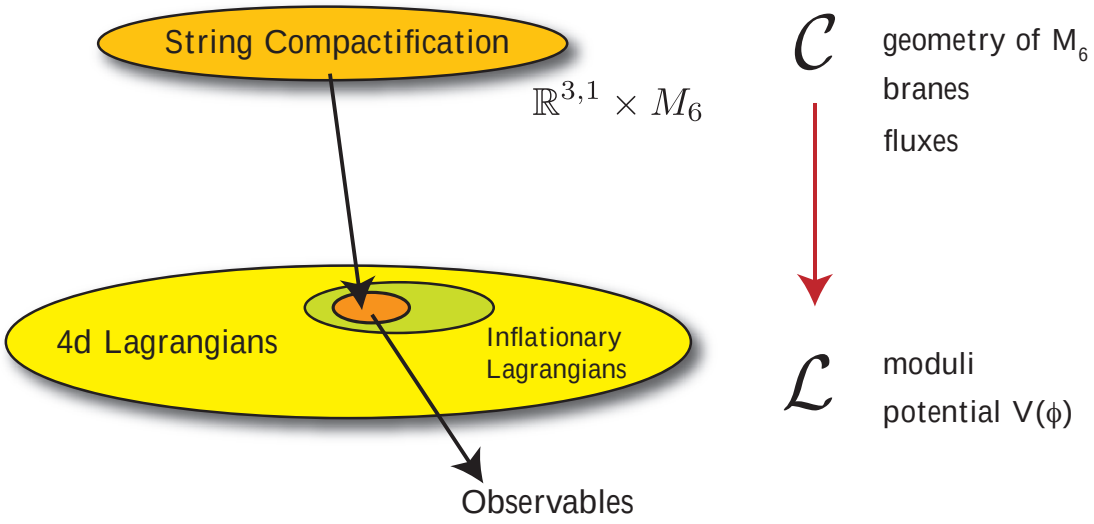


FIGURE 1. From String Compactification Data to Low Energy Lagrangian to Inflation. String theory specifies discrete compactification data $\mathcal{C}$ (geometry and topology of extra dimensions, amount and types of branes, amount and types of fluxes, etc.) At low energies, four-dimensional physics is described by an effective field theory with Lagrangian $\mathcal{L}$. In this thesis we study the correspondence between $\mathcal{C}$ and $\mathcal{L}$ and search for configurations that allow inflationary solutions.

Starting from a consistent string theory configuration with given compactification data $\mathcal{C}$ the aim is to derive the low energy 4d Lagrangian $\mathcal{L}$. The input $\mathcal{C}$ amounts to specifying the compactification geometry, the background fluxes and the configuration of branes. From this the effective four-dimensional physics can in principle be derived. The parameters in the four-dimensional Lagrangians $\mathcal{L}$ will be defined in terms of the more fundamental input parameters in $\mathcal{C}$. In this thesis we will be investigating this correspondence between the fundamental parameters of a string compactification and the effective four-dimensional physics.

Generically, a given string compactification will not lead to low energy Lagrangians that permit cosmological inflation to occur. An important application of string theory to early universe cosmology therefore is to identify the subset of Lagrangians that do allow inflationary solutions. A systematic study of the correspondence $\mathcal{C} \to \mathcal{L}$ should ultimately allow us to determine which models of inflation are possible in string theory. One can then search for signatures that are (un)natural or (un)characteristic in string inflation. This is to be compared to the results for inflation in the context of quantum field theory. It is hoped that inflationary models derived from string theory are more restricted and therefore more predictive.

Making explicit the correspondence between higher-dimensional string theory input and four-dimensional effective Lagrangians is highly non-trivial. To study inflation requires having exquisite control over classical and quantum contributions to the inflaton potential. To compute the inflaton mass requires understanding gravity corrections to the potential up to dimension six, $\delta V = \frac{1}{M_{\rm pl}^2}\mathcal{O}_6$. This requires knowing $g_s$ and $\alpha'$ corrections, backreaction effects, etc. Common approximations like the classical limit, non-compact or large volume treatments and probe approximations for D-branes are often insufficient. In addition, as we will see, the inflaton potential often depends sensitively on the inclusion of moduli stabilization effects.

In this thesis we focus on a specific, concrete model of inflation in string theory, warped D-brane inflation, with the aim of understanding corrections to the inflaton potential as fully and explicitly as possible. This gives substantial progress towards an *existence proof* of an inflationary scenario derived from the microscopic compactification data of string theory.

### 3. Compactification Effects in D-brane Inflation

Warped D-brane inflation has received considerable theoretical attention as a framework where explicit computations can be performed. In particular, the inflaton potential is in principle completely computable from string theory. In practice, computing the D3-brane potential in sufficient detail to determine whether it can be flat enough for inflation is very challenging.

Kachru, Kallosh, Linde, Maldacena, McAllister and Trivedi (KKLMMT) [95] established that the Coulomb part of the brane-antibrane potential in a warped background is sufficiently flat for inflation. However, they also showed that compactification effects induced by the stabilization of moduli fields lead to crucial correction terms that generically spoil the delicate flatness of the potential and lead to an incarnation of the supergravity eta-problem. At the time of Ref. [95], not all terms of the inflaton potential could be computed explicitly, but the hope was expressed that the individual contributions to the inflaton mass could cancel in special fine-tuned configurations. However, this expectation required certain assumptions about the functional form of a specific unknown correction term which we call the 'superpotential correction'. An explicit computation was needed to assess the real status of the eta-problem for brane inflation models.

In this thesis we compute the missing term in the D3-brane potential [18]. We are then equipped with the full inflaton Lagrangian. In fact, we find that the missing term and hence the resulting potential is *not* of the functional form anticipated in earlier work. This lends a new perspective to the brane inflation scenario. The

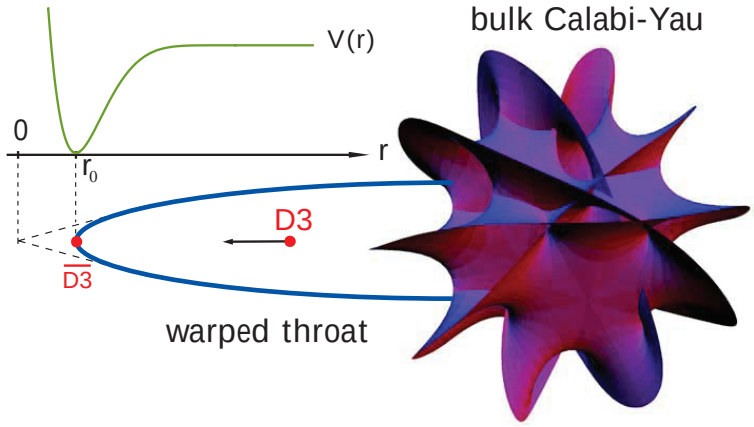


FIGURE 2. The KKLMMT Scenario. The 3-branes are spacetime-filling and therefore pointlike in the extra dimensions. The net force on the D3-brane is associated with the inflaton potential.

inflaton potential can be flat only locally over a small range of values for the inflaton field. Fine-tuned inflation is restricted to the region near an inflection point of the potential.

An important aspect of our analysis is the consistent treatment of compactification constraints. The higher-dimensional theory determines the following aspects of the four-dimensional effective theory:

(1) *Functional form of correction terms.*

As mentioned above and as we will explain in much more detail below (Chapters 5, 6 and 7), considerations of holomorphicity and the dimensionality of the compact space dictate the functional form of the superpotential correction to the inflaton potential. This severely restricts the possibility of fine-tuning the shape of the potential.

(2) *Range of parameters in the Lagrangian.*

After deriving the effective Lagrangian $\mathcal{L}$ from explicit string theory data $\mathcal{C}$ it is important to remember the relation been the effective parameters in the four-dimensional Lagrangian and the higher-dimensional input (this in contrast to "string-inspired" models where this connection is unknown or subsequently forgotten). In particular, more often than not there are

important compactification constraints on the input parameters in $\mathcal{C}$ that restrict the allowed values of the parameters in $\mathcal{L}$.

For example, in Ref. [21] Liam McAllister and I derived that the range of the canonical inflaton field in this scenario is bounded by the size of the compactification manifold

$$\frac{\Delta\phi}{M_{\rm pl}} < \frac{2}{\sqrt{N}} \ll 1\,. \tag{1.1}$$

(Here, $N$ is a large integer defined below.) Any parameter in the Lagrangian that relates to a coordinate on the compact space has to satisfy this constraint. In later chapters we explain the relevance of this bound for the fine-tuning of slow-roll models of brane inflation, for the viability of DBI inflation and for the amplitude of inflationary gravitational waves.

(3) *Correlation of parameters in the Lagrangian.*

Knowing the explicit relation between the parameters in $\mathcal{L}$ and the data in $\mathcal{C}$ allows us to identify important correlations between the parameters in $\mathcal{L}$. The effective parameters often cannot be treated independently but are linked by virtue of having a common origin in the compactification of the higher-dimensional Lagrangian. This perspective is lost in string-inspired models without an explicit derivation of the Lagrangian.

## 4. String Theory and Primordial Gravitational Waves

Some of the simplest inflationary models ($V(\phi) = m^2\phi^2, \lambda\phi^4, \dots$) have the inflaton field evolving over a super-Planckian range, $\Delta\phi > M_{\rm pl}$. In particular, this is required of all models with an observable gravitational wave signal [122]. So far it has been challenging to derive such 'large-field' models from an explicit string compactification. It is therefore interesting to ask whether these models can arise from a consistent string compactification $\mathcal{C}$ or if there are any fundamental obstructions. In the context

of effective field theory with a Planck scale cutoff $\Lambda = M_{\rm pl}$ it has been argued [122] that the effective potential $V(\phi)$ can only be reliably computed over a domain $\Delta\phi < M_{\rm pl}$. The question of the implications of super-Planckian field excursions is UV-sensitive and therefore provides an interesting window into microphysics (while inflation usually hides UV-physics!). In addition, there is the possibility that these considerations might be forced on us by a future observation of a primordial gravitational wave signal. To explain such a signal from a microscopic point of view will be an interesting theoretical challenge. In this thesis we ask whether scalar fields in string theory can have $\Delta\phi > M_{\rm pl}$ *and* controllably flat potential (*i.e.* $V'$, $V'' \ll V$ for $\Delta\phi > M_{\rm pl}$).

## 5. Outline of the Thesis

The structure of this thesis is as follows:

■ Part I: Review

In Chapters 2, 3 and 4 we review key aspects of cosmology and string theory. This sets the stage for the discussion in the following chapters. However, readers with a background in cosmology and string theory may skip directly to Chapter 5 without loss of continuity.

Our review of the fundamentals of modern cosmology (Chapter 2) emphasizes observations and the physical mysteries (dark matter, dark energy, and inflation) that they reveal. After a discussion of the homogeneous background cosmology we present an analysis of cosmological fluctuations. An understanding of these fluctuations is essential for observational tests of the inflationary paradigm. We then describe the dark energy puzzle and its impact on fundamental physics. Finally, we end our discussion of cosmology with a review of basic elements of inflation and an assessment of the future prospects for cosmological observations.

To preface our discussion of string cosmology we then give an overview of recent techniques of moduli stabilization in string theory (Chapter 3). In particular, we describe type IIB flux compactifications and the KKLT scenario. Finally, we review

the Klebanov-Strassler (KS) geometry as an important example of a warped background space whose metric is explicitly known. The KS solution will be an important background for our study of string inflation.

We end our review of string cosmology with an assessment of the state of the 'art' of inflation in string theory (Chapter 4). We describe warped D-brane inflation in some detail, emphasizing the eta-problem and the DBI mechanism. Finally, we summarize the progress and challenges of other models of string inflation.

■ Part II: The Inflaton Potential $V(\phi)$

Chapter 5 is a technical calculation of a crucial correction to the non-perturbative superpotential. This correction depends on the position of any mobile D3-branes in the compactification geometry and therefore forms a key ingredient for computing the inflaton potential in warped D-brane inflation (Chapters 6 and 7). We explain how the gauge theory effect can be translated into a geometric calculation via open-closed string duality. In particular, we compute the D3-brane backreaction on the warped volume of the four-cycle wrapped by a stack of D7-branes. We prove that the final result for the superpotential is then given by the holomorphic embedding condition of the D7-branes.

Chapter 6 is a summary of the implications of the results of Chapter 5 for models of D-brane inflation, while Chapter 7 is a long version of Chapter 6 that derives all results and extends the discussion. First, we derive the D3-brane potential in warped backgrounds. The multi-field potential depends on the radial coordinate $r$ and the five real angular coordinates of the KS throat as well as the complex modulus associated with the overall volume of the compact space. We integrate out the volume and the angles to get an effective single-field potential $V(r)$. We identify parameters in the inflaton potential with the microscopic input data of the string compactification. Imposing all consistency conditions on the compactification, we search for inflationary solutions in the effective theory. We find that inflationary

solutions would be easy to find if compactification constraints were ignored. Imposing constraints from the compactification geometry significantly restricts the parameter space of successful models. In particular, the potential can be made flat only locally and inflation is possible only close to an approximate inflection point of the potential. This leads to a model that is very sensitive to the model parameters and the initial conditions. We called this "A Delicate Universe" [20].

■ Part III: String Theory and Gravitational Waves

Chapter 8 derives a microscopic bound on the field evolution during warped D-brane inflation. In particular, we show that $\Delta\phi < M_{\rm pl}$. This bound is model-independent in the sense that it does not depend on the form of the potential and other details of inflation. Via a result by Lyth [122] this geometric bound on the field range is translated into a limit on the primordial gravitational wave amplitude. We also discuss the implications of the field range bound for the viability of DBI inflation on Calabi-Yau cones. The simplest models of DBI inflation overproduce primordial non-Gaussianity if the microscopic compactification constraint is imposed on the D3-brane position.

Chapter 9 speculates about possible generalizations of the result of Chapter 8. We describe the important challenge of deriving explicit models of string inflation that predict observable tensors, providing an important connection between microscopic physics and macroscopic observables.

■ Part IV: Conclusion

Chapters 10 and 11 offer some conclusions and perspectives.

In Chapter 10 we summarize the three main UV challenges/opportunities of string inflation: the eta-problem of $V(\phi)$, a microscopically consistent realization of large-field models with observable gravitational wave amplitude $r$ and a microscopically consistent realization of models with large non-Gaussianity $f_{\rm NL}$.

In Chapter 11 we make some concluding remarks and give a personal perspective on future directions.

■ Appendices

The appendices contain many original and new results. We consider them an essential aspect of this work.

In Appendix A we review Maldacena's beautiful calculation of the inflationary two- and three-point functions and cite the corresponding results for more general inflation models like DBI inflation. These classic results are used throughout the thesis as they form the basis for all modern comparisons of the inflationary predictions with cosmological data. Appendix B, C and D give technical details of the computations presented in Chapter 5, while Appendix E, F G and H give technical details of the computations presented in Chapters 6 and 7. Finally, Appendix J is a reference of key results used in this dissertation.

*Note on collaboration.* Modern theoretical physics is largely a collaborative effort. This thesis would not have been possible without the input and guidance of my outstanding collaborators. However, I was intimately involved in all the research reported in this dissertation. Furthermore, in each project the majority of the writing and rewriting of our results was done by Liam McAllister and myself. At the end my contributions and those of my collaborators have been woven together and there is no meaningful way to partition the final product.

# Part 1

# Review of String Cosmology

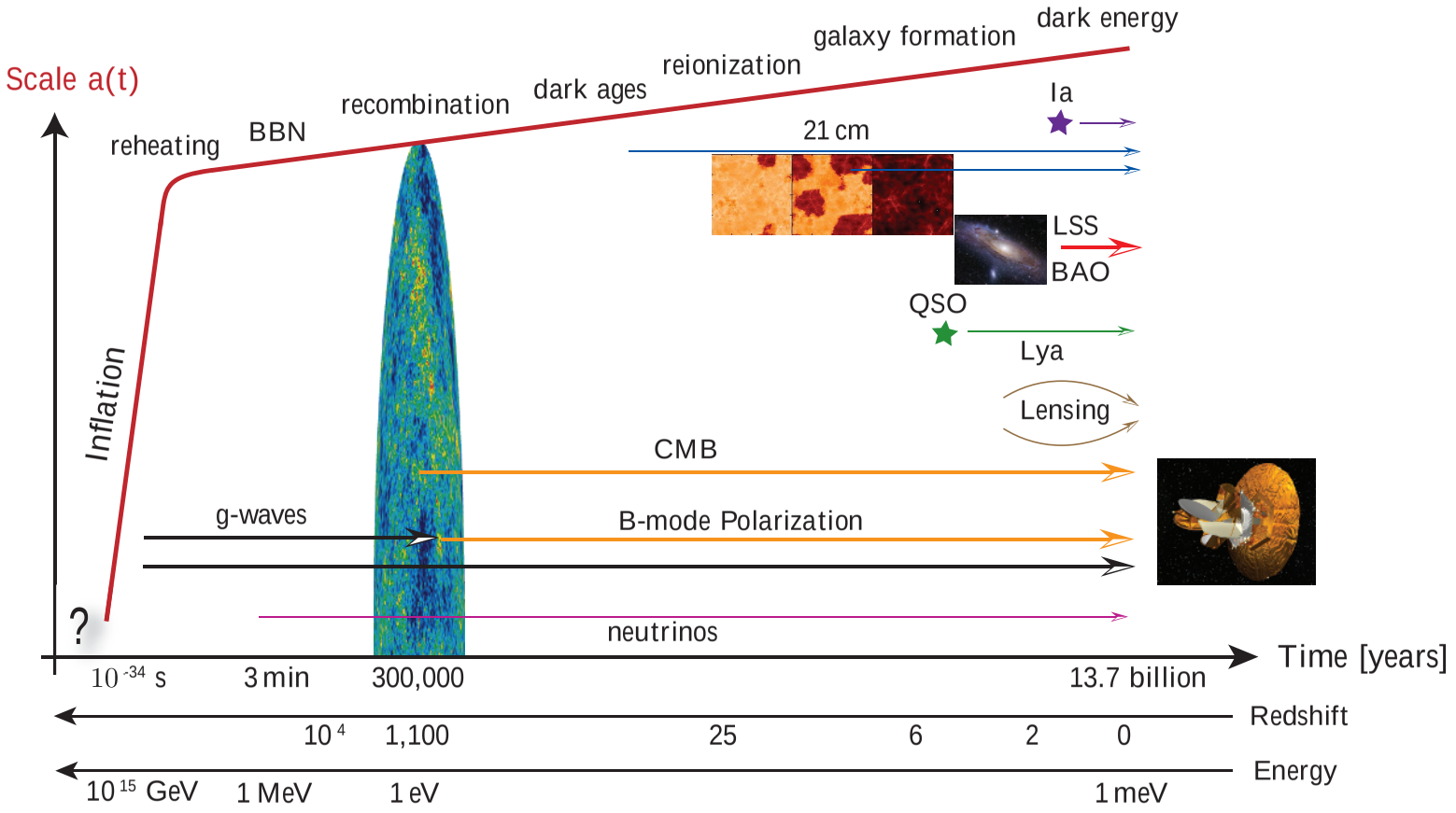
Scale a(t)
dark energy
galaxy formation
reionization
dark ages
recombination
BBN
reheating
Inflation
?
Ia
21 cm
LSS
BAO
QSO
Lya
Lensing
CMB
g-waves
B-mode Polarization
neutrinos
Time [years]
10 -34 s
3 min
300,000
13.7 billion
Redshift
10 4
1,100
25
6
2
0
Energy
10 15 GeV
1 MeV
1 eV
1 meV

CHAPTER 2

# Aspects of Modern Cosmology

In this chapter we present a review of basic cosmology (see also [62, 130, 160]). The emphasis is on observations and the physical mysteries that they reveal. Readers familiar with this background material may skip directly to Chapter 3.

We preface this chapter with a qualitative description of the thermal history of the universe (§1). In §2 we then give the theoretical background for understanding the status of observational cosmology. After describing the geometry and dynamics of the homogeneous background spacetime we define fluctuations around the smooth background. We focus on fluctuations in the density and the metric (gravitational waves). We describe how cosmological observations of these fluctuations are related to the physics of the early universe. Next, we devote two sections to the mystery of cosmic acceleration. We introduce dark energy and inflation in §3 and §4, respectively. While we restrict our treatment of dark energy to brief and mostly qualitative remarks, we discuss inflation in some detail. We explain the Big Bang puzzles and their resolution by a period of accelerated expansion in the early universe. We then introduce the inflaton potential $V(\phi)$ and the slow-roll conditions. Finally, we make the important connection between cosmological observables (§2) and quantum fluctuations around the classical inflationary dynamics (Appendix A).

## 1. A Brief History of the Universe

"Why is the universe *big*, *flat* and *empty*?" "What is the origin of structure?" These ancient questions have sharpened in recent years as a result of significant theoretical advances and high precision cosmological experiments. Remarkably, we now have quantitative answers to these questions based on fundamental physics applied to conditions in the early universe. Even more remarkably, for the first time in history our theories can be tested against cosmological observations. Data from the cosmic microwave background (CMB) [151] (Figure 1) and the large-scale structure (LSS) [156] (Figure 2) have given us detailed views of the early universe and its late time evolution. In this section we give a qualitative description of our modern understanding of the cosmos. We fill in the quantitative details in later sections.

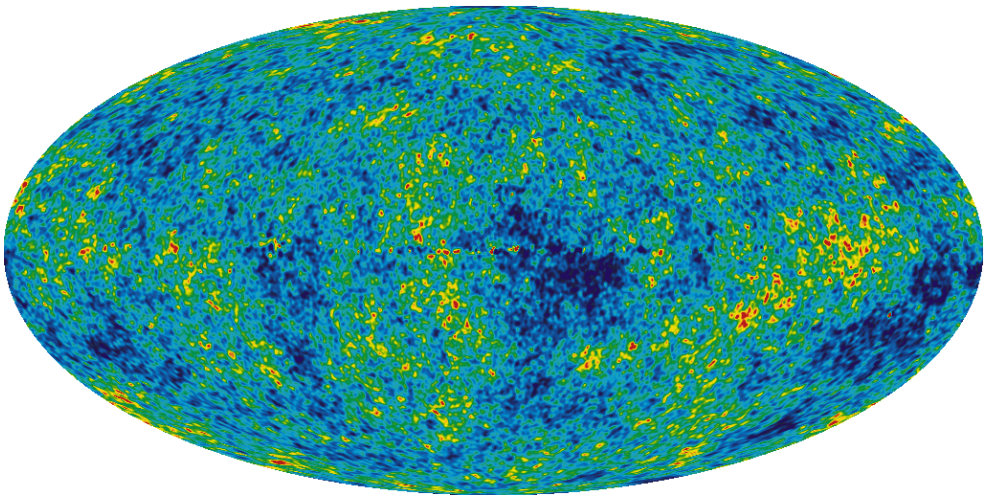

FIGURE 1. Temperature fluctuations in the cosmic microwave background (CMB). Blue spots represent directions on the sky where the CMB temperature is $\sim 10^{-4}$ below the mean, $\bar{T}_0 = 2.7$ K. This corresponds to photons losing energy while climbing out of the gravitational potentials of overdense regions in the early universe. Yellow and red indicate hot (underdense) regions. The statistical properties of these fluctuations contain important information about both the background evolution and the initial conditions of the universe (see Figures 3 and 4).

**1.1. Physics in an Expanding Universe.** There is undeniable evidence for the expansion of the universe: the light from distant galaxies is systematically shifted

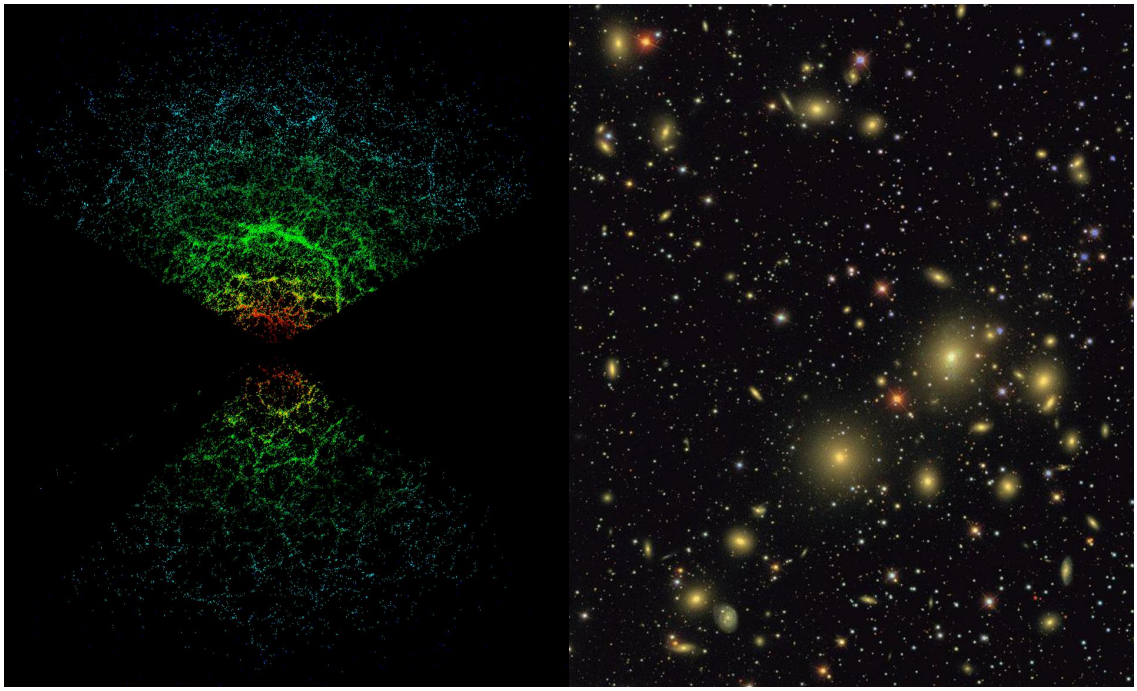

FIGURE 2. Distribution of galaxies. The Sloan Digital Sky Survey (SDSS) has measured the positions and distances (redshifts) of nearly a million galaxies. Galaxies first identified on 2d images, like the one shown above on the right, have their distances measured to create the 3d map. The left image shows a slice of such a 3d map. The statistical properties of the measured distribution of galaxies reveal important information about the structure and evolution of the late time universe.

towards the red end of the spectrum [89], the observed abundances of the light elements (H, He, and Li) matches the predictions of Big Bang Nucleosynthesis (BBN) [6], and the only explanation for the cosmic microwave background is a relic radiation from a hot early universe [60].

Two principles characterize thermodynamics and particle physics in an expanding universe:

(1) interactions between particles freeze out when the interaction rate $\Gamma = \sigma n v$ drops below the expansion rate $H$.

(2) broken symmetries in the laws of physics may be restored at high energies.

Table 1 shows the thermal history of the universe and various phase transitions related to symmetry breaking events. In the following we will give a qualitative summary of

TABLE 1. Major Events in the History of the Universe

| | Time | Energy | |
|---|---|---|---|
| Planck Epoch? | $< 10^{-43}$ s | $10^{18}$ GeV | |
| String Scale? | $\lesssim 10^{-43}$ s | $\lesssim 10^{18}$ GeV | |
| Grand Unification? | $\sim 10^{-36}$ s | $10^{15}$ GeV | |
| Inflation? | $\lesssim 10^{-34}$ s | $\lesssim 10^{15}$ GeV | |
| SUSY Breaking? | $> 10^{-10}$ s | $> 1$ TeV | |
| Baryogenesis? | $> 10^{-10}$ s | $> 1$ TeV | |
| Electroweak Unification | $10^{-10}$ s | 1 TeV | |
| Quark-Hadron Transition | $10^{-4}$ s | $10^2$ MeV | |
| Nucleon Freeze-out | 0.01 s | 10 MeV | |
| Neutrino Decoupling | 1 s | 1 MeV | |
| BBN | 3 min | 0.1 MeV | |
| | | | Redshift |
| Matter-Radiation Equality | $10^4$ yrs | 1 eV | $10^4$ |
| Recombination | $10^5$ yrs | 0.1 eV | 1,100 |
| Dark Ages | $10^5 - 10^8$ yrs | | $> 25$ |
| Reionization | $10^8$ yrs | | $25 - 6$ |
| Galaxy Formation | $\sim 6 \times 10^8$ yrs | | $\sim 10$ |
| Dark Energy | $\sim 10^9$ yrs | | $\sim 2$ |
| Solar System | $8 \times 10^9$ yrs | | 0.5 |
| Albert Einstein born | $14 \times 10^9$ yrs | 1 meV | 0 |

these milestones in the evolution of our universe. We will emphasize which aspects we consider certain and which are still more speculative.

**1.2. From Electroweak Symmetry Breaking to Recombination.** From $10^{-10}$ seconds to 380,000 years the history of the universe is based on well understood and tested(!) laws of particle, nuclear and atomic physics. We are therefore justified to have some confidence about the events shaping the universe during that time.

Enter the universe at 100 GeV, the time of the electroweak phase transition ($10^{-10}$ s). Above 100 GeV the electroweak symmetry is restored and the $Z$ and $W^{\pm}$ bosons are massless. Interactions are strong enough to keep quarks and leptons in thermal equilibrium. Below 100 GeV the symmetry between the electromagnetic and the weak forces is broken, $Z$ and $W^{\pm}$ bosons acquire mass and the cross-section of

weak interactions decreases as the temperature of the universe drops. As a result, at 1 MeV, neutrinos decouple from the rest of the matter. Shortly after, at 1 second, the temperature drops below the electron rest mass and electrons and positrons annihilate efficiently. Only an initial matter-antimatter asymmetry of one part in a billion survives. The resulting photon-baryon fluid is in equilibrium.

Around 0.1 MeV the strong interaction becomes important and protons and neutrons combine into the light elements (H, He, Li) during Big Bang Nucleosynthesis (BBN) ($\sim 200\,\mathrm{s}$). The successful prediction of the H, He and Li[1] abundances is one of the most striking consequences of the Big Bang theory.

The matter and radiation densities are equal around 1 eV ($10^{11}\,\mathrm{s}$). Charged matter particles and photons are strongly coupled in the plasma and fluctuations in the density propagate as cosmic 'sound waves'. Around 0.1 eV (380,000 yrs) protons and electrons combine into neutral hydrogen atoms. Photons decouple and form the free-streaming cosmic microwave background (CMB). 13.7 billion years later these photons give us the earliest snapshot of the universe (Figure 1).

**1.3. Evolution of Cosmic Structure.** Small density perturbations in the early universe, $\delta \equiv \frac{\delta\rho}{\rho}$, grow via gravitational instability to form the large scale structures observed in the late universe (Figure 2). During radiation domination the growth is slow, $\delta \sim \ln a$ (where $a(t)$ is the scale factor, see below). Clustering becomes more

[1]BBN predicts the primordial abundances of the light elements deuterium D, helium-3 $^3$He, helium-4 $^4$He and lithium-7 $^7$Li as a function of the baryon-to-photon ratio. These predictions are tested by reconstructing the primordial abundances from astronomical observations. To reduce systematic uncertainties the observations are limited to astronomical objects in which very little stellar nucleosynthesis has taken place (*e.g.* dwarf galaxies) or to objects that are very distant and therefore in an early stage of their evolution (*e.g.* quasars). The agreement between the theory and observations is excellent for deuterium and helium, but less perfect for lithium [47]. However, because the $^7$Li abundance in old Population II stars may be depleted, the observed lithium abundance depends both on stellar models and the consistency of BBN. We consider it more likely that the 'Li problem' is explained by systematic errors in the measurements and uncertainties in astrophysical modeling than by a fundamental problem with early universe cosmology. It should also be noted that the baryon-to-photon ratio preferred by BBN is consistent with the value inferred independently from CMB measurements.

efficient after matter dominates the background density, $\delta \sim a$. Small scales become non-linear first, $\delta \sim 1$, and form gravitationally bound objects that decouple from the overall expansion. This leads to a picture of hierarchical structure formation (see Table 2) with small scale structures (like stars and galaxies) forming first and then merging into larger structures (clusters and superclusters of galaxies).

TABLE 2. Typical Length Scales in the Universe

| | meters | | |
|---|---|---|---|
| Planck Scale | $10^{-35}$ m | | |
| String Scale? | $\sim 10^{-30}$ m | | |
| "LHC Scale" | $10^{-18}$ m | | |
| Quark, Electron | $< 10^{-18}$ m | | |
| Proton | $10^{-15}$ m | | |
| Nucleus | $10^{-14}$ m | | |
| Atom | $10^{-10}$ m | | |
| DNA | $10^{-8}$ m | | |
| Virus | $10^{-7}$ m | | |
| Cell | $10^{-4}$ m | | |
| | | light years | parsec |
| Earth | $10^{8}$ m | | |
| Earth-Moon | $10^{9}$ m | | |
| Earth-Sun | $10^{11}$ m | 8 min | |
| Earth-Star | $10^{18}$ m | 100 yrs | 30 pc |
| Galaxy | $10^{21}$ m | $10^{5}$ yrs | 10 kpc |
| Local Group | $10^{22}$ m | $10^{5}$ yrs | 100 kpc |
| Virgo Cluster | $10^{23}$ m | $10^{6}$ yrs | 1 Mpc |
| Supercluster | $10^{24}$ m | $10^{7}$ yrs | 10 Mpc |
| Observable Universe | $4.3 \times 10^{26}$ m | $45 \times 10^{9}$ yrs | $1.4 \times 10^{4}$ Mpc |

Around redshift $z = 25$, high energy photons from the first stars begin to ionize the hydrogen in the inter-galactic medium (IGM). This process of 'reionization' is completed at $z \approx 6$. Meanwhile, the most massive stars run out of nuclear fuel and explode as 'supernovae'. In these explosions the heavy elements (C, O, ...) necessary for the formation of life are created, leading to the slogan "we are all stardust".

At $z \approx 1$, a negative pressure 'dark energy' comes to dominate the universe. The background spacetime is accelerating and the growth of structure ceases, $\delta \sim$ const.

**1.4. The First $10^{-10}$ Seconds.** The fundamental laws of high energy physics are well-established up to the energies reached by current particle accelerators ($\sim$ 1 TeV). Our ideas about the *very early* universe on the other hand are based on more speculative physics. In this section we sketch the implications of physics beyond the Standard Model for early universe cosmology.

*Grand Unification.* In the history of physics symmetry principles and unification have been reliable guides towards the true nature of the world. The giants of physics, Newton, Maxwell and Einstein, each provided important unifying principles that revolutionized the way we see the world (physics+astronomy, electricity+magnetism, space+time). Grand Unified Theories (GUTs) are a set of gauge theories that unify the electromagnetic force with the strong and the weak nuclear forces at high energies ($\sim 10^{15}$ GeV). GUTs have a number of interesting theoretical consequences. Generic versions of GUTs predict proton decay and the existence of magnetic monopoles. Neither phenomenon is observed in nature.[2] GUTs also predict a phase transition as the temperature of the universe drops below $10^{15}$ GeV. Initially there was some hope that this might be the physical origin of cosmological inflation (see below). However, it now seems that this hope cannot be realized when details of the inflationary dynamics are considered in the context of GUTs.

Finally, at the GUT scale, interactions violate baryon number and CP, while the GUT phase transition provides out of equilibrium conditions. GUT physics therefore can provide a plausible explanation for the observed baryon asymmetry of the universe (alternatively, there are many models in which the baryon asymmetry is produced at lower energies by electroweak processes).

[2]Indeed, one of Guth's original motivations for inflation was to explain the absence of GUT monopoles. Today, experimental limits on the proton lifetime rule out the simplest versions of grand unified theories raising some doubts about the idea of the unification of forces at the GUT scale.

*Inflation.* The observed expansion of the universe implies serious initial conditions problems (see §4) unless a period of accelerated expansion[3] – inflation – is postulated to have occurred somewhere between the GUT scale, $10^{15}$ GeV, and the electroweak scale, 1 TeV. The large uncertainty in the energy scale of inflation reflects our lack of understanding of the fundamental physical origin of the inflationary era. We defer a detailed discussion of speculations on the "physics of inflation" to the remainder of this thesis. Here, we would only like to mention that small quantum fluctuations around the classical inflationary dynamics are stretched by inflation to cosmological scales and seed primordial density fluctuations. Inflation therefore provides a very elegant mechanism to explain the initial conditions relevant to the formation of large-scale structure via gravitational instability.

*Quantum Foam.* At *very very early* times ($10^{-43}$ s), corresponding to high energies ($10^{18}$ GeV) and short length scales ($10^{-35}$ m), quantum mechanics becomes important for the structure and dynamics of the universe. Classical notions of space and time lose their familiar meanings. The uncertainty principle allows (virtual) particles to briefly come into existence, and then annihilate, without violating energy conservation. The energy of these virtual particles can be large if the space that is considered is small. Since energy curves spacetime, this suggests that on very small scales space looks nothing like the smooth large scale spacetime that characterizes the universe today. On small scales violent quantum fluctuations produce a foam-like structure [161]. A quantitative understanding of the physics of that era requires applying a theory of quantum gravity to fluctuations at the Planck scale. The absence of such a theory limits us to hand-waving and speculation.

[3]The cyclic model [154] proposes a radically different solution to the initial conditions problems and a very different cosmic history. In the cyclic model the Big Bang singularity was not the beginning of time but only marked the transition from a slow contracting universe to an expanding universe. The standard initial conditions problems are solved by a long period of dark energy domination followed by slow contraction and a bounce.

*String Cosmology.* It is now believed that general relativity is only an effective theory valid at low energies and large distances. As we just sketched heuristically, at very high energy and short distances, new symmetries and degrees of freedom of a more fundamental theory are likely to become important. In the context of string theory some of these qualitative ideas can be made more concrete (for a review see *e.g.* [128]). Quantitatively, one expects a treatment based on quantum field theory (QFT) and general relativity (GR) to break down down, either when the Hubble scale $H$ increases to the scale of some new physics (like the string scale $M_s \equiv \frac{1}{\sqrt{\alpha'}} \sim g_s M_{\rm pl} \ll M_{\rm pl}$) or when spatial fluctuations shrink to the string scale $l_s$. In many cases, string degrees of freedom (characterizing the extended nature of strings) become important in this limit.[4] Perturbative and non-perturbative stringy dynamics has been suggested as a way to resolve the cosmological Big Bang singularity and to explain why our universe has three large space dimensions [42]. Due to lack of space and expertise we cannot do justice to these interesting applications of string theory to the very early universe in this work. For a recent survey of ideas we refer the reader to Ref. [128].

## 2. Status of Observational Cosmology

**2.1. ΛCDM.** The recent data of fluctuations in the cosmic microwave background [151] (Figure 1) and the distribution of galaxies [156] (Figure 2) has led to the emergence of a standard cosmological model. On the largest observed scales the universe is homogeneous and isotropic, while on small scales tiny primordial fluctuations in the overall density have grown by gravitational instability to form galaxies, stars, and planets. Galaxies and clusters of galaxies would be unstable if it weren't

[4]For the remainder of this thesis it will be important that we assume that the string scale $M_s$ is significantly above the inflation scale $M_{\rm inf} \sim (H_{\rm inf} M_{\rm pl})^{1/2}$. At energies below $M_s$, string theory reduces to supergravity with corrections that can be treated perturbatively. In practice, we will also assume that the inflation scale is below the compactification (or Kaluza-Klein) scale $M_c \sim L^{-1}$, where $L$ is a typical length scale of the compactification manifold. In that case, an effective four-dimensional description is possible.

for the gravitational effect of cold dark matter (CDM). Finally, the observations show that the present universe is dominated by a mysterious form of dark energy ($\Lambda$) that causes the expansion of the universe to accelerate.

All the cosmological data can be well fit by a six parameter model: $\{\Omega_b,\ \Omega_{dm},\ h,\ \tau\}$ describes the homogeneous background (§2.2), while $\{A_s,\ n_s\}$ characterizes the primordial fluctuations (§2.3). In this section we consider the observational evidence for the $\Lambda$CDM model, before discussing the theoretical issues that the model raises (§3 and §4).

### 2.2. Homogeneous Background.

*Geometry.* Averaged over very large scales the universe is nearly homogeneous and isotropic. The spacetime is then described by the Friedmann-Robertson-Walker (FRW) metric

$$\mathrm{d}s^2 = -\mathrm{d}t^2 + a(t)^2\left(\frac{\mathrm{d}r^2}{1-kr^2} + r^2(\mathrm{d}\theta^2 + \sin^2\theta\mathrm{d}\phi^2)\right). \tag{2.1}$$

Here, the scale factor $a(t)$ describes the relative size of spacelike hypersurfaces $\Sigma_3$ at different times. The curvature parameter $k$ is $+1$ for positively curved $\Sigma_3$, 0 for flat $\Sigma_3$, and $-1$ for negatively curved $\Sigma_3$. Equation (2.1) uses comoving coordinates – the universe expands as $a(t)$ increases, but galaxies keep fixed coordinates[5] $r$, $\theta$, $\phi$. If we define the scale factor to be unity today, $a(t_0) \equiv 1$, then the redshifting of light between emission at time $t$ and observation today at $t_0$ is given by

$$1 + z = \frac{\lambda_{\text{observed}}}{\lambda_{\text{emitted}}} = \frac{1}{a(t)}. \tag{2.2}$$

The expansion rate of the universe is characterized by the Hubble parameter $H(t) \equiv \partial_t \ln a$. This is arguably the most important function in cosmology. It is measured

[5]This statement only applies to the Hubble flow and ignores the peculiar velocities of galaxies $\mathbf{v}_{\text{pec}} = (\dot{r}, \dot{\theta}, \dot{\phi})$.

rather indirectly by determining separately the distances and redshifts of astronomical objects. Since measuring distances in cosmology is notoriously difficult (see *e.g.* [62, 134]), the value of the Hubble constant has historically been associated with large uncertainties and fierce debates [134]. In defining cosmological distances a fundamental quantity is the comoving distance to an object at redshift $z$[6]

$$\chi(z) \equiv \int_0^z \frac{\mathrm{d}z'}{H(z')}\,. \tag{2.3}$$

It relates to two important distance measures: the 'angular diameter distance' and the 'luminosity distance'. Angular diameter distance is defined as the ratio of an object's physical transverse size to its angular size

$$d_A(z) = \frac{1}{1+z}\begin{cases} \frac{\sinh[\sqrt{\Omega_k}H_0\chi(z)]}{[H_0\sqrt{\Omega_k}]} & k=+1 \\ \chi(z) & k=0 \\ \frac{\sin[\sqrt{\Omega_k}H_0\chi(z)]}{[H_0\sqrt{\Omega_k}]} & k=-1 \end{cases} \tag{2.4}$$

Observations of cosmic microwave background anisotropies provide a measure of the angular diameter distance to the last scattering surface[7] $d_A(z_{\mathrm{CMB}})$. This provides an accurate measure of the average geometry of the universe[8] (see Figures 3 and 4). Supernova observations on the other hand measure luminosity distances which relate the observed apparent magnitudes to the absolute luminosity emitted by the stellar explosion

$$d_L(z) = (1+z)\chi(z)\,. \tag{2.5}$$

[6]This is the distance along radial null geodesics of (2.1).

[7]CMB observations measure the angular diameter of the sound horizon at baryon-photon decoupling. We here point out that the angular size of CMB anisotropies only provides a measure of the *integrated* Hubble parameter to the last scattering surface. However, through baryon acoustic oscillations in large-scale structure correlations and the Alcock-Paczynski effect angular diameter distances to objects at lower redshifts can be measured. This might provide interesting constraints on the late time evolution of $H$ and the dynamics of dark energy.

[8]From (2.4) we see that a measurement of $\Omega_k$ requires an independent estimate of the Hubble constant $H_0$.

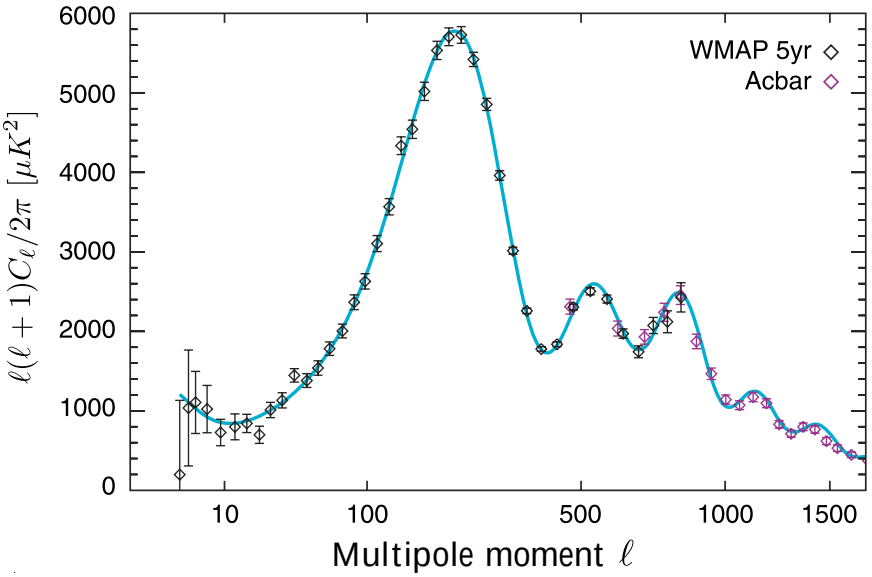


FIGURE 3. Power spectrum of CMB temperature fluctuations. The data is in perfect agreement with the theoretical prediction (solid line) of the ΛCDM model with a nearly scale-invariant input spectrum for the primordial density perturbations (as predicted by inflation). The position of the first peak measures the angular diameter distance to the recombination surface.

This gives a late time measurement of the evolution of the Hubble parameter $H(z)$. Analysis of data from type IA supernova explosions led to the discovery of the accelerating universe [137, 142].

*Dynamics.* So far we have described the *kinematics* of the FRW spacetime as defined by the metric (2.1). To characterize the *dynamics* we relate the background spacetime to the energy-momentum tensor of the universe. Einstein's gravitational field equations ($M_{\rm pl}^2 G_{\mu\nu} = T_{\mu\nu}$) for a FRW universe (2.1) filled with a perfect fluid, $T^\mu_{\ \nu} = \mathrm{diag}(-\rho, p, p, p)$, take the form of the Friedmann equations

$$H^2 = \frac{1}{3M_{\rm pl}^2}\rho - \frac{k}{a^2}\,, \tag{2.6}$$

$$\frac{\ddot{a}}{a} = -\frac{1}{6M_{\rm pl}^2}(\rho + 3p)\,. \tag{2.7}$$

Here, $\rho$ and $p$ are the energy density and the pressure of the fluid, respectively. For a multi-component fluid, it is convenient to define the density parameter in a species $i$

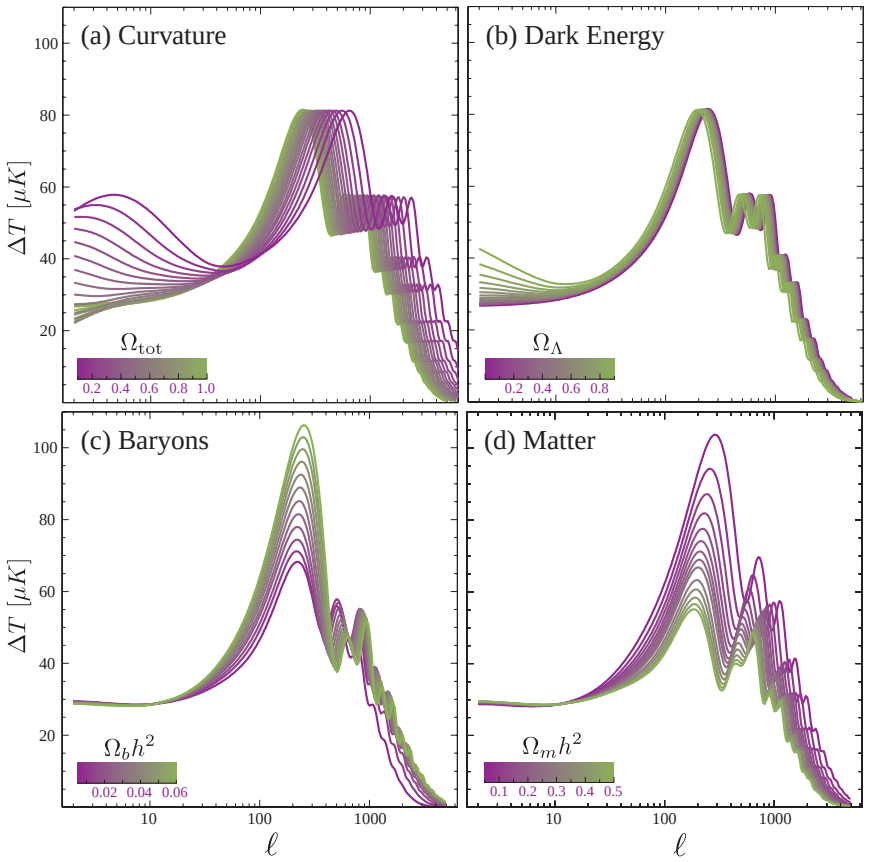


FIGURE 4. Fluctuations in the cosmic microwave background as a function of the parameters of the background cosmology [figure courtesy of Wayne Hu]. (a) Variation of the total density (or curvature) shifts the positions of the peaks of the spectrum. The CMB is therefore a probe of the background geometry. (b) Increasing the dark energy contribution increases power on large scales via the integrated Sachs-Wolfe effect. (c) The baryon density affects the relative peak heights. The observed relative peak heights are consistent with Big Bang nucleosynthesis values for $\Omega_b$. (d) Increasing the matter content uniformly damps power on all scales.

relative to the critical density for a flat universe is $\rho_c \equiv 3M_{\rm pl}^2 H^2$

$$\Omega_i \equiv \frac{\rho_i}{\rho_c}\,. \tag{2.8}$$

The Friedmann equation (2.6) then becomes

$$\Omega(t) - 1 = \frac{k}{H^2 a^2} \equiv \Omega_k\,, \tag{2.9}$$

where

$$\Omega = \sum_i \Omega_i = \Omega_r + \Omega_b + \Omega_{dm} + \Omega_\Lambda + \cdots \,. \tag{2.10}$$

Here, we consider radiation (photons and neutrinos)[9] ($r$), baryons ($b$), dark matter ($dm$) and dark energy ($\Lambda$). The CMB+LSS best fit parameters for the composition of the universe *today* are [151]

| | |
|---|---|
| $\Omega_r$ | $8.518 \times 10^{-5}$ |
| $\Omega_b$ | $0.046 \pm 0.003$ |
| $\Omega_{dm}$ | $0.231 \pm 0.026$ |
| $\Omega_m \equiv \Omega_b + \Omega_{dm}$ | $0.277 \pm 0.029$ |
| $\Omega_\Lambda$ | $0.723 \pm 0.029$ |
| $\Omega_k$ | $-0.0052 \pm 0.0064$ |
| $\Omega$ | $\sim 1 \pm 10^{-2}$ |

This is consistent with a spatially flat universe, a theoretical prejudice inspired by inflation (see §4). In the remainder of this thesis we will therefore set $\Omega_k \equiv 0$.

Notice from the second Friedmann equation (2.7) that accelerated expansion, $\ddot{a} > 0$, as observed for the late universe (dark energy) and as postulated for the early universe (inflation), requires a negative pressure component, $p < -\frac{1}{3}\rho$. To explain this from fundamental physics is one of the biggest challenges of theoretical physics.

**2.3. Fluctuations.** As we mentioned before, galaxies are formed by gravitational instability of minute density fluctuations $\delta\rho$, *i.e.* small perturbations of the homogeneous FRW background (2.1). Observations of the cosmic microwave background radiation provide the earliest snapshot of these fluctuations. The metric of a flat FRW universe with small perturbations is

$$\mathrm{d}s^2 = \Big[\bar{g}_{\mu\nu} + \delta g_{\mu\nu}\Big]\mathrm{d}x^\mu \mathrm{d}x^\nu \,. \tag{2.11}$$

[9]We use $\Omega_r = \Omega_\gamma(1 + 0.2271 N_{\rm eff})$, where $\Omega_\gamma$ is the photon density and $N_{\rm eff} \approx 3.04$ is the effective number of relativistic neutrino species.

For the important discussion of the gauge dependence of this split into background variables ($\bar{g}_{\mu\nu}$, $\bar{\rho}$) and perturbations ($\delta g_{\mu\nu}$, $\delta\rho$) we refer the reader to the excellent treatment in Ref. [130]. Here, we restrict ourselves to a summary of the basic technical results of first-order cosmological perturbation theory. (Further details are given in Appendix A.) The metric perturbations $\delta g_{\mu\nu}$ can be decomposed into three distinct types: *scalar*, *vector* and *tensor* perturbations. This classification describes the transformation properties of the perturbations under spatial coordinate reparameterizations [130]. At linear order scalar, vector and tensor perturbations do not interact.

*Scalars.* Scalar perturbations are characterized by 4 scalar functions and 2 gauge degrees of freedom. In Newtonian gauge the perturbed metric takes the following form

$$\mathrm{d}s^2 = -(1+2\Phi)\mathrm{d}t^2 + a(t)^2(1-2\Psi)\delta_{ij}\mathrm{d}x^i\mathrm{d}x^j\,. \tag{2.12}$$

In the absence of anisotropic stress ($T_{ij}=0$) $\Phi=\Psi$ and scalar metric perturbations are described by a single function, the Newtonian potential $\Phi(t,\mathbf{x})$. In Fourier space the fluctuation amplitude is

$$\Phi_{\mathbf{k}}(t) = \int \mathrm{d}^3\mathbf{x}\, e^{-i\mathbf{k}\cdot\mathbf{x}}\Phi(t,\mathbf{x})\,. \tag{2.13}$$

The *initial* power spectrum of $\Phi$ is[10]

$$\langle\Phi_{\mathbf{k}}(t_i)\Phi_{\mathbf{k}'}(t_i)\rangle \equiv (2\pi)^3\delta(\mathbf{k}+\mathbf{k}')\mathcal{P}_s(k)\,, \qquad P_s(k)\equiv\frac{k^3}{2\pi^2}\mathcal{P}_s(k)\,. \tag{2.14}$$

Assuming a power law, $P_s(k)=A_s k^{n_s-1}$, we define the spectral index of the primordial power spectrum

$$n_s - 1 \equiv \frac{\mathrm{d}\ln P_s}{\mathrm{d}\ln k}\,. \tag{2.15}$$

[10]By "initial" we mean any time $t_i$ between the end of inflation and the horizon re-entry of a given Fourier mode (see §4). The normalization of $P_s(k)$ is chosen such that the real space variance of $\Phi$ is $\langle\Phi\Phi\rangle = \int_0^\infty P_s(k)\,\mathrm{d}\ln k$.

The value $n_s = 1$ corresponds to a scale-invariant Harrison-Zeldovich spectrum. The scalar metric perturbations $\Phi$ are induced by inhomogeneities in the energy density,

$$\rho(t, \mathbf{x}) = \bar{\rho}(t)[1 + \delta(t, \mathbf{x})] \,. \tag{2.16}$$

Density perturbations $\delta$ and metric perturbations $\Phi$ are related by a Poisson equation on subhorizon scales ($k > aH$) and by a constant rescaling on superhorizon scales ($k < aH$). On subhorizon scales, gravity acts as an amplifier of these fluctuations, which leads to the formation of the large-scale structure of the universe. The evolution of density fluctuations is characterized by the growth function $g_k(t)$[11]

$$\delta_{\mathbf{k}}(t) \equiv \frac{g_k(t, t_i)}{a} \delta_{\mathbf{k}}(t_i) \,. \tag{2.17}$$

CMB and LSS observations measure the density power spectrum at late times (Figure 5). To relate this to the primordial spectrum one needs to take into account the post-processing of the spectrum as given by the growth factor $g_k(t)$. Assuming validity of general relativity and using the measured cosmological parameters to fix the background cosmology we can factor out the cosmological evolution and extract the spectrum of primordial fluctuations $P_s(k)$. The precise shape of this spectrum provides an accurate test of inflationary perturbations as the origin of cosmic structure (see §4 and Figure 6).

*Vectors.* Vector perturbations are related to rotational motion of the fluid. They decay with the expansion of the universe and therefore do not affect the late time properties of the universe. We will not consider them further.

[11]The function $g_k(t)$ depends on theory of gravity and the matter content of the universe. The growth of structure therefore provides an important consistency test for the applicability of general relativity on very large scales.

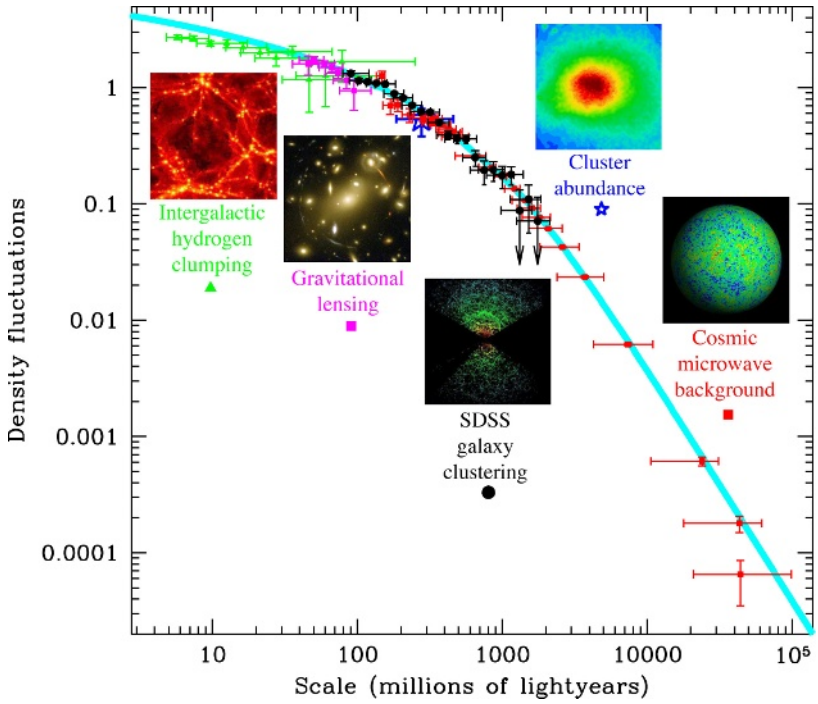


FIGURE 5. Density fluctuations as a function of scale and relevant observational probes [figure courtesy of Max Tegmark].

*Tensors.* Tensor perturbations describe *gravitational waves*, *i.e.* perturbations to the spatial metric of the form

$$\mathrm{d}s^2 = -\mathrm{d}t^2 + a(t)^2(\delta_{ij} + h_{ij})\mathrm{d}x^i\mathrm{d}x^j\,, \tag{2.18}$$

where $\partial_i h_{ij} = h^i_i = 0$. A stochastic background of gravitational waves is a unique prediction of inflationary cosmology (see §4). At linear order gravitational waves do not couple to perturbations in the fluid.[12] They therefore redshift like radiation and their amplitudes decays with the expansion of the universe. The tensor perturbation $h_{ij}$ can be written in terms of two polarization modes: $h_{ij} = h_+ e^+_{ij} + h_\times e^\times_{ij}$. The primordial power spectrum for each polarization mode is

$$\langle h_{\mathbf{k}} h_{\mathbf{k}'}\rangle = (2\pi)^3\delta(\mathbf{k}+\mathbf{k}')\mathcal{P}_t(k)\,, \qquad P_t(k) \equiv \frac{k^3}{2\pi^2}\mathcal{P}_t(k)\,. \tag{2.19}$$

[12]Second order couplings between scalar and tensor modes have been considered in [8, 23, 129], but they are small by virtue of the scalar amplitude being small, $\Phi \sim 10^{-5}$.

CMB polarization experiments will be sensitive to the tensor-to-scalar ratio

$$r \equiv \frac{P_t}{P_s} \,. \tag{2.20}$$

The data has now reached a precision that allows meaningful constraints to be placed on $n_s$ (2.15) and $r$ (2.20) (see Figure 6).

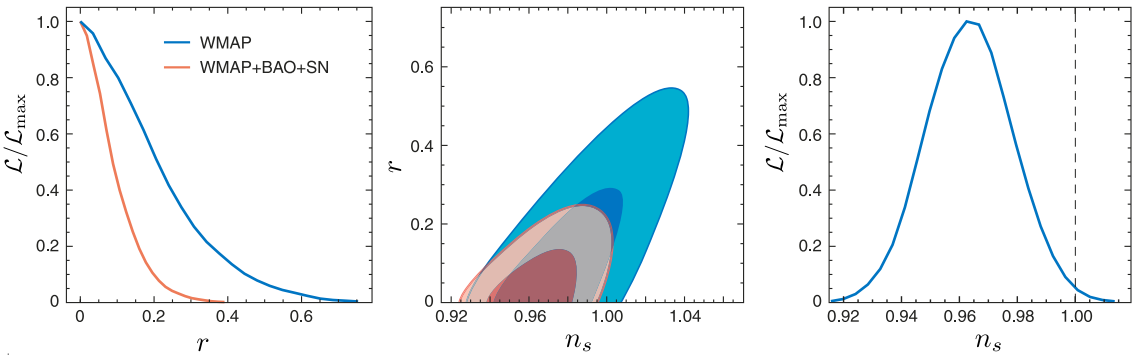


FIGURE 6. Constraints on the inflationary parameters $n_s$ and $r$ from recent cosmic microwave background and large-scale structure observations [151].

**2.4. Summary.** This is a golden age of cosmology. New precision data is testing theoretical ideas about the structure and evolution of the universe. These observations have revealed three problems that challenge the foundations of theoretical physics: dark matter, dark energy, and inflation. We now know that 95% of the universe is not ordinary atoms! However, we have yet to make sense of it! We have some ideas for what the dark matter might be, but dark energy and inflation lack any explanation in fundamental physics.

## 3. Dark Energy

**3.1. The Dark Energy Crisis.** Explaining the nature of dark energy is one of the greatest challenges of fundamental physics. Paul Steinhardt calls the discovery of dark energy "one of the most surprising and profound discoveries in the history of science" [152], while Steven Weinberg notes that "physics thrives on crisis" [159].

Two questions summarize the dark energy crisis:

- *Why is the vacuum energy so unnaturally small?*

  The energy momentum tensor of the universe $T_{\mu\nu}$ is expected to contain a term $\Lambda g_{\mu\nu}$ coming from the quantum mechanical energy density of the vacuum. Computations in quantum field theory[13] suggest that the natural value of the constant $\Lambda$ should be in the range $(\mathrm{TeV})^4 \leq \Lambda_{\mathrm{theory}} \leq (10^{19}\,\mathrm{GeV})^4$. According to Einstein's equations, $M_{\mathrm{pl}}^2 G_{\mu\nu} = T_{\mu\nu}$, such a term admits de Sitter space as a solution. It is therefore natural to propose vacuum energy as the cause of the observed acceleration of the universe today. Unfortunately, the observed value of the cosmological constant $\Lambda_{\mathrm{obs}} \sim (\mathrm{meV})^4$ is some 120 orders of magnitude smaller than its natural value, $\Lambda_{\mathrm{obs}}/\Lambda_{\mathrm{theory}} = 10^{-123}$. This is the biggest disagreement between theory and experiment in the history of science. It is the famous *cosmological constant problem*: "Why is the vacuum energy density so small?" And, "If it is so small, why is it not zero?"

- *Why did acceleration start only in the recent past?*

  To make matters worse, the energy density of dark energy is observed to be of the same order of magnitude as the present matter density. This is

[13]The following provides an estimate of the energy density of empty space: Consider summing the zero-point energies of all normal modes of some field of mass $m$ up a wavenumber cutoff $\Lambda^{1/4} \gg m$. This yields the following vacuum energy density

$$\langle\rho\rangle = \int_0^{\Lambda^{1/4}} \frac{4\pi k^2 \mathrm{d}k}{(2\pi)^3} \frac{1}{2} \sqrt{k^2 + m^2} \approx \frac{\Lambda}{16\pi^2}\,. \tag{2.21}$$

If $\Lambda^{1/4}$ is set to any particle physics scale ($M_{\mathrm{pl}}$, $M_{\mathrm{SUSY}}$, $\Lambda_{\mathrm{QCD}}^{1/4}$, $m_e$), one gets a version of the cosmological constant problem.

puzzling since the vacuum energy density $\rho_\Lambda \propto a^0$ remains constant during the evolution of the universe, whereas the matter energy density $\rho_m \propto a^{-3}$ decreases as the universe expands. The two energy densities being nearly the same today means that their ratio $\rho_\Lambda/\rho_m$ had to be incredibly small in the early universe, but fine-tuned to become nearly equal today. In other words, one might think that we are living at a special epoch when the dark energy density and the matter density are nearly equal in magnitude. During most of the history and the future of the universe this is not the case. This has become known as the *cosmic coincidence problem* (the "why now?" problem).

**3.2. Dark Energy in String Theory.** The cosmological constant problem points to a deep conflict between the physics of the very large and the very small. Quantum mechanics describes the microscopic world of elementary particles, atoms and molecules, while Einstein's general relativity provides an elegant mathematical formulation for the evolution of the universe on the largest scales. Both theories are fantastically successful in describing fundamental features of the world. However, whenever forced to apply quantum mechanics and general relativity simultaneously one is led to troubling inconsistencies. String theory in contrast is a consistent theory of quantum gravity and hence has the potential to address fundamental questions about the initial Big Bang singularity and the center of black holes. It is therefore justified to imagine that string theory will also give us new insights into the vacuum energy problem. So far this hope has not been realized, although string theory has provided some interesting new ideas for addressing the problem. In particular, formulating de Sitter space in string theory has been a challenge that was overcome only recently by the first explicit constructions of metastable de Sitter solutions (see Chapter 3). The multiplicity of these vacuum solutions can explain the vacuum energy problem by anthropic reasoning [39].

## 4. Inflation

"SPECTACULAR REALIZATION:
This kind of supercooling can explain why the universe today is so incredibly flat and therefore resolve the fine-tuning paradox pointed out by Bob Dicke in his Einstein day lectures."
*Alan Guth*, Dec 7, 1979.

**4.1. Shortcomings of the Big Bang Theory.** Despite the success of the Big Bang theory in explaining basic cosmological observations (see §2) it was realized (*e.g.* by Dicke) that the uniform expansion of the universe poses serious conceptual problems.

*Homogeneity Problem.* The standard model of cosmology assumes that the universe is homogeneous and isotropic. Indeed observations confirm this. However, the conventional Big Bang theory does not explain this fact. As we discussed above, inhomogeneities are gravitationally unstable and therefore tend to grow with time. Observations of the CMB for instance verify that the fluctuations were much smaller at the last scattering epoch than today. One thus expects that these inhomogeneities were still smaller further back in time. How to explain a universe so smooth in its past?

*Flatness Problem.* Spacetime in general relativity is dynamical, curving in response to matter in the universe. Why then is the universe so closely approximated by flat Euclidean space? To understand the severity of the problem consider the Friedmann equation in the form (2.9)

$$\Omega(a) - 1 = \frac{k}{(aH)^2}\,. \tag{2.22}$$

In the conventional Big Bang theory the comoving Hubble radius $(aH)^{-1}$ grows with time and $|\Omega - 1|$ hence diverges with time. (A flat universe with $\Omega = 1$ is an unstable

fixed point.) In the context of the standard Big Bang model, the quasi-flatness observed today, $\Omega(a_0) \sim 1$, therefore requires extreme fine-tuning of $\Omega$ near 1 in the early universe, *e.g.* the deviation from flatness at BBN, during the GUT era and at the Planck scale, respectively has to satisfy the following conditions: $|\Omega(a_{\rm BBN}) - 1| \leq \mathcal{O}(10^{-16})$, $|\Omega(a_{\rm GUT}) - 1| \leq \mathcal{O}(10^{-55})$, $|\Omega(a_{\rm pl}) - 1| \leq \mathcal{O}(10^{-61})$.

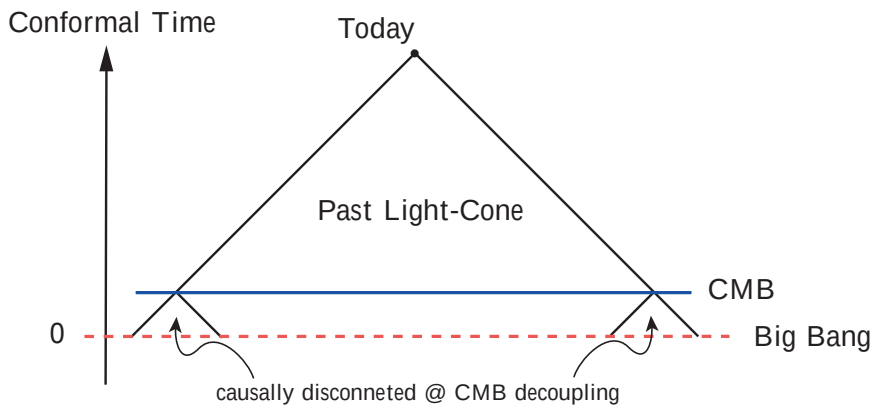


FIGURE 7. Conformal spacetime of conventional Big Bang cosmology. The CMB at last scattering consists of $10^5$ causally disconnected regions!

*Horizon Problem.* Consider radial null geodesics in a flat FRW spacetime (2.1)

$$\mathrm{d}r = \pm \frac{\mathrm{d}t}{a(t)} \equiv \mathrm{d}\tau \,. \tag{2.23}$$

We define the *comoving horizon*, $\tau$, as the causal horizon, *i.e.* the distance a light ray travels between time 0 and time $t$

$$\tau \equiv \int_0^t \frac{\mathrm{d}t'}{a(t')} = \int_0^a \frac{\mathrm{d}a}{Ha^2} = \int_0^a \mathrm{d}\ln a \, (aH)^{-1} \,. \tag{2.24}$$

During the standard cosmological expansion the increasing *comoving Hubble radius*, $(aH)^{-1}$, is therefore associated with an increasing *comoving horizon*[14], $\tau$, and the *fraction of the universe in causal contact increases with time*. However, the near-homogeneity of the CMB tells us that the universe was quasi-homogeneous at the

[14]This explains the common practice of often using the terms 'comoving Hubble radius' and 'comoving horizon' interchangeably. Although these terms should conceptually be clearly distinguished, this inaccurate use of language has become standard.

time of last scattering on a scale encompassing many regions that are a priori causally independent (see Figure 7). Why then is the CMB uniform on large scales (of order the present horizon)?

*Comment on Initial Conditions.* It should be emphasized that the flatness and horizon problems are *not* strict inconsistencies of the standard cosmological model. If one assumes that the initial value of $\Omega$ was extremely close to unity and that the universe began homogeneously (but with just the right level of inhomogeneity to explain structure formation) then the universe would have continued to evolve homogeneously in agreement with observations. The flatness and horizon problems are therefore just severe shortcomings in the predictive power of the Big Bang model. The dramatic flatness of the early universe cannot be predicted by the standard model, but must instead be assumed in the initial conditions. Likewise, the striking large-scale homogeneity of the universe is not explained or predicted by the model, but instead must simply be assumed. Inflation removes these assumptions about initial conditions.

**4.2. The Basic Idea of Inflation.** All the Big Bang puzzles are solved by a beautifully simple idea: '*invert the behavior of the comoving Hubble radius*' $(aH)^{-1}$ *i.e.* make it *decrease* sufficiently in the very early universe. A decreasing Hubble radius corresponds to *accelerated expansion*

$$\frac{\mathrm{d}}{\mathrm{d}t}(aH)^{-1} < 0 \qquad \Rightarrow \qquad \frac{\mathrm{d}^2 a}{\mathrm{d}t^2} > 0\,. \tag{2.25}$$

A flat universe then becomes an attractor solution (see Equation (2.22)) and the observed CMB sky was in causal contact in the past (see Figure 8). A period of acceleration in the early universe therefore very elegantly solves the problems with the standard Big Bang theory. However, it raises the question: What is the physics of inflation? Twenty-five years after inflation was introduced by Guth it remains a paradigm in search of a theory. From the second Friedmann equation (2.7) we see

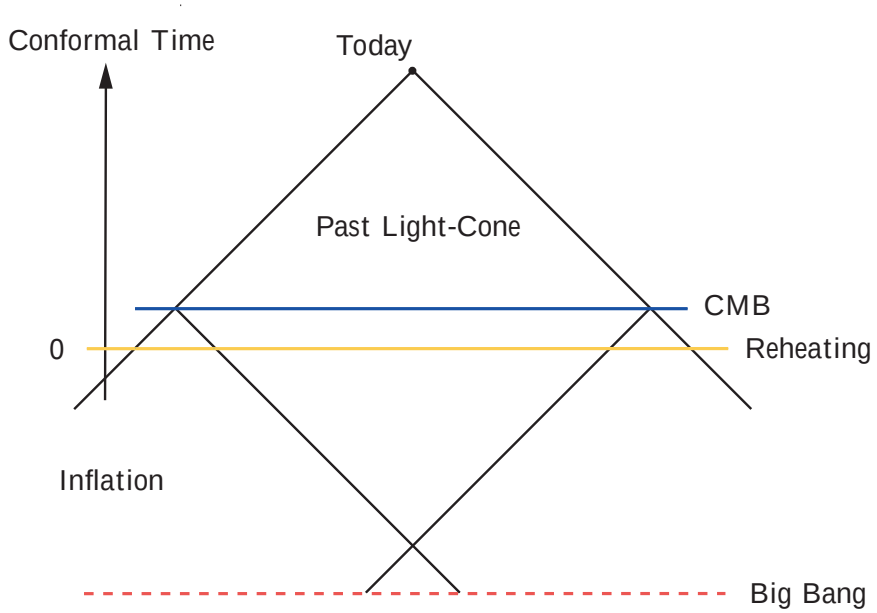


FIGURE 8. Conformal spacetime of the inflationary universe. The horizon problem is solved by extending conformal time to negative values. In inflationary cosmology the Big Bang is at $\tau = -\infty$, while without inflation it is at $\tau = 0$ (see Figure 7).

that accelerated inflationary expansion, like dark energy, requires a negative pressure component to dominate the universe

$$\frac{\mathrm{d}^2 a}{\mathrm{d}t^2} > 0 \qquad \Rightarrow \qquad \rho + 3p < 0\,. \tag{2.26}$$

Furthermore, the two Friedmann equations (2.6) and (2.7) may be combined into the continuity equation

$$\frac{\mathrm{d}\rho}{\mathrm{d}t} = -3H(\rho + p)\,. \tag{2.27}$$

During inflation $p \approx -\rho$, so the inflationary expansion requires that the early universe was dominated by a nearly constant energy density, $\dot{\rho} \approx 0$. This is unlike any physical phenomenon we are familiar with.

**4.3. Slow-Roll Inflation.** In the absence of a better theoretical understanding of inflation it is standard practice to parameterize our ignorance by a scalar field $\phi$ with potential $V(\phi)$ (see Figure 9). Consider therefore the scalar field Lagrangian

$$\mathcal{L} = -\frac{1}{2} g^{\mu\nu} \partial_\mu \phi \partial_\nu \phi - V(\phi) \,. \tag{2.28}$$

Computing the energy-momentum tensor associated with $\mathcal{L}$, we find that the homo-

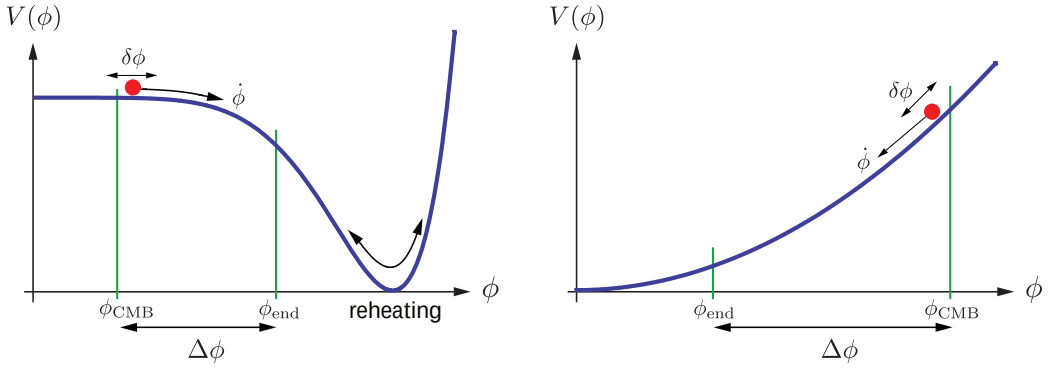


FIGURE 9. The Inflaton Potential. Acceleration occurs when the potential energy of the field $V$ dominates over its kinetic energy $\frac{1}{2}\dot\phi^2$. Inflation ends at $\phi_{\rm end}$ when the slow-roll conditions are violated, $\epsilon \to 1$. CMB fluctuations are created by quantum fluctuations $\delta\phi$ about 60 $e$-folds before the end of inflation. At reheating, the energy density of the inflaton is converted into radiation.
*Left*: A typical small-field potential. *Right*: A typical large-field potential.

geneous mode $\phi(t)$ acts like a perfect fluid with equation of state

$$w \equiv \frac{p}{\rho} = \frac{\frac{1}{2}\dot\phi^2 - V}{\frac{1}{2}\dot\phi^2 + V} \,. \tag{2.29}$$

The equation of motion of the inflaton field in an FRW background is the Klein-Gordon equation

$$\ddot\phi + 3H\dot\phi + V'(\phi) = 0 \,. \tag{2.30}$$

From equation (2.29) we see that accelerated expansion, $w < -\frac{1}{3}$, occurs when the potential energy density dominates over the kinetic energy, $V \gg \frac{1}{2}\dot\phi^2$. From the equation of motion (2.30) we further note that this condition is sustained if $\ddot\phi \ll V'$. These two conditions for prolonged inflation are summarized by restrictions on

the form of the inflaton potential $V(\phi)$ and its derivatives. Quantitatively, inflation requires smallness of the slow-roll parameters

$$\epsilon \equiv \frac{M_{\rm pl}^2}{2}\left(\frac{V'}{V}\right)^2, \tag{2.31}$$

$$\eta \equiv M_{\rm pl}^2\frac{V''}{V}. \tag{2.32}$$

The conditions for inflation, $\epsilon, |\eta| \ll 1$, constrain the shape of the inflaton potential. Whether and how naturally such flat potentials are achievable in string theory is an important open question which we will address in the bulk of this thesis.

**4.4. Quantum Origin of Structure.** So far we have only discussed the classical evolution of the inflaton field. Something remarkable happens when one considers quantum fluctuations of the inflaton: inflation combined with quantum mechanics provides an elegant mechanism for generating the initial seeds of all structure in the universe.

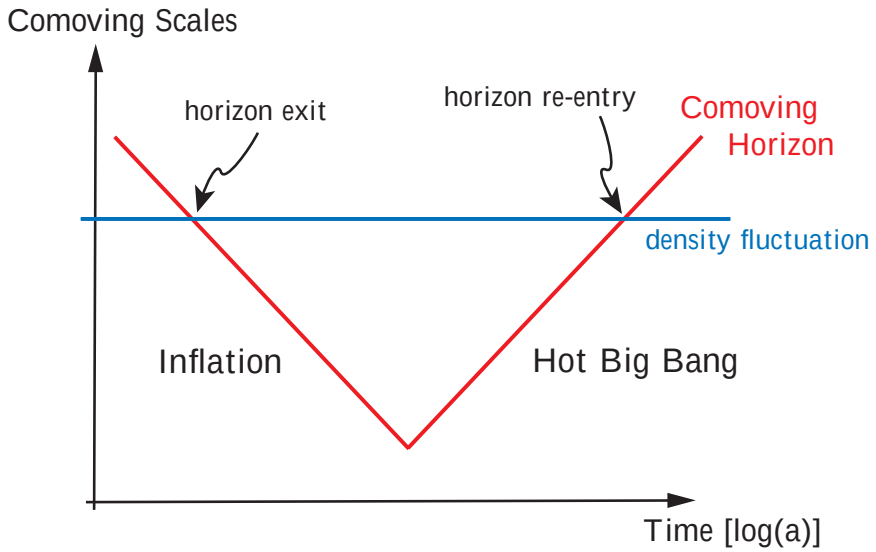


FIGURE 10. Creation and evolution of perturbations in the inflationary universe. Fluctuations are created quantum mechanically on sub-horizon scales. While comoving scales remain constant the comoving Hubble radius during inflation shrinks and the perturbations exit the horizon. Causal physics cannot act on superhorizon perturbations and they freeze until horizon re-entry at late times.

A very intuitive way of understanding how the quantum fluctuations of the inflaton field $\delta\phi(\mathbf{x})$ translate into density fluctuations $\delta\rho(\mathbf{x})$ is via the time-delay formalism developed by Guth and Pi [84].[15] The basic idea is that $\phi$ controls the time at which inflation ends (see Figure 9). Small quantum fluctuations in the value of the inflaton field $\delta\phi(\mathbf{x}) \sim H$ translate into differences in the end of inflation ($\epsilon \equiv 1$) for different regions of space $\delta t(\mathbf{x})$. Regions acquiring a negative frozen fluctuation $\delta\phi$ remain potential-dominated longer than regions where $\delta\phi$ is positive. Hence, fluctuations of the field $\phi$ lead to a local delay of the end of inflation

$$\delta t = \frac{\delta\phi}{\dot{\phi}} \sim \frac{H}{\dot{\phi}} \,. \tag{2.33}$$

For the field fluctuation we have used the result of the zero-point calculation in de Sitter space, $\delta\phi \sim H$. After reheating, the energy density evolves as $\rho = 3M_{\rm pl}^2 H^2$ where $H \sim t^{-1}$, so that

$$\frac{\delta\rho}{\rho} \sim 2\frac{\delta H}{H} \sim H\delta t \sim H\,\frac{H}{\dot{\phi}} \,. \tag{2.34}$$

This process therefore induces tiny density variations $\delta\rho$ which via gravitational instability grow to form the observed large-scale structure of the universe. In addition, quantum fluctuations during inflation excite tensor metric perturbations, $\delta g \sim \frac{H}{M_{\rm pl}}$. Future experiments hope to detect this stochastic background of gravitational waves from inflation.

[15] Strictly speaking the time-delay formalism is only valid when inflation is well-described by the de Sitter solution and the equation of state is nearly unchanging [158]. We refer the reader to Appendix A for an improved derivation of the inflationary perturbation spectra.

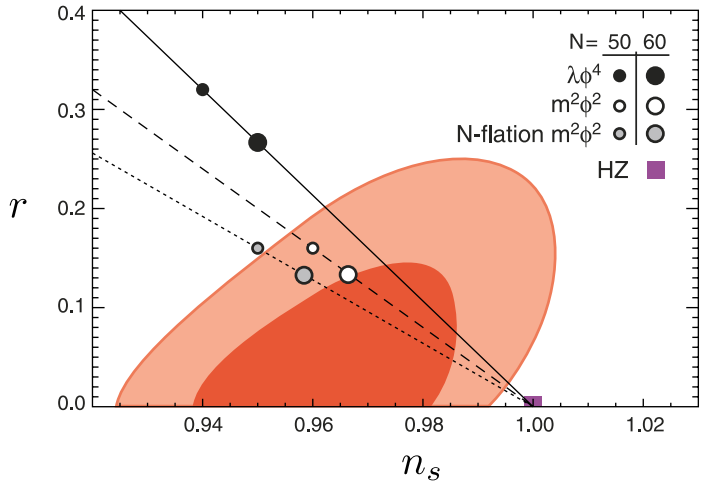


FIGURE 11. Constraints on inflationary models from recent cosmic microwave background and large-scale structure observations [151].

### 4.5. Cosmological Observables.

*Power Spectra.* The computation we just sketched gives the following results for primordial scalar and tensor power spectra (see Appendix A for details)

$$P_s = \left(\frac{H}{2\pi}\right)^2 \left(\frac{H}{\dot\phi}\right)^2 \approx \frac{1}{24\pi^2 M_{\rm pl}^4}\frac{V}{\epsilon} \tag{2.35}$$

$$P_t = \frac{2}{\pi^2}\left(\frac{H}{M_{\rm pl}}\right)^2 \approx \frac{2}{3\pi^2}\frac{V}{M_{\rm pl}^4}\,. \tag{2.36}$$

Here, the r.h.s. should be evaluated when the fluctuation mode freezes after crossing the horizon, $k = aH$, (see Figure 10) and the second equality made use of the slow-roll approximation. In a power law description, $P_s = A_s k^{n_s-1}$ and $P_t = A_t k^{n_t}$, the spectral indices in terms of the slow-roll parameters are

$$n_s - 1 = 2\eta - 6\epsilon\,, \tag{2.37}$$

$$n_t = -2\epsilon\,. \tag{2.38}$$

The deviation from scale-invariance ($n_s = 1, n_t = 0$) may be traced to a small time evolution of the Hubble parameter during inflation. From (2.35) and (2.36) we define

the tensor-to-scalar ratio

$$r = 16\epsilon\,. \tag{2.39}$$

Measurements of $n_s$ and $r$ are strong discriminators of inflationary models (see Figure 11).

*Inflationary Gravitational Waves.* Detection of a stochastic background of primordial gravitational waves is widely regarded as a 'smoking gun' signature of inflation. The best hope for detecting such a signal is via the subtle imprints they leave in the polarization of the CMB (B-modes).[16] It is important to make *pre*-dictions for the expected gravitational wave amplitude before the next generation of CMB polarization experiments comes online. In the context of string theory we discuss this challenge in Chapters 8, 9 and 10.

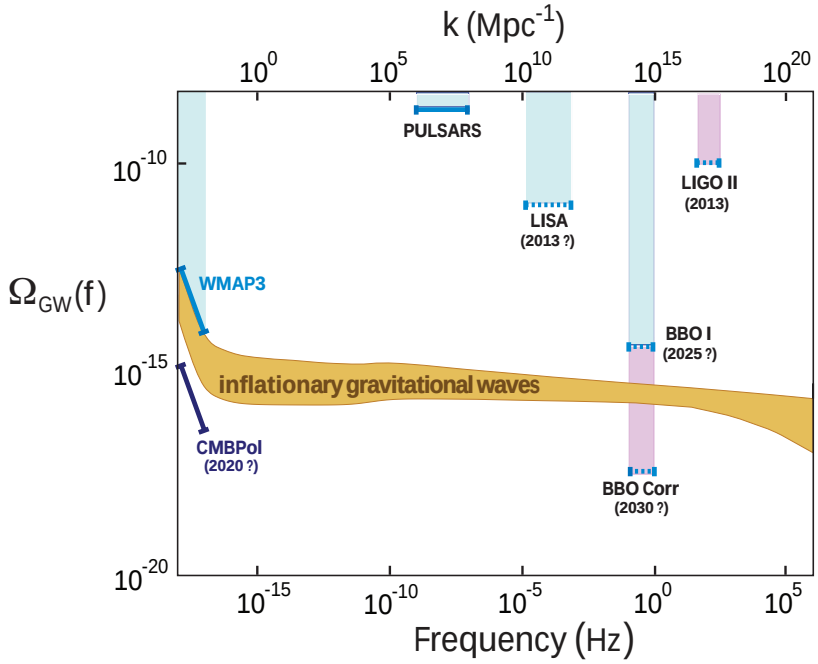


FIGURE 12. Current and future constraints on the inflationary gravitational wave background (Figure adapted from Boyle et al. [41]). Shown is the theoretical prediction for "minimally tuned" inflationary models as defined in [41].

[16] In the future it might also become feasible to measure inflationary gravitational waves at late times with direct-detection experiments like the Big Bang Observer (BBO) (see Figure 12)

A conservative estimate for the minimal gravitational wave amplitude that is accessible to future experiments is $r > 0.01$. Any signal that is much smaller than this will be very hard to extract from astrophysical foregrounds [150]. A detection of the primordial tensor-to-scalar ratio $r$ would be truly revolutionary, as $r$ encodes two crucial pieces of information about the inflationary era:

(1) *Energy scale of inflation*

The measured amplitude of scalar perturbations $P_s \approx 2.4 \times 10^{-9}$ implies a relation between the energy scale of inflation $V^{1/4}$ and the tensor-to-scalar ratio $r$

$$\boxed{V^{1/4} = 1.06 \times 10^{16}\,\mathrm{GeV}\left(\frac{r}{0.01}\right)^{1/4}}. \tag{2.40}$$

Detecting tensors ($r > 0.01$) would therefore imply that inflation occurred at very high energies.

(2) *Super-Planckian field variation*

There is a one-to-one correspondence between the tensor-to-scalar ratio $r$ and the evolution of the inflaton during inflation $\Delta\phi \equiv |\phi_{\mathrm{CMB}} - \phi_{\mathrm{end}}|$ [122] (see Figure 9 for a definition of $\Delta\phi$ and Chapter 8 for a derivation of the Lyth bound)

$$\boxed{\frac{\Delta\phi}{M_{\mathrm{pl}}} > \mathcal{O}(1)\left(\frac{r}{0.01}\right)^{1/2}}. \tag{2.41}$$

Observable gravitational waves ($r > 0.01$) therefore require super-Planckian field excursions $\Delta\phi > M_{\mathrm{pl}}$ while keeping the potential controllably flat. In Chapters 8 and 9 we discuss whether this is realizable in a consistent microscopic theory like string theory.

*Primordial Non-Gaussianity.* Gaussian fluctuations are completely described by their two-point correlation function (or the power spectrum). The primordial fluctuations created during slow-roll inflation are predicted to be highly Gaussian (see

Appendix A) and the CMB power spectrum therefore reveals most of their statistical properties. However, large non-Gaussianity can arise for non-minimal models with non-trivial kinetic terms and/or multiple fields. This non-Gaussianity is best extracted from the three-point function (or bi-spectrum)

$$\langle \Phi_{\mathbf{k}_1} \Phi_{\mathbf{k}_2} \Phi_{\mathbf{k}_3} \rangle = (2\pi)^3 \delta(\mathbf{k}_1 + \mathbf{k}_2 + \mathbf{k}_3) F(k_1, k_2, k_3) \,, \tag{2.42}$$

where the momentum dependence of the function $F$ contains important clues about the physics of inflation.

A simple way to characterize the non-Gaussianity of $\Phi$ is to assume that it can be parameterized by a field redefinition of the form

$$\Phi = \Phi_L + f_{\rm NL} \Phi_L^2 \,, \tag{2.43}$$

where $\Phi_L$ is Gaussian and the constant $f_{\rm NL}$ measures the amount of non-Gaussianity of $\Phi$. Equation (2.43) is often called *local* non-Gaussianity. For single-field slow-roll inflation $f_{\rm NL} < 1$ (see Appendix A). Since it is generally believed that non-Gaussianity is only observable if $f_{\rm NL} \gtrsim 1$, we conclude that primordial non-Gaussianities from slow-roll inflation are unobservable. However, the non-Gaussianity can easily be one or two orders of magnitude bigger in non-minimal models of inflation. The search for primordial non-Gaussianity is therefore an important aspect of the experimental efforts to test the physics of inflation.

**4.6. What is the Physics of Inflation?** Understanding the (micro)physics of inflation remains one of the most important open problems in modern cosmology and theoretical physics. Explicit particle physics models of inflation remain elusive, so that a natural microscopic explanation for inflation has yet to be uncovered.[17] Nevertheless, there have recently been interesting efforts to derive inflation from string theory. The search for inflationary solutions in string compactifications will be the main focus of this thesis.

[17]At this point it should be emphasized that the inflationary era in the early universe is an *unproven hypothesis*. It is therefore important to keep an open mind about creative alternative solutions to the horizon and flatness problems and the generation of cosmological perturbations. The most interesting proposals to date are the ekpyrotic/cyclic scenarios [43, 100, 154]. In these models a period of slow contraction before the Big Bang expanding phase replaces inflation.

CHAPTER 3

# Elements of String Compactifications

In this chapter we review fundamental aspects of string compactifications. The formal developments described here form the basis for modern studies of string cosmology. We make no attempt at a complete and/or pedagogical introduction to string theory. For a more thorough treatment of this vast and rapidly evolving subject the reader may be referred to [27, 79, 138, 164].

After describing the moduli problem in §1 we present flux compactifications and the KKLT scenario in §2 and §3, respectively. These constructions fix all moduli and allow metastable de Sitter solutions. In addition, compactifications with fluxes generically have warped regions whose local geometry we review in §4.

## 1. The Moduli-Stabilization Problem

Low energy effective actions arising from string theory typically contain many scalar fields collectively called *moduli*. In particular, the compact manifolds satisfying the string equations of motion generally come in continuous families whose parameters (controlling the size and shape of the extra dimensions) become scalar fields in the four-dimensional effective theory. Compactifications containing branes have additional moduli that parameterize their relative positions and orientations. Finally, any string compactification always contains the massless dilaton field.

Before considering potentials arising from fluxes and non-perturbative effects, these string moduli fields are massless and their couplings are of gravitational

strength. the existence of these fields therefore raises generic cosmological problems – The late time evolution of moduli fields affects low energy observables like the couplings of the Standard Model, Newton's gravitational constant, and the fine-structure constant. In addition, light moduli fields can lead to fifth force-type violations of the equivalence principle. All of these effects are strongly constrained by experiments. The presence of light moduli fields may also lead to problems in the early universe: *e.g.* successful Big Bang nucleosythesis (BBN) requires a moduli mass $m_\chi$ in excess of 30 TeV. If $m_\chi \lesssim 100$ MeV then the energy stored in the moduli fields overcloses the universe while if 100 MeV $\lesssim m_\chi \lesssim$ 30 TeV then the moduli decay dilutes the BBN products [110]. Phenomenologically viable models of particle physics and cosmology therefore require a solution to the moduli-stabilization problem.

## 2. Flux Compactification

The moduli-stabilization problem has been solved only recently in the context of flux compactifications of type IIB string theory [76], [82], [93]. Here we summarize the basic elements of this program. For more details we refer the reader to the review by Douglas and Kachru [63] or the recent Les Houches lectures by Denef [57].

**2.1. Basic Ingredients.** The basic ingredients of type IIB flux compactifications are fluxes, branes and warped extra dimensions. The type IIB limit of string theory contains D3-, D5-, and D7-branes as well as O(rientifold)-planes. The action for a Dp-brane is the sum of a Dirac-Born-Infeld (DBI) term and a Chern-Simons (CS)-term [139]

$$S_{Dp} = S_{\rm DBI} + S_{\rm CS}\,. \tag{3.1}$$

The DBI action describes the worldvolume of the brane which in string frame is[1]

$$S_{\rm DBI} = -T_p \int {\rm d}^{p+1}\xi\, e^{-\Phi}\sqrt{-\det(G_{AB})}\,. \tag{3.2}$$

[1]This result is to leading order in $\alpha'$ and for the case of vanishing worldvolume field strength.

Here, $T_p = (2\pi)^{-p} g_s^{-1} (\alpha')^{-(p+1)/2}$ is the D-brane tension in terms of the string coupling $g_s$ and the fundamental string length $\sqrt{\alpha'}$. The field $\Phi$ is the dilaton and $G_{AB}$ is the pullback of the metric onto the brane worldvolume. The Chern-Simons-term[2] describes the electric coupling of a Dp-brane to the R-R $(p+1)$-form $C_{p+1}$

$$S_{\rm CS} = \mu_p \int C_{p+1}\,, \qquad |\mu_p| = T_p e^{-(p-3)\Phi/4}\,. \tag{3.3}$$

Branes are therefore sources for form-field fluxes $F_{p+2} = {\rm d}C_{p+1}$. The total flux of these fields through topologically non-trivial surfaces in the extra dimensions is quantized, *e.g.*

$$\frac{1}{(2\pi)^2\alpha'}\int_A F_3 = M\,, \qquad \frac{1}{(2\pi)^2\alpha'}\int_B H_3 = -K\,, \tag{3.4}$$

where $A$ and $B$ are 3-cycles of the compact manifold, $F_3 = {\rm d}C_2$ and $H_3 = {\rm d}B_2$ are 3-form fluxes and $M$ and $K$ are integers.

Finally, the presence of branes and fluxes sources locally warped spacetime regions,

$${\rm d}s^2 = h^{1/2}(y)\underbrace{g_{\mu\nu}{\rm d}x^\mu{\rm d}x^\nu}_{4D} + h^{-1/2}(y)\underbrace{g_{ij}{\rm d}y^i{\rm d}y^j}_{6D}\,. \tag{3.5}$$

These regions are important backgrounds for quantitative studies of string cosmology (see §4 and Chapter 4).

**2.2. Moduli Potential.** In the following we provide a lightning review of the four-dimensional low-energy effective description of the KKLT proposal. We work in the limit of $\mathcal{N}=1$ supergravity, where the moduli potential $V_F$ is characterized by a superpotential $W$ and a Kähler potential $\mathcal{K}$

$$V_F = e^{\mathcal{K}/M_{\rm pl}^2}\left[\mathcal{K}^{i\bar{j}} D_i W \overline{D_j W} - \frac{3}{M_{\rm pl}^2}|W|^2\right]\,, \tag{3.6}$$

where $D_i W \equiv \partial_i W + \frac{1}{M_{\rm pl}^2}(\partial_i \mathcal{K})W$ and $\mathcal{K}_{i\bar{j}} \equiv \partial_i \partial_{\bar{j}} \mathcal{K}$. The compactification typically contains 3-form flux $G_3 \equiv F_3 - \tau H_3$ which contributes to the superpotential via the

[2]More general forms of the Chern-Simons term may be found in [139].

Gukov-Vafa-Witten (GVW) term [82]

$$W_{\rm flux} = \int G_3 \wedge \Omega \,, \tag{3.7}$$

where $\Omega$ denotes the holomorphic three-form on the Calabi-Yau three-fold and $\tau \equiv C_0 + ie^{-\Phi}$ is the axio-dilaton. The Kähler potential for the complex structure moduli and the dilaton is

$$\mathcal{K} = -M_{\rm pl}^2 \ln \left[ \int \Omega \wedge \bar{\Omega} \right] - M_{\rm pl}^2 \ln[\tau + \bar{\tau}] \,. \tag{3.8}$$

Turning on generic $G_3$-flux induces a potential $V_F$ that usually fixes all the complex structure moduli ($\chi_\alpha$) and the dilaton ($\tau$) [76]. The potential (3.6) is minimized for $D_{\chi_\alpha} W_{\rm flux} = D_\tau W_{\rm flux} = 0$.

## 3. De Sitter Vacua in String Theory

**3.1. Non-perturbative Effects.** The (classical) flux background fixes the *shape* (complex structure moduli) of the extra dimensions, but leaves the overall *size* (Kähler moduli $\rho$) unfixed [76] (see Figure 1). Recently, Kachru, Kallosh, Linde and Trivedi (KKLT) [93] provided a framework for stabilizing the overall size of the compact manifold by including non-perturbative (quantum) effects *e.g.* gaugino condensation on D7-branes or Euclidean D3-instantons. These effects are parameterized by the following superpotential

$$W_{\rm np} = A e^{-a\rho} \,, \tag{3.9}$$

for $a$ constant. With $\mathcal{K} = -3M_{\rm pl}^2 \ln[\rho + \bar{\rho}]$ the F-term potential (3.6) then leads to supersymmetric anti-de Sitter (SUSY AdS) vacua, $D_\rho W = D_\rho(W_{\rm flux} + W_{\rm np}) = 0$, with stabilized Kähler modulus. The compactification is stabilized at large volume, $\rho_\star \gg 1$, iff the flux superpotential is a small negative constant $W_{\rm flux}(\chi_\alpha^\star, \tau^\star) \equiv W_0 \sim -10^{-4}$ (in units where $M_{\rm pl} \equiv 1$).

**3.2. de Sitter Space.** Having negative cosmological constant, these solutions cannot yet describe our universe, $V_F = -\frac{3}{M_{\rm pl}^2}|W|^2 e^{\mathcal{K}/M_{\rm pl}^2}$. KKLT therefore uplifted the AdS minima to positive energies by adding anti-D3-branes. This 'D-term' uplifting adds the following term to the moduli potential

$$V_D = \frac{D}{(\rho+\bar{\rho})^2}\,, \tag{3.10}$$

where $D$ is a constant that depends on the D3-brane tension and the warping of the background. The final potential for the volume modulus $\sigma \equiv \mathrm{Re}(\rho)$ is shown in Figure 1

$$V(\sigma) = \frac{aA}{2M_{\rm pl}^2}\frac{e^{-a\sigma}}{\sigma^2}\left(\frac{1}{3}a\sigma A e^{-a\sigma} + W_0 + A e^{-a\sigma}\right) + \frac{1}{4}\frac{D}{\sigma^2}\,. \tag{3.11}$$

Notice that the de Sitter minimum is *metastable*. The magnitude of the cosmological

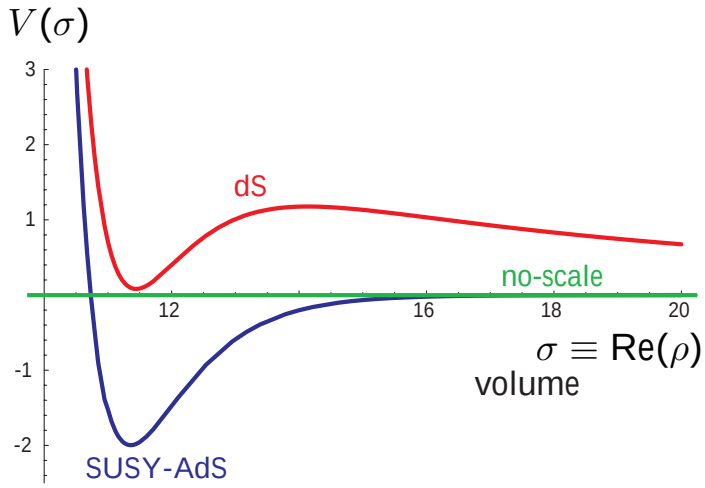


FIGURE 1. KKLT compactification: Potential for the volume modulus $\sigma = \mathrm{Re}(\rho)$. Fluxes fix the complex structure and the dilaton field, but leave the overall volume modulus unfixed (green curve). Non-perturbative effects stabilize the volume in a supersymmetric minimum with negative cosmological constant (blue curve). Anti-D3 branes provide the uplifting energy to a metastable de Sitter minimum (red curve).

constant associated with the minimum depends on the choice of flux quanta (3.4) and is therefore tunable. The discretuum of vacua in type IIB flux compactifications has been employed for an anthropic solution to the cosmological constant problem [39].

## 4. Klebanov-Strassler Geometry

The moduli spaces of compact Calabi-Yau spaces generically contain conifold singularities. The local description of these singularities is called the *conifold*, a non-compact Calabi-Yau three-fold whose geometry is given by a cone. In contrast to general Calabi-Yau backgrounds the metric data for the conifold is explicitly known. This makes these backgrounds very interesting for detailed studies of string cosmology and particle phenomenology.

In this section we cite basic geometrical facts about the conifold (for more details we refer the reader to the recent Les Houches lectures by Benna and Klebanov [29]).

**4.1. Singular Conifold.** The *(singular) conifold* is defined by the complex equation

$$\sum_{i=1}^{4} z_i^2 = 0\,, \qquad z_i \in \mathbb{C}\,. \tag{3.12}$$

The constraint equation (3.12) describes a cone over $X_5 = S^2 \times S^3$. To see this note that if $z^i$ is a solution to (3.12) then so is $\lambda z^i$ with $\lambda \in \mathbb{C}$. Also, letting $z^i \equiv x^i + iy^i$, the complex equation (3.12) may be recast into three real equations

$$\vec{x}\cdot\vec{x} = \frac{1}{2}\rho^2\,, \qquad \vec{y}\cdot\vec{y} = \frac{1}{2}\rho^2\,, \qquad \vec{x}\cdot\vec{y} = 0\,. \tag{3.13}$$

The first equation defines a 3-sphere $S^3$ with radius $\rho/\sqrt{2}$.[3] The last two equations then describe a 2-sphere $S^2$ fibred over the $S^3$. The Calabi-Yau metric on the conifold is

$$\mathrm{d}s_6^2 = \mathrm{d}r^2 + r^2 \mathrm{d}s_{T^{1,1}}^2\,, \tag{3.14}$$

if we define the radial coordinate $r \equiv \sqrt{3/2}\rho^{2/3}$ or $r^3 \equiv \sum_{i=1}^4 |z_i|^2$.

[3]Here, the variable $\rho$ is of course not to be confused with the Kähler modulus introduced in §3.

The base of the cone is the $T^{1,1}$ coset space $[SU(2)_A \times SU(2)_B]/U(1)_R$ which has the topology $S^2 \times S^3$. The metric of $T^{1,1}$ in angular coordinates $\theta_i \in [0, \pi]$, $\phi_i \in [0, 2\pi]$, $\psi \in [0, 4\pi]$ is

$$\mathrm{d}s^2_{T^{1,1}} = \frac{1}{6}\Big(\mathrm{d}\psi + \sum_{i=1}^{2} \cos\theta_i \mathrm{d}\phi_i\Big)^2 + \frac{1}{6}\sum_{i=1}^{2}(\mathrm{d}\theta_i^2 + \sin^2\theta_i \mathrm{d}\phi_i^2)\,. \tag{3.15}$$

**4.2. Deformed Conifold.** The space defined by (3.12) is singular at the tip of the cone, $r = 0$. Various prescriptions exist for removing this singularity – *e.g.* consider the *deformed conifold* defined by

$$\sum_{i=1}^{4} z_i^2 = \varepsilon^2\,, \tag{3.16}$$

where $\varepsilon \in \mathbb{C}$. By a phase rotation of the $z_i$ coordinates we can always choose $\varepsilon \in \mathbb{R}^+$. This defines a one-dimensional moduli space. For large $r$ the deformed conifold geometry reduces to the singular conifold with $\varepsilon = 0$. Moving from large $r$ towards the origin, the sizes of the $S^2$ and the $S^3$ both decrease. Decomposing the $z_i$ into real and imaginary parts we now find

$$\varepsilon^2 = \vec{x}\cdot\vec{x} - \vec{y}\cdot\vec{y}\,, \tag{3.17}$$

and

$$\rho^2 = \vec{x}\cdot\vec{x} + \vec{y}\cdot\vec{y}\,. \tag{3.18}$$

This shows that the range of $\rho$ (or $r$) is limited by

$$\varepsilon^2 \leq \rho^2 < \infty \tag{3.19}$$

and the singularity at $r = 0$ is avoided for $\varepsilon^2 > 0$. It also shows that as $\rho^2 \to \varepsilon^2$ the $S^2$ disappears ($\vec{y}\cdot\vec{y} \to 0$) leaving just an $S^3$ with finite radius.

**4.3. Warped Throat.** A stack of $N$ D3-branes placed at the singularity $z_i = 0$ backreacts on the geometry, producing a warped background with the following ten-dimensional line element

$$\mathrm{d}s^2 = h^{1/2}(z) g_{\mu\nu} \mathrm{d}x^\mu \mathrm{d}x^\nu + h^{-1/2}(z) g_{i\bar{\jmath}} \mathrm{d}z^i \mathrm{d}z^{\bar{\jmath}} \,, \tag{3.20}$$

where $g_{i\bar{\jmath}}$ is the metric (3.14) and the warp factor is

$$h(r) = \frac{R^4}{r^4} \,, \qquad R^4 \equiv \frac{27\pi}{4} g_s N (\alpha')^2 \,. \tag{3.21}$$

This AdS background is an explicit realization of the Randall-Sundrum scenario [140, 141] in string theory. In the spirit of AdS/CFT [124] the $AdS_5 \times T^{1,1}$ geometry (3.20) has a dual gauge theory interpretation. The dual $\mathcal{N} = 1$ supersymmetric conformal gauge theory was constructed in [107]. It is an $SU(N) \times SU(N)$ gauge theory coupled to bifundamental chiral superfields. If one further adds $M$ D5-branes wrapped over the $S^2$ inside $T^{1,1}$, then the gauge group becomes $SU(N + M) \times SU(N)$, giving a cascading gauge theory [105, 106]. The three-form flux induced by the wrapped D5-branes (fractional D3-branes) satisfies

$$\frac{1}{(2\pi)^2 \alpha'} \int_{S^3} F_3 = M \,. \tag{3.22}$$

The warp factor $h(r)$ for this case was found by Klebanov and Strassler (KS) [105]. For large $r$ it is [106]

$$h(r) = \frac{27\pi(\alpha')^2}{4r^4} \left[ g_s N + \frac{3}{2\pi} (g_s M)^2 \ln\Big(\frac{r}{r_0}\Big) + \frac{3}{8\pi} (g_s M)^2 \right] , \tag{3.23}$$

where $r_0 \sim \varepsilon^{2/3} e^{2\pi N/(3 g_s M)}$.

The Klebanov-Strassler warped conifold background (also refered to as the *warped throat*) is the basis for our explicit studies of warped D-brane inflation.

CHAPTER 4

# Inflation in String Theory

Understanding the physics of inflation is one of the main challenges of fundamental physics and modern cosmology. Since string theory remains the most promising candidate for a UV-completion of the Standard Model that unifies gauge and gravitational interactions in a consistent quantum theory, it seems natural to search within string theory for an explicit realization of the inflationary scenario. This search has so far revealed two distinct classes of inflationary models which identify the inflaton field with either open string modes (*e.g.* brane inflation [64, 95], DBI inflation [4, 147], assisted M5-brane inflation [26], D3/D7 inflation [56], wrapped brane inflation [148]), or closed string modes (*e.g.* Kähler moduli inflation [54], racetrack inflation [35, 36], N-flation [61, 67]). In this chapter we review these theoretical developments.

We begin in §1 with general remarks about the promise of studying UV-physics in string theory models of inflation. In §2 we review warped brane inflation with particular emphasis on the eta-problem [95] and the DBI mechanism [147]. In §3 we provide a brief survey of other models of string inflation. We describe their prospects and problems. Finally, in §4 we explain the ambitious goal of deriving inflationary models from explicit string compactifications.

For more details on these and related aspects of inflation in string theory we refer the reader to the excellent review by McAllister and Silverstein [128] or the upcoming review by Liam McAllister and myself [22].

## 1. UV Challenges/Opportunities

We first make some preliminary remarks on the promise of studying inflation in the context of string theory. Specifically, we will emphasize three problems in inflationary cosmology that benefit most directly from the application of a UV-complete theory.[1]

**1.1. $V(\phi)$ and the Eta–Problem.** As the rest of this thesis will illustrate with the example of brane inflation, the main challenge in string inflation is *not* to find a flat potential, but to prove that it is *the* potential. After a modulus field with (naively) flat potential has been identified, the challenge is to prove that the delicate flatness of the potential is protected against corrections. More specifically, consider an inflation model with some potential $V(\phi)$. A robust model requires understanding gravity corrections up to (at least) dimension six

$$\delta V \sim \frac{V}{M_{\rm pl}^2}\phi^2 \,. \tag{4.1}$$

These terms can induce $\mathcal{O}(H)$ corrections to the inflaton mass, which shift the inflationary eta parameter by order unity

$$\Delta\eta \sim \mathcal{O}(1) \,. \tag{4.2}$$

For a controllable model one needs to demonstrate explicitly that these dangerous terms are absent, suppressed or cancel. This requires some knowledge of Planck scale physics or quantum gravity.

**1.2. Gravitational Waves.** The Lyth bound [122] shows that observable tensors ($r > 0.01$, say) require super-Planckian field excursions during inflation,

$$\Delta\phi > M_{\rm pl} \,. \tag{4.3}$$

[1]The following remarks are inspired by discussions with Shamit Kachru, Eva Silverstein and Liam McAllister.

An effective field theory (EFT) description of inflation integrates out all heavy fields above a cutoff $M$ and only retains the light inflaton degree of freedom. It is argued (*e.g.* [123]) that this procedure generically gives a tree-level potential of the following form

$$V(\phi) = V_0 + \frac{1}{2}m^2\phi^2 + \frac{1}{4}\lambda\phi^4 + \phi^4\sum_{n=1}^{4}\lambda_n\Big(\frac{\phi}{M}\Big)^n\,. \tag{4.4}$$

Here we have separated the potential in a renormalizable part and an infinite series of irrelevant terms which are supressed by the cut-off scale $M$. Since it is usually assumed that $\lambda_n \sim \mathcal{O}(1)$ and $M \lesssim M_{\rm pl}$, this suggests a breakdown of the EFT for $\phi > M_{\rm pl}$. Of course, this argument does not prove the impossibility of super-Planckian vevs, but it suggests that capturing the dynamics over a super-Planckian range requires going beyond EFT. Whether large-field models of inflation are under (microphysical) theoretical control can therefore be addressed unambiguously only in a UV-complete theory such as string theory.

**1.3. Non-Gaussianity.** In single-field slow-roll models of inflation the primordial fluctuations are very nearly Gaussian with the amount of non-Gaussianity suppressed by powers of the slow-roll parameters [125]. To obtain observable non-Gaussianity during inflation requires extensions of the simplest models by including multiple fields and/or non-trivial kinetic effects. In single-field models with higher-derivative corrections to the canonical kinetic term the non-Gaussianity can be large if and only if these operators are important to the inflationary background dynamics [55]. From an effective field theory point of view this means living dangerously close to the limit of control with a large number of higher-derivative corrections all being simultaneously important. Such models therefore cry for UV-completion. String theory has recently provided a number of interesting realizations for such models, *e.g.* DBI inflation [147] (see §2).

## 2. Warped D-brane Inflation

**2.1. Setup.** Warped D-brane inflation is arguably the most developed inflationary scenario in string theory. In this setup inflation is described by the motion of a D3-brane in a warped background (like the Klebanov-Strassler throat [105] introduced in the previous chapter). The D3-brane fills four-dimensional spacetime and is pointlike in the compact extra dimensions (see Figure 1). The position of the brane in the extra dimensions serves as the inflaton field.

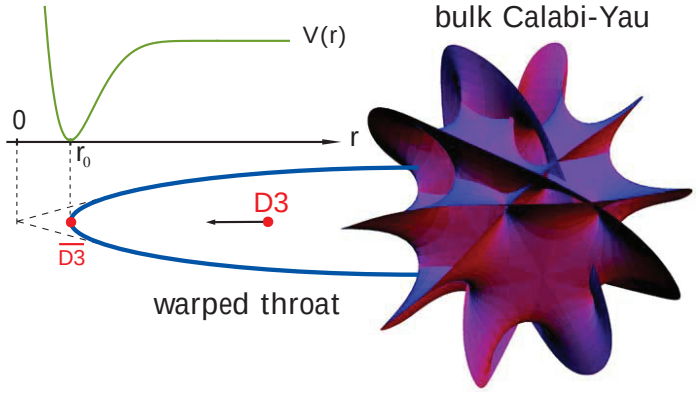


FIGURE 1. The KKLMMT Scenario. The 3-branes are spacetime-filling and therefore pointlike in the extra dimensions. The net force on the D3-brane is associated with the inflaton potential.

The kinetic term for the motion of the brane arises from the Dirac-Born-Infeld (DBI) action (3.2) in the background (3.20)

$$\mathcal{L}_{\rm DBI} = -f^{-1}(\phi)\sqrt{1-2f(\phi)X} + f^{-1}(\phi)\,. \tag{4.5}$$

Here, $X \equiv -\frac{1}{2}g^{\mu\nu}\partial_\mu\phi\partial_\nu\phi$, where $\phi^2 = T_3 r^2$ parameterizes the inflaton field, and $f^{-1} = T_3 h^{-1}$ is the warped tension of the brane. In the slow-roll limit ($fX \ll 1$) we recover the familiar canonical kinetic term $\mathcal{L}_{\rm DBI} \approx X$.

The original brane inflation proposal by Dvali and Tye [64] considered a brane-antibrane pair in an unwarped background (*e.g.* a torus). The brane then feels a Coulomb-like force from the anti-brane that acts as a potential for the inflaton. However, in the scenario of Dvali and Tye this force is too strong to allow slow-roll

inflation. In addition, the moduli stabilization problem had not been addressed. Kachru, Kallosh, Linde, Maldacena, McAllister and Trivedi (KKLMMT) made the important observation that a brane in a *warped* background feels a much weaker force. Warping suppresses the brane-antibrane force sufficiently to make slow-roll possible. In addition, KKLMMT showed how to embed the model into a concrete KKLT compactification with fixed moduli. However, in the process they discovered that compactification effects add correction terms to the potential that generically spoil slow-roll.

**2.2. The Eta–Problem.** Consider a KKLT compactification with an additional mobile D3-brane. As argued by Ganor [71], the non-perturbative superpotential (3.9) now depends on the D3-brane position $\phi \propto r$

$$W_{\rm np} = A(\phi) e^{-a\rho} \,. \tag{4.6}$$

At this point $A(\phi)$ is an unknown function. The Kähler potential in such a setup was given by DeWolfe and Giddings [58]

$$\mathcal{K} = -3M_{\rm pl}^2 \ln[\rho + \bar{\rho} - k(\phi, \bar{\phi})] \equiv -3M_{\rm pl}^2 \ln U(\rho, \phi) \,, \tag{4.7}$$

where $k(\phi, \bar{\phi}) \approx \phi\bar{\phi}$ is the Kähler potential on the moduli space of the D3-brane (*e.g.* a warped throat region). The inflaton potential may then be computed from the F- and D-term potentials

$$V(\phi) = V_F(\phi) + V_D(\phi) \,. \tag{4.8}$$

Here, $V_F(\phi)$ is the moduli potential (3.6) and $V_D(\phi) = DU^{-2}$ parameterizes the the energy of the brane-antibrane pair (see (3.10)). To arrive at a single field potential for $\phi$ the volume modulus $\rho$ has been integrated out. The slow-roll eta parameter corresponding to (4.8) is

$$\eta = \frac{2}{3} + \Delta\eta(\phi) \,, \tag{4.9}$$

where $\Delta\eta(\phi)$ has isolated the terms that arise from the dependence of the superpotential on $\phi$ (4.6) . Notice that if $A = constant$ then $\eta = \frac{2}{3}$ and inflation is impossible. However, we know that it is inconsistent to assume that $A$ is a pure constant independent of the brane position $\phi$. KKLMMT therefore expressed the hope that the functional form of $A(\phi)$ would be such that it allowed a fine-tuned cancellation of the $\frac{2}{3}$ in (4.9). Since at the time the function $A(\phi)$ was not known, this expectation remained only a hope that had to be checked against an explicit computation. In other words, to assess the true status of warped D-brane inflation one needed to compute $A(\phi)$ (Chapter 5) and determine $\Delta\eta(\phi)$ (Chapters 6 and 7). The first computation of $A(\phi)$ [18] is one of the main results of this thesis. We find that inflation is harder to achieve than was generally assumed.

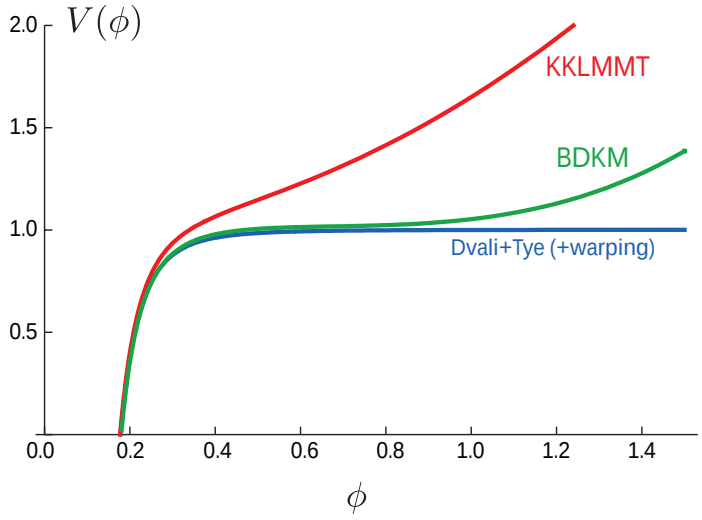


FIGURE 2. Computations of the brane potential.
a) Dvali+Tye (+warping) [64, 95]: $V_{\rm Coulomb}(\phi) = V_0(1 - c\phi^{-4})$.
b) KKLMMT [95]: $V_{\rm KKLMMT}(\phi) = V_{\rm Coulomb}(\phi) + \beta\phi^2$.
c) BDKM [19]: $V_{\rm BDKM}(\phi) = V_{\rm Coulomb}(\phi) + \lambda_1(\phi - \phi_0) + \lambda_3(\phi - \phi_0)^3$.

**2.3. Physical Interpretation of the Brane Potential.** We digress briefly to give a more physical interpretation of the different contributions to the brane potential (see Figure 2). A brane experiences (at least) three forces in a KKLT background:

(1) *Coulomb interaction with the anti-D3:*

The Coulomb-like interaction between the brane-antibrane pair may be understood as follows: The energy density of the branes perturbs the warp factor of the background geometry. Schematically, the perturbation $\delta h_i$ satisfies the following equation of motion

$$\nabla^2 \delta h_i = \mathcal{C}\, \delta(r - r_i) \qquad \Rightarrow \qquad \delta h_i \propto \frac{1}{|r - r_i|^4}\,, \tag{4.10}$$

where $r_i$ parameterizes the positions of the D3-brane and the anti-D3-brane. The D3-brane hence feels a $1/r^4$ force from the perturbed geometry sourced by the anti-brane. The force is suppressed by warping and gives a negligible contribution to the inflationary $\eta$-parameter.

(2) *D3-brane backreaction on the volume:*

Similarly, the D3-brane energy backreacts on the overall compactification volume, so that the physical volume becomes dependent on the brane position $\mathcal{V}(r)$. Since powers of the volume appear in the rescaling of the action from string frame to Einstein frame[2]

$$\mathcal{L}_{\text{Einstein}} = \frac{1}{\mathcal{V}^n(r)} \mathcal{L}_{\text{string}}\,, \qquad n \in \mathbb{Z}\,, \tag{4.11}$$

this gravitational interaction between the D3-brane and the compact space induces a force on the D3-brane (first computed by KKLMMT [95]). This is the physical origin of the $\frac{2}{3}$-term in equation (4.9).

[2]Strictly speaking, only a breathing mode appears in the dimensional reduction (see Appendix F).

(3) *D3/D7 interaction:*

In a KKLT compactification the overall volume is stabilized by non-perturbative effects on wrapped D7-branes. One therefore is obliged to include the force between the D3-brane and the D7-branes. The effect can be small if the D7-branes are far from the throat region (in which case inflation will be impossible) or it can be large if the D7-branes are in or near the throat. In the hope of deriving inflationary solutions, we therefore consider D7-branes wrapping a 4-cycle reaching into the throat. The presence of the D3-brane changes the (warped) volume of the 4-cycle. A change in the 4-cycle volume in turn changes the effective gauge coupling on the D7-brane world-volume, $g(r)$, and hence modifies the strength of the non-perturbative effect in a way that depends on the location of the D3-brane, $W_{\rm np} \propto \exp(1/g^2(r))$ (see (4.6)). This induces a force on the mobile D3-brane (first computed by BDKMMM [18]; Chapter 5). We discuss the D3/D7 interaction in more detail in the bulk of this thesis. It produces the $\Delta\eta(\phi)$-contribution in (4.9).

**2.4. DBI Inflation.** Silverstein and Tong [147] recently proposed an interesting mechanism that potentially obviates the eta-problem of slow-roll brane inflation. Their model (called DBI inflation) is driven by non-linear kinetic effects exhibited by the action (4.5) and does not rely on the delicate flatness of the inflaton potential.

While slow-roll brane inflation corresponds to non-relativistic brane motion, the non-linearities of the DBI action become important in the relativistic limit. The relativistic limit of brane motion in a warped background may be characterized by the parameter $\gamma$ (defined in analogy to the Lorentz factor of relativistic particle dynamics)[3]

$$\gamma \equiv \frac{1}{\sqrt{1 - f(\phi)\dot{\phi}^2}}\,. \tag{4.12}$$

[3]For simplicity we here restrict the discussion to the homogeneous mode $\phi(t)$.

Positivity of the argument of the square-root in (4.12) imposes a local speed limit on the brane motion, $\dot{\phi}^2 \leq f^{-1}(\phi) = T_3 h^{-1}(\phi)$ (in units where $c = 1$). The presence of strong warping in the throat, $h^{-1} \ll 1$, can make this maximal speed of the brane much smaller than the speed of light. The parameter $\gamma$ is large when $\dot{\phi}$ is close to this speed limit.

From the inflaton action $\mathcal{L} = \mathcal{L}_{\rm DBI} - V$ we find the homogeneous energy density in the field

$$\rho = 2X\mathcal{L}_{,X} - \mathcal{L} = (\gamma - 1)f^{-1} + V\,, \tag{4.13}$$

while the pressure is

$$p = \mathcal{L} = (1 - \gamma^{-1})f^{-1} - V\,. \tag{4.14}$$

The energy and pressure of the inflaton source the dynamics of the homogeneous background spacetime, $\mathrm{d}s^2 = -\mathrm{d}t^2 + a(t)^2\mathrm{d}\mathbf{x}^2$, as described by the Friedmann equations

$$3M_{\rm pl}^2 H^2 = \rho\,, \qquad 2M_{\rm pl}^2 \dot{H} = -(\rho + p)\,. \tag{4.15}$$

Inflation requires that the variation of the Hubble parameter $H$ is small

$$\epsilon \equiv -\frac{\dot{H}}{H^2} = \frac{3}{2}(1 + w) < 1\,, \tag{4.16}$$

where

$$w \equiv \frac{p}{\rho} = \frac{(1 - \gamma^{-1})f^{-1} - V}{(\gamma - 1)f^{-1} + V}\,. \tag{4.17}$$

From the expression for the equation of state parameter (4.17) we see that although the brane moves relativistically in the DBI limit, $\gamma \gg 1$, inflation still requires that the potential energy $V$ dominates over the kinetic energy of the brane $(\gamma - 1)T_3 h^{-1}$. This is possible because the kinetic energy of the brane is suppressed by the large warping of the internal space, $h^{-1} \ll 1$.

In addition to providing an elegant solution to the eta-problem, DBI inflation makes exciting phenomenological predictions. The primordial fluctuations produced

during DBI inflation are highly non-Gaussian ($f_{\rm NL} \propto \gamma^2 \gg 1$) at a level easily detectable by near future experiments [147]. This makes DBI inflation very falsifiable. In fact, as we will show in Chapter 8, DBI inflation on Calabi-Yau cones is already very constrained by a combination of experimental and microscopic considerations [21].

## 3. Models of String Inflation

Models of inflation in string theory can be divided into two categories: models where the inflaton is an open string or closed string degree of freedom.

**3.1. Open String Models.** Crudely speaking, open string moduli parameterize the positions and orientations of D-branes. Using these moduli, many variants and complements of brane-antibrane inflation and DBI inflation have been constructed (*e.g.* assisted M5-brane inflation [26], D3/D7 inflation [56], wrapped brane inflation [148], etc.). We refer the reader to the original papers and recent reviews [96] for a more comprehensive summary of these developments. Since we described brane inflation in some detail in the previous section we here restrict ourselves to a few comments on models of inflation coming from the closed string sector.

**3.2. Closed String Models.** Closed string moduli are the Kähler moduli, the complex structure moduli, the dilaton and the corresponding axions. The associated inflationary models include racetrack inflation [35, 36], Kähler moduli inflation [54], Roulette inflation [38], and N-flation [61, 67]. For no reason other than personal taste we here select to describe Kähler moduli inflation and N-flation in more detail.

■ **Kähler moduli inflation** by Conlon and Quevedo [54] is an interesting attempt to embed inflation in the LARGE volume compactifications of [15]. An attractive feature of these models is that most corrections to the inflaton potential are suppressed by factors of the exponentially large volume.

Let the Kähler potential for three Kähler moduli $\rho_i$ be

$$\mathcal{K} = -2M_{\rm pl}^2 \ln\Big[\lambda_1(\rho_1+\bar\rho_1)^{3/2} + \lambda_2(\rho_2+\bar\rho_2)^{3/2} + \lambda_3(\rho_3+\bar\rho_3)^{3/2} + \xi\Big] \quad (4.18)$$

$$\equiv -2M_{\rm pl}^2 \ln[\mathcal{V}(\phi)]\,, \quad (4.19)$$

where $\xi$ parameterizes $\alpha'$ corrections. The superpotential has the same structure as in KKLT (see Chapter 3)

$$W = W_0 + \sum_{i=1}^{3} A_i e^{a_i\rho_i}\,. \quad (4.20)$$

For $W_0 = \mathcal{O}(1)M_{\rm pl}^4$ this leads to a minimum at exponentially large volume $\mathcal{V}_\star \sim \mathcal{O}(10^{14})$. (Recall that the KKLT solution corresponds to the limit $W_0 \approx -10^{-4}M_{\rm pl}^4$.)

At least three Kähler moduli are required to stabilize the overall volume $\mathcal{V}$ during inflation. $\rho_1$ and $\rho_2$ are fixed, while a blow-up four-cycle $\rho_3$ plays the role of the evolving inflaton $\phi$. In [54] the axion $\mathrm{Im}(\rho_3)$ was frozen at its minimum and the inflaton reduced to $\mathrm{Re}(\rho_3)$. The more general case was considered in [38]. There, the two complex fields $\rho_1$ and $\rho_2$ are again fixed, but in $\rho_3 \equiv \phi + i\theta$, both the volume modulus $\phi$ and the axion $\theta$ evolve during inflation. The resulting potential is periodic in $\theta$ and exponentially flat in $\phi$. In this multi-field case, the inflationary trajectories are of course not unique, but depend on the initial conditions.

To date, it has not been proven rigorously that the eta-problem is really absent in Kähler moduli inflation. Most corrections to the potential are suppressed by factors of the overall (exponentially large) volume. However, as noted in [38, 54], there are additional corrections to the Kähler potential of the form $f(\phi)\mathcal{V}^{-n}$ that could depend on the inflaton. For generic functions $f(\phi)$ this gives an eta-problem. Proving the absence of these terms remains an important step towards establishing the viability of models of Kähler moduli inflation.

■ **N-flation** [61, 67] is unique amongst inflationary models in string theory in that it predicts an observable amplitude of gravitational waves. As we explained in

Chapter 2, observable gravity waves are associated with super-Planckian field excursions during inflation. In Chapters 8, 9 and 10 we explain why we think it may be very challenging to embed large-field models of inflation in a consistent string compactification. This makes it particularly interesting to discuss whether N-flation is a serious exception to this general expectation.

N-flation overcomes the super-Planckian problem by the mechanism of assisted inflation [115]. Let us first describe assisted inflation in effective field theory and then present its string theoretic realization. We consider $N$ fields $\phi_i$ with separable potentials $V(\phi) = \sum_i V_i(\phi_i)$. The individual fields do not exceed Planckian vevs. The crucial point of the assistance effect is that each individual field feels the combined Hubble friction of all fields, $3M_{\rm pl}^2 H^2 = \sum_i V_i$, but only the force from its own potential

$$\ddot{\phi}_i + 3H\dot{\phi}_i = -\partial_i V_i \,. \tag{4.21}$$

(Note that cross-couplings between the fields can easily destroy the assistance effect). Imagine a large number of fields with small initial displacements away from the minima of their potentials, $\Delta\phi_i \ll M_{\rm pl}$. The potentials $V_i$ are then approximated by a quadratic expansion about the minima $V_i \approx \frac{1}{2} m_i^2 \phi_i^2$. For simplicity, we also take all masses to be equal $m_i = m$ [61] (the case of a distribution of different masses was considered by Easther and McAllister [67]). The effective inflaton potential then becomes, $V = \frac{1}{2} m^2 \left[\phi_1^2 + \phi_2^2 + \cdots + \phi_N^2\right] \equiv \frac{1}{2} m^2 \Phi^2$. Here, we have defined the effective inflaton as the Pythagorean sum of the individual fields $\Phi^2 \equiv \sum_i \phi_i^2$. If the initial field displacements are equal, $\phi_i \equiv \phi$, we can write $\Phi = \sqrt{N}\phi_i$. If the number of fields $N$ is large enough, then the effective inflaton can have a super-Planckian displacement $\Delta\Phi > M_{\rm pl}$ even if $\Delta\phi_i \ll M_{\rm pl}$. For string theory axions the required number of field turns out to be $N \geq \mathcal{O}(1000)$ [61, 67, 102].

We now come to the concrete realization of this idea using the many axions of string theory – our treatment parallels that of Ref. [67]. A large number of axions

are generically present in string compactifications. The axion Lagrangian is

$$\mathcal{L} = \frac{1}{2} M_{\rm pl}^2 \mathcal{K}_{ij} \nabla_\mu \phi^i \nabla^\mu \phi^j - V \,, \tag{4.22}$$

where

$$V = \exp\left(\frac{\mathcal{K}}{M_{\rm pl}^2}\right) \left[\mathcal{K}^{AB} D_A W \overline{D_B W} - 3\frac{|W|^2}{M_{\rm pl}^2}\right] . \tag{4.23}$$

Here $A, B$ run over the dilaton $\tau$, the complex structure moduli $\chi_\alpha$ and the Kähler moduli $\rho_i \equiv \sigma_i - i\phi_i$. The Kähler potential only depends on the real part of the Kähler moduli and in particular is independent of the axions $\phi_i$. Meanwhile, in the KKLT superpotential the dependence on the axions is as follows

$$W_i = A_i e^{-2\pi\sigma_i} e^{2\pi i \phi_i} \equiv C_i e^{2\pi i \phi_i} \,. \tag{4.24}$$

*Assuming* that the complex structure moduli and the volume cycles $\sigma_i$ have relaxed to their minima, we focus on the evolution of the axion fields $\phi_i$ (we discuss this assumption below). The complete superpotential from fluxes and nonperturbative effects is

$$W = W_0(\tau^\star, \chi_\alpha^\star) + \sum_i W_i(\sigma_i^\star, \phi_i) \,. \tag{4.25}$$

Substituting (4.25) into (4.23) and performing a Taylor expansion around $\phi_i = 0$ one finds [67] (using F-flatness $D_A W|_{\phi_i=0} = 0$)

$$V = (2\pi)^2 \hat{M}_{ij} \phi^i \phi^j + \mathcal{O}(\phi^3) \,, \tag{4.26}$$

where

$$\hat{M}_{ij} \equiv \frac{1}{M_{\rm pl}^2} e^{\mathcal{K}/M_P^2} \left(\mathcal{K}^{AB} D_A C_i D_B C_j - 3 C_i C_j\right) . \tag{4.27}$$

At this point, neither the kinetic terms, nor the mass matrix are diagonal. Hence, the potential does *not* take the uncoupled form required for the assistance effect described above. However, Ref. [67] showed that the cross-couplings in $\hat{M}_{ij}$ are suppressed for statistical reasons (see Appendix A of [67]). Furthermore, the metric $\mathcal{K}_{ij}$ can be

diagonalized by an orthogonal rotation

$$O_i{}^k \mathcal{K}_{kl} O_j{}^l = \frac{f_i^2}{M_{\rm pl}^2}\delta_{ij}\,. \tag{4.28}$$

The eigenvalues $f_i$ are the axion decay constants. Finally, after absorbing the $f_i$ into a rescaling of the $\phi_i$ to make the kinetic terms canonical, the Lagrangian becomes

$$\mathcal{L} = \frac{1}{2}\partial_\mu\phi_i\partial^\mu\phi^i - M_{ij}\phi^i\phi^j\,, \tag{4.29}$$

where

$$M_{ij} = (2\pi)^2\frac{e^{\mathcal{K}}}{f_i f_j}O_i{}^k\left(D_A C_k D^A C_l - 3C_k C_l\right)O_j{}^l\,. \tag{4.30}$$

In the limit where only the quadratic terms in (4.26) are retained a further orthogonal rotation diagonalizes $M_{ij}$. The eigenvalues of $M_{ij}$ are the masses $m_i$ of $N$ canonically normalized, uncoupled axions

$$\mathcal{L} = \frac{1}{2}\partial_\mu\phi_i\partial^\mu\phi^i - \sum_i \frac{1}{2}m_i^2\phi_i^2\,. \tag{4.31}$$

(Ref. [67] went further and characterized the statistical properties of these eigenvalues using random matrix theory). This seems to establish the Lagrangian assumed for assisted $N$ axion inflation. However, the devil is in the details. Are the cross-couplings really small enough to allow the assistance effect? What happens when higher-order corrections to the quadratic approximations for the potentials are included? Most importantly there is a question of initial conditions: is it consistent to assume that the real parts of the Kähler moduli have all relaxed to their minima before the axionic counterparts? This assumption requires that the mass in the $\sigma_i$-directions is much larger than in the $\phi_i$-directions. Finally, the string compactifications of N-flation are at the limit of control of the $\alpha'$ and $g_s$ expansions [61]. Unknown higher corrections in $\alpha'$ and $g_s$ could spoil the success of the scenario. It therefore remains to be established

explicitly whether N-flation is a consistent realization of large-field inflation in string theory.[4]

### 4. Inflation from Explicit String Compactifications

None of the models in §3 have been derived from an explicit string compactification that includes a computation of all relevent correction terms. In this thesis we make important steps towards this goal.

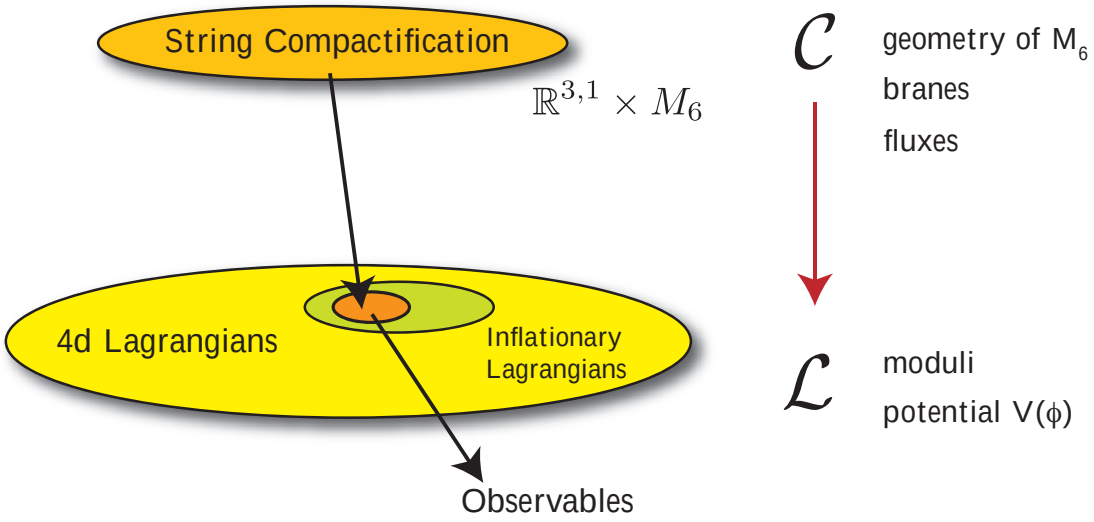


FIGURE 3. From String Compactification Data to Low Energy Lagrangian to Inflation. String theory specifies discrete compactification data $\mathcal{C}$ (geometry and topology of extra dimensions, amount and types of branes, amount and types of fluxes, etc.) At low energies, four-dimensional physics is described by an effective field theory with Lagrangian $\mathcal{L}$. In this thesis we study the correspondence between $\mathcal{C}$ and $\mathcal{L}$ and search for configurations that allow inflationary solutions.

In the following chapters, we formulate the standard that we would like to require from an explicit model of string inflation. We illustrate this program with a concrete computation of the inflaton potential for models of warped D-brane inflation. We draw conclusions about the possibilities and impossibilities of effective field theories derivable from this setup. We will find that although naively these scenarios lead to

[4]At the time of writing the most detailed discussions of these issues can be found in [80] and [98] .

effective Lagrangians that should easily allow inflationary solutions, the parameter space of successful models is dramatically reduced by microphysical constraints arising from the compactification geometry.

# Part 2

# The Inflaton Potential

CHAPTER 5

# On D3-brane Potentials in Compact Spaces

We begin our study of D-brane motion in warped background spacetimes by computing a crucial ingredient to the D3-brane potential.[1] Technical details of the computations presented in this chapter are relegated to Appendices B, C and D.

## 1. Introduction

**1.1. Motivation.** As we emphasized in Part I of this thesis, a truly satisfactory model of inflation in string theory should include a complete specification of a string compactification, together with a reliable computation of the resulting four-dimensional effective theory. While some models come close to this goal, we have seen that very small corrections to the potential can spoil the delicate flatness conditions required for slow-roll inflation [153]. In particular, gravitational corrections typically induce inflaton masses of order the Hubble parameter $H$, which are fatal for slow-roll. String theory provides a framework for a systematic computation of these corrections, but so far it has rarely been possible, in practice, to compute all the relevant effects. However, there is no obstacle in principle, and one of our main goals in this work is to improve the status of this problem.

It is well-known that a D3-brane probe of a 'no-scale' compactification [76] with imaginary self-dual three-form fluxes experiences no force: gravitational attraction

[1]The material of this chapter is based on Daniel Baumann, Anatoly Dymarsky, Igor Klebanov, Juan Maldacena, Liam McAllister and Arvind Murugan, "On D3-brane Potentials in Compactifications with Fluxes and Wrapped D-branes", JHEP **0611**, 031 (2006).

and Ramond-Ramond repulsion cancel, and the brane can sit at any point of the compact space with no energy cost. This no-force result is no longer true, in general, when the volume of the compactification is stabilized. The D-brane moduli space is lifted by the same nonperturbative effect that fixes the compactification volume. This has particular relevance for inflation models involving moving D-branes.

In the warped brane inflation model of Kachru et al. [95] (see Chapter 4) it was established that the interaction potential of a brane-antibrane pair in a warped throat geometry is exceptionally flat, in the approximation that moduli-stabilization effects are neglected. However, incorporating these effects yielded a potential that generically was not flat enough for slow roll. That is, certain correction terms to the inflaton potential arising from the Kähler potential[2] and from volume-inflaton mixing [95] could be computed in detail, and gave explicit inflaton masses of order $H$.[3] One further mass term, arising from a one-loop correction to the volume-stabilizing nonperturbative superpotential, was known [71] to be present, but was not computed. The authors of [95] argued that in some small percentage of possible models, this one-loop mass term might take a value that approximately canceled the other inflaton mass terms and produced an overall potential suitable for slow-roll. This was a fine-tuning, but *not* an explicit one: lacking a concrete computation of the one-loop correction, it was not possible to specify fine-tuned microscopic parameters, such as fluxes, geometry, and brane locations, in such a way that the total mass term was known to be small. In this chapter we give an explicit computation of this key, missing inflaton mass term for brane motion in general warped throat backgrounds. Applications of our results to brane inflation will be discussed in Chapters 6 and 7.

[2]These terms are those associated with the usual supergravity eta problem.

[3]Similar problems are expected to affect other warped throat inflation scenarios, such as [65]. Indeed, concerns about the Hubble-scale corrections to the inflaton potential of [65] have been raised in [44], but the effects of compactification were not considered there.

**1.2. Method.** The inflaton mass problem described in [95] appears in any model of slow-roll inflation involving D3-branes moving in a stabilized flux compactification. Thus, it is necessary to search for a general method for computing the dependence of the nonperturbative superpotential on the D3-brane position. Ganor [71] studied this problem early on, and found that the correction to the superpotential is a section of a bundle called the 'divisor bundle', which has a zero at the four-cycle where the wrapped brane is located. The problem was addressed more explicitly by Berg, Haack, and Körs (BHK) [32], who computed the threshold corrections to gaugino condensate superpotentials in toroidal orientifolds. This gave a substantially complete[4] potential for brane inflation models in such backgrounds. However, their approach involved a challenging open-string one-loop computation that is difficult to generalize to more complicated Calabi-Yau geometries and to backgrounds with flux and warping, such as the warped throat backgrounds relevant for a sizeable fraction of current models. Moreover, KKLT-type volume stabilization often proceeds via a superpotential generated by Euclidean D3-branes [163], not by gaugino condensation or other strong gauge dynamics; this requires computing semiclassical corrections around the instanton background.

Following work by Giddings and Maharana [77], we overcome these difficulties by viewing the correction to the mobile D3-brane potential as arising from a distortion, sourced by the D3-brane itself, of the background near the four-cycle wrapped by the D7-branes or Euclidean D3-brane responsible for the non-perturbative effect. This corrects the warped volume of the four-cycle, changing the magnitude of the nonperturbative effect. Specifically, we assume that the Kähler moduli are stabilized by nonperturbative effects, arising either from Euclidean D3-branes or from strong gauge dynamics (such as gaugino condensation) on D7-branes. In either case, the

[4]Corrections to the Kähler potential provide one additional effect; see [33, 75].

nonperturbative superpotential is associated with a particular four-cycle, and has exponential dependence on the warped volume of this cycle. Inclusion of a D3-brane in the compact space slightly modifies the supergravity background, changing the warped volume of the four-cycle and hence the gauge coupling in the D7-brane gauge theory. Due to gaugino condensation this in turn changes the superpotential of the four-dimensional effective theory. The result is an energy cost for the D3-brane that depends on its location.

This method may be viewed as the closed-string dual of the open-string computation of BHK [32]. In §4.2 we compute the correction for a toroidal compactification, where an explicit comparison is possible, and verify that the closed-string method exactly reproduces the result of [32]. We view this as a highly nontrivial check of the closed-string method.

Employing the closed-string perspective allows us to study the potential for a D3-brane in a warped throat region, such as the warped deformed conifold [105] or its generalizations [48, 65], glued into a flux compactification. This is a case of direct phenomenological interest. To model the four-cycle bearing the most relevant nonperturbative effect, we compute the change in the warped volume of a variety of holomorphic four-cycles, as a function of the D3-brane position. We find that most of the details of the geometry far from the throat region are irrelevant. Note that the supergravity method is applicable provided that the internal manifold has large volume.

The distortion produced by moving a D3-brane in a warped throat corresponds to a deformation of the gauge theory dual to the throat by expectation values of certain gauge-invariant operators [108]. Hence, it is possible, and convenient, to use methods and perspectives from the AdS/CFT correspondence [124] (see [2, 103] for reviews).

**1.3. Outline.** The organization of this chapter is as follows. In §2 we recall the problem of determining the potential for a D3-brane in a stabilized flux compactification. We stress that a consistent computation must include a one-loop correction to the volume-stabilizing nonperturbative superpotential. In §3 we explain how this correction may be computed in supergravity, as a correction to the warped volume of each four-cycle producing a nonperturbative effect. We present the Green's function method (*cf.* Ref. [77]) for determining the perturbation of the warp factor at the location of the four-cycle in §4. We argue that supersymmetric four-cycles provide a good model for the four-cycles producing nonperturbative effects in general compactifications, and in particular in warped throats. In §5 we compute in detail the corrected warped volumes of certain supersymmetric four-cycles in the singular conifold. We also give results for corrected volumes in some other asymptotically conical spaces. In §6 we give an explicit and physically intuitive solution to the 'rho problem' [32], *i.e.* the problem of defining a holomorphic volume modulus in a compactification with D3-branes. We also discuss the important possibility of model-dependent effects from the bulk of the compactification. We conclude in §7.

Technical details of the computations in this chapter are relegated to a number of appendices. In Appendix B we present some facts about Green's functions on conical geometries, as needed for the computation of §5. Details of our computation for warped conifolds are given in Appendix C. The equivalent calculation for $Y^{p,q}$ cones is presented in Appendix D.

## 2. D3-branes and Volume Stabilization

**2.1. Nonperturbative Volume Stabilization.** For realistic applications to cosmology and particle phenomenology, it is important to stabilize all the moduli. The flux-induced superpotential [82] stabilizes the dilaton and the complex structure moduli [76], but is independent of the Kähler moduli. However, nonperturbative

terms in the superpotential do depend on the Kähler moduli, and hence can lead to their stabilization [93]. There are two sources for such effects:

(1) Euclidean D3-branes wrapping a four-cycle in the Calabi-Yau [163].

(2) Gaugino condensation or other strong gauge dynamics on a stack of $N_{D7}$ spacetime-filling D7-branes wrapping a four-cycle in the Calabi-Yau.

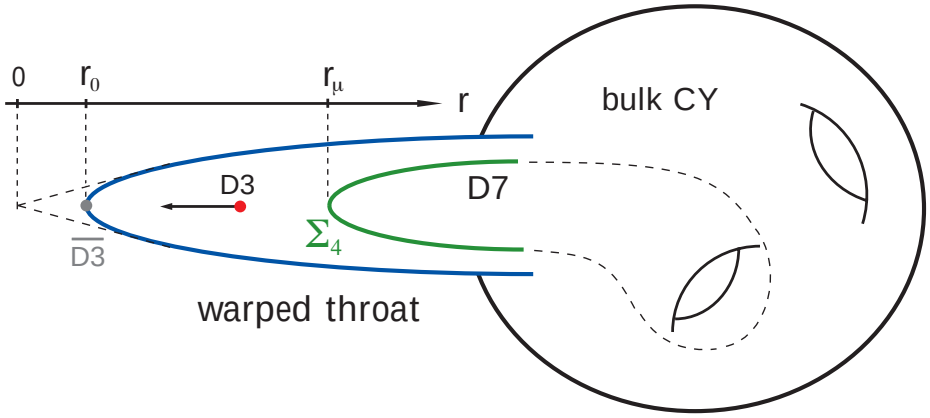


FIGURE 1. Cartoon of an embedded stack of D7-branes wrapping a four-cycle $\Sigma_4$, and a mobile D3-brane, in a warped throat region of a compact Calabi-Yau. In the scenario of [95] the D3-brane feels a force from an anti-D3-brane at the tip of the throat. Alternatively, in [65] it was argued that a D3-brane in the resolved warped deformed conifold background feels a force even in the absence of an anti-D3-brane. In this work we consider an additional contribution to the D3-brane potential, coming from nonperturbative effects on D7-branes.

Let $\rho$ be the volume of a given four-cycle that admits a nonperturbative effect.[5] The resulting superpotential is expected to be of the form [93]

$$W_{\rm np}(\rho) = A(\chi, X) e^{-a\rho} \,. \tag{5.1}$$

Here $a$ is a numerical constant and $A(\chi, X)$ is a holomorphic function of the complex structure moduli $\chi \equiv \{\chi_1, \ldots, \chi_{h^{2,1}}\}$ and of the positions $X$ of any D3-branes in the

[5]In general, there are $h^{1,1}$ Kähler moduli $\rho_i$. For notational simplicity we limit our discussion to a single Kähler modulus $\rho$, but point out that our treatment straightforwardly generalizes to many moduli. The identification of a holomorphic Kähler modulus, *i.e.* a complex scalar belonging to a single chiral superfield, is actually quite subtle. We address this important point in §6.1. At the present stage $\rho$ may simply be taken to be the volume as defined in *e.g.* [76].

internal space.[6] The functional form of $A$ will depend on the particular four-cycle in question.

The prefactor $A(\chi, X)$ arises from a one-loop correction to the nonperturbative superpotential. For a Euclidean D3-brane superpotential, $A(\chi, X)$ represents a one-loop determinant of fluctuations around the instanton. In the case of D7-brane gauge dynamics the prefactor comes from a threshold correction to the gauge coupling on the D7-branes.

In the original KKLT proposal, the complex structure moduli acquired moderately large masses from the fluxes, and no probe D3-brane was present. Thus, it was possible to ignore the moduli-dependence of $A(\chi, X)$ and treat $A$ as a constant, albeit an unknown one. In the case of present interest (as in [95]), the complex structure moduli are still massive enough to be negligible, but there is at least one mobile D3-brane in the compact space, so we must write $A = A(X)$. (See [71] for a very general argument that no prefactor $A$ can be independent of a D3-brane location $X$.)

The goal of this chapter is to compute $A(X)$. As we explained in the introduction, this has already been achieved in certain toroidal orientifolds [32], and the relevance of $A(X)$ for brane inflation has also been recognized [32, 95]. Here we will use a closed-string channel method for computing $A(X)$, allowing us to study more general compactifications. In particular, we will give the first concrete results for $A(X)$ in the warped throats relevant for many brane inflation models.

**2.2. D3-brane Potential After Volume Stabilization.** The F-term part of the supergravity potential is

$$V_F = e^{\kappa^2 \mathcal{K}} \left[ \mathcal{K}^{i\bar{j}} D_i W \overline{D_j W} - 3\kappa^2 |W|^2 \right] , \qquad \kappa^2 = M_{\rm pl}^{-2} = 8\pi G \, . \tag{5.2}$$

[6] Strictly speaking, there are three complex fields, corresponding to the dimensionality of the internal space, but we will refer to a single field for notational convenience.

DeWolfe and Giddings [58] showed that the Kähler potential $\mathcal{K}$ in the presence of mobile D3-branes is

$$\kappa^2\mathcal{K} = -3\ln\left[\rho+\bar{\rho}-\gamma k(X,\bar{X})\right] \equiv -2\ln\mathcal{V}\,, \tag{5.3}$$

where $k(X,\bar{X})$ is the Kähler potential for the Calabi-Yau metric, *i.e.* the Kähler potential on the putative moduli space of a D3-brane probe, $\mathcal{V}$ is the physical volume of the internal space, and $\gamma$ is a constant.[7] We address this volume-inflaton mixing in more detail in §6.1. For clarity we have assumed here that there is only one Kähler modulus, but our later analysis is more general.

The superpotential $W$ is the sum of a constant flux term [82] $W_{\rm flux}(\chi_\star) = \int G_3\wedge\Omega \equiv W_0$ at fixed complex structure $\chi_\star$ and a term $W_{\rm np}$ (5.1) from nonperturbative effects,

$$W = W_0 + A(X)e^{-a\rho}\,. \tag{5.4}$$

Equations (7.13) to (7.14) imply three distinct sources for corrections to the potential for D3-brane motion:

(1) $m_{\mathcal{K}}$: The $X$-dependence of the Kähler potential $\mathcal{K}$ leads to a mass term familiar from the supergravity eta problem.

(2) $m_D$: Sources of $D$-term energy, if present, will scale with the physical volume $\mathcal{V}$ and hence depend on the D3-brane location. This leads to a mass term for D3-brane displacements.

(3) $m_A$: The prefactor $A(X)$ in the superpotential (7.14) leads to a mass term[8] via the F-term potential (7.13).

[7] In §6.1 we will find that $\gamma \equiv \frac{1}{3}\kappa^2 T_3$, where $T_3$ is the D3-brane tension.

[8] After the appearance of [18] (Chapter 5) we realized in [19] (Chapter 7) that $A(X)$ can never lead to a pure mass term. We should therefore imagine a local definition of the mass $m_A(X)$ as the second derivative of the potential. As indicated here (and proven in [19]) this 'mass' will depend on the field value $X$. This is to be contrasted with $m_{\mathcal{K}}$ and $m_D$ which are constants.

The masses $m_{\mathcal{K}}$ and $m_D$ were calculated explicitly in [95] and shown to be of order the Hubble parameter $H$. On the other hand, $m_A$ has been computed only for the toroidal orientifolds of [32]. It has been suggested [95] that there might exist non-generic configurations in which $m_A$ cancels against the other two terms. It is in these fine-tuned situations that D3-brane motion could produce slow-roll inflation. By computing $m_A$ explicitly, one can determine whether or not this hope is realized [19].

## 3. Warped Volumes and the Superpotential

**3.1. The Role of the Warped Volume.** The nonperturbative effects discussed in §2.1 depend exponentially on the warped volume of the associated four-cycle: the warped volume governs the instanton action in the case of Euclidean D3-branes, and the gauge coupling in the case of strong gauge dynamics on D7-branes. To see this, consider a warped background with the line element

$$\mathrm{d}s^2 = G_{\mu\nu}\mathrm{d}x^\mu \mathrm{d}x^\nu + G_{ij}\mathrm{d}Y^i\mathrm{d}Y^j \equiv h^{-1/2}(Y)g_{\mu\nu}\mathrm{d}x^\mu\mathrm{d}x^\nu + h^{1/2}(Y)g_{ij}\mathrm{d}Y^i\mathrm{d}Y^j\,, \quad (5.5)$$

where $Y^i$ and $g_{ij}$ are the coordinates and the unwarped metric on the internal space, respectively, and $h(Y)$ is the warp factor.

The Yang-Mills coupling $g_7$ of the $7+1$ dimensional gauge theory living on a stack of D7-branes is given by[9]

$$g_7^2 \equiv 2(2\pi)^5 g_s(\alpha')^2\,. \quad (5.6)$$

The action for gauge fields on D7-branes that wrap a four-cycle $\Sigma_4$ is

$$S = \frac{1}{2g_7^2}\int_{\Sigma_4}\mathrm{d}^4\xi\sqrt{g^{ind}}\,h(Y)\cdot\int\mathrm{d}^4x\sqrt{-g}\;g^{\mu\alpha}g^{\nu\beta}\,\mathrm{Tr}\,F_{\mu\nu}F_{\alpha\beta}\,, \quad (5.7)$$

where $\xi_i$ are coordinates on $\Sigma_4$ and $g^{ind}$ is the metric induced on $\Sigma_4$ from $g_{ij}$. A key point is the appearance of a single power of $h(Y)$ [77]. Defining the warped volume

[9] In the notation of [139], $g_7^2 = 2g_{D7}^2$.

of $\Sigma_4$,

$$V^w_{\Sigma_4} \equiv \int_{\Sigma_4} \mathrm{d}^4\xi \sqrt{g^{ind}}\, h(Y)\,, \tag{5.8}$$

and recalling the D3-brane tension

$$T_3 \equiv \frac{1}{(2\pi)^3 g_s (\alpha')^2}\,, \tag{5.9}$$

we read off the gauge coupling of the four-dimensional theory from (5.7):

$$\frac{1}{g^2} = \frac{V^w_{\Sigma_4}}{g_7^2} = \frac{T_3 V^w_{\Sigma_4}}{8\pi^2}\,. \tag{5.10}$$

In $\mathcal{N} = 1$ super-Yang-Mills theory, the Wilsonian gauge coupling is the real part of a holomorphic function which receives one-loop corrections, but no higher perturbative corrections [7, 143–145]. The modulus of the gaugino condensate superpotential in $SU(N_{D7})$ super-Yang-Mills with ultraviolet cutoff $M_{\mathrm{UV}}$ is given by

$$|W_{\mathrm{np}}| = 16\pi^2 M_{\mathrm{UV}}^3 \exp\Big(-\frac{1}{N_{D7}}\frac{8\pi^2}{g^2}\Big) \propto \exp\Big(-\frac{T_3 V^w_{\Sigma_4}}{N_{D7}}\Big)\,. \tag{5.11}$$

The mobile D3-brane adds a flavor to the $SU(N_{D7})$ gauge theory, whose mass $m$ is a holomorphic function of the D3-brane coordinates. In particular, the mass vanishes when the D3-brane coincides with the D7-brane. In such a gauge theory, the superpotential is proportional to $m^{1/N_{D7}}$ [91]. Our explicit closed-string channel calculations will confirm this form of the superpotential.

In the case that the nonperturbative effect comes from a Euclidean D3-brane, the instanton action is

$$S = T_3 \int_{\Sigma_4} \mathrm{d}^4\xi \sqrt{G^{ind}} = T_3 \int_{\Sigma_4} \mathrm{d}^4\xi \sqrt{g^{ind}}\, h(Y) \equiv T_3 V^w_{\Sigma_4}\,, \tag{5.12}$$

so that, just as in (5.7), the action depends on a single power of $h(Y)$. The modulus of the nonperturbative superpotential is then

$$|W_{\mathrm{np}}| \propto \exp\Big(-T_3 V^w_{\Sigma_4}\Big)\,. \tag{5.13}$$

**3.2. Corrections to the Warped Volumes of Four-Cycles.** The displacement of a D3-brane in the compactification creates a slight distortion $\delta h$ of the warped background, and hence affects the warped volumes of four-cycles. The correction takes the form

$$\delta V^w_{\Sigma_4} \equiv \int_{\Sigma_4} \mathrm{d}^4 Y \sqrt{g^{ind}(X;Y)}\, \delta h(X;Y)\,. \tag{5.14}$$

By computing this change in volume we will extract the dependence of the superpotential on the D3-brane location $X$. In the non-compact throat approximation, we will calculate $\delta V^w_{\Sigma_4}$ explicitly, and find that it is the real part of a holomorphic function $\zeta(X)$.[10] Its imaginary part is determined by the integral of the Ramond-Ramond four-form perturbation $\delta C_4$ over $\Sigma_4$ (we will not compute this explicitly, but will be able to deduce the result using the holomorphy of $\zeta(X)$).

The nonperturbative superpotential of the form (5.1), generated by the gaugino condensation, is then determined by

$$A(X) = A_0 \exp\Big(-\frac{T_3\,\zeta(X)}{N_{D7}}\Big)\,. \tag{5.15}$$

We have introduced an unimportant constant $A_0$ that depends on the values at which the complex structure moduli are stabilized, but is independent of the D3-brane position. As remarked above, computing (5.15) is equivalent to computing the dependence of the threshold correction to the gauge coupling on the mass $m$ of the flavor coming from strings that stretch from the D7-branes to the D3-brane.

In the case of Euclidean D3-branes, the change in the instanton action is proportional to the change in the warped four-cycle volume. Hence, the nonperturbative

[10] In the compact case, it is no longer true that $\delta V^w_{\Sigma_4}$ is the real part of a holomorphic function. This is related to the 'rho problem' [32], and in fact leads to a resolution of the problem, as we shall explain in §6.1 (see also [77]). The result is that in terms of an appropriately-defined holomorphic Kähler modulus $\rho$ (5.62), the holomorphic correction to the gauge coupling coincides with the holomorphic result of our non-compact calculation.

superpotential is of the form (5.1) with

$$A(X) = A_0 \exp\Big(-T_3\,\zeta(X)\Big)\,. \tag{5.16}$$

In this case, computing (5.14) is equivalent to computing the D3-brane dependence of an instanton fluctuation determinant.

Finally, we can write a unified expression that applies to both sources of nonperturbative effects:

$$A(X) = A_0 \exp\Big(-\frac{T_3\,\zeta(X)}{n}\Big)\,, \tag{5.17}$$

where $n = N_{D7}$ for the case of gaugino condensation on D7-branes and $n = 1$ for the case of Euclidean D3-branes.

## 4. D3-brane Backreaction

**4.1. The Green's Function Method.** A D3-brane located at some position $X$ in a six-dimensional space with coordinates $Y$ acts as a point source for a perturbation $\delta h$ of the geometry:

$$-\nabla^2_Y \delta h(X;Y) = \mathcal{C}\,\left[\frac{\delta^{(6)}(X-Y)}{\sqrt{g(Y)}} - \rho_{bg}(Y)\right]\,. \tag{5.18}$$

That is, the perturbation $\delta h$ is a Green's function for the Laplace problem on the background of interest. Here $\mathcal{C} \equiv 2\kappa_{10}^2 T_3 = (2\pi)^4 g_s(\alpha')^2$ ensures the correct normalization of a single D3-brane source term relative to the four-dimensional Einstein-Hilbert action. A consistent flux compactification contains a background charge density $\rho_{bg}(Y)$ which satisfies

$$\int \mathrm{d}^6 Y \sqrt{g}\,\rho_{bg}(Y) = 1 \tag{5.19}$$

to account for the Gauss's law constraint on the compact space [76].

To solve (5.18), we first solve

$$-\nabla^2_{Y'}\Phi(Y;Y') = -\nabla^2_{Y}\Phi(Y;Y') = \frac{\delta^{(6)}(Y-Y')}{\sqrt{g}} - \frac{1}{V_6}\,, \tag{5.20}$$

where $V_6 \equiv \int \mathrm{d}^6 Y \sqrt{g}$. The solution to (5.18) is then

$$\delta h(X;Y) = \mathcal{C}\left[\Phi(X;Y) - \int \mathrm{d}^6 Y' \sqrt{g}\, \Phi(Y;Y') \rho_{bg}(Y')\right]. \tag{5.21}$$

We note for later use that

$$-\nabla_X^2 \delta h(X;Y) = \mathcal{C}\left[\frac{\delta^{(6)}(X-Y)}{\sqrt{g(X)}} - \frac{1}{V_6}\right]. \tag{5.22}$$

This relation is independent of the form of the background charge $\rho_{bg}$.

To compute $A(X)$ from (7.15), we simply solve for the Green's function $\delta h$ obeying (5.18) and then integrate $\delta h$ over the four-cycle of interest, according to (5.14).

**4.2. Comparison with the Open-String Approach.** Let us show that this supergravity (closed-string channel) method is consistent with the results of BHK [32], where the correction to the gaugino condensate superpotential was derived via a one-loop open-string computation.[11]

The analysis of [32] applied to configurations of D7-branes and D3-branes on certain toroidal orientifolds, *e.g.* $T^2 \times T^4/\mathbb{Z}_2$. We introduce a complex coordinate $X$ for the position of the D3-branes on $T^2$, as well as a complex structure modulus $\tau$ for $T^2$, and without loss of generality we set the volume of $T^4/\mathbb{Z}_2$ to unity. Let us consider the case where all the D7-branes wrap $T^4/\mathbb{Z}_2$ and sit at the origin $X = 0$ in $T^2$.

The goal is to determine the dependence of the gauge coupling on the position $X$ of a D3-brane. (The location of the D3-brane in the $T^4/\mathbb{Z}_2$ wrapped by the D7-branes is immaterial.) For this purpose, we may omit terms computed in [32] that depend only on the complex structure and not on the D3-brane location. Such terms will only affect the D3-brane potential by an overall constant.

[11] Analogous pairs of closed-string and open-string computations exist in the literature, *e.g.* [17].

Then, the relevant terms from equation (44) of [32], in our notation[12], are

$$\delta\Big(\frac{8\pi^2}{g^2}\Big) = \frac{1}{4\pi\,\mathrm{Im}(\tau)}\Big[\mathrm{Im}(X)\Big]^2 - \frac{1}{2}\ln\left|\vartheta_1\left(\frac{X}{2\pi}\Big|\tau\right)\right|^2 + \dots\,. \tag{5.23}$$

Let us now compare (5.23) to the result of the supergravity computation. In principle, the prescription of equation (5.14) is to integrate the Green's function on a six-torus over the wrapped four-torus. However, we notice that this procedure of integration will reduce the six-dimensional Laplace problem to the Laplace problem on the two-torus parametrized by $X$,

$$-\nabla_X^2\delta h(X;0) = \mathcal{C}\,\left[\delta^{(2)}(X) - \frac{1}{V_{T^2}}\right]\,, \tag{5.24}$$

where $V_{T^2} = 8\pi^2\,\mathrm{Im}(\tau)$. The correction to the gauge coupling, in the supergravity approach, is then proportional to $\delta h(X;0)$. Solving (5.24) and using (5.10), we get exactly (5.23). We conclude that our method precisely reproduces the results of [32], at least for those terms that directly enter the D3-brane potential.

**4.3. A Model for the Four-Cycles.** The closed-string channel approach to calculating $A(X)$ is well-defined for any given background, but further assumptions are required when no complete metric for the compactification is available. Fortunately, explicit metrics are available for many non-compact Calabi-Yau spaces, and at the same time, the associated warped throat regions are of particular interest for inflationary phenomenology. For a given warped throat geometry, our approach is to compute the D3-brane backreaction on specific four-cycles in the non-compact, asymptotically conical space. We will demonstrate that this gives an excellent approximation to the backreaction in a compactification in which the same warped throat is glued into a compact bulk. In particular, we will show in §6.2 that the physical effect in question is localized in the throat, *i.e.* is determined primarily by the shape

[12]After the replacement $X \to w$, our definitions of the theta functions and torus coordinates correspond to those of [139]; our $X$ differs from the $A$ of [32] by a factor of $2\pi$.

of the four-cycle in the highly warped region.[13] The model therefore only depends on well-known data, such as the specific warped metric and the embedding equations of the four-cycles, and is insensitive to the unknown details of the unwarped bulk. In principle, our method can be extended to general compact models for which metric data is available.

It still remains to identify the four-cycles responsible for nonperturbative effects in this model of a warped throat attached to a compact space. Such a space will in general have many Kähler moduli, and hence, assuming that stabilization is possible at all, will have many contributions to the nonperturbative superpotential. The most relevant term, for the purpose of determining the D3-brane potential, is the term corresponding to the four-cycle closest to the D3-brane. For a D3-brane moving in the throat region, this is the four-cycle that reaches farthest down the throat. In addition, the gauge theory living on the corresponding D7-branes should be making an important contribution to the superpotential.

The nonperturbative effects of interest are present only when the four-cycle satisfies an appropriate topological condition [163], which we will not discuss in detail. This topological condition is, of course, related to the global properties of the four-cycle, whereas the effect we compute is dominated by the part of the four-cycle in the highly-warped throat region, and is insensitive to details of the four-cycle in the unwarped region. That is, our methods are not sensitive to the distinction between four-cycles that do admit nonperturbative effects, and those that do not. We therefore propose to model the four-cycles producing nonperturbative effects with four-cycles that are merely supersymmetric, *i.e.* can be wrapped supersymmetrically by D7-branes. Many members of the latter class are not members of the former, but as

[13]To be precise, the physical effect is localized near the D3-brane, which may be taken to be far from the bulk, in the region where the throat is well-approximated by the non-compact metric. This is also the region where the background warping is large.

the shape of the cycle in the highly-warped region is the only important quantity, we expect this distinction to be unimportant.

We are therefore led to consider the backreaction of a D3-brane on the volume of a stack of supersymmetric D7-branes wrapping a four-cycle in a warped throat geometry. The simplest configuration of this sort is a supersymmetric 'flavor brane' embedding of several D7-branes in a conifold [9, 99, 133].

## 5. Backreaction in Warped Conifold Geometries

We now recall some relevant geometry. The singular conifold[14] is a non-compact Calabi-Yau threefold defined as the locus

$$\sum_{i=1}^{4} z_i^2 = 0 \tag{5.25}$$

in $\mathbb{C}^4$. After a linear change of variables ($w_1 = z_1 + iz_2, w_2 = z_1 - iz_2,$ *etc.*), the constraint (5.25) becomes

$$w_1 w_2 - w_3 w_4 = 0\,. \tag{5.26}$$

The Calabi-Yau metric on the conifold is

$$\mathrm{d}s_6^2 = \mathrm{d}r^2 + r^2 \mathrm{d}s_{T^{1,1}}^2\,. \tag{5.27}$$

The base of the cone is the $T^{1,1}$ coset space $(SU(2)_A \times SU(2)_B)/U(1)_R$ whose metric in angular coordinates $\theta_i \in [0,\pi], \phi_i \in [0,2\pi], \psi \in [0,4\pi]$ is

$$\mathrm{d}s_{T^{1,1}}^2 = \frac{1}{9}\Big(\mathrm{d}\psi + \sum_{i=1}^{2} \cos\theta_i\, \mathrm{d}\phi_i\Big)^2 + \frac{1}{6}\sum_{i=1}^{2}\Big(\mathrm{d}\theta_i^2 + \sin^2\theta_i\, \mathrm{d}\phi_i^2\Big)\,. \tag{5.28}$$

[14]The KS geometry [105] and its generalizations [48] are warped versions of the *deformed* conifold, defined by $\sum_{i=1}^{4} z_i^2 = \varepsilon^2$. When the D3-branes and D7-branes are sufficiently far from the tip of the deformed conifold, it will suffice to consider the simpler case of the warped singular conifold constructed in [106].

A stack of $N$ D3-branes placed at the singularity $w_i = 0$ backreacts on the geometry, producing the ten-dimensional metric

$$\mathrm{d}s_{10}^2 = h^{-1/2}(r)\mathrm{d}x_4^2 + h^{1/2}(r)\mathrm{d}s_6^2 \ , \tag{5.29}$$

where the warp factor is

$$h(r) = \frac{27\pi g_s N(\alpha')^2}{4r^4} \ . \tag{5.30}$$

This is the $AdS_5 \times T^{1,1}$ background of type IIB string theory, whose dual $\mathcal{N} = 1$ supersymmetric conformal gauge theory was constructed in [107]. The dual is an $SU(N) \times SU(N)$ gauge theory coupled to bifundamental chiral superfields $A_1, A_2, B_1, B_2$, each having $R$-charge 1/2. Under the $SU(2)_A \times SU(2)_B$ global symmetry, the superfields transform as doublets. If we further add $M$ D5-branes wrapped over the two-cycle inside $T^{1,1}$, then the gauge group changes to $SU(N+M) \times SU(N)$, giving a cascading gauge theory [105, 106]. The metric remains of the form (5.29), but the warp factor is modified to [106]

$$h(r) = \frac{27\pi(\alpha')^2}{4r^4}\Big[g_s N + b(g_s M)^2 \ln\Big(\frac{r}{r_0}\Big) + \frac{1}{4}b(g_s M)^2\Big] \ , \tag{5.31}$$

with $b \equiv \frac{3}{2\pi}$, and $r_0 \sim \varepsilon^{2/3} e^{2\pi N/(3g_s M)}$. If an extra D3-brane is added at small $r$, it produces a small change of the warp factor, $\delta h = \frac{27\pi g_s(\alpha')^2}{4r^4} + \mathcal{O}(r^{-11/2})$. A precise determination of $\delta h$ on the conifold, using the Green's function method, is one of our goals in this chapter. As discussed above, this needs to be integrated over a supersymmetric four-cycle.

**5.1. Supersymmetric Four-Cycles in the Conifold.** The complex coordinates $w_i$ can be related to the real coordinates $(r, \theta_i, \phi_i, \psi)$ via

$$w_1 = r^{3/2} e^{\frac{i}{2}(\psi-\phi_1-\phi_2)} \sin\frac{\theta_1}{2} \sin\frac{\theta_2}{2}\,, \tag{5.32}$$

$$w_2 = r^{3/2} e^{\frac{i}{2}(\psi+\phi_1+\phi_2)} \cos\frac{\theta_1}{2} \cos\frac{\theta_2}{2}\,, \tag{5.33}$$

$$w_3 = r^{3/2} e^{\frac{i}{2}(\psi+\phi_1-\phi_2)} \cos\frac{\theta_1}{2} \sin\frac{\theta_2}{2}\,, \tag{5.34}$$

$$w_4 = r^{3/2} e^{\frac{i}{2}(\psi-\phi_1+\phi_2)} \sin\frac{\theta_1}{2} \cos\frac{\theta_2}{2}\,. \tag{5.35}$$

It was shown in [9] that the following holomorphic four-cycles admit supersymmetric D7-branes:[15]

$$f(w_i) \equiv \prod_{i=1}^{4} w_i^{p_i} - \mu^P = 0\,. \tag{5.36}$$

Here $p_i \in \mathbb{Z}$, $P \equiv \sum_{i=1}^4 p_i$, and $\mu \in \mathbb{C}$ are constants defining the embedding of the D7-branes. In real coordinates the embedding condition (5.36) becomes

$$\psi(\phi_1, \phi_2) = n_1\phi_1 + n_2\phi_2 + \psi_s\,, \tag{5.37}$$

$$r(\theta_1, \theta_2) = r_{\min}\left[x^{1+n_1}(1-x)^{1-n_1} y^{1+n_2}(1-y)^{1-n_2}\right]^{-1/6}\,, \tag{5.38}$$

where

$$r_{\min}^{3/2} \equiv |\mu|\,, \tag{5.39}$$

$$\frac{1}{2}\psi_s \equiv \arg(\mu) + \frac{2\pi s}{P}\,, \quad s \in \{0, 1, \ldots, P-1\}\,. \tag{5.40}$$

We have defined the coordinates

$$x \equiv \sin^2\frac{\theta_1}{2}\,, \quad y \equiv \sin^2\frac{\theta_2}{2} \tag{5.41}$$

[15]This is not an exhaustive list: another holomorphic embedding was used in [114].

and the rational winding numbers

$$n_1 \equiv \frac{p_1 - p_2 - p_3 + p_4}{P}\,, \quad n_2 \equiv \frac{p_1 - p_2 + p_3 - p_4}{P}\,. \tag{5.42}$$

To compute the integral over the four-cycle we will need the volume form on the wrapped D7-brane, which is

$$\mathrm{d}\theta_1\mathrm{d}\theta_2\mathrm{d}\phi_1\mathrm{d}\phi_2\,\sqrt{g^{ind}} = \frac{V_{T^{1,1}}}{16\pi^3}\,r^4\,\mathcal{G}(x,y)\,\mathrm{d}x\mathrm{d}y\mathrm{d}\phi_1\mathrm{d}\phi_2\,, \tag{5.43}$$

where

$$\begin{aligned}\mathcal{G}(x,y) &\equiv \frac{(1+n_1)^2}{2}\frac{1}{x(1-x)} - 2n_1\frac{1}{1-x} \\ &+ \frac{(1+n_2)^2}{2}\frac{1}{y(1-y)} - 2n_2\frac{1}{1-y} - 1\,.\end{aligned} \tag{5.44}$$

In (5.43) we defined the volume of $T^{1,1}$

$$V_{T^{1,1}} \equiv \int \mathrm{d}^5\Psi\sqrt{g_{T^{1,1}}} = \frac{16\pi^3}{27}\,, \tag{5.45}$$

with $\Psi$ standing for all five angular coordinates on $T^{1,1}$.

For applications to brane inflation, we are interested in four-cycles that do not reach the tip of the conifold ($|n_i| \leq 1$). This condition is obeyed when the $p_i$ are nonnegative, and we shall restrict to this case for the remainder of the chapter. Two particularly simple special cases of (5.36) are:

- *Ouyang embedding* [133]: $w_1 = \mu\,.$
- *Karch-Katz embedding* [99]: $w_1 w_2 = \mu^2\,.$

Analogous supersymmetric four-cycles are known [50] in some more complicated asymptotically conical spaces, such as cones over $Y^{p,q}$ manifolds. We will consider this case in §5.4 and in Appendix D.

**5.2. Relation to the Dual Gauge Theory Computation.** The calculation of $\delta h$ and its integration over a holomorphic four-cycle is not sensitive to the background warp factor. Let us discuss a gauge theory interpretation of the calculation when we choose the background warp factor from (5.30), *i.e.* we ignore the effect of $M$ wrapped D5-branes. Here the gauge theory is exactly conformal, and we may invoke the AdS/CFT correspondence to give a simple meaning to the multipole expansion of $\delta h$,

$$\delta h = \frac{27\pi g_s(\alpha')^2}{4r^4}\left[1+\sum_i \frac{c_i f_i(\theta_1,\theta_2,\phi_1,\phi_2,\psi)}{r^{\Delta_i}}\right] . \tag{5.46}$$

In the dual gauge theory, the $c_i$ are proportional to the expectation values of gauge-invariant operators $\mathcal{O}_i$ determined by the position of the D3-brane [108]. Among these operators a special role is played by the chiral operators of $R$-charge $k$, $\mathrm{Tr}[A_{\alpha_1}B_{\dot\beta_1}A_{\alpha_2}B_{\dot\beta_2}\ldots A_{\alpha_k}B_{\dot\beta_k}]$, symmetric in both the dotted and the undotted indices. These operators have exact dimensions $\Delta_i^{\rm chiral}=3k/2$ and transform as $(k/2,k/2)$ under the $SU(2)_A\times SU(2)_B$ symmetry. In addition to these operators, many non-chiral operators, whose dimensions $\Delta_i$ are not quantized [81], acquire expectation values and therefore affect the multipole expansion of the warp factor. But remarkably, *all* these non-chiral contributions vanish upon integration over a holomorphic four-cycle. Therefore, the contributing terms in $\delta h$ have the simple form [108]

$$\delta h_{\rm chiral} = \frac{27\pi g_s(\alpha')^2}{4r^4}\left[1+\sum_{k=1}^{\infty}\frac{(f_{a_1\ldots a_k}\widehat{z}_{a_1\ldots a_k}+c.c.)}{r^{3k/2}}\right] , \tag{5.47}$$

where $f_{a_1\ldots a_k}\sim \bar\epsilon_{a_1}\bar\epsilon_{a_2}\ldots\bar\epsilon_{a_k}$ for a D3-brane positioned at $z_a=\epsilon_a$. Above, $\widehat{z}_{a_1\ldots a_k}$ are the normalized spherical harmonics on $T^{1,1}$ that transform as $(k/2,k/2)$ under the $SU(2)_A\times SU(2)_B$. The normalization factors are defined in Appendix B.

The leading term in (5.46), which falls off as $1/r^4$, gives a logarithmic divergence at large $r$ when integrated over a four-cycle. We note that this term does not appear if we define $\delta h$ as the solution of (5.18) with $\sqrt{g}\,\rho_{bg}(Y)=\delta^{(6)}(Y-X_0)$. This corresponds to evaluating the change in the warp factor, $\delta h$, created by moving the D3-brane to

$X$ from some reference point $X_0$. If we choose the reference point $X_0$ to be at the tip of the cone, $r = 0$, then (5.46) is modified to

$$\delta h = \frac{27\pi g_s(\alpha')^2}{4r^4}\left[\sum_i \frac{c_i f_i(\theta_1,\theta_2,\phi_1,\phi_2,\psi)}{r^{\Delta_i}}\right] . \tag{5.48}$$

An advantage of this definition is that now there is a precise correspondence between our calculation and the expectation values of operators in the dual gauge theory.

**5.3. Results for the Conifold.** We are now ready to compute the D3-brane-dependent correction to the warped volume of a supersymmetric four-cycle in the conifold. Using the Green's function on the singular conifold (B.9), which we derive in Appendix B, and the explicit form of the induced metric $\sqrt{g^{ind}}$ (5.43), we carry out integration term by term and find that most terms in (5.14) do not contribute. We relegate the details of this computation to Appendix C. As we demonstrate in Appendix C, the terms that do not cancel are precisely those corresponding to (anti)chiral deformations of the dual gauge theory.

Integrating (5.48) term by term as prescribed in (5.14), we find that the final result for a general embedding (5.36) is

$$T_3\,\delta V^w_{\Sigma_4} = T_3\,\mathrm{Re}\,(\zeta(w_i)) = -\mathrm{Re}\left(\ln\left[\frac{\mu^P - \prod_{i=1}^4 w_i^{p_i}}{\mu^P}\right]\right) , \tag{5.49}$$

so that

$$A = A_0\left(\frac{\mu^P - \prod_{i=1}^4 w_i^{p_i}}{\mu^P}\right)^{1/n} . \tag{5.50}$$

Comparing to (5.36), we see that $A$ is proportional to a power of the holomorphic equation that specifies the embedding. For $n = N_{D7}$ coincident D7-branes, this power is $1/n$. This behavior agrees with the results of [71]; note in particular that when $n = 1$, (5.50) has a simple zero everywhere on the four-cycle, as required by [71].

Finally, let us specialize to the two cases of particular interest, the Ouyang [133] and Karch-Katz [99] embeddings in which the four-cycle does not reach all the way

to the tip of the throat. For the Ouyang embedding we find

$$A(w_1) = A_0 \left( \frac{\mu - w_1}{\mu} \right)^{1/n} , \tag{5.51}$$

whereas for the Karch-Katz embedding we have

$$A(w_1, w_2) = A_0 \left( \frac{\mu^2 - w_1 w_2}{\mu^2} \right)^{1/n} . \tag{5.52}$$

**5.4. Results for $Y^{p,q}$ Cones.** Recently, a new infinite class of Sasaki-Einstein manifolds $Y^{p,q}$ of topology $S^2 \times S^3$ was discovered [73, 74]. The $\mathcal{N} = 1$ superconformal gauge theories dual to $AdS_5 \times Y^{p,q}$ were constructed in [30]. These quiver theories, which live on $N$ D3-branes at the apex of the Calabi-Yau cone over $Y^{p,q}$, have gauge groups $SU(N)^{2p}$, bifundamental matter, and marginal superpotentials involving both cubic and quartic terms. Addition of $M$ D5-branes wrapped over the $S^2$ at the apex produces a class of cascading gauge theories whose warped cone duals were constructed in [86]. A D3-brane moving in such a throat could also serve as a model of D-brane inflation [65].

Having described the calculation for the singular conifold in some detail, we now cite the results of an equivalent computation for cones over $Y^{p,q}$ manifolds. More details can be found in Appendix D.

Supersymmetric four-cycles in $Y^{p,q}$ cones are defined by the following embedding condition [50]

$$f(w_i) \equiv \prod_{i=1}^{3} w_i^{p_i} - \mu^{2p_3} = 0 \, , \tag{5.53}$$

where the complex coordinates $w_i$ are defined in Appendix D. Integration of the Green's function over the four-cycle leads to the following result for the perturbation to the warped volume

$$T_3 \, \delta V^w_{\Sigma_4} = T_3 \, \mathrm{Re} \left( \zeta(w_i) \right) = -\mathrm{Re} \left( \ln \left[ \frac{\mu^{2p_3} - \prod_{i=1}^{3} w_i^{p_i}}{\mu^{2p_3}} \right] \right) , \tag{5.54}$$

so that

$$A = A_0 \left( \frac{\mu^{2p_3} - \prod_{i=1}^{3} w_i^{p_i}}{\mu^{2p_3}} \right)^{1/n} . \tag{5.55}$$

**5.5. General Compactifications.** The arguments in [71], which were based on studying the change in the theta angle as one moves the D3-brane around the D7-branes, indicate that the correction is a section of a bundle called the 'divisor bundle'. This section has a zero at the location of the D7-branes. The correction has to live in a non-trivial bundle since a holomorphic function on a compact space would be a constant. In the non-compact examples we considered above we can work in only one coordinate patch and obtain the correction as a simple function, the function characterizing the embedding. Strictly speaking, the arguments in [71] were made for the case that the superpotential is generated by wrapped D3-instantons. But the same arguments can be used to compute the correction for the gauge coupling on D7-branes.

In summary, we have explicitly computed the modulus of $A$, and found a result in perfect agreement with the analysis of the phase of $A$ in [71]. One has a general answer of the form

$$A(w_i) = A_0 \left( f(w_i) \right)^{1/n} , \tag{5.56}$$

where $f$ is a section of the divisor bundle and $f(w_i) = 0$ specifies the location of the D7-branes.

## 6. Compactification Effects

**6.1. Holomorphy of the Gauge Coupling.** In compactifications with mobile D3-branes, the identification of holomorphic Kähler moduli and holomorphic gauge couplings is quite subtle. This has become known as the 'rho problem' [32].[16] Let us recall the difficulty. In the internal metric $g_{ij}$ appearing in (5.5), we can identify the

[16]Similar issues were discussed in [162].

breathing mode of the compact space via

$$\mathrm{d}s^2 = h^{-1/2}(Y)e^{-6u}g_{\mu\nu}\mathrm{d}x^\mu \mathrm{d}x^\nu + h^{1/2}(Y)e^{2u}\tilde{g}_{ij}\mathrm{d}Y^i\mathrm{d}Y^j\,. \tag{5.57}$$

Here $\tilde{g}_{ij}$ is a fiducial metric for the internal space, $e^{2u}$ is the breathing mode, and $g_{\mu\nu}$ is the four-dimensional Einstein-frame metric. In the following, all quantities computed from $\tilde{g}_{ij}$ will be denoted by a tilde. The Born-Infeld kinetic term for a D3-brane, expressed in Einstein frame and in terms of complex coordinates $X, \bar{X}$ on the brane configuration space, is then

$$S_{\mathrm{kin}} = -T_3 \int \mathrm{d}^4x\sqrt{-g}e^{-4u}\partial_\mu X^i \partial^\mu \bar{X}^{\bar{j}}\tilde{g}_{i\bar{j}}\,. \tag{5.58}$$

DeWolfe and Giddings argued in [58] that to reproduce this volume scaling, as well as the known no-scale, sequestered property of the D3-brane action in this background, the Kähler potential must take the form

$$\kappa^2\mathcal{K} = -3\ln e^{4u}\,, \tag{5.59}$$

with the crucial additional requirement that

$$\partial_i\partial_{\bar{j}}e^{4u} \propto \tilde{g}_{i\bar{j}}\,, \tag{5.60}$$

so that $e^{4u}$ contains a term proportional to the Kähler potential $k(X,\bar{X})$ for the fiducial Calabi-Yau metric. Comparing (5.58) to the kinetic term derived from (5.59), we find in fact

$$\partial_i\partial_{\bar{j}}e^{4u} = -\left(\frac{\kappa^2 T_3}{3}\right)k_{,i\bar{j}}\,. \tag{5.61}$$

We can now define the holomorphic volume modulus $\rho$ as follows. The real part of $\rho$ is given by

$$\rho + \bar{\rho} \equiv e^{4u} + \left(\frac{\kappa^2 T_3}{3}\right)k(X,\bar{X}) \tag{5.62}$$

and the imaginary part is the axion from the Ramond-Ramond four-form potential. As explained in [95], this is consistent with the fact that the axion moduli space is a circle that is non-trivially fibered over the D3-brane moduli space.

Next, the gauge coupling on a D7-brane is easily seen to be proportional to the breathing mode of the metric, $e^{4u} \equiv \rho + \bar{\rho} - \left(\frac{1}{3}\kappa^2 T_3\right) k(X, \bar{X})$, which is *not* the real part of a holomorphic function on the brane moduli space. However, supersymmetry requires that the gauge kinetic function is a holomorphic function of the moduli. This conflict is the rho problem.

We can trace this problem to an incomplete inclusion of the backreaction due to the D3-brane. Through (5.62), the physical volume modulus $e^{4u}$ has been allowed to depend on the D3-brane position. That is, the difference between the holomorphic modulus $\rho$ and the physical modulus $e^{4u}$ is affected by the D3-brane position. This was necessary in order to recover the known properties of the brane/volume moduli space. Notice from (5.62) that the strength of this open-closed mixing is controlled by $\kappa^2 T_3$, and so is manifestly a consequence of D3-brane backreaction in the compact space. However, as we explained in §3, the warp factor $h$ also depends on the D3-brane position, again via backreaction. To include the effects of the brane on the breathing mode, but not on the warp factor, is not consistent.[17] One might expect that consideration of the correction $\delta h$ to the warp factor would restore holomorphy and resolve the rho problem. This was suggested in [77], and we now carry out an explicit calculation that confirms this.

What we find is that the uncorrected warped volume $(V^w_{\Sigma_4})_0$, as well as the correction $\delta V^w_{\Sigma_4}$, are both non-holomorphic, but their non-holomorphic pieces precisely cancel, so that the *corrected* warped volume $V^w_{\Sigma_4}$ is the real part of a holomorphic function of the moduli $\rho$ and $X$.

[17] Let us point out that this is precisely the closed-string dual of the resolution found in [32]: careful inclusion of the open-string one-loop corrections to the gauge coupling resolved the rho problem. In that language, the initial inconsistency was the inclusion of only some of the one-loop effects.

First, we separate the constant, zero-mode, piece of the warp factor:

$$h(X;Y) = h_0 + \delta h(X;Y)\,. \tag{5.63}$$

By definition $\delta h(X;Y)$ integrates to zero over the compact manifold,

$$\int \mathrm{d}^6 Y \sqrt{g(Y)}\,\delta h(X;Y) = 0\,. \tag{5.64}$$

This implies that the factor of the volume that appears in the four-dimensional Newton constant is unaffected by $\delta h$. Thus we have $\kappa^{-2} = \kappa_{10}^{-2} h_0 \tilde{V}_6$. We define the uncorrected warped volume via

$$(V^w_{\Sigma_4})_0 \equiv \int_{\Sigma_4} \mathrm{d}^4\xi \sqrt{g^{ind}}\, h_0 = e^{4u(X,\bar{X})}\, h_0\, \tilde{V}_{\Sigma_4}\,. \tag{5.65}$$

This is non-holomorphic because of the prefactor $e^{4u(X,\bar{X})}$. In particular, using (5.62), we have

$$(V^w_{\Sigma_4})_0 = -\left(\frac{\kappa^2 T_3}{3}\right) \tilde{V}_{\Sigma_4}\, h_0\, k(X,\bar{X}) + [\text{hol.} + \text{antihol.}]\,. \tag{5.66}$$

We next consider $\delta h$. When the D3-brane is not coincident with the four-cycle of interest, we find from (5.22) that $\delta h$ obeys

$$\nabla^2_X \delta h(X;Y) = \frac{\mathcal{C}}{V_6} \tag{5.67}$$

where $\mathcal{C} \equiv 2\kappa_{10}^2 T_3 = 2\kappa^2 T_3 h_0 \tilde{V}_6$. Hence, $\delta h$ is *not* the real part of a holomorphic function of $X$. The source of the deviation from holomorphy is the term $\frac{1}{V_6}$ in (5.22). Although this term is superficially similar to a constant background charge density, it is independent of the density $\rho_{bg}(Y)$ of physical D3-brane charge in the internal space, which has coordinates $Y$. Instead, $\frac{1}{V_6}$ may be thought of as a 'background charge' on the D3-brane moduli space, which has coordinates $X$. From this perspective, it is the Gauss's law constraint on the D3-brane moduli space that forces $\delta h$ to be non-holomorphic.

In complex coordinates, using the metric $\tilde{g}$, and noting that $\tilde{V}_6 = V_6\, e^{-6u}$, (5.67) may be written as

$$\tilde{g}^{i\bar{j}}\partial_i\partial_{\bar{j}}\delta h = \kappa^2 T_3\, h_0\, e^{-4u}\,, \tag{5.68}$$

where because the compact space is Kähler, we can write the Laplacian using partial derivatives. It follows that, to leading order in $\kappa^2$,

$$\delta h = \left(\frac{\kappa^2 T_3}{3}\right) h_0\, e^{-4u} k(X,\bar{X}) + [\text{hol.} + \text{antihol.}]\,. \tag{5.69}$$

The omitted holomorphic and antiholomorphic terms are precisely those that we computed in the preceding sections. Furthermore, recalling the definition (5.14), we have

$$\delta V^w_{\Sigma_4} = \left(\frac{\kappa^2 T_3}{3}\right) h_0\, \tilde{V}_{\Sigma_4} k(X,\bar{X}) + [\zeta(X) + \overline{\zeta(X)}]\,. \tag{5.70}$$

The non-holomorphic first term in (5.70) precisely cancels the non-holomorphic term in $(V^w_{\Sigma_4})_0$ (5.66), so that

$$V^w_{\Sigma_4} = (V^w_{\Sigma_4})_0 + \delta V^w_{\Sigma_4} = \tilde{V}_{\Sigma_4}\, h_0\, (\rho + \bar{\rho}) + [\zeta(X) + \overline{\zeta(X)}]\,. \tag{5.71}$$

We conclude that $V^w_{\Sigma_4}$ can be the real part of a holomorphic function.[18] This supports the role of the warped four-volume in the definition of holomorphic coordinates proposed in [77].

To summarize, we have seen that the background charge term in (5.22), which was required by a constraint analogous to Gauss's law on the D3-brane moduli space, causes $\delta V^w_{\Sigma_4}$ to have a non-holomorphic term proportional to $k(X,\bar{X})$. Furthermore, the DeWolfe-Giddings Kähler potential produces a well-known non-holomorphic term, also proportional to $k(X,\bar{X})$, in the uncorrected warped volume $(V^w_{\Sigma_4})_0$. We found that these two terms precisely cancel, so that the total warped volume $V^w_{\Sigma_4} = (V^w_{\Sigma_4})_0 +$

[18] Strictly speaking, we have shown only that $V^w_{\Sigma_4}$ is in the kernel of the Laplacian; the r.h.s. of (5.69) and (5.71) could in principle contain extra terms that are annihilated by the Laplacian but are not the real parts of holomorphic functions. However, the obstruction to holomorphy presented by $k(X,\bar{X})$ has disappeared, and we expect no further obstructions.

$\delta V_{\Sigma_4}^w$ can be holomorphic. Thus, the corrected gauge coupling on D7-branes, and the corrected Euclidean D3-brane action, are holomorphic.[19]

Note that, as a consequence of this discussion, the holomorphic part of the correction to the volume changes under Kähler transformations of $k(X, \bar{X})$. This implies that the correction is in a bundle whose field strength is proportional to the Kähler form.

**6.2. Model-Dependent Effects from the Bulk.** In §2.2, we listed three contributions to the potential for D3-brane motion. The first two were given explicitly in [95], and we have computed the third. It is now important to ask whether this is an exhaustive list: in other words, might there be further effects that generate D3-brane mass terms of order $H$? In particular, could coupling of the throat to a compact bulk generate corrections to our results, and hence adjust the brane potential?[20]

First, let us justify our approach of using noncompact warped throats to model D3-brane potentials in compact spaces with finite warped throat regions. The idea is that the effect of the D3-brane on a four-cycle is localized in that portion of the four-cycle that is deepest in the throat. Comparing (5.43) to (5.48), we see that all corrections to the warped volume scale inversely with $r$, and are therefore supported in the infrared region of the throat. Hence, as anticipated in §4.3, the effects of interest are automatically concentrated in the well-understood region of high warping, far from the model-dependent region where the throat is glued into the rest of the compact space. This is true even though a typical four-cycle will have most of its volume in the bulk, outside the highly warped region. The perturbation due to the D3-brane already falls off faster than $r^{-4}$ in the throat, where the measure factor is $r^4$, and in the bulk the perturbation will diminish even more rapidly. Except in remarkable

[19]To complete the identification of the holomorphic variable, we note that the constant $a$ appearing in (5.1) is $a \equiv 2T_3\tilde{V}_{\Sigma_4}h_0/n$. The resulting dependence on $g_s$ could be absorbed by a redefinition of $\rho$, as in [93].

[20]The bulk corrections considered in [1] are generically smaller than those we consider here.

cases, the diminution of the perturbation will continue to dominate the growth of the measure factor. A similar argument reinforces our assertion that the dominant effect on a D3-brane comes from whichever wrapped brane descends farthest into the throat.

We conclude that the effects of the gluing region, where the throat meets the bulk, and of the bulk itself, produce negligible corrections to the terms we have computed. Fortunately, the leading effects are concentrated in the highly warped region, where one has access to explicit metrics and can do complete computations.

We have now given a complete account of the nonperturbative superpotential. However, the Kähler potential is not protected against perturbative corrections, which could conceivably contribute to the low-energy potential for D3-brane motion. Explicit results are not available for general compact spaces (see, however, [33, 75]); here we will simply argue that these corrections can be made subleading. Recall that the DeWolfe-Giddings Kähler potential provides a mixing between the volume and the D3-brane position that generates brane mass terms of order $H$. Any *further* corrections to the Kähler potential, whether from string loops or sigma-model loops, will be subleading in the large-volume, weak-coupling limit, and will therefore generically give mass terms that are small compared to $H$. In addition, the results of [70] give some constraints on $\alpha'$ corrections to warped throat geometries. We leave a systematic study of this question for the future.

## 7. Implications and Conclusion

We have used a supergravity approach (see also [77]) to study the D3-brane corrections to the nonperturbative superpotential induced by D7-branes or Euclidean D3-branes wrapping four-cycles of a compactification. This has been a key, unknown element of the potential governing D3-brane motion in such a compactification. We integrated the perturbation to the background warping due to the D3-brane over the wrapped four-cycle. The resulting position-dependent correction to the warped

four-cycle volume modifies the strength of the nonperturbative effect, which in turn implies a force on the D3-brane. This computation is the closed-string channel dual of the threshold correction computation of [32], and we showed that the closed-string method efficiently reproduces the results of [32].

We then investigated the D3-brane potential in explicit warped throat backgrounds with embedded wrapped branes. We showed that for holomorphic embeddings, only those deformations corresponding to (anti)chiral operators in the dual gauge theory contribute to correcting the superpotential. This led to a strikingly simple result: the superpotential correction is given by the embedding condition for the wrapped brane, in accord with [71].

An important application of our results is to cosmological models with moving D3-branes, particularly warped brane inflation models [95]. It is well-known that these models suffer from an eta problem and hence produce substantial inflation only if the inflaton mass term is fine-tuned to fall in a certain range. Our result determines a 'missing' contribution to the inflaton potential that was discussed in [95], but was not computed there. Equipped with this contribution, one can quantify the fine-tuning in warped brane inflation by considering specific choices of throat geometries and of embedded wrapped branes, and determining whether prolonged inflation occurs [19]. This amounts to a microscopically justified method for selecting points or regions within the phenomenological parameter space described in [69]. This approach was initiated in [32], but the open-string method used there does not readily extend beyond toroidal orientifolds, and is especially difficult for warped throats in flux compactifications. In contrast, our concrete computations were performed in warped throat backgrounds, and thus apply directly to warped brane inflation models, including backgrounds with fluxes.

Our approach also led to an explicit solution of the 'rho problem', *i.e.* the apparent non-holomorphy of the gauge coupling on wrapped D7-branes in backgrounds with

D3-branes. This problem arises from incomplete inclusion of D3-brane backreaction effects, and in particular from omission of the correction to the warped volume that we computed in this work. We observed that the correction is itself non-holomorphic, as a result of a Gauss's law constraint on the D3-brane moduli space. Moreover, the non-holomorphic correction cancels precisely against the non-holomorphic term in the uncorrected warped volume, leading to a final gauge kinetic function that is holomorphic.

Let us emphasize that the problem of fine-tuning in D-brane inflation models has *not* disappeared, but can now be made more explicit. A detailed analysis of this will be presented in Chapters 6 and 7.

CHAPTER 6

# Compactification Obstacles to D-brane Inflation

We proceed by analyzing the cosmological implications of the results of the previous chapter. This chapter summarizes our findings,[1] while in the next chapter we present more technical aspects of our computations.

## 1. Introduction

String theory is a promising candidate for the theoretical underpinning of the inflationary paradigm [3, 83, 120], but explicit and controllable models of inflation in string theory have remained elusive. In this chapter we ask whether explicit working models are possible in the setting of slow-roll warped D-brane inflation [64, 95], in which the inflaton field is identified with the location of a mobile D3-brane in a warped throat region [105] of the compactification manifold. As explained in Chapter 5, moduli stabilization introduces potentially fatal corrections to the inflaton potential in this scenario. Some of these corrections arise from complicated properties of the compactification [32] and have been computed only recently [18].

The attitude taken in most of the literature on the subject (*cf.* [95, 118]) is that because of the vast number and complexity of string vacua, in some nonzero fraction of them it should be the case that the different corrections to the inflaton potential cancel to high precision, leaving a suitable inflationary model. This expectation or

[1]This chapter is based on Daniel Baumann, Anatoly Dymarsky, Igor Klebanov, Liam McAllister and Paul Steinhardt, "A Delicate Universe: Compactification Obstacles to D-brane Inflation", Phys. Rev. Lett. **99**, 141601 (2007).

hope has never been rigorously justified, and there is no guarantee that the correction terms can ever cancel: for example, it may be the case that the correction terms invariably have the same sign, so that no cancellation can occur. In this chapter we report the results of a systematic investigation into whether or not this hope of fine-tuned cancellation can in fact be realized. While this chapter is a non-techincal summary of our conclusions, all the technical subtleties that we had to consider are carefully spelt out in Chapter 7.

The new ingredient that makes this work possible is the result of [18] for a correction to the volume-stabilizing nonperturbative superpotential. As explained in Chapter 5, this effect corresponds to the interaction between the inflationary D3-brane and the moduli-stabilizing wrapped branes, *i.e.* D7-branes or Euclidean D3-branes wrapping a four-cycle of the Calabi-Yau. The location of these wrapped branes therefore becomes a crucial parameter in the D3-brane potential.

In a recent paper [45], Burgess et al. showed that for a particular embedding of the D7-branes, the Ouyang embedding [133], the correction to the inflaton potential from the term computed in [18] vanishes identically. In this case the potential is always too steep for inflation, independent of fine-tuning. Here, we consider a different holomorphic embedding due to Kuperstein [114]. For fine-tuned values of the microphysical parameters, the potential for radial motion of a D3-brane in this background contains an approximate inflection point around which slow-roll inflation can occur. This potential is not of the form anticipated by previous authors: the D7-brane has no effect whatsoever on the quadratic term in the inflaton potential, but instead causes the potential to flatten in a small region far from the tip of the conifold. We emphasize that arranging for this inflection point to occur inside the throat region, where the metric is known and our construction is self-consistent, imposes a severe constraint on the compactification parameters. Moreover, inflation only occurs for

a bounded range about the inflection point, which requires a high degree of control over the initial conditions of the inflaton field.

## 2. The Compactification

Our setting is a flux compactification [63, 76] of type IIB string theory on an orientifold of a Calabi-Yau threefold, or, more generally, an F-theory compactification. We suppose that the fluxes are chosen so that the internal space has a warped throat region, and that $n > 1$ D7-branes supersymmetrically wrap a four-cycle that extends into this region (see Figure 1 in Chapter 5). As a concrete example of this local geometry, we consider the warped version [105] of the deformed conifold $\sum z_i^2 = \varepsilon^2$, where $z_i$ are coordinates on $\mathbb{C}^4$. Assuming that the D3-brane is far from the tip of the conifold, we may neglect the deformation $\varepsilon$. We choose $z_\alpha = (z_1, z_2, z_3)$ as the three independent complex D3-brane coordinates, and use the conifold constraint to express $z_4$ in terms of them. We suppose that this throat is glued into a compact space, as in [76], and for simplicity we take this space to have a single Kähler modulus $\rho$. Moduli stabilization [93] relies on the fact that strong gauge dynamics on suitable D7-branes generates a nonperturbative superpotential, $W_{\rm np} = A(z_\alpha)\exp[-a\rho]$, where $a = \frac{2\pi}{n}$. The D7-brane embedding is specified by a single holomorphic equation, $f(z_\alpha) = 0$, and the result of [18] is that

$$A(z_\alpha) = A_0 \left(\frac{f(z_\alpha)}{f(0)}\right)^{1/n} , \tag{6.1}$$

where $A_0$ is independent of the D3-brane position $z_\alpha$. Including the flux superpotential [82] $W_{\rm flux} = \int G_3 \wedge \Omega \equiv W_0$, the total superpotential is $W = W_0 + A(z_\alpha)\exp[-a\rho]$.

The DeWolfe-Giddings Kähler potential [58] is[2]

$$\mathcal{K}(\rho, \bar\rho, z_\alpha, \bar z_\alpha) = -3\ln[\rho + \bar\rho - \gamma k] \equiv -3\ln U\,, \tag{6.2}$$

[2]In this chapter, we employ natural units where $M_{\rm pl}^{-2} = 8\pi G \equiv 1$.

where $k(z_\alpha, \bar{z}_\alpha)$ is the Kähler potential of the Calabi-Yau space, and $\gamma$ is a constant [19]. Well inside the throat but far from the tip, we may use the Kähler potential of the conifold [49],

$$k = \frac{3}{2}\left(\sum_{i=1}^{4}|z_i|^2\right)^{2/3} = \frac{3}{2}r^2\,. \tag{6.3}$$

Then the F-term potential is [19, 45]

$$\begin{aligned} V_F &= \frac{1}{3U^2}\Bigg[(\rho+\bar{\rho})|W_{,\rho}|^2 - 3(\overline{W}W_{,\rho} + c.c.) \\ &\quad + \frac{3}{2}(\overline{W_{,\rho}}z^\alpha W_{,\alpha} + c.c.) + \frac{1}{\gamma}k^{\alpha\bar{\beta}}W_{,\alpha}\overline{W_{,\beta}}\Bigg]\,, \end{aligned} \tag{6.4}$$

where

$$k^{\alpha\bar{\beta}} = r\left[\delta^{\alpha\bar{\beta}} + \frac{1}{2}\frac{z_\alpha\bar{z}_\beta}{r^3} - \frac{z_\beta\bar{z}_\alpha}{r^3}\right]. \tag{6.5}$$

To this we add the contribution of an anti-D3-brane at the tip of the deformed conifold [95],

$$V_D = D(r)U^{-2}\,, \qquad D(r) \equiv D\left(1 - \frac{3D}{16\pi^2}\frac{1}{(T_3 r^2)^2}\right)\,, \tag{6.6}$$

where $D = 2T_3/h_0$, $T_3$ is the D3-brane tension, and $h_0$ is the KS warp factor at the tip.

## 3. Towards Fine-Tuned Inflation

To derive the effective single-field potential, we consider radial trajectories that are stable in the angular directions, so that the dynamics of the angular fields becomes trivial. We also integrate out the massive volume modulus, incorporating the crucial fact that the volume shifts as the D3-brane moves [19]. Then the canonically normalized inflaton field $\phi = r\sqrt{\frac{3}{2}T_3}$ parameterizes the motion along the radial direction of the throat. To investigate the possibility of sustained inflation, we consider the slow-roll parameter $\eta = V''/V$. We find $\eta = \frac{2}{3} + \Delta\eta(\phi)$, where $\Delta\eta$ arises from the dependence (6.1) of the superpotential on $\phi$. Slow-roll inflation is possible near

$\phi = \phi_0$ if $\Delta\eta(\phi_0) \approx -\frac{2}{3}$. Here, using the explicit result of [18] for $A(\phi)$, we compute $\Delta\eta$ and determine whether the full potential can be flat enough for inflation.[3]

A reasonable expectation implicit in prior work on the subject is that there exist fine-tuned values of the microphysical parameters for which $\Delta\eta(\phi) \approx -\frac{2}{3}$, *i.e.* the correction to the inflaton potential arising from $A(\phi)$ includes a term quadratic in $\phi$, which, for a fine-tuned value of its coefficient, causes $\eta$ to be small for a considerable range of $\phi$. However, we make the important observation that the functional form of (6.1) implies that there is actually *no* purely quadratic correction. To see this we note that $A$ is a holomorphic function of the $z_\alpha$ coordinates, which, by (6.3), scale with radius as $z_\alpha \propto \phi^{3/2}$. Thus, the presence of $A(\phi)$ in the form (6.1) does not lead to new quadratic terms in (7.13). This is concrete evidence against the hope of a fine-tuned cancellation of the inflaton mass over an extended range of $\phi$.

However, as we now explain, there exists a simple example in which a different sort of cancellation can occur. Kuperstein [114] studied the D7-brane embedding $z_1 = \mu$, where we may assume that $\mu \in \mathbb{R}^+$. This embedding, and the potential in this background, preserve an $SO(3)$ subgroup of the $SO(4)$ global symmetry acting on the $z_i$ coordinates of the deformed conifold. To find a purely radial trajectory that is stable in the angular directions, we consider the variation $\delta z_1$ while keeping the radius $r$ fixed. We then require the first variation of the potential $\delta V = V(z_1 + \delta z_1, r, \rho) - V(z_1, r, \rho)$ to vanish for all $r$ and the second variation $\delta^2 V$ to be non-negative. The extremality constraint $\delta V = 0$ specifies the radial trajectory $z_1 = \pm\frac{1}{\sqrt{2}} r^{3/2}$, $z_2 = \pm i z_1$. A detailed study of the angular mass matrix $\delta^2 V$ reveals that the trajectory along $z_1 = +\frac{1}{\sqrt{2}} r^{3/2}$ is unstable, while the potential along the negative axis, $z_1 = -\frac{1}{\sqrt{2}} r^{3/2}$, is stable in all angular directions. After integrating out the imaginary part of the Kähler modulus

[3]For the special case of the Ouyang embedding, $z_1 + i z_2 = \mu$, Burgess et al. proved a simple no-go result for fine-tuned brane inflation [45]. They found that for this particular example, $\Delta\eta$ vanishes along the angularly stable trajectory. We have found similar 'delta-flat' trajectories [19] for all embeddings in the infinite class studied in [9]. These trajectories cannot support slow-roll inflation, no matter how the parameters of the potential are tuned. Here, we study an embedding for which there is no delta-flat direction.

$\rho$, the potential is given in terms of the radius $r$ (or the canonical inflaton $\phi$) and the real-valued volume modulus $\sigma \equiv \frac{1}{2}(\rho + \bar{\rho})$, as [19]

$$V(\phi,\sigma) = \frac{a|A_0|^2}{3}\frac{e^{-2a\sigma}}{U^2(\phi,\sigma)}g(\phi)^{2/n}\left[2a\sigma + 6 - 6e^{a\sigma}\frac{|W_0|}{|A_0|}\frac{1}{g(\phi)^{1/n}} + \frac{3c}{n}\frac{\phi}{\phi_\mu}\frac{1}{g(\phi)^2} - \frac{3}{n}\frac{1}{g(\phi)}\frac{\phi^{3/2}}{\phi_\mu^{3/2}}\right] + \frac{D(\phi)}{U^2(\phi,\sigma)}\,. \tag{6.7}$$

Here $g(\phi) \equiv \frac{f(\phi)}{f(0)} = 1 + \left(\frac{\phi}{\phi_\mu}\right)^{3/2}$, and $\phi_\mu^2 \equiv T_3(2\mu^2)^{2/3}$ denotes the minimal radial location of the D7-branes. We have also introduced $c^{-1} \equiv 4\pi\gamma(2\mu^2)^{2/3}$, used [19] $\gamma = \sigma_0 T_3/3$, and defined $U(\phi,\sigma) \equiv 2\sigma - \frac{\sigma_0}{3}\phi^2$. The parameter $\sigma_0$ is the stabilized value of the Kähler modulus in the absence of the D3-brane (or when the D3-brane is near the bottom of the throat). Now, for each value of $\phi$ we carry out a constrained minimization of the potential to find $\sigma_\star(\phi)$, *i.e.* we find $\sigma_\star(\phi)$ such that $\frac{\partial V}{\partial \sigma}\big|_{\sigma_\star(\phi)} = 0$. The function $\sigma_\star(\phi)$ may either be computed numerically or fitted to high accuracy by the approximate expression [19]

$$\sigma_\star(\phi) \approx \sigma_0\left[1 + \frac{1}{n\,a\sigma_0}\left(1 - \frac{1}{2a\sigma_0}\right)\left(\frac{\phi}{\phi_\mu}\right)^{3/2}\right]. \tag{6.8}$$

Substituting $\sigma_\star(\phi)$ into (6.7), we find the effective single-field potential $\mathbb{V}(\phi) \equiv V(\phi,\sigma_\star(\phi))$.

For generic values of the compactification parameters, $\mathbb{V}$ has a metastable minimum at some distance from the tip. In fact, one can show that the potential has negative curvature near the tip and positive curvature far away, so that by continuity, $\eta$ vanishes at some intermediate value $\phi_0$. Then, one can find fine-tuned values of the D7-brane position $\phi_\mu$ for which this minimum is lifted to become an inflection point (see Figure 2). This transition from metastability to monotonicity guarantees that $\epsilon = \frac{1}{2}(V'/V)^2$ can be made extremely small, so that prolonged slow-roll inflation is possible. In our scenario, then, the potential contains an approximate inflection point

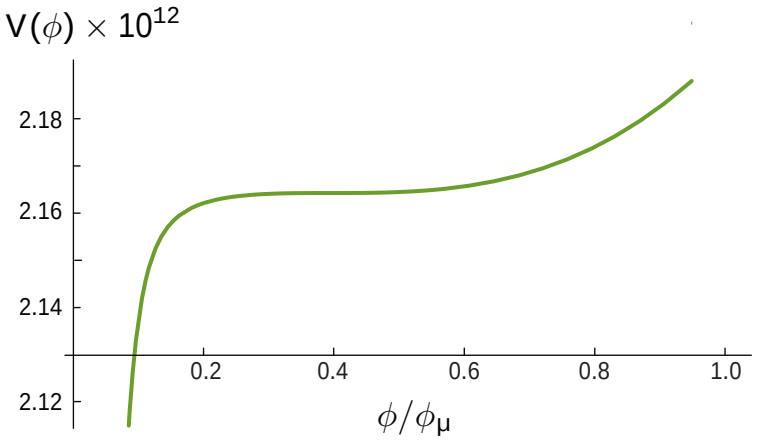


FIGURE 1. **Example of Inflation near an Inflection Point.** *Compactification data*: $n = 8$, $\phi_\mu = \frac{1}{4}$, $A_0 = 1$, $a\sigma_0 = 10$, $W_0 = -\frac{1}{3}e^{-2a\sigma_0}(2a\sigma_0 + 3)$, $D = 1.1 \times \frac{2a^2}{3}\sigma_0 e^{-2a\sigma_0}$.

at $\phi = \phi_0$, where $\mathbb{V}$ is very well approximated by the cubic

$$\mathbb{V} = V_0 + \lambda_1(\phi - \phi_0) + \frac{1}{3!}\lambda_3(\phi - \phi_0)^3\,, \tag{6.9}$$

for some $V_0, \lambda_1, \lambda_3$.

The number of $e$–folds derived from the effective potential (7.58) is

$$N_e(\phi) = \int_{\phi_{\rm end}}^{\phi} \frac{{\rm d}\phi}{\sqrt{2\epsilon}} = \sqrt{\frac{2V_0^2}{\lambda_1\lambda_3}}\arctan\left(\frac{V_0\eta(\phi)}{\sqrt{2\lambda_1\lambda_3}}\right)\Bigg|_{\phi_{\rm end}}^{\phi}\,. \tag{6.10}$$

Since $\eta$ is small only for a limited range of inflaton values, the number of $e$–folds is large only when $\epsilon$ is very small. This forces these models to be of the small field type. The scalar spectrum on scales accessible to cosmic microwave background (CMB) experiments can be red, scale-invariant, or blue, depending on how flat the potential is. That is, $n_s - 1 = (2\eta - 6\epsilon)|_{\phi_{\rm CMB}} \approx 2\eta(\phi_{\rm CMB})$, where $\phi_{\rm CMB}$ corresponds to the field value when observable scales exit the horizon during inflation, say between $e$-folds 55 and 60. The sign of $\eta(\phi_{\rm CMB})$, and hence of $n_s - 1$, depends on where $\phi_{\rm CMB}$ is relative to the inflection point. If inflation only lasts for the minimal number of $e$–folds to solve the horizon and flatness problems then the scalar spectrum is blue. If the potential is made more flat, so that $\epsilon$ is smaller, inflation lasts longer, and $\phi_{\rm CMB}$

is reduced, the spectrum can be red. This sensitivity to the details of the potential reduces the predictivity of the scenario.

## 4. Microscopic Constraints

A crucial consistency requirement is that the inflationary region around $\phi_0$, and the location $\phi_\mu$ of the tip of the wrapped D7-branes, should fit well inside the throat, where the metric is known. As shown in [21] (see Chapter 8), the range of $\phi$ in Planck units is geometrically limited,

$$\Delta\phi < \frac{2}{\sqrt{N}}\,, \tag{6.11}$$

where $N \gg 1$ is the background D3-brane charge of the throat. When combined with the Lyth bound [122], this yields a sharp upper bound on the tensor signal in these models [21]. Here we find that this same bound actually poses an obstacle to inflation itself: for an explicit inflationary model with the Kuperstein embedding of D7-branes, $\phi_\mu$ and $\phi_0$ must obey (6.11). Although one can find examples [19] in which this requirement is met, this imposes significant restrictions on the compactification. In particular, $N$ cannot be too large, implying that corrections to the supergravity approximation could be significant.

## 5. Conclusions

We have assessed the prospects for an explicit model of warped D-brane inflation by including the known dangerous corrections to the inflaton potential. In particular, we have studied whether the hope of fine-tuning superpotential corrections to the inflaton potential to reduce the slow-roll parameter $\eta$ can be justified. For a large class [9] of holomorphic embeddings of wrapped D7-branes there are trajectories where the potential is too steep for inflation, with no possibility of fine-tuning to avoid this conclusion [45], [19]. For the Kuperstein embedding [114], fine-tuning is possible

in principle, and inflation can occur in a small region near an inflection point of the potential. The requirement (6.11) that this inflection point lies well inside the throat provides stringent constraints on the compactification. Detailed construction of compactifications where such constraints are satisfied remains an open problem.

This study illustrates the care that must be taken in assessing the prospects for inflationary cosmology in string theory. It appeared that warped D-brane inflation involved many adjustable parameters, including the D7-brane embedding and other compactification data, and so it was reasonable to expect that working examples would exist. However, the compactification geometry constrains these microphysical parameters so that there is much less freedom to adjust the shape of the potential than simple parameter counting would suggest.

The problem of constructing a fully explicit model of inflation in string theory remains important and challenging. Diverse corrections to the potential that are negligible for many other purposes can be fatal for inflation, and one cannot reasonably claim success without understanding all these contributions. We have made considerable progress towards this goal, but have not yet succeeded: a truly exhaustive search for further corrections to the inflaton potential remains necessary.

Finally, there is a pressing need for a more natural model of string inflation than the one we have presented here.

CHAPTER 7

# Towards an Explicit Model of D-brane Inflation

For the dedicated reader this chapter presents the technical details behind the results presented in Chapter 6.[1] Appendices E, F, G, and H are an integral part of this work.

## 1. Introduction

**1.1. Review and Motivation.** In this chapter we will be concerned with making progress towards an *explicit* model of inflation in string theory, by which we mean a model in which the fields and parameters in the low-energy Lagrangian are derived from the data of a string compactification. In such a scenario, questions about the structure of the inflaton potential can be resolved by concrete string theory computations. This should be contrasted with string-inspired models constructed directly in effective field theory, for which naturalness is the final arbiter of the form of the potential. We will not quite reach the ambitious goal of an entirely explicit model of inflation derived from string theory, and indeed one main point of this work is that truly explicit models of string inflation can be rather intricate, involving multiple nontrivial microscopic constraints that are surprising from the low-energy perspective.

As before, we will work in the setting of D-brane inflation [64, 95], a promising framework that has attracted considerable interest, but in which concrete, working

[1]This chapter is based on Daniel Baumann, Anatoly Dymarsky, Igor Klebanov and Liam McAllister, "Towards an Explicit Model of D-brane Inflation", JCAP **0801**, 024 (2008).

models remain scarce. In previous chapters we reviewed that moduli stabilization gives rise to corrections to the inflaton potential. Some of these corrections arise from complicated properties of the compactification and have been computed only recently [18].[2]

The attitude taken in most of the literature on the subject (see *e.g.* [95, 118]) is that because of the vast number and complexity of string vacua, in some nonzero fraction of them it should be the case that the corrections to the inflaton potential cancel to high precision, leaving a suitable inflationary model. However, there is no guarantee that this hope can be realized: for example, the correction terms may invariably have the same sign so that no cancellation can ever occur. Moreover, the precise nature of the cancellation will affect the detailed predictions of the model. In this chapter we will systematically address the question of whether or not this hope of fine-tuned cancellation can in fact be realized. The new ingredient that makes this investigation possible is the result of Chapter 5 for the one-loop correction to the volume-stabilizing nonperturbative superpotential. As we explained in Chapter 5, this effect is due to the interaction [32, 77] between the inflationary D3-brane and the moduli-stabilizing wrapped branes, *i.e.* D7-branes wrapping a four-cycle within the Calabi-Yau threefold.[3] The location of these wrapped branes therefore becomes a crucial parameter in the D3-brane potential.

With this theoretical input we ask whether the known correction terms to the inflaton potential can indeed cancel for specific values of the microphysical input parameters. To investigate this, we study D3-brane motion in warped conifold backgrounds [105, 106] for a large class of wrapped brane embeddings. By identifying radial trajectories that are stable in the angular directions, we integrate out the angular degrees of freedom and arrive at an effective two-field potential for the inflaton –

[2]For important earlier work, see [32, 71, 77].

[3]Alternatively, one could consider Euclidean D3-branes wrapping this four-cycle. Their effect on the nonperturbative superpotential is very similar to that of the D7-branes.

corresponding to the radial direction in the throat – and the compactification volume. Because we work in a framework with explicitly stabilized moduli, the compactification volume has a positive mass-squared. However, this mass is not so large that the volume remains fixed at a single value during inflation. Instead, the minimum of the potential for the volume shifts as the D3-brane moves: the compact space shrinks slightly as the D3-brane falls down the throat. Properly incorporating this phenomenon leads to a nontrivial change in the effective single-field inflaton potential. Thus, we find that an approximation that keeps the volume fixed at its KKLT [93] minimum during inflation is not sufficiently accurate for a D-brane inflation model. Our improved approximation is that the volume changes adiabatically, remaining in an inflaton-dependent minimum, as the D3-brane moves.

Equipped with the effective single-field potential, we ask whether the trajectories that are stable in the angular directions can enjoy flat potentials. For the large class of holomorphic wrapped brane embeddings described in [9], we find trajectories that are too steep to permit inflation, even with an arbitrary amount of fine-tuning of the compactification parameters: the functional form of the leading corrections to the potential makes fine-tuning impossible. (Our conclusions are consistent with those reached in [45] for the special case of the Ouyang embedding [133].) This illustrates a key virtue of the explicit, top-down approach: by direct computation we can refute the very reasonable expectation that fine-tuning is generically possible.

Undeterred by this no-go result for a wide class of D3-brane trajectories, we devote a large portion of this paper to showing that in a particularly simple and symmetric embedding due to Kuperstein [114], the stable trajectory is *not* necessarily steep. We then establish that for fine-tuned values of the microphysical parameters, a D3-brane following this stable trajectory leads to sustained slow-roll inflation near an inflection point of the potential. Finally, we derive nontrivial constraints, due to the consistency of the embedding of the warped throat in a flux compactification,

that relate the microscopic parameters of the inflaton Lagrangian. These constraints sharply restrict the parameter space of the model, and in fact exclude most, but not all, of the parameter space that permits sustained inflation.

Our result provides evidence for the existence of successful warped D-brane inflation models based on concrete microscopic data of a flux compactification. However, we emphasize that inflation is non-generic in this class of D-brane models. In fact, because of the geometric constraints, it is surprisingly difficult, though not impossible, to achieve inflation.

**1.2. Outline.** The outline of this chapter is as follows: In §2 we briefly review D-brane inflation in warped backgrounds. We then provide results for the complete D3-brane potential in a warped throat region of the compactification. This includes an important correction to the volume-stabilizing nonperturbative superpotential first computed in [18]. In §3 we present a detailed study of a simple example, the case of the Kuperstein embedding [114] of the wrapped branes. By integrating out the complex Kähler modulus and the angular positions of the D3-brane, we derive effective single-field potentials for different brane trajectories. In §4 we then prove the existence of a stable inflationary trajectory, but also discuss important constraints on microscopic parameters that make inflation challenging to achieve. In §5 we comment on generalizations to other embeddings. We then take the opportunity, in §6, to make some general remarks about the problem of relating string compactification data to the low energy Lagrangian. We conclude in §7.

In order to make this chapter more readable, we have relegated a number of more technical results to a series of appendices. Although most of these results are new, they could be omitted on a first reading. Appendix E gives details of the conifold geometry and of the supergravity F-term potential. In Appendix F we dimensionally reduce the ten-dimensional string action and derive microscopic constraints on the inflaton field range and the warped four-cycle volume. In particular, we explain how

to generalize the field range bound of [21] to a compactification with a nontrivial breathing mode. We also derive a new constraint that relates the field range and the volume of the wrapped four-cycle. Appendix G provides more technical aspects of the proof that the inflationary trajectory is stable against angular fluctuations. In Appendix H we derive the dependence of the compactification volume on the D3-brane position. This is an important improvement on the typical approach of keeping the volume fixed as the D3-brane moves.

## 2. D3-brane Potential in Warped Backgrounds

**2.1. The Compactification.** Our setting is a flux compactification [76] (see Chapter 3 or Ref. [63] for a review) of type IIB string theory on an orientifold of a Calabi-Yau threefold (or an F-theory compactification on a Calabi-Yau fourfold). We suppose that the fluxes are chosen so that the internal space has a warped throat region. As a simple, concrete example of this local geometry, we consider the warped deformed conifold [105]. The deformed conifold is a subspace of complex dimension three in $\mathbb{C}^4$ defined by the constraint equation

$$\sum_{i=1}^{4} z_i^2 = \varepsilon^2 \,, \tag{7.1}$$

where $\{z_i, i = 1, 2, 3, 4\}$ are complex coordinates in $\mathbb{C}^4$. The deformation parameter $\varepsilon$ can be made real by an appropriate phase rotation. The region relevant to our modeling of D-brane inflation lies far from the bottom of the throat, where the right hand side of (7.1) can be ignored and the metric of the deformed conifold is well-approximated by that of the singular conifold,

$$\mathrm{d}s_6^2 = \mathrm{d}\hat{r}^2 + \hat{r}^2 \mathrm{d}s_{T^{1,1}}^2 \,, \tag{7.2}$$

where $\mathrm{d}s_{T^{1,1}}^2$ is the metric of the Einstein manifold $T^{1,1}$, the base of the cone (see Appendix A). This Calabi-Yau metric is obtained from the Kähler potential [49]

$$k = \frac{3}{2}\left(\sum_{i=1}^{4} |z_i|^2\right)^{2/3} = \frac{3}{2} r^2 = \hat{r}^2 \,. \tag{7.3}$$

The warping is achieved by turning on $M$ units of $F_3$ flux through the A-cycle of the deformed conifold (the three-sphere at the bottom) and $-K$ units of $H_3$ flux through the dual B-cycle. The resulting warped deformed conifold background is given in [87, 105]. If $\hat{r}_{\mathrm{UV}}$ is the maximum radial coordinate where the throat is

glued into a compact manifold, then for $\varepsilon^{2/3} \ll \hat{r} \ll \hat{r}_{\rm UV}$ the background is well-approximated by the warped conifold [106]

$$\mathrm{d}s_{10}^2 = h^{-1/2}(\hat{r})\mathrm{d}s_4^2 + h^{1/2}(\hat{r})\mathrm{d}s_6^2\,, \tag{7.4}$$

with the warp factor [87, 106]

$$h(\hat{r}) = \frac{L^4}{\hat{r}^4}\ln\frac{\hat{r}}{\varepsilon^{2/3}}\,, \qquad L^4 = \frac{81}{8}(g_s M\alpha')^2\,. \tag{7.5}$$

We also have [76, 87]

$$\ln\frac{\hat{r}_{\rm UV}}{\varepsilon^{2/3}} \approx \frac{2\pi K}{3g_s M}\,. \tag{7.6}$$

The scale of supersymmetry breaking associated with an anti-D3-brane at the bottom of the throat is $D = 2T_3 h_0^{-1}$, where $h_0$ is the warp factor there. The approximation (7.5) is not accurate enough to determine the warp factor at the bottom of the throat; its value is [87, 105]

$$h_0 = a_0(g_s M\alpha')^2 2^{2/3}\varepsilon^{-8/3}\,, \qquad a_0 \approx 0.71805\,, \tag{7.7}$$

which is approximately $h_0 \approx e^{8\pi K/3g_s M}$ [76].

Following [93], we require that all the closed string moduli are stabilized,[4] by a combination of fluxes and nonperturbative effects. Each nonperturbative effect may arise either from Euclidean D3-branes wrapping a four-cycle, or from strong gauge dynamics, such as gaugino condensation, on a stack of $n > 1$ D7-branes wrapping a four-cycle. Finally, as in [18], we require that at least one of the four-cycles bearing nonperturbative effects descends a finite distance into the warped throat. For simplicity of presentation we will refer to the nonperturbative effects on this cycle as originating on D7-branes, but all our results apply equally well to the case in which Euclidean D3-branes are responsible for this effect.

[4]This condition is necessary for a realistic model, and amounts to a nontrivial selection criterion on the space of compactifications.

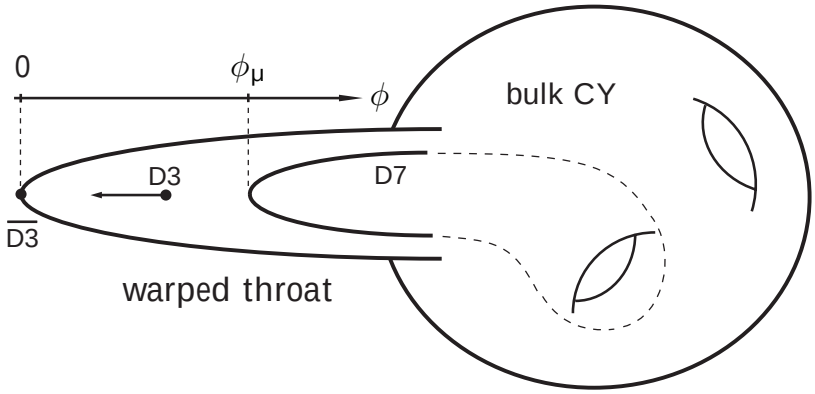


FIGURE 1. Cartoon of an embedded stack of D7-branes wrapping a four-cycle $\Sigma_4$, and a mobile D3-brane, in a warped throat region of a compact Calabi-Yau. The D3-brane feels a force from the D7-branes and from an anti-D3-brane at the tip of the throat.

An embedding is specified by the number $n = N_{D7} > 1$ of D7-branes and the minimal radial coordinate $r_\mu$ reached by the D7-branes. The stabilization of $r_\mu$ is a potentially confusing issue, so we pause to explain it. In the construction [114] of supersymmetric wrapped D7-branes in the noncompact KS throat, $r_\mu$ is a free parameter. One might therefore think that the wrapped D7-branes are not stabilized, and that there is a massless field corresponding to changes in $r_\mu$. However, in the F-theory picture, $r_\mu$ is determined by the complex structure of the fourfold. For generic choices of four-form fluxes, this complex structure is entirely fixed [121] (see also [78]), just as the threefold complex structure is fixed in type IIB compactifications with generic three-form fluxes [76]. Moreover, the scale of the associated mass terms (see *e.g.* [94]), $m_{\text{flux}} \sim \frac{\alpha'}{\sqrt{V_6}}$, with $V_6$ the volume of the compact space, is considerably higher than the (warped) energy scale associated with the brane–antibrane pair under consideration. Hence, for our purposes the D7-brane moduli are massive enough to be ignored. Next, the stabilized value of $r_\mu$ is determined by the fluxes in the bulk of the fourfold. In a generic compactification the number of choices of such fluxes is vast, so we expect that for a given compactification and for any desired value $r_\mu^\star$, there exist choices of flux that fix the D7-brane to a location $r_\mu \approx r_\mu^\star$.

**2.2. D3-brane Potential from Moduli Stabilization.** The effect of moduli stabilization on the D3-brane is captured by the F-term potential of $\mathcal{N} = 1$ supergravity,

$$V_F = e^{\kappa^2 \mathcal{K}} \Big[ D_\Sigma W \mathcal{K}^{\Sigma\overline{\Omega}} \overline{D_\Omega W} - 3\kappa^2 W \overline{W} \Big] , \qquad \kappa^2 = M_{\rm pl}^{-2} \equiv 8\pi G , \tag{7.8}$$

where $\{Z^\Sigma\} \equiv \{\rho, z_\alpha; \alpha = 1, 2, 3\}$ and $D_\Sigma W = \partial_\Sigma W + \kappa^2 (\partial_\Sigma \mathcal{K}) W$. The combined Kähler potential for the volume modulus, $\rho$, and the three open string moduli (D3-brane positions), $z_\alpha$, is of the form postulated by DeWolfe and Giddings [58][5]

$$\kappa^2 \mathcal{K}(\rho, \overline{\rho}, z_\alpha, \overline{z_\alpha}) = -3 \ln[\rho + \bar{\rho} - \gamma k(z_\alpha, \overline{z_\alpha})] \equiv -3 \ln U , \tag{7.9}$$

where in general $k(z_\alpha, \overline{z_\alpha})$ denotes the Kähler potential of the Calabi-Yau manifold. The normalization constant $\gamma$ in (7.9) is derived in Appendix F and may be expressed as

$$\gamma \equiv \frac{\sigma_0}{3} \frac{T_3}{M_{\rm pl}^2} , \tag{7.10}$$

where $2\sigma_0 \equiv 2\sigma_\star(0) = \rho_\star(0) + \bar{\rho}_\star(0)$ is the stabilized value of the Kähler modulus when the D3-brane is near the tip of the throat.

The Kähler metric $\mathcal{K}_{\Omega\overline{\Sigma}} \equiv \mathcal{K}_{,\Omega\overline{\Sigma}}$ assumes the form

$$\mathcal{K}_{\Omega\overline{\Sigma}} = \frac{3}{\kappa^2 U^2} \left( \begin{array}{c|c} 1 & -\gamma k_{\overline{\beta}} \\ \hline -\gamma k_\alpha & U\gamma k_{\alpha\overline{\beta}} + \gamma^2 k_\alpha k_{\overline{\beta}} \end{array} \right) , \tag{7.11}$$

where $k_{\alpha\overline{\beta}} \equiv \partial_\alpha \partial_{\overline{\beta}} k$ is the Calabi-Yau metric, and $k_\alpha \equiv k_{,\alpha}$.

[5] In [46] it was suggested that this result may receive corrections in strongly-warped scenarios. However, the proposed corrections do not affect the metric on the Kähler moduli space, and thus are irrelevant for most of the considerations presented here. However, a truly thorough search for possible effects of such corrections on our analysis must await a more complete understanding of the structure of corrections to the Kähler potential.

The problem of finding the inverse metric, $\mathcal{K}^{\Delta\overline{\Gamma}}\mathcal{K}_{\overline{\Gamma}\Omega} = \delta^{\Delta}_{\Omega}$, was solved in [45]:

$$\mathcal{K}^{\Delta\overline{\Gamma}} = \frac{\kappa^2 U}{3}\left(\begin{array}{c|c} U + \gamma k_\gamma k^{\gamma\overline{\delta}} k_{\overline{\delta}} & k_\gamma k^{\gamma\overline{\beta}} \\ \hline k^{\alpha\overline{\delta}} k_{\overline{\delta}} & \frac{1}{\gamma} k^{\alpha\overline{\beta}} \end{array}\right) . \tag{7.12}$$

After some calculation, these results lead to the F-term potential

$$\begin{aligned} V_F(\rho, z_\alpha) &= \frac{\kappa^2}{3U^2}\Bigg[\Big(\rho + \overline{\rho} + \gamma(k_\gamma k^{\gamma\overline{\delta}} k_{\overline{\delta}} - k)\Big)|W_{,\rho}|^2 - 3(\overline{W}W_{,\rho} + c.c.) \\ &\qquad + \underbrace{(k^{\alpha\overline{\delta}} k_{\overline{\delta}} \overline{W_{,\rho}} W_{,\alpha} + c.c.) + \frac{1}{\gamma} k^{\alpha\overline{\beta}} W_{,\alpha} \overline{W_{,\beta}}}_{\Delta V_F}\Bigg] . \end{aligned} \tag{7.13}$$

The label $\Delta V_F$ has isolated the terms in F-term potential (7.13) that arise exclusively from the dependence of the nonperturbative superpotential on the brane position [18]. The remainder of (7.13) is the standard KKLT F-term potential [93].

The superpotential $W$ is the sum of the constant Gukov-Vafa-Witten flux superpotential [82], $W_{\rm flux} = \int G_3 \wedge \Omega \equiv W_0$, and a term from nonperturbative effects, $W_{\rm np} = A(z_\alpha)e^{-a\rho}$,

$$W(\rho, z_\alpha) = W_0 + A(z_\alpha)e^{-a\rho} , \qquad a \equiv \frac{2\pi}{n} . \tag{7.14}$$

By a choice of phases we can arrange that $W_0$ is real and negative. The nonperturbative term $W_{\rm np}$ arises either from strong gauge dynamics on a stack of $n > 1$ D7-branes or from Euclidean D3-branes (with $n = 1$ ). We assume that either sort of brane supersymmetrically wraps a four-cycle in the warped throat that is specified by a holomorphic embedding equation $f(z_\alpha) = 0$. The warped volume of the four-cycle governs the magnitude of the nonperturbative effect, by affecting the gauge coupling on the D7-branes (equivalently, the action of Euclidean D3-branes) wrapping this four-cycle. The presence of a D3-brane gives rise to a perturbation to the warp factor, and this leads to a correction to the warped four-cycle volume. This correction depends on the D3-brane position and is responsible for the prefactor $A(z_\alpha)$ [77]. In

[18], in collaboration with J. Maldacena and A. Murugan, we computed the D3-brane backreaction on the warped four-cycle volume. This gave the result[6]

$$A(z_\alpha) = A_0 \left( \frac{f(z_\alpha)}{f(0)} \right)^{1/n} . \tag{7.15}$$

See [18] for a derivation of this result, and for a more complete discussion of the setup, which we have only briefly reviewed here.

**2.3. Potential in the Warped Conifold Throat.** In this section we apply the general formulae of the previous section to the case of a D3-brane moving in a warped deformed conifold. We will assume that both the mobile D3-brane and the fixed D7-branes are located far enough from the tip that the deformation parameter $\varepsilon$ may be neglected. If we use $z_\alpha = \{z_1, z_2, z_3\}$ as the three independent variables, the conifold constraint allows us to express $z_4 = \pm i(\sum_{\alpha=1}^3 z_\alpha^2)^{1/2}$. Using this basis, and the Kähler potential (7.3), we obtain the conifold metric

$$k_{\alpha\overline{\beta}} = \frac{3}{2} \frac{\partial^2}{\partial z_\alpha \partial \overline{z_\beta}} \left( \sum_{\gamma=1}^3 |z_\gamma|^2 + \left| \sum_{\gamma=1}^3 z_\gamma^2 \right| \right)^{2/3} \tag{7.16}$$

$$= \frac{1}{r} \left[ \delta_{\alpha\overline{\beta}} + \frac{z_\alpha \overline{z_\beta}}{|z_4|^2} - \frac{1}{3r^3} \left( z_\alpha \overline{z_\beta} + z_\beta \overline{z_\alpha} - \frac{z_4}{\overline{z_4}} \overline{z_\alpha z_\beta} - \frac{\overline{z_4}}{z_4} z_\alpha z_\beta \right) \right] . \tag{7.17}$$

Its inverse assumes the simple form

$$k^{\alpha\overline{\beta}} = r \left[ \delta^{\alpha\overline{\beta}} + \frac{1}{2} \frac{z_\alpha \overline{z_\beta}}{r^3} - \frac{z_\beta \overline{z_\alpha}}{r^3} \right] . \tag{7.18}$$

Expression (7.13) for the F-term potential simplifies significantly when we substitute (7.18) and note that

$$U(\rho, r) = \rho + \overline{\rho} - \frac{3\gamma}{2} r^2 , \qquad k^{\gamma\overline{\delta}} k_{\overline{\delta}} = \frac{3}{2} z_\gamma , \quad k_\gamma k^{\gamma\overline{\delta}} k_{\overline{\delta}} = k . \tag{7.19}$$

[6]The D3-brane-independent factor $A_0$ in (7.15) arises from threshold corrections that depend on the complex structure moduli. This quantity is not known except in special cases, but is a relatively unimportant constant in our scenario, because the complex structure moduli are stabilized by the flux background, and because, as we shall see, $A_0$ appears in the final potential only as an overall constant prefactor.

The remaining term in the potential is the contribution of an anti-D3-brane at the tip of the conifold, including its Coulomb interaction with the mobile D3-brane [95]

$$V_D(\rho, r) = \frac{D(r)}{U^2(\rho, r)}\,, \qquad D(r) \equiv D\left[1 - \frac{3D}{16\pi^2}\frac{1}{(T_3 r^2)^2}\right] + D_{\rm other} \approx D + D_{\rm other}\,, \quad (7.20)$$

where $D \equiv 2h_0^{-1}T_3$ is twice the warped D3-brane tension at the tip[7] and $D_{\rm other}$ represents a possible contribution from distant sources of supersymmetry breaking, *e.g.* in other throats.

The complete inflaton potential is then the sum of the F-term potential from moduli stabilization, plus the contribution of the antibrane,

$$V = V_F(\rho, z_\alpha) + V_D(\rho, r)\,. \quad (7.21)$$

The canonical inflaton $\phi$ is proportional to $r$, the radial location of the D3-brane (see §F.3 for details). Using (7.21) to compute the slow-roll parameter

$$\eta \equiv M_{\rm pl}^2 \frac{V_{,\phi\phi}}{V}\,, \quad (7.22)$$

we find

$$\eta = \frac{2}{3} + \Delta\eta(\phi)\,, \quad (7.23)$$

where $\Delta\eta$ arises from the dependence of the superpotential on $\phi$. If $A$ were a constant independent of $\phi$, slow-roll inflation would be impossible [95], because in that case $\eta = \frac{2}{3}$. In this paper, using the explicit result of [18] for $A(\phi)$, we will compute $\Delta\eta$ and determine whether the full potential can be flat enough for inflation. Note that the sign of $\Delta\eta$, while crucial, is not obvious *a priori*.

[7] A similar potential for a mobile D3-brane arises if instead of including the antibrane we generalize the throat background [65].

### 3. Case Study: Kuperstein Embedding

Let us consider a particularly simple and symmetric holomorphic embedding due to Kuperstein [114], which is defined by the algebraic equation

$$f(z_1) = \mu - z_1 = 0\,, \tag{7.24}$$

where, without loss of generality, we will consider the case in which $\mu \in \mathbb{R}^+$. This embedding preserves an $SO(3)$ subgroup of the $SO(4)$ global symmetry acting on the $z_i$ coordinates of the deformed conifold. Kuperstein showed that this is a supersymmetric embedding not just for the singular conifold, but also in the full warped deformed conifold background with three-form fluxes. (For comparison, the embeddings of [9, 133] have so far been studied explicitly only in the $AdS_5 \times T^{1,1}$ background). Adding just a mobile D3-brane does not break supersymmetry in the case of the non-compact throat. Therefore, the interaction between the D3-branes and D7-branes must vanish in that limit. When the throat is embedded in a compactification, the D3-brane potential can receive a contribution from the nonperturbative superpotential (7.14).

The inflaton potential $V(\rho, r, z_i)$ is in general a complicated function of the Kähler modulus and of the radial and angular coordinates of the D3-brane. In this section we systematically integrate out all fields except the radial coordinate, leading to an effective single-field potential for the radial inflaton.

### 3.1. Multi-field Potential.

*F-term potential.* By the results of [18], equation (7.24) implies

$$A(z_1) = A_0 \left(1 - \frac{z_1}{\mu}\right)^{1/n} , \tag{7.25}$$

and the F-term potential (7.13) is

$$\begin{aligned} V_F &= \frac{\kappa^2 a |A(z_1)|^2 e^{-a(\rho+\bar{\rho})}}{3U(\rho,r)^2} \Bigg[ \Big(a(\rho+\bar{\rho})+6\Big) + 6\, W_0 \,\mathrm{Re}\Big(\frac{e^{a\rho}}{A(z_1)}\Big) \\ &\qquad - 3\,\mathrm{Re}(\alpha_{z_1} z_1) + \frac{r}{a\gamma}\Big(1 - \frac{|z_1|^2}{2r^3}\Big)|\alpha_{z_1}|^2 \Bigg] , \end{aligned} \tag{7.26}$$

where

$$\alpha_{z_1} \equiv \frac{A_{z_1}}{A} = -\frac{1}{n(\mu - z_1)} , \tag{7.27}$$

and

$$\mathrm{Re}(\alpha_{z_1} z_1) = -\frac{1}{2n} \frac{\mu(z_1 + \overline{z_1}) - 2|z_1|^2}{|\mu - z_1|^2} . \tag{7.28}$$

Note that the potential (7.26) depends only on $r$, $z_1$, and $\rho$. Therefore, it is invariant under the $SO(3)$ that acts on $z_2, z_3, z_4$.

*Angular degrees of freedom.*

*Imaginary part of the Kähler modulus.* First, to reduce the complexity of the multi-field potential, we integrate out the imaginary part of the Kähler modulus. Setting $\rho \equiv \sigma + i\tau$, equation (7.26) becomes

$$\begin{aligned} V_F &= \frac{\kappa^2 a |A|^2 e^{-2a\sigma}}{3U^2} \Bigg[ \Big(2a\sigma + 6\Big) + 6\, W_0 e^{a\sigma} \underline{\underline{\,\mathrm{Re}\Big(\frac{e^{ia\tau}}{A}\Big)\,}} \\ &\qquad - 3\,\mathrm{Re}(\alpha_{z_1} z_1) + \frac{r}{a\gamma}\Big(1 - \frac{|z_1|^2}{2r^3}\Big)|\alpha_{z_1}|^2 \Bigg] . \end{aligned} \tag{7.29}$$

We see that only the underlined term depends on $\tau$, and the potential for $\tau$ is minimized when this term is as small as possible. Because $W_0$ is negative, integrating out

$\tau(z_1, r) = \mathrm{Im}(\rho)$ then amounts to the replacement

$$\frac{e^{ia\tau}}{A} \to \frac{1}{|A|}\,. \tag{7.30}$$

Notice that this is *not* the same as setting $\tau \equiv 0$. In particular, $\tau(z_1, r)$ might be a complicated function, but all we need to know is (7.30).

*Angular directions.* The D3-brane position is described by the radial coordinate $r$ and five angles $\Psi_i$ on the base of the cone. The angles are periodic coordinates on a compact space, so the potential in $\Psi_i$ is either constant or else has discrete minima at some values $\Psi_i^\star$. We are interested in trajectories that are stable in the angular directions, so that the motion occurs purely along the radial direction.

We can therefore reduce the number of degrees of freedom by fixing the angular coordinates to the positions that minimize the potential. In Appendix G we show that for any Kuperstein-like embedding $f(z_1) = 0$, these extrema in the angular directions occur only for trajectories satisfying

$$z_1 = \pm\frac{r^{3/2}}{\sqrt{2}}\,, \qquad \Leftrightarrow \qquad \frac{\partial V}{\partial \Psi_i} = 0\,. \tag{7.31}$$

Furthermore, in Appendix G we examine the matrix of second derivatives, $\frac{\partial^2 V}{\partial\Psi_i \partial\Psi_j}$, and find the conditions under which these extrema are stable minima. For the present discussion we only need one result from that section: for small $r$, the trajectory (7.31) is stable against angular fluctuations for negative $z_1$ and unstable for positive $z_1$. In Appendix F we show that the canonical inflaton field $\phi$ is well-approximated by a constant rescaling of the radial coordinate $r$,

$$\phi^2 \equiv T_3 \hat{r}^2 = \frac{3}{2} T_3 r^2\,. \tag{7.32}$$

An important parameter of the brane potential is the minimal radial coordinate of the D7-brane embedding [18, 114], $r_\mu^3 \equiv 2\mu^2$, or $\phi_\mu^2 = \frac{3}{2}T_3(2\mu^2)^{2/3}$. The potential

along the trajectory (7.31) may then be written as

$$V(\phi,\sigma) = V_F(\phi,\sigma) + V_D(\phi,\sigma)\,, \tag{7.33}$$

where

$$\begin{aligned} V_F(\phi,\sigma) &= \frac{\kappa^2 a|A_0|^2}{3}\frac{\exp(-2a\sigma)}{U(\phi,\sigma)^2}g(\phi)^{2/n}\Bigg[2a\sigma+6-6\exp(a\sigma)\frac{|W_0|}{|A_0|}\frac{1}{g(\phi)^{1/n}} \\ &\qquad +\frac{3}{n}\left(c\frac{\phi}{\phi_\mu}\pm\left(\frac{\phi}{\phi_\mu}\right)^{3/2}-\left(\frac{\phi}{\phi_\mu}\right)^{3}\right)\frac{1}{g(\phi)^2}\Bigg]\,, \end{aligned} \tag{7.34}$$

$$V_D(\phi,\sigma) = \frac{D(\phi)}{U(\phi,\sigma)^2}\,, \tag{7.35}$$

and

$$g(\phi)\equiv\left|1\mp\left(\frac{\phi}{\phi_\mu}\right)^{3/2}\right|\,,\qquad U(\phi,\sigma)\equiv 2\sigma-\frac{\sigma_0}{3}\frac{\phi^2}{M_{\rm pl}^2}\,. \tag{7.36}$$

Here we have introduced the constant

$$c\equiv\frac{1}{4\pi\gamma r_\mu^2}=\frac{9}{4n\,a\sigma_0\frac{\phi_\mu^2}{M_{\rm pl}^2}}\,. \tag{7.37}$$

This two-field potential is the input for our numerical study in §4.3.

### 3.2. Effective Single-Field Potential.

*Real part of the Kähler modulus.* Having reduced the potential to a function of two real fields, $\phi$ and $\sigma$, we integrate out $\sigma$ by assuming[8] that it evolves adiabatically while remaining in its instantaneous minimum $\sigma_\star(\phi)$, which is defined implicitly by

$$\partial_\sigma V\big|_{\sigma_\star(\phi)} = 0\,. \tag{7.38}$$

[8]We are assuming that $\sigma$ is much more massive than $\phi$. This may not be valid for a truly generic configuration of a D3-brane in a compact space, but we are specifically interested in cases in which the potential for $\phi$ has been fine-tuned to be flat. Thus, when slow-roll inflation is possible at all, the adiabatic approximation is justified. See also [135].

This leads to the effective single-field potential

$$\mathbb{V}(\phi) \equiv V(\sigma_\star(\phi), \phi)\,. \tag{7.39}$$

In general, we are not able to solve equation (7.38) analytically for $\sigma_\star(\phi)$, so we perform this final step numerically (§4.3). Nevertheless, in Appendix H we derive useful approximate analytical solutions for the stabilized volume modulus and its dependence on $\phi$ (similar results were derived independently in [113]). Here, we cite the basic results of that section. First, the critical value $\sigma_F$ of the Kähler modulus before uplifting is determined by $D_\rho W|_{\phi=0,\,\sigma_F} = 0$, or equivalently [93],

$$3\frac{|W_0|}{|A_0|}e^{a\sigma_F} = 2a\sigma_F + 3 \qquad \Rightarrow \qquad \left.\frac{\partial V_F}{\partial \sigma}\right|_{\sigma_F} = 0\,. \tag{7.40}$$

We now show how the Kähler modulus is shifted away from $\sigma_F$ by the inclusion of a brane-antibrane pair.

(1) **Shift induced by the uplifting**

Adding an anti-D3-brane to lift the KKLT AdS minimum to a dS minimum induces a small shift in the stabilized volume, $\sigma_F \to \sigma_F + \delta\sigma \equiv \sigma_\star(0) \equiv \sigma_0$, where

$$\delta\sigma \approx \frac{s}{a^2\sigma_F} \ll 1 \ll \sigma_F\,. \tag{7.41}$$

Here we found it convenient to define the ratio of the antibrane energy to the F-term energy *before* uplifting, *i.e.* when $\sigma = \sigma_F$,

$$s \equiv \frac{(D + D_{\rm other})U^{-2}(0,\sigma_F)}{|V_F(0,\sigma_F)|}\,, \tag{7.42}$$

where stability of the volume modulus in a metastable de Sitter vacuum requires $1 < s \lesssim \mathcal{O}(3)$. Although $\delta\sigma$ is small, it appears in an exponent in (7.34), so that its effect there has to be considered,

$$3\frac{|W_0|}{|A_0|}e^{a\sigma_0} \approx 2a\sigma_0 + 3 + 2s\,. \tag{7.43}$$

When the D3-brane is near the tip, $\phi \approx 0$, the Kähler modulus remains at $\sigma_0$. Using this constant value even when the brane is at finite $\phi$ suffices for understanding the basic qualitative features of the potential (7.34). However, important quantitative details of the potential depend sensitively on the dependence of $\sigma_\star$ on $\phi$; see Appendix D and Ref. [135].

(2) **Shift induced by D3-brane motion**

In Appendix H we derive the following analytic approximation to the dependence of the stabilized volume on the D3-brane position:

$$\sigma_\star(\phi) \approx \sigma_0 \left[1 + c_{3/2} \left(\frac{\phi}{\phi_\mu}\right)^{3/2}\right] , \tag{7.44}$$

where

$$c_{3/2} \approx \frac{1}{n}\frac{1}{a\sigma_F}\left[1 - \frac{1}{2a\sigma_F}\right] . \tag{7.45}$$

This expression is valid along $z_1 = -\frac{r^{3/2}}{\sqrt{2}}$, which we argue below is the interesting case in which the potential is stable in the angular directions.

*Analytic single-field potential.* Along the trajectory $z_1 = -\frac{r^{3/2}}{\sqrt{2}}$, the inflaton potential is

$$\begin{aligned}\mathbb{V}(\phi) \;=\; & \frac{\kappa^2 a|A_0|^2}{3}\frac{\exp(-2a\sigma_\star(\phi))}{U(\phi,\sigma_\star(\phi))^2} g(\phi)^{2/n}\Bigg[2a\sigma_\star(\phi) + 6 - 6\exp(a\sigma_\star(\phi))\frac{|W_0|}{|A_0|}\frac{1}{g(\phi)^{1/n}} \\ & + \frac{3c}{n}\frac{\phi}{\phi_\mu}\frac{1}{g(\phi)^2} - \frac{3}{n}\left(\frac{\phi}{\phi_\mu}\right)^{3/2}\frac{1}{g(\phi)}\Bigg] + \frac{D(\phi)}{U(\phi,\sigma_\star(\phi))^2} ,\end{aligned} \tag{7.46}$$

where $\sigma_\star(\phi)$ can be determined numerically or approximated analytically by (7.44). Using the analytic result (7.44) in (7.46) captures the basic qualitative features of the potential, but is insufficient to assess detailed quantitative questions. In particular, by using (7.44) one systematically underestimates the total number of $e$-folds supported by the potential (see Appendix D and Ref. [135]).

The inflaton potential (7.46) is one of our main results.

## 4. Search for an Inflationary Trajectory

In the preceding section, we derived the inflaton potential (7.46) along the angularly-stable trajectory $z_1 = -\frac{r^{3/2}}{\sqrt{2}}$. We will now explore this potential and establish that slow roll inflation is possible for a certain range of parameters. First, in §4.1, we present a few analytic results about the curvature of the potential. Then, in §4.2, we describe the constraints on the parameters of the model that are dictated by the structure of the compactification. Finally, in §4.3, we present the results of a numerical study of the potential.

**4.1. Analytic Considerations.** Let us briefly recall the reason for computing the effect of $A(\phi)$ on the inflaton potential. Kachru et al. [95] derived $\eta = \frac{2}{3}$ for the case $A = const.$, and suggested that the inflaton-dependence of the nonperturbative superpotential, $A(\phi)$, could contribute corrections to the inflaton mass, which, if of the right sign, could accidentally make $\eta$ small. This reasonable expectation hinges on the presence of quadratic corrections to the inflaton potential.

We now argue that in view of the result (7.15), wrapped D7-branes give *no* purely quadratic corrections to the inflaton potential. To see this, we note that the holomorphic coordinates on the conifold scale as fractional powers of $\phi$, $|z_i| \propto \phi^{3/2}$, and $A(z_i)$ is a holomorphic function of the $z_i$ coordinates [18]. This observation implies that the inflaton potential is of the form

$$\frac{\mathbb{V}(\phi)}{\mathbb{V}(0)} = 1 + \frac{1}{3}\frac{\phi^2}{M_{\rm pl}^2} + v(\phi)\,, \tag{7.47}$$

where $v(\phi)$ contains no quadratic terms. The slow roll parameter $\eta$, which needs to be very small for sustained slow roll inflation, is

$$\eta \equiv M_{\rm pl}^2 \frac{\mathbb{V}_{,\phi\phi}}{\mathbb{V}} = \frac{2}{3} + M_{\rm pl}^2 v_{,\phi\phi}\,. \tag{7.48}$$

Because $v_{,\phi\phi}$ contains no constant term, there is no possibility of cancelling the $\frac{2}{3}$ uniformly, for the entire range of $\phi$. Instead, we can at best hope to cancel the $\frac{2}{3}$ at some special point(s) $\phi_0$ obeying $v_{,\phi\phi}(\phi_0) = -\frac{2}{3}$.

Using the explicit form (7.46) and expanding for small $\phi/\phi_\mu$, we find

$$\eta = \frac{2}{3} - \eta_{-1/2} \left(\frac{\phi}{\phi_\mu}\right)^{-1/2} + \cdots , \tag{7.49}$$

where

$$\eta_{-1/2} \approx \frac{M_{\rm pl}^2}{\phi_\mu^2} \frac{3(4s-3)}{8n(s-1)} \frac{1}{a\sigma_0} > 0 . \tag{7.50}$$

Hence, $\eta < 0$ sufficiently close to the tip. On the other hand, we find that for $\phi \gg \phi_\mu$, $\eta > 0$. By continuity, $\eta$ must vanish at some intermediate location $\phi_0$.

The precise location of $\phi_0$ is a parameter-dependent question. For this purpose, the most important parameter is the minimal radius $\phi_\mu$ of the D7-branes. Notice that (7.48) can be written as

$$\eta = \frac{2}{3} + \frac{M_{\rm pl}^2}{\phi_\mu^2} v_{,xx} , \tag{7.51}$$

where $x \equiv \frac{\phi}{\phi_\mu}$ and $v_{xx}$ is insensitive to $\phi_\mu$ (see (7.46)). From (7.49) we see that the second term in (7.51) dominates near the tip, giving a large negative $\eta$. This implies the opportunity for a small $\eta$ by cancellation against the positive $\frac{2}{3}$. However, only if $\phi_\mu$ is not too small can this cancellation be achieved inside the throat. Otherwise, $\eta$ remains negative throughout the regime of interest. We conclude that for small $\phi_\mu$, $\phi_0$ is outside the throat, and hence outside the validity of our construction.

**4.2. Parameters and Microscopic Constraints.** Let us describe the microscopic parameters that determine the inflaton potential (7.46). In view of (7.42), the D-term $D_{\rm other} + 2T_3 h_0^{-1}$ and $W_0$ are represented by $s$ and by $\omega_F = a\sigma_F$, respectively. Next, the prefactor $A_0$ only appears as an overall constant rescaling the height of the potential, so we set $A_0 \equiv 1$. The shape of the inflaton potential is therefore determined by $n$, $\omega_F$, $s$ and $\phi_\mu$. As we now explain, microscopic constraints lead to

important restrictions on the allowed parameter ranges and induce non-trivial correlations among the above parameters.

First, the range of the radial coordinate $r$ affects the four-dimensional Planck mass, because a longer throat makes a larger contribution to the volume of the compact space. In [21] Liam McAllister and I showed that this creates a strong constraint on the allowed field range of the inflaton field $\phi$ (see also Appendix F)

$$\frac{\Delta\phi}{M_{\rm pl}} < \frac{2}{\sqrt{N}}\,. \tag{7.52}$$

Here we use the field range bound (7.52) to constrain the microscopically viable range of $\phi_\mu$, the minimal radial extent of the D7-branes in canonical units. For this purpose we find it convenient to write the bound in the form

$$\frac{\phi_\mu^2}{M_{\rm pl}^2} = \frac{1}{Q_\mu^2}\frac{1}{B_6}\frac{4}{N}\,, \tag{7.53}$$

where $B_6 \equiv \frac{V_6^w}{(V_6^w)_{\rm throat}} > 1$ parameterizes the relative contribution of the throat to the total (warped) volume of the compact space, and

$$Q_\mu \equiv \frac{r_{\rm UV}}{r_\mu} \tag{7.54}$$

is a measure of how far into the throat the four-cycle extends. Applicability of the results of [18] requires $Q_\mu = \frac{\phi_{\rm UV}}{\phi_\mu} > 1$.

Second, the warped volume $V_{\Sigma_4}^w$ of the wrapped four-cycle $\Sigma_4$ is bounded below by the warped volume in the throat region,

$$V_{\Sigma_4}^w = (V_{\Sigma_4}^w)_{\rm throat} + (V_{\Sigma_4}^w)_{\rm bulk} \geq (V_{\Sigma_4}^w)_{\rm throat}\,. \tag{7.55}$$

In Appendix F.2 we compute $(V_{\Sigma_4}^w)_{\rm throat}$ for the Kuperstein embedding

$$T_3(V_{\Sigma_4}^w)_{\rm throat} = \frac{3}{2}N\ln Q_\mu\,. \tag{7.56}$$

In §2 we explained how the unperturbed warped four-cycle volume relates to the Kähler modulus of the compactification (more details can be found in Refs. [18, 77] and Appendix F). If we use $B_4 \equiv \frac{V^w_{\Sigma_4}}{(V^w_{\Sigma_4})_{\rm throat}} > 1$ to parameterize the relative contribution of the throat to the total warped volume of the four-cycle wrapped by the D7-branes, then we can relate the vev of the Kähler modulus to microscopic parameters of the compactification

$$\omega_F \approx \omega_0 \approx \frac{3}{2}\frac{N}{n} B_4 \ln Q_\mu \,. \tag{7.57}$$

We require $\omega_0 < \mathcal{O}(30)$, because otherwise the inflation scale will be too low – see Appendix F.

The constraints (7.53), (7.57) will play an essential role in our analysis. We will find that inflationary configurations are rather easy to find if these constraints are neglected, but imposing them dramatically decreases the parameter space suitable for inflation.

*Bulk contributions to the volume.* We have just introduced two parameters, $B_4 = \frac{V^w_{\Sigma_4}}{(V^w_{\Sigma_4})_{\rm throat}}$ and $B_6 = \frac{V^w_6}{(V^w_6)_{\rm throat}}$, that represent ratios of total volumes to throat volumes. In the throat, we have access to an explicit Calabi-Yau metric and can compute the volumes directly. This metric data in the throat is one of the main reasons that warped D-brane inflation can be studied explicitly. In contrast, we have very little data about the bulk, so we cannot compute $B_4$ and $B_6$.

Fortunately, these parameters do not directly enter the potential. Instead, they appear in the compactification constraints (7.53) and (7.57), and thereby affect the microscopically allowable ranges of the other parameters, such as $\phi_\mu$ and $Q_\mu$. In particular, when $B_6$ is large, the range of $\phi_\mu$ is reduced, because the throat is shorter in four-dimensional Planck units. In the numerical investigation of §4.3, we find that inflation is possible inside the throat, and our construction is self-consistent, provided that $B_4/B_6 \gtrsim 2$. For concreteness, we take $B_4 \sim 9$, $B_6 \sim 1.5$ in the remainder. This

means that the throat contributes a greater share of the total six-volume than it does of the wrapped four-cycle volume: in other words, the wrapped four-cycle only enters the upper reaches of the throat. Although we expect that such a configuration can be realized, it will be valuable to find a fully explicit construction. We note, however, that a very large value of $B_4$, implying that the D7-brane is hardly in the throat at all, would mean that the result of [18] is inapplicable, because the correction to the four-cycle volume is then dominated by the correction to the uncomputable bulk portion of the volume.

*Parameter choices.* Although a systematic study of the full multi-dimensional parameter space would undoubtedly be instructive, we here employ a simpler and more transparent strategy that we believe nevertheless accurately portrays the range of possibilities. To this end, we set some of the discrete parameters to reasonable values and then scan over the remaining parameters. Let us emphasize that although the precise values chosen here are not important, it is important that we were able to find regions in parameter space where all our approximations are valid and all the compactification constraints are satisfied.

First, we fix $n \to 8$. This helps to reduce the degree to which the volume shifts during inflation, as from (7.45), $c_{3/2} \propto n^{-1}$. Numerical study of the case $n = 2$ yields results qualitatively similar to those we present here, but the analytical treatment is more challenging. To ignore backreaction of the wrapped branes on the background geometry, we require that the background D3-brane charge exceeds the number of wrapped branes, $\frac{N}{n} > 1$. For concreteness, we use $N = 32$. Finally, as previously stated, we take $B_4 \sim 5$, $B_6 \sim 2$.

This allows us to impose the microscopic constraints (7.53), (7.57) on the compactification volume $\omega_F$ and the wrapped brane location $\phi_\mu$ in terms of a single parameter $Q_\mu$. The remaining parameters that determine the potential are then $Q_\mu$ (7.54) and $s$ (7.42).

To search for inflationary solutions, we scanned over $Q_\mu$ and $s$, treating both as continuous parameters, although they are in principle determined by discrete flux input. Here, for simplicity of presentation, we will fix $Q_\mu$ to a convenient value, $Q_\mu = 1.2$, and only exhibit the scanning over $s$. To interpret this scanning in microphysical terms, we recall that, for fixed F-term potential and for fixed supersymmetry breaking (corresponding to the parameter $D_{\rm other}$) outside the throat, $s$ is determined by $D = 2T_3 h_0^{-1}$, where $h_0$ is given in (7.7) and is of order $h_0 \approx \exp\left(\frac{8\pi K}{3 g_s M}\right)$. The values of $h_0$ we will consider can be achieved for reasonable values of $K, M, g_s$.

In summary, we have arranged that all consistency conditions are satisfied, and all parameters except for the amount of uplifting, $s$, are fixed. As we vary the uplifting, the shape of the potential (7.46) will change. As we shall now see, for a certain range of values of $s$ the potential becomes flat enough for prolonged inflation.

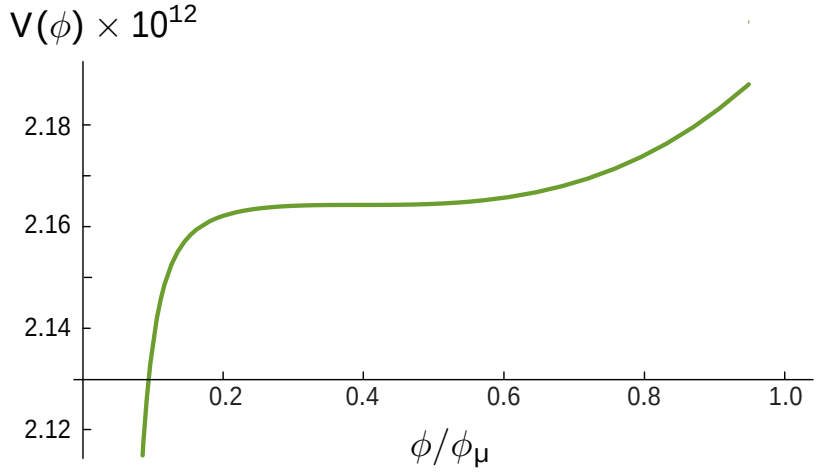


FIGURE 2. **Inflaton potential** $\mathbb{V}(\phi)$**.**
*Compactification data:* $n = 8$, $\omega_F = 10$, $N = 32$, $Q_\mu = 1.2$, $B_6 = 1.5$, $B_4 = 9$, $s = 1.1$, which implies $\phi_\mu = 0.25$, $W_0 = -3.432 \times 10^{-4}$, $D + D_{\rm other} = 1.2 \times 10^{-8}$, $\omega_0 \approx 10.1$.

**4.3. Numerical Results.** The first observation we make about (7.46) is that, near the parameter values we have indicated, it is generically non-monotonic. In fact, the potential has a metastable minimum[9] at some distance from the tip. We are

[9]A D3-brane located in this metastable minimum contributes to the breaking of supersymmetry. It would be extremely interesting to use a configuration of a D3-brane and a

confident that this is a minimum and not a saddle point, because we have explicitly shown in the Appendices that the curvature of the potential in the angular directions is non-negative. (The curvature is zero along directions protected by the unbroken $SO(3)$ symmetry of the background, and positive in the other directions.) Moreover, we have shown that the potential is stable with respect to changes in the Kähler modulus.

Next, we notice that as we vary $s$, the metastable minimum grows more shallow, and the two zeroes of $V'$, the local maximum and the local minimum, approach each other. A zero of $V''$ is trapped in the shrinking range between these two zeroes of $V'$. For a critical value of $s$, the zero of $V''$ and the two zeroes of $V'$ coincide, and the potential has an inflection point. As $s$ changes further, the potential becomes strictly monotonic.

We therefore find that there exists a range of $s$ for which both the first and second derivatives of the potential approximately vanish. This is an approximate inflection point. In the next section we discuss a phenomenological model that captures the essential features of (7.46) in the vicinity of this inflection point.

**4.4. Phenomenological Model: Cubic Inflation.** We have shown that inflationary solutions in the Kuperstein embedding arise near an inflection point at $\phi = \phi_0$, where the potential is very well approximated by the cubic form [88, 123][10]

$$\mathbb{V} = V_0 + \lambda_1(\phi - \phi_0) + \frac{1}{3!}\lambda_3(\phi - \phi_0)^3 \,. \tag{7.58}$$

moduli-stabilizing D7-brane stack to uplift to a de Sitter vacuum. Here we have not quite accomplished this: we have, of course, included an anti-D3-brane as well, which is well-known to accomplish the uplifting by itself [93]. If this antibrane is removed, the structure of the potential changes, and it is not clear from our results so far that a remaining D3-brane would suffice to uplift to a de Sitter vacuum. We leave this as a promising direction for future work.

[10]Ref. [5] has developed an inflation model within the minimal supersymmetric standard model (MSSM) that has a similar cubic phenomenology. We thank Justin Khoury for bringing this model to our attention. Inflection point inflation in the context of string theory, with the inflaton corresponding to the compactification volume, has been considered in [92].

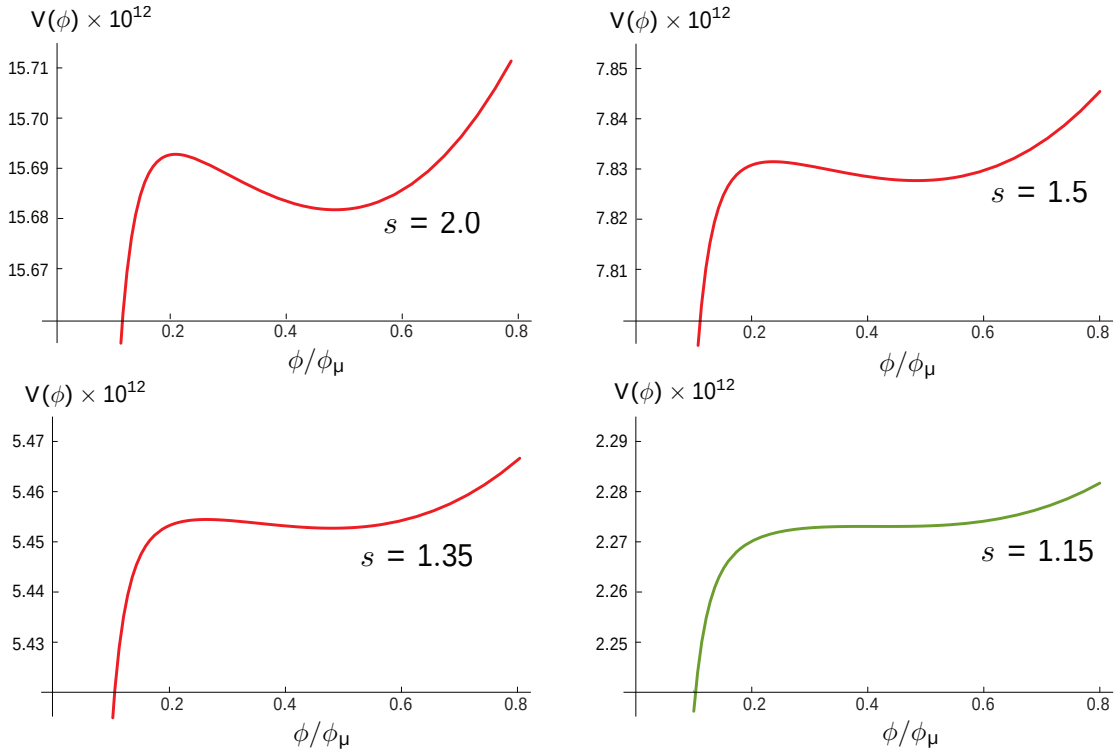


FIGURE 3. **The inflaton potential $\mathbb{V}(\phi)$ as a function of $s$.**
The transition from metastability to monotonicity is shown; old inflation and new inflation are continuously connected.

Prolonged inflation requires smallness of the slow roll parameters, $\epsilon, \eta \ll 1$. From (7.58) we find[11]

$$\epsilon \equiv \frac{1}{2}\left(\frac{\mathbb{V}_{,\phi}}{\mathbb{V}}\right)^2 \approx \frac{1}{2}\left(\frac{\lambda_1 + \frac{1}{2}\lambda_3(\phi-\phi_0)^2}{V_0}\right)^2 , \tag{7.59}$$

$$\eta \equiv \frac{\mathbb{V}_{,\phi\phi}}{\mathbb{V}} \approx \frac{\lambda_3}{V_0}(\phi-\phi_0)\,. \tag{7.60}$$

The number of $e$–folds between some value $\phi$ and the end of inflation $\phi_{\rm end}$ is then

$$N_e(\phi) = \int_{\phi_{\rm end}}^{\phi} \frac{{\rm d}\phi}{\sqrt{2\epsilon}} = \frac{N_{\rm tot}}{\pi}\arctan\left(\frac{\eta(\phi)}{2\pi N_{\rm tot}^{-1}}\right)\Bigg|_{\phi_{\rm end}}^{\phi} , \tag{7.61}$$

where

$$N_{\rm tot} \equiv \int_{-\infty}^{\infty} \frac{{\rm d}\phi}{\sqrt{2\epsilon}} = \pi\sqrt{\frac{2V_0^2}{\lambda_1\lambda_3}}\,. \tag{7.62}$$

[11] In this section we set $M_{\rm pl} \equiv 1$.

In (7.59) and (7.60) we have set $\mathbb{V}(\phi) \approx V_0$ in the denominators, while in (7.62) we extended the integral from the range where $|\eta| < 1$ to infinity. These approximations are very good in the regime

$$\frac{V_0}{\lambda_3} \ll 1 \,, \qquad \frac{V_0}{\sqrt{\lambda_1 \lambda_3}} \gg 1 \,. \tag{7.63}$$

The first of these conditions guarantees that inflation is of the small-field type, while the second implies that $N_{\rm tot} \gg 1$. We will be interested in $N_{\rm tot} \geq N_{\rm CMB} \sim 60$.

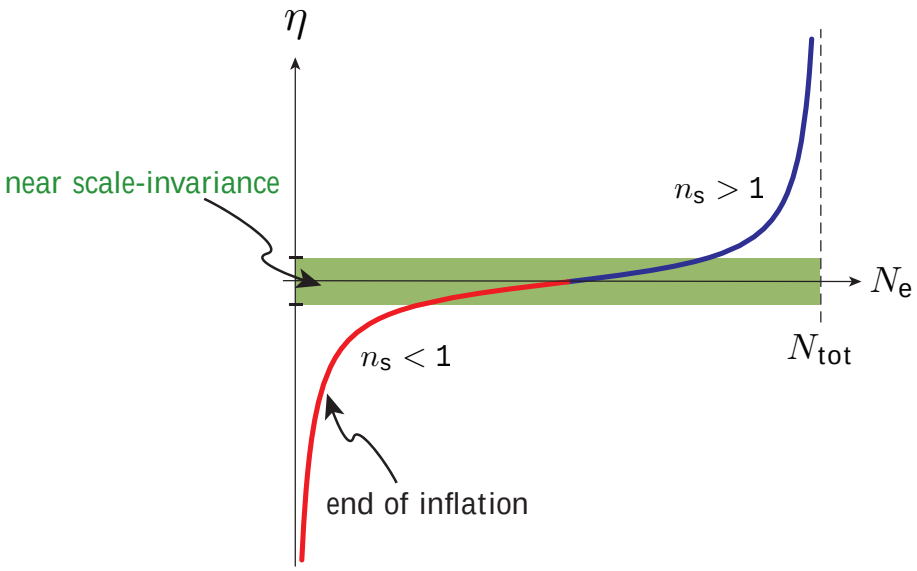


FIGURE 4. $\eta(\phi)$ **as a function of the number of** $e$**-folds of inflation,** $N_e$. In the green band, $|\eta| < 2\pi N_{\rm tot}^{-1}$.

Equation (7.61) shows that there are $\frac{1}{2}N_{\rm tot}$ $e$–folds during which $|\eta| < 2\pi N_{\rm tot}^{-1}$; see Figure 4. For large $N_{\rm tot}$ this implies that there is a large range of $e$–folds where $\eta$ is small and the scalar perturbation spectrum is nearly scale-invariant. Predicting the scalar spectral index in these models is non-trivial:

$$n_s - 1 = (2\eta - 6\epsilon)|_{\phi_{\rm CMB}} \approx 2\eta(\phi_{\rm CMB}) \,. \tag{7.64}$$

The scalar spectral index on CMB scales can be red, blue or even perfectly scale-invariant depending on where $\phi_{\rm CMB}$ is relative to the inflection point. If inflation only

lasts for the minimal number of $e$-folds to solve the horizon and flatness problems then the scalar spectrum is blue. If the potential is flatter than this, so that $\epsilon$ is smaller, inflation lasts longer and $\phi_{\rm CMB}$ is more likely to be smaller than $\phi_0$. The spectrum is then red, since $\eta(\phi_{\rm CMB} < \phi_0) < 0$.

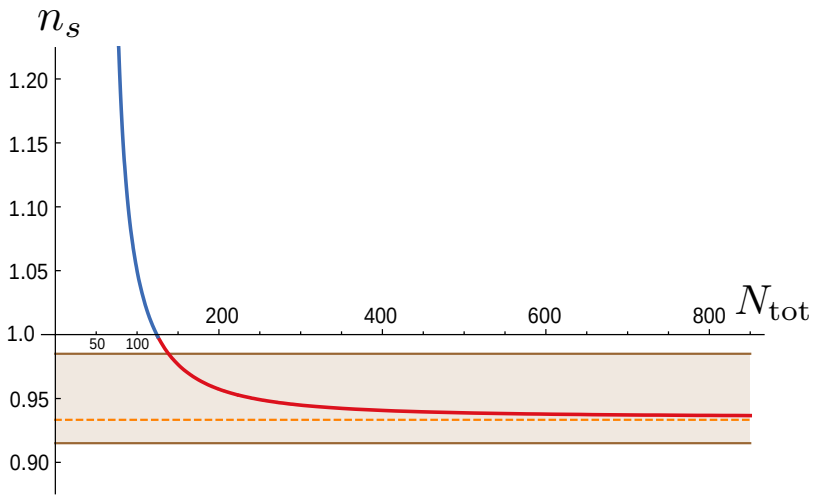


FIGURE 5. **Spectral index** $n_s$, evaluated on CMB scales, as a function of the total number of $e$-folds of inflation, $N_{\rm tot}$. The light band gives the WMAP3 $2\sigma$ limit on $n_s$ (for $r \equiv 0$) [151].

More concretely, we can evaluate $n_s$ by inverting (7.61) at $\phi_{\rm CMB}$ where $N_e(\phi_{\rm CMB}) \equiv N_{\rm CMB} \sim 60$, and using $\eta(\phi_{\rm end}) = -1$. This gives

$$n_s - 1 = \frac{4\pi}{N_{\rm tot}} \tan\left(\pi \frac{N_{\rm CMB}}{N_{\rm tot}} - \arctan\left(\frac{N_{\rm tot}}{2\pi}\right)\right) . \tag{7.65}$$

Using $\arctan x = \frac{\pi}{2} - x^{-1} + \mathcal{O}(x^{-3})$ we furthermore find

$$n_s - 1 = \frac{4\pi}{N_{\rm tot}} \tan\left(\pi \frac{N_{\rm CMB} + 2}{N_{\rm tot}} - \frac{\pi}{2} + \mathcal{O}(N_{\rm tot}^{-3})\right) . \tag{7.66}$$

Using $N_{\rm CMB} + 2 \approx N_{\rm CMB} \gg 1$, we may simplify this to

$$n_s - 1 \approx -\frac{4\pi}{N_{\rm tot}} \cot\left(\pi \frac{N_{\rm CMB}}{N_{\rm tot}}\right) , \tag{7.67}$$

which has the expansion

$$n_s - 1 \approx -\frac{4}{N_{\rm CMB}} + \frac{4\pi^2}{3}\frac{N_{\rm CMB}}{N_{\rm tot}^2} + \mathcal{O}\Big(\frac{N_{\rm CMB}^3}{N_{\rm tot}^4}\Big)\,. \tag{7.68}$$

Equation (7.67) is plotted in Figure 5. We note the following properties of this result. For $N_{\rm tot}$ not much greater than $N_{\rm CMB}$ the spectrum is strongly blue and the model is hence ruled out by recent observations [151] (in this regime the slow-roll formulae we have used are not good approximations, but a more exact treatment gives similar results). For $N_{\rm tot} \approx 2N_{\rm CMB}$ the spectrum on CMB scales is exactly scale-invariant. For $N_{\rm tot} \gtrsim 2N_{\rm CMB}$ the spectrum is red and asymptotes to the lower limit $n_s \to 1 - 4/N_{\rm CMB} \approx 0.93$ for $N_{\rm tot} \gg N_{\rm CMB}$. This asymptotic limit, which has been noted in studies of inflation near an inflection point [5, 92], is more strongly red than is typical in single-field inflation models.

Given the explicit expression (7.67) for the spectral index $n_s(N_e)$ we can compute its scale-dependence or 'running':

$$\alpha_s \equiv \frac{dn_s}{d\ln k} = -\left.\frac{dn_s}{dN_e}\right|_{N_e=N_{\rm CMB}} = -\frac{4\pi^2}{N_{\rm tot}^2}\sin^{-2}\left(\pi\frac{N_{\rm CMB}}{N_{\rm tot}}\right)\,, \tag{7.69}$$

$$\approx -\frac{4}{N_{\rm CMB}^2} - \frac{4\pi^2}{3}\frac{1}{N_{\rm tot}^2} + \mathcal{O}\Big(\frac{N_{\rm CMB}^2}{N_{\rm tot}^4}\Big)\,. \tag{7.70}$$

The running can be large for models with blue spectral tilt ($N_{\rm tot} \sim N_{\rm CMB}$), but is small for models with red spectra. The asymptotic value for $N_{\rm tot} \gg N_{\rm CMB}$ is $\alpha_s \to -4/N_{\rm CMB}^2 \approx -10^{-3}$. Notice that because both the tilt $n_s - 1$ and the running $\alpha_s$ are determined by $N_{\rm tot}$ alone (for fixed $N_{\rm CMB}$), this phenomenological model is predictive.

It is possible to arrange for the magnitude of scalar perturbations on CMB scales to be small,

$$\Delta_{\mathcal{R}}^2 = \left.\frac{1}{24\pi^2}\frac{\mathbb{V}}{\epsilon}\right|_{\phi_{\rm CMB}} \approx 2.4\times 10^{-9}\,, \tag{7.71}$$

by adjusting the overall scale of inflation $V_0$.

Let us comment briefly on some general difficulties in inflection point inflation. Since inflation is restricted to a small region around the inflection point, an immediate concern is the question of initial conditions. In particular, how sensitive is the present scenario to the initial position and velocity of the D3-brane? What fraction of initial conditions lead to overshoot rather than to inflation? These questions have recently been analyzed by Bret Underwood [157] who finds that including the effects of the DBI kinetic term dramatically improves naive estimates on the amount of fine-tuning of initial conditions necessary for inflation.

Since this is a small-field model, it is sensitive to small corrections in the slope of the potential (see §6). These corrections are important for both the background evolution, *i.e.* the number of $e$–folds of inflation, and for the perturbation spectrum.

Finally, we note that the appearance of the inflection point feature depends sensitively on the use of the adiabatic approximation for integrating out the volume modulus. One might therefore be worried about cases in which the exact two-field evolution is not well captured by this approximation and a more detailed numerical study of the two-field evolution is required.[12]

## 5. Comments on Other Embeddings

The previous two sections contained a detailed discussion of the D3-brane potential for the Kuperstein embedding. We derived important microscopic constraints, analyzed the fine-tuning problem involved in realizing inflationary solutions, and studied the resulting cosmological dynamics.

In this section we will make some brief remarks about other embeddings. When applicable we will emphasize the differences and similarities to the Kuperstein case. This will illustrate the special status of the Kuperstein embedding.

[12]This important problem has been explored in the subsequent work [135] where the validity of the adiabatic approximation is explicitly confirmed.

First, we give a simple proof that for an infinite class of D7-brane embeddings, the ACR embeddings, there always exist trajectories for which no amount of fine-tuning can flatten the inflaton potential. Areán, Crooks and Ramallo (ACR) [9] studied supersymmetric four-cycles in the conifold described by the embedding equations

$$f(w_i) = \mu^P - \prod_{i=1}^{4} w_i^{p_i} = 0\,, \tag{7.72}$$

where $p_i \in \mathbb{Z}$, $P \equiv \sum_{i=1}^{4} p_i$ and $\mu^P \in \mathbb{C}$ are constants defining the embedding. Here $w_i \in \mathbb{C}$ are alternative coordinates on the conifold that follow from the $z_i$ coordinates by a linear transformation (see Appendix E). The conifold constraint in these coordinates is $w_1 w_2 - w_3 w_4 = 0$. By requiring that the $p_i$ are non-negative we can restrict attention to four-cycles that do not reach the tip of the conifold. Two simple special cases of the ACR embeddings (7.72) are the *Ouyang embedding* [133], $w_1 = \mu$, and the *Karch-Katz embedding* [99], $w_1 w_2 = \mu^2$.

To study the ACR embeddings in a unified way we define a collective coordinate $\Phi$

$$\Phi^P \equiv \prod_{i=1}^{4} w_i^{p_i}\,, \tag{7.73}$$

such that

$$A(\Phi^P) = A_0 \left(1 - \frac{\Phi^P}{\mu^P}\right)^{1/n}\,, \tag{7.74}$$

and

$$\sum_i w_i \alpha_{w_i} = \sum_i p_i \Phi^P \alpha_{\Phi^P} = P \Phi^P \alpha_{\Phi^P}\,, \tag{7.75}$$

where

$$\alpha_{\Phi^P} \equiv \frac{1}{A}\frac{\partial A}{\partial \Phi^P} = -\frac{1}{n}\frac{1}{\mu^P - \Phi^P}\,. \tag{7.76}$$

Next, we consider the part of the F-term potential that depends on derivatives of the superpotential with respect to the brane coordinates

$$\Delta V_F = -\frac{\kappa^2 a |A|^2 e^{-2a\sigma}}{U^2}\left[3\,\mathrm{Re}(w^i \alpha_{w_i}) - \frac{1}{a\gamma}\hat{k}_w^{i\bar{j}} \alpha_{w_i} \alpha_{\overline{w_j}}\right], \tag{7.77}$$

where

$$\mathrm{Re}(w^i \alpha_{w_i}) = P\,\mathrm{Re}(\Phi^P \alpha_{\Phi^P}) \tag{7.78}$$

and

$$\frac{1}{\gamma}\hat{k}_w^{i\bar{j}}\alpha_{w_i}\alpha_{\overline{w_j}} \;=\; \frac{1}{\gamma r^2}\left|\alpha_{\Phi^P}\right|^2\left|\Phi^P\right|^2\left\{\frac{1}{2}P^2 + (p_1-p_2)^2 + (p_3-p_4)^4 + Z(w_i)\right\}. \tag{7.79}$$

Here, we found it convenient to write the Kähler metric $\hat{k}_w^{i\bar{j}}$ in $SO(4)$–invariant form (see Appendix E) and defined the function

$$\begin{aligned} Z \;\equiv\; &+\left|p_1\frac{w_4}{w_1}+p_3\frac{w_2}{w_3}\right|^2+\left|p_1\frac{w_3}{w_1}+p_4\frac{w_2}{w_4}\right|^2 \\ &+\left|p_2\frac{w_3}{w_2}+p_4\frac{w_1}{w_4}\right|^2+\left|p_2\frac{w_4}{w_2}+p_3\frac{w_1}{w_3}\right|^2 . \end{aligned} \tag{7.80}$$

**5.1. Delta-flat Directions.** We now show that there is always a radial trajectory, $\Phi = 0$, along which $\partial W/\partial w_i$ is orthogonal to $w_i$ and lies in the null direction of $\hat{k}_w^{i\bar{j}}$. The term $\Delta V_F$ in (7.77) then vanishes and the prefactor $A$ of the superpotential becomes independent of the brane position. We call this a *delta-flat direction*. For the Ouyang embedding this trajectory was first found by Burgess et al. [45]. As noted in [45], delta-flat directions are noteworthy because they have $\Delta\eta = 0$ and therefore imply a well-known no-go result for inflation [95].

More concretely, we see that for (7.78) to vanish one requires

$$\Phi = 0\,, \tag{7.81}$$

*i.e.* at least one of the $w_i$ that enter the embedding must vanish. In fact, we notice that (7.78) vanishes whenever (7.79) does, so we can restrict our attention to (7.79). If *any* $p_i > 1$, then we see immediately from the overall factor $|\Phi^P|^2 = |w_1|^{2p_1}|w_2|^{2p_2}|w_3|^{2p_3}|w_4|^{2p_4}$ that (7.79) vanishes on $w_i = 0$. For $p_i \leq 1$ there are only a few distinct cases: $\Phi = w_1$, $\Phi^2 = w_1w_2$, $\Phi^2 = w_1w_3$, $\Phi^3 = w_1w_2w_3$, and

$\Phi^4 = w_1 w_2 w_3 w_4$. In the next section we will illustrate the argument for the important case of the Ouyang embedding, $\Phi = w_1$; the proof is easily generalized to the remaining cases. This completes the proof that all ACR embeddings have delta-flat trajectories.

**5.2. Comparison of the Ouyang and Kuperstein Embeddings.** Recently the result of [18] has been applied [45, 113] to compactifications involving the Ouyang embedding $w_1 = \mu$. In this case, the correction to the F-term potential is

$$\Delta V_F = \frac{\kappa^2}{3U^2}\left[\frac{3}{2}(\overline{W_{,\rho}} w_1 W_{,w_1} + c.c.) + \frac{1}{\gamma}\hat{k}_w^{1\bar{1}} W_{,w_1}\overline{W_{,w_1}}\right], \tag{7.82}$$

where

$$\hat{k}_w^{1\bar{1}} = r\Big(1 + \frac{|w_1|^2}{2r^3} - \frac{|w_2|^2}{r^3}\Big). \tag{7.83}$$

There are two kinds of radial extremal trajectories: the delta-flat trajectory $w_1 = w_3 = w_4 = 0$, for which $\Delta V_F = 0$ [45], and also a trajectory $w_2 = w_3 = w_4 = 0$, $w_1 \in \mathbb{R}$ used in [113].

The Kuperstein scenario is closely related to the Ouyang scenario except for two subtle differences which we now discuss:

(1) There exists *no* delta-flat direction for the Kuperstein embedding.

(2) The single-field potential along the non-delta-flat direction for the Ouyang embedding is identical in shape to that along the corresponding Kuperstein trajectory. However, the angular stability is different (see Appendix G). This trajectory in the Kuperstein embedding is stable for small $r$, while in the Ouyang embedding it is unstable in that regime.

To see this compare the correction to the F-term potential for the Ouyang embedding, (7.82), with the corresponding term for the Kuperstein embedding,

$$\Delta V_F = \frac{\kappa^2}{3U^2}\left[\frac{3}{2}(\overline{W_{,\rho}} z_1 W_{,z_1} + c.c.) + \frac{1}{\gamma}k^{1\bar{1}} W_{,z_1}\overline{W_{,z_1}}\right], \tag{7.84}$$

where

$$k^{1\bar{1}} = r\Big(1 - \frac{1}{2}\frac{|z_1|^2}{r^3}\Big)\,. \tag{7.85}$$

This shows immediately that the Kuperstein embedding does not have a delta-flat direction, since $k^{1\bar{1}}$ cannot vanish for $r > 0$. This is to be viewed in contrast to the Ouyang case for which (7.83) vanishes on $w_1 = 0$.

Considering $k^{1\bar{1}}, \hat{k}_w^{1\bar{1}}$ for each case one may further show that the trajectories $2|z_1|^2 = r^3$ and $|w_1|^2 = r^3$ lead to identical shapes for the single-field potential. However, 'off-shell', *i.e.* away from the extremal path, $\hat{k}_w^{1\bar{1}}$ for the Ouyang embedding is of a different form from $k^{1\bar{1}}$ for the Kuperstein embedding. It is for this reason that the angular stability of the two scenarios is different (see Appendix G for details). In particular, while for the Kuperstein embedding the trajectory is stable for the regime of interest, for the Ouyang embedding it is unstable.

To discuss the issue of stability in simple terms, we consider $\theta_1 = \theta_2 = \theta$ and $\tilde{\psi} \equiv \psi - \phi_1 - \phi_2$, so that $w_1 = e^{\frac{i}{2}\tilde{\psi}} r^{3/2} \sin^2(\theta/2)$. Then, as shown in [45] for $n = 1$,

$$V_F(\theta) = V_1 \sin^2(\theta/2) + V_2 \sin^4(\theta/2) + const.\,, \tag{7.86}$$

where

$$V_1 = \frac{\kappa^2 |A_0|^2 e^{-2a\sigma}}{3U^2}\frac{r}{\gamma\mu^2}\left(2 - a\mu\gamma\sqrt{r}\cos\frac{\tilde{\psi}}{2}\left(9 + 4a\sigma + 6W_0\frac{e^{a\sigma}}{|A_0|}\right)\right)\,, \tag{7.87}$$

$$V_2 = \frac{1}{4}\frac{\kappa^2 |A_0|^2 e^{-2a\sigma}}{3U^2}\frac{r}{\gamma\mu^2}\Big(-2 + a\gamma r^2(12 + 8a\sigma)\Big)\,. \tag{7.88}$$

We see that $\frac{\partial V_F}{\partial\theta}$ vanishes for $\theta = 0$ or $\pi$.

The $\theta = 0$ trajectory is delta-flat [45]. For this trajectory, $\frac{\partial^2 V_F}{\partial\theta^2} = \frac{1}{2}V_1$ which is clearly positive for small $r$ and stays positive up to some critical radius $r_c$. To compute $r_c$ we evaluate $V_1$ at $\sigma = \sigma_0$ using

$$4a\sigma_0 + 9 - 6W_0\frac{e^{a\sigma_0}}{|A_0|} \approx 3 - 4s\,. \tag{7.89}$$

We find

$$V_1 \approx \frac{\kappa^2 |A_0|^2 e^{-2a\sigma_0}}{3U^2} \frac{r}{\gamma\mu^2} \left( 2 + a\mu\gamma(4s-3)\sqrt{r}\cos\frac{\tilde{\psi}}{2} \right). \tag{7.90}$$

For $s > 3/4$ and for real positive $\mu$, the potential is minimized at $\tilde{\psi} = 2\pi$, where

$$V_1 \approx \frac{\kappa^2 |A_0|^2 e^{-2a\sigma_0}}{3U^2} \frac{r}{\gamma\mu^2} \left( 2 - a\mu\gamma(4s-3)\sqrt{r} \right), \tag{7.91}$$

This is positive as long as $r$ is less than $r_c$, where

$$\frac{r_c}{r_\mu} = \frac{1}{(4s-3)^2} \left( \frac{9}{a\sigma_0} \right)^2 \frac{M_{\rm pl}^4}{\phi_\mu^4}. \tag{7.92}$$

Applying the field range bound in the form $\frac{\phi_\mu^2}{M_{\rm pl}^2} < \frac{4}{N}$ one finds

$$\frac{r_c}{r_\mu} > \frac{N^2}{4^2} \frac{1}{(4s-3)^2} \left( \frac{9}{a\sigma_0} \right)^2. \tag{7.93}$$

For typical parameters we therefore conclude that $r_c \geq r_\mu$ and the delta-flat direction is hence stable from the tip to at least the location $r_\mu$ of the D7-branes.

For the $\theta = \pi$ trajectory, $\frac{\partial^2 V_F}{\partial\theta^2} = -\frac{1}{2}V_1$. This is negative for $r < r_c$ and the $\theta = \pi$ trajectory is therefore unstable in this regime. This analysis was carried out for $n = 1$ but it illustrates the essential qualitative point (for a more general analysis with the same conclusion, see Appendix C.2).

In Appendix G.4 we show that for all ACR embeddings there are alternative trajectories with $\Phi \neq 0$ that are not delta-flat. This is important because it implies that, for a D3-brane moving along such a trajectory, $\eta$ can be different from $\frac{2}{3}$. We postpone a more general treatment of such trajectories for the future (but see Appendix G.4 for some preliminary remarks).

## 6. Discussion

In this section we will briefly take stock of our progress towards an explicit model of D-brane inflation. For this purpose, it is useful to consider the more general problem of deriving a low-energy Lagrangian from the data of a string compactification.

In principle, the data of a compactification – such as the background geometry, brane positions, and fluxes – determine the low-energy effective Lagrangian in full. In practice, one typically begins by deriving the leading-order effective Lagrangian, which follows from dimensional reduction of the classical ten-dimensional supergravity action, including the effect of fluxes but treating D-branes as probes. Then, one can include corrections to this action, including such things as nonperturbative terms in the superpotential, D-brane backreaction effects, string loop corrections to the Kähler potential, and $\alpha'$ corrections to the Kähler potential. Except in cases with extended supersymmetry, it is typically impossible to obtain results beyond leading order in either series of corrections to the Kähler potential.

For the present purpose, an instructive way to organize these corrections is according to their effects on the slow-roll parameter $\eta$, as follows. The leading order classical four-dimensional Lagrangian we denote $\mathcal{L}_0$. Correction terms are well-known to give rise to inflaton masses of order $H$, and hence corrections of order unity to $\eta$. When all such effects, from any source whatsoever, have been added to $\mathcal{L}_0$, we denote this corrected Lagrangian $\mathcal{L}_1$. By definition, this is the Lagrangian whose inflaton mass term is a good approximation to the 'true' mass term that would follow from a dimensional reduction incorporating corrections of arbitrarily high degree. (Notice that the leading-order classical Lagrangian $\mathcal{L}_0$ may itself contain large inflaton mass terms.) Finally, if to $\mathcal{L}_1$ we add the leading terms that give corrections to $\eta$ that are parametrically small compared to unity, we call the resulting Lagrangian $\mathcal{L}_2$. In sum, we propose to organize corrections to the Lagrangian according to the degree of

their effects on $\eta$, even though such an organization does not correspond to a literal expansion parameter such as the string coupling.

To determine whether a given model gives rise to prolonged slow-roll inflation, one needs to know $\mathcal{L}_1$. However, it is rarely true that all the required results are available. For example, in the warped brane inflation model of [95], the inflaton-dependence of the threshold factor $A(\phi)$ of the nonperturbative superpotential was not known until recently [18, 32]. Similarly, in Kähler moduli inflation [54], a particular term in the Kähler potential that could give $\Delta\eta \sim 1$ has not yet been computed (though it has been conjectured that this term might vanish.) Although such partial data is generally insufficient to determine whether a model is successful, even this degree of detail is relatively rare: a fair fraction of proposed models of string inflation include only the $\mathcal{L}_0$ data, without any corrections at all.

In this chapter, we have made progress towards a full understanding of the Lagrangian $\mathcal{L}_1$ for the warped brane inflation models of [95]. However, as we will now explain, further work is necessary.

First, let us briefly recall the best-understood correction terms. The D3-brane potential receives contributions from the mixing between the volume and the D3-brane position in the DeWolfe-Giddings Kähler potential (7.9). Moreover, the nonperturbative superpotential receives the correction (7.15) sourced by the backreaction of the D3-brane on the warp factor. Holomorphy of the gauge kinetic function ensures that this correction, which corresponds to a one-loop threshold factor, is the only perturbative correction to the superpotential. The only additional contributions to the superpotential come from multi-instantons, which give a negligibly small effect.

The Kähler potential, however, is not protected by holomorphy, and in general receives $\alpha'$ and $g_s$ corrections. In the large-volume, weak-coupling limit, these corrections are suppressed relative to the leading terms in the DeWolfe-Giddings Kähler potential, and so generate mass terms that are generically smaller than $H$ by powers

of the inverse volume or powers of the string coupling. Hence, by our above definition, these corrections correspond to terms in $\mathcal{L}_2$. Although complete results for these terms are not available for a general compactification, the work of Berg, Haack, and Körs [33, 34] in the toroidal orientifold case gives substantial guidance. These authors found that the leading D3-brane-dependent corrections to $\mathcal{K}$ are of two types, one suppressed by an additional power of $\rho$ compared to the DeWolfe-Giddings result, and the other suppressed by one power of $g_s$. For $\rho \gg 1$, $g_s \ll 1$, these terms give a parametrically small correction to the D3-brane potential, and so belong to what we have called $\mathcal{L}_2$. Even better, in some cases [33] the expectations of naive dimensional analysis are borne out, and the numerical prefactors of these higher-order terms are moderately small.[13]

Corrections due to the fluxes are a further possibility. The best-understood $\alpha'$ corrections arise from the term $(\alpha')^3 R^4$ in ten dimensions, with $R^4$ standing for an appropriate contraction of four powers of the Riemann tensor. In the presence of three-form flux $G_3$, there are additional terms from $(G_3)^2 R^3$, and it is less clear how these correct the Kähler potential [25]. However, it has been argued that at large volume, hence low flux density, this effect is subleading [15].

Finally, and perhaps most importantly, perturbations of the background fields in the throat, which can arise from sources in the bulk, can give substantial corrections to the D3-brane potential.[14] It was argued in [59] (see also [113]) that in special cases these effects may be small compared to the forces from the D7-brane. However, lacking a more complete understanding of these effects, we do not claim that the potential we have presented is completely general. Instead, our construction is representative of a particulay tractable class of situations in which the bulk effects are small.

[13]We thank M. Berg for helpful discussions of this point.
[14]We thank S. Kachru for explanations of this point.

## 7. Conclusions

In this chapter we have systematically studied the potential for a D3-brane in a warped throat containing holomorphically-embedded D7-branes. This system is a promising candidate for an explicit model of inflation in string theory. However, the warped brane inflation model of [95] is well-known to suffer from an inflaton mass problem, in that corrections from moduli stabilization tend to curve the potential and make slow-roll inflation impossible. The true severity of this problem – and, correspondingly, the status of the model – have remained unclear, because the functional form of one particular correction term, arising from a threshold correction to the nonperturbative superpotential, was unavailable before the recent result of [18]. In this work, building on [18], we have studied the corrected potential in detail. This equipped us to assess the true status of the warped brane inflation model [95] and to ascertain whether prolonged slow-roll inflation is indeed possible.

Our method for analyzing the potential involved several nontrivial improvements over existing approximations. First, we systematically identified stable minima in the angular directions of the conifold, and showed how the radial potential depends on the choice of angular minimum. Second, we showed that the common assumption that the compactification volume remains stabilized at its minimum during inflation is inadequate: the volume shrinks slightly as the D3-brane falls down the throat, and this leads to non-negligible corrections to the effective D3-brane potential. We gave an analytic expression for the volume as a function of the D3-brane position and showed that this is an excellent approximation to the full result.

For a large class of embeddings of the wrapped branes, the ACR embeddings, we showed that the radial potential for a D3-brane at a particular angular extremum is necessarily too steep to support inflation, because the contributions computed in [18] vanish along the trajectory, and so the no-go result of [95] applies. This was first explained in [45] for a special ACR embedding, the Ouyang embedding [133]. Our

results here generalize this to the full ACR class. It follows that these trajectories in throats containing wrapped branes with ACR embeddings do not permit slow roll D-brane inflation, even if one allows an arbitrary degree of fine-tuning: there is simply no parameter that can be varied to flatten the potential in such a case. However, we also showed that all ACR embeddings have alternative trajectories, corresponding to other choices of the angular extremum, for which this no-go result does not apply.

Our main result was an analysis of a very simple and symmetric embedding, the Kuperstein embedding, that does allow a flat D3-brane potential. We found that for certain fine-tuned ranges of the compactification parameters, the potential is flat enough to allow prolonged inflation. However, the resulting potential is not as simple as that conjectured in [95] and further elaborated in [68]: moduli stabilization gives rise to a potential that is much more complicated than a mass term for radial motion. Furthermore, adjusting the potential by varying microscopic parameters changes features in the potential instead of just rescaling the mass term. In particular, one can fine-tune to arrange for a flat region suitable for inflation, but we found that this will occur around an inflection point away from the origin. Hence, when inflation occurs, it does so near an approximate inflection point, rather than in a shallow quadratic potential centered on the origin. In short, we found that a low-order Taylor expansion of the potential around the minimum at the tip of the throat does not properly describe those regions of the potential where inflation is possible. Instead, one is obliged to use the complete potential presented here. Our result implies that the phenomenology of some classes of warped D-brane inflation models is well-described by an effective single-field potential with a constant and cubic term. As we explained, models of this sort (see [5] for an analogous example in the MSSM) are particularly sensitive to the initial conditions. Moreover, the tilt of the scalar spectrum is exquisitely sensitive to the slope of the potential near the approximate inflection point.

One important, general lesson of our work is that there is considerably less freedom to adjust the parameters of this system than one might expect from the low-energy effective action. First, the functional form of $A(\phi)$ derived in [18] is rather special: most importantly, $A(\phi)$ contains no quadratic term, and does not lead to any new quadratic terms in the inflaton potential. This implies that the potential cannot be flattened uniformly, and $\eta$ can only be small in a limited region. Second, the range of $\phi$ is limited by the microscopic constraint of [21]. Finally, the field range is linked to the scale of inflation, because of a new geometric constraint linking the size of the wrapped four-cycle and the length of the throat. Using these results, we found that although this system depends on many microscopic parameters, in many cases it is nevertheless impossible to choose these parameters in such a way that the slow-roll parameter $\eta$ is fine-tuned to vanish. This occurs because constraints originating in the geometry of the compactification correlate the microscopic quantities, so that the true number of adjustable parameters is much smaller than a naive estimate would suggest.

An important direction for future work is a more comprehensive understanding of any additional corrections to the potential, such as $\alpha'$ corrections, string loop corrections, and perturbations of the throat metric due to bulk sources. We have argued that in some cases the presence of such effects is not fatal for inflation, but precise observational predictions will certainly depend on these effects.

**Symbols used in this Chapter**

TABLE 1. Definitions of symbols and notation used in this chapter and in Appendices E, F, G, and H.

| Variable | Description | Definition |
|---|---|---|
| $z_i$ | complex conifold coordinates | $\sum_i z_i^2 = 0$, (E.4)–(E.7) |
| $w_i$ | complex conifold coordinates | $w_1 w_2 - w_3 w_4 = 0$, (E.8)–(E.11) |
| $\varepsilon$ | conifold deformation parameter | $\sum_i z_i^2 = \varepsilon$, equation (7.1) |
| $r$ | radial coordinate on the conifold | $r^3 = \sum_i \lvert z_i\rvert^2$ |
| $\hat{r}$ | radial coordinate on the conifold | $\hat{r}^2 = \frac{3}{2} r^2$, $\mathrm{d}s^2 = \mathrm{d}\hat{r}^2 + \ldots$ |
| $\tilde{r}$ | radial coordinate on the conifold | $\tilde{r} = e^u \hat{r}$ |
| $e^u$ | breathing mode | equation (F.1) |
| $g_{\alpha\bar{\beta}}$ | fiducial metric | |
| $\tilde{g}_{\alpha\bar{\beta}}$ | physical metric | $\tilde{g}_{\alpha\bar{\beta}} = e^{2u} g_{\alpha\bar{\beta}}$ |
| $k$ | Kähler potential | $g_{\alpha\bar{\beta}} = k_{,\alpha\bar{\beta}}$, $k = \frac{3}{2}(\sum_i z_i^2)^{2/3}$ |
| $\phi_i$, $\theta_i$, $\psi$ | angular coordinates on $T^{1,1}$ | equations (E.4)–(E.7) |
| $h(r)$ | warp factor | equation (7.4) |
| $r_{\mathrm{UV}}$ | radius at the UV end | $\ln r_{\mathrm{UV}}/\varepsilon^{2/3} = 2\pi K/(3 g_s M)$ |
| $\phi$ | inflaton field | $\phi^2 = T_3 \hat{r}^2$ |
| $\varphi$ | canonical inflaton field | Appendix F, $\varphi^2 \approx \frac{\sigma_c^{(0)}}{\sigma(\phi)} \phi^2$ |
| $\mathcal{K}$ | Kähler potential | $\kappa^2 \mathcal{K} = -3 \ln U$ |
| $W$ | superpotential | |
| $U$ | argument of Kähler potential [58] | $U = \rho + \bar{\rho} - \gamma k$ |
| $\rho$ | complex Kähler modulus | |
| $\sigma$ | real part of $\rho$ | $2\sigma = \rho + \bar{\rho}$ |
| $\tau$ | imaginary part of $\rho$ | $2i\,\tau = \rho - \bar{\rho}$ |
| $\sigma_\star$ | stabilized volume modulus | $\partial_\sigma V\big\rvert_{\sigma_\star} = 0$ |
| $\omega_\star$ | rescaled volume modulus | $\omega_\star \equiv a \sigma_\star$ |
| $W_0$ | GVW-flux superpotential | $W_0 = \int G \wedge \Omega$ |
| $W_{\mathrm{np}}$ | non-perturbative superpotential | $W_{\mathrm{np}} = A(z_i) e^{-a\rho}$ |
| $f(z_i)$ | embedding equation | $A(z_i) \propto (f(z_i))^{1/n}$ |
| $g(z_i)$ | embedding equation | $g(z_i) = f(z_i)/f(0)$ |
| $A_0$ | prefactor of $W_{\mathrm{np}}$ | $A_0 = A(z_i = 0)$ |
| $V_F$ | F-term potential | equation (7.8) |
| $V_D$ | D-term potential | $V_D = D U^{-2}$; equation (7.20) |
| $D$ | scale of D-term energy | $D \equiv 2 h_0^{-1} T_3$ |
| $\epsilon$, $\eta$ | slow-roll parameters | $\epsilon = \frac{1}{2}(V'/V)^2$, $\eta = V''/V$ |
| $g_s$ | string coupling | |
| $T_3$ | D3-brane tension | $T_3^{-1} = (2\pi)^3 g_s (\alpha')^2$ |

| Variable | Description | Definition |
|---|---|---|
| $\mu$ | embedding parameter | $z_1 = \mu$ |
| $n$ | # of embedded D7's | |
| $a$ | parameter in $W_{\rm np}$ | $a = 2\pi/n$ |
| $r_\mu$ | minimal radius of D7 | $r_\mu^3 = 2\mu^2$ |
| $\phi_\mu$ | rescaled $r_\mu$ | $\phi_\mu^2 = \frac{3}{2}T_3 r_\mu^2$ |
| $M$, $K$ | flux on the $A$ and $B$ cycle | |
| $N$ | five-form flux | $N \equiv MK$ |
| $L$ | AdS radius | equation (F.21) |
| $M_{\rm pl}$ | 4d Planck mass | $M_{\rm pl}^2 = \frac{1}{\pi}(T_3)^2 V_6^w$ |
| $V_6^w$ | warped 6-volume | |
| $V_{\Sigma_4}^w$ | warped 4-cycle volume | Appendix F |
| $s$ | ratio of D- and F-term | |
| $x$ | ratio of $r$ and $r_\mu$ | $x = r/r_\mu$ |
| $x_0$ | location of $\eta = 0$ | |
| $Q_\mu$ | ratio of $r_{\rm UV}$ and $r_\mu$ | $Q_\mu = r_{\rm UV}/r_\mu > 1$ |
| $B_6$ | bulk contribution to $V_6^w$ | $(V_6^w)_{\rm bulk} = B_6 (V_6^w)_{\rm throat}$ |
| $B_4$ | bulk contribution to $V_{\Sigma_4}^w$ | $(V_{\Sigma_4}^w)_{\rm bulk} = B_4 (V_{\Sigma_4}^w)_{\rm throat}$ |
| $\omega_F$ | Kähler modulus *before* uplifting | equation (H.2) |
| $\omega_0$ | Kähler modulus *after* uplifting | $\omega_0 \approx \omega_F + s/\omega_F$ |
| $\Gamma$ | factor in $\mathcal{K}$ | $\Gamma = 2\sigma_0$ |
| $\tilde{\Gamma}$ | factor in $\mathcal{K}$ | $\tilde{\Gamma} \equiv \Gamma e^{4u} = U$ |
| $\gamma$ | prefactor in the Kähler potential | $\gamma = \frac{\Gamma}{6}\frac{T_3}{M_{\rm pl}^2} = \frac{\sigma_0}{3}\frac{T_3}{M_{\rm pl}^2}$ |
| $c$ | factor in $V_F$ | $c^{-1} = 4\pi\gamma r_\mu^2$ |
| $c_{3/2}$ | factor in volume shift | equation (7.45) |
| $X$, $X+Y$ | eigenvalues of Hessian | Appendix G |
| $P$ | degree of ACR embeddings | $\prod_i w_i^{p_i} = \mu^P$ |
| $p_i$ | embedding parameter | $p_i \in \mathbb{Z}$ |
| $\Phi$ | collective coordinate for ACR | $\Phi^P \equiv \prod_i w_i^{p_i}$ |

# Part 3

# String Theory and Gravitational Waves

"I never thought that anybody would ever actually measure these things.
I thought we were just calculating for the fun of it."

*Alan Guth*

CHAPTER 8

# A Microscopic Limit on Gravitational Waves

We conclude our analysis of D-brane inflation by exposing a geometric limit on the maximal amplitude of gravitational waves attainable in these models.[1]

## 1. Introduction

In the foreseeable future it may be possible to detect primordial gravitational waves [37] produced during inflation [3, 83, 120]. This would be a spectacular opportunity to reveal physics at energy scales that are unattainable in terrestrial experiments. In light of this possibility, it is essential to understand the predictions made by various inflationary models for gravitational wave production. As we shall review, a result of Lyth [122] connects detectably large gravitational wave signals to motion of the inflaton over Planckian distances in field space. It is interesting to know when suitably flat potentials over such large distances are attainable in string compactifications, allowing a potentially observable tensor signal in the associated string inflation models. In this chapter we analyze this issue for the case of warped D-brane inflation models [64, 95], and use compactification constraints to derive a firm upper bound on the inflaton field range in Planck units.

[1]This chapter is based on Daniel Baumann and Liam McAllister, "A Microscopic Limit on Gravitational Waves from D-brane Inflation," Phys. Rev. D **75**, 123508 (2007). The computation was originally suggested to us by Juan Maldacena and we received important initial input from Igor Klebanov.
The numerical estimates of Ref. [21] have been updated to the WMAP 5-year data [111]. The sign of $f_{\rm NL}$ for DBI inflation has been corrected. These changes strengthen the conclusions of Ref. [21].

For slow-roll warped brane inflation, our result implies that the gravitational wave signal is undetectably small. This constraint is model-independent and holds for any slow-roll potential. For DBI inflation [4, 147], the limit on the field range forces the tensor signal to be much smaller than the current observational bound. Detection in a future experiment may be possible only if $r$ decreases rapidly soon after scales observable in the cosmic microwave background exit the horizon. This does occur in some models, but it has a striking correlate: the scalar spectrum will typically have a strong blue tilt and/or be highly non-Gaussian during the same epoch.

We also consider compactification constraints on the special case of DBI inflation with a quadratic potential. We find that observational constraints, together with our bound on the field range, exclude scenarios with a large amount of five-form flux. For a DBI model realized in a warped cone over an Einstein manifold $X_5$, this translates into a very strong requirement on the volume of $X_5$ at unit radius. However, we show that manifolds obeying this constraint do exist, at least in noncompact models. This translates the usual problem of accommodating a large flux into the problem of arranging that $X_5$ has small volume.

## 2. The Lyth Bound

In slow-roll inflation[2] the tensor fluctuation two-point function is[3]

$$P_t = \frac{2}{\pi^2}\left(\frac{H}{M_{\rm pl}}\right)^2 , \tag{8.1}$$

where $H$ is the Hubble expansion rate. The scalar fluctuation two-point function is

$$P_s = \left(\frac{H}{2\pi}\right)^2 \left(\frac{H}{\dot\varphi}\right)^2 . \tag{8.2}$$

The first factor in (8.2) represents the two-point function of the scalar field, while the second factor comes from the conversion of fluctuations of the scalar field into

[2]By *slow-roll inflation* we mean standard single-field inflation with canonical kinetic term.
[3]See Chapter 2 and Appendix A for details of the results cited in this section.

fluctuations of the scale factor in the metric (or scalar curvature fluctuations). The ratio between the tensor and scalar two-point functions is

$$r \equiv \frac{P_t}{P_s} = 8\left(\frac{\dot{\varphi}}{HM_{\rm pl}}\right)^2 = 8\left(\frac{d\varphi}{d\mathcal{N}}\frac{1}{M_{\rm pl}}\right)^2, \tag{8.3}$$

where $\mathrm{d}\mathcal{N} = H\mathrm{d}t$ represents the differential of the number of $e$-folds. This implies that the total field variation during inflation is

$$\frac{\Delta\varphi}{M_{\rm pl}} = \frac{1}{8^{1/2}}\int_0^{\mathcal{N}_{\rm end}} \mathrm{d}\mathcal{N}\, r^{1/2}\,, \tag{8.4}$$

where $\mathcal{N}_{\rm end} \sim 60$ is the total number of $e$-folds from the time the CMB quadrupole ($\mathcal{N} \equiv 0$) exits the horizon to the end of inflation.

In any given model of inflation, $r$ is determined as a function of $\mathcal{N}$. As a measure of the evolution of $r$ we define the following quantity

$$\mathcal{N}_{\rm eff} \equiv \int_0^{\mathcal{N}_{\rm end}} \mathrm{d}\mathcal{N}\left(\frac{r}{r_{\rm CMB}}\right)^{1/2}, \tag{8.5}$$

so that

$$\frac{\Delta\varphi}{M_{\rm pl}} = \left(\frac{r_{\rm CMB}}{8}\right)^{1/2}\mathcal{N}_{\rm eff}\,. \tag{8.6}$$

Here $r_{\rm CMB}$ denotes the tensor-to-scalar ratio $r$ evaluated on CMB scales, $0 < \mathcal{N} < \mathcal{N}_{\rm CMB} \approx 4$. We use $\mathcal{N}_{\rm eff}$ to parameterize how far beyond $\mathcal{N}_{\rm CMB}$ the support of the integral in (8.4) extends. If $r$ is precisely constant then $\mathcal{N}_{\rm eff} = \mathcal{N}_{\rm end}$, if $r$ is monotonically increasing then $\mathcal{N}_{\rm eff} > \mathcal{N}_{\rm end}$, and if $r$ decreases then $\mathcal{N}_{\rm eff} < \mathcal{N}_{\rm end}$. For a detailed discussion of related issues, see [66].

Equation (8.6) relates the amount of gravitational waves observable in CMB polarization experiments to the field variation $\Delta\varphi$ during inflation

$$r_{\rm CMB} = \frac{8}{(\mathcal{N}_{\rm eff})^2}\left(\frac{\Delta\varphi}{M_{\rm pl}}\right)^2. \tag{8.7}$$

To make use of the relation (8.7), we need to estimate $\mathcal{N}_{\rm eff}$, which amounts to determining $r(\mathcal{N})$. In slow-roll inflation $r$ is proportional to the slow-roll parameter

$$\epsilon \equiv -\frac{d\ln H}{d\mathcal{N}}\,. \tag{8.8}$$

We can define a second slow roll parameter $\tilde{\eta}$ as the fractional variation of $\epsilon$ during one $e$-fold. Then we have

$$\frac{d\ln r}{d\mathcal{N}} = \frac{d\ln \epsilon}{d\mathcal{N}} = \tilde{\eta}\,. \tag{8.9}$$

Equivalently, we can write (8.9) in terms of the spectral indices of the scalar and tensor power spectra

$$\begin{aligned}\frac{d\ln r}{d\mathcal{N}} &= n_t - (n_s - 1) \\ &= -\left[(n_s-1) + \frac{r}{8}\right]\,,\end{aligned} \tag{8.10}$$

where we have used the usual single-field consistency condition, $n_t = -r/8$. Hence, observational constraints on $n_s$ and $r$ give limits on the evolution of $r$ to first order in slow-roll.

We notice that $\mathcal{N}_{\rm eff} < \mathcal{N}_{\rm end}$ only if $\tilde{\eta}$ is negative. Present observations [151, 156] indicate that $|\tilde{\eta}_{\rm CMB}|$ is very small on scales probed by CMB ($\mathcal{N} \lesssim 4$) and large-scale structure observations ($\mathcal{N} \lesssim 10$). In particular, $\tilde{\eta}_{\rm CMB} \gtrsim -0.03$. Since the variation of $\tilde{\eta}$ is second order in slow-roll we may assume that $\tilde{\eta}$ remains small throughout inflation. Integrating (8.9), we find a range $\mathcal{N}_{\rm eff} \sim 30 - 60$ in (8.7). Nearly all of the range for $\tilde{\eta}_{\rm CMB}$ allowed by WMAP3+SDSS [151, 156] actually corresponds to $\mathcal{N}_{\rm eff} \gtrsim 50$. To get a conservative bound, we have considered the most negative values of $\tilde{\eta}_{\rm CMB}$ allowed at the $2\sigma$-level, corresponding to the largest allowed values of $n_s - 1$ and $r$. This gives $\mathcal{N}_{\rm eff} \sim 30$. Direct observation of gravitational waves by some futuristic gravitational wave detector such as the Big Bang Observer (BBO) would put a similar lower bound on $\mathcal{N}_{\rm eff}$ (see *e.g.* [40]).

With this input, the *Lyth bound* [122] for slow-roll inflation becomes

$$r_{\rm CMB} \lesssim \frac{8}{30^2}\Big(\frac{\Delta\varphi}{M_{\rm pl}}\Big)^2 . \tag{8.11}$$

This bound implies that a model producing a detectably large quantity of gravitational waves necessarily involves field variations of order the Planck mass. We will now determine whether such large field variations are possible in a class of string inflation models.

## 3. Constraint on Field Variation in Compact Spaces

In this section we determine the maximum field range of the inflaton in warped D-brane inflation. By (8.7) or (8.11), this will imply an upper limit on gravitational wave production in this scenario. As we will show, this geometrical restriction leads to a strong, model-independent constraint.

**3.1. Warped Throat Compactifications.** Consider a warped flux compactification of type IIB string theory to four dimensions [63], with the line element

$$\mathrm{d}s^2 = h^{-1/2}(y) g_{\mu\nu}\mathrm{d}x^\mu \mathrm{d}x^\nu + h^{1/2}(y) g_{ij}\mathrm{d}y^i \mathrm{d}y^j \,, \tag{8.12}$$

where $\mu,\nu \in 0\ldots3$ are spacetime indices and $i,j \in 4\ldots9$ are internal space indices.

We will be interested in the case that the internal space has a conical throat, *i.e.* a region in which the metric is locally of the form[4]

$$g_{ij}\mathrm{d}y^i\mathrm{d}y^j = \mathrm{d}\rho^2 + \rho^2 \mathrm{d}s^2_{X_5} \,, \tag{8.13}$$

for some five-manifold $X_5$. The metric on this cone is Calabi-Yau provided that $X_5$ is a Sasaki-Einstein space. If the background contains suitable fluxes, the metric in the throat region can be highly warped.

[4]We use $\rho$ to denote the radial direction, because the conventional symbol $r$ is already in use.

Many such warped throats can be approximated locally, *i.e.* for a small range of $\rho$, by the geometry $AdS_5 \times X_5$, with the warp factor

$$h(\rho) = \left(\frac{R}{\rho}\right)^4, \tag{8.14}$$

where $R$ is the radius of curvature of the $AdS$ space. In the case that the background flux is generated entirely by $N$ dissolved D3-branes placed at the tip of the cone, we have the relation [81]

$$\frac{R^4}{(\alpha')^2} = 4\pi g_s N \frac{\pi^3}{\mathrm{Vol}(X_5)}\,. \tag{8.15}$$

Here $\mathrm{Vol}(X_5)$ denotes the dimensionless volume of the space $X_5$ with unit radius.[5] Generically, we expect this volume to obey $\mathrm{Vol}(X_5) = \mathcal{O}(\pi^3)$, *e.g.* $\mathrm{Vol}(S^5) = \pi^3$, $\mathrm{Vol}(T^{1,1}) = \frac{16}{27}\pi^3$. However, very small volumes are possible, for example by performing orbifolds.

Warped throats have complicated behavior both in the infrared and the ultraviolet. For almost all $X_5$, no smooth tip geometry, analogous to that of the Klebanov-Strassler throat [105], is known. Furthermore, the ultraviolet end of the throat, where the conical metric is supposed to be glued into a compact bulk, is poorly understood. These regions are geometric realizations of what are called the 'IR brane' and 'Planck brane' in Randall-Sundrum models. In this note we study constraints that are largely independent of the properties of these boundaries. We take the throat to extend from the tip at $\rho = 0$ up to a radial coordinate $\rho_{\mathrm{UV}}$, where the ultraviolet end of the throat is glued into the bulk of the compactification. Background data, in particular three-form fluxes, determine $\rho_{\mathrm{UV}}$, but we will find that $\rho_{\mathrm{UV}}$ cancels from the quantities of interest.

To summarize our assumptions: we consider a throat that is a warped cone over some Einstein space $X_5$, but may have complicated modifications in the infrared and

[5] An equivalent definition of $\mathrm{Vol}(X_5)$, which may be more clear when it is difficult to define a radius, is as the angular factor in the integral defining the volume of a cone over $X_5$.

ultraviolet. This very large class of geometries includes the backgrounds most often studied for warped brane inflation, but it would be interesting to understand even more general warped throats.

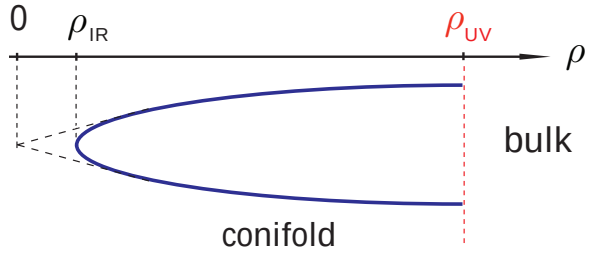


FIGURE 1. Conifold geometry. The throat volume (bounded by $\rho_{\rm IR}$ and $\rho_{\rm UV}$) gives a lower limit on the total compactification volume. This provides a lower limit on the four-dimensional Planck mass.

**3.2. A Lower Bound on the Compactification Volume.** Standard dimensional reduction gives the following relation between the four-dimensional Planck mass $M_{\rm pl}$, the warped volume of the compact space $V_6^w$, the inverse string tension $\alpha'$, and the string coupling $g_s$:

$$M_{\rm pl}^2 \equiv \frac{V_6^w}{\kappa_{10}^2}\,, \tag{8.16}$$

where $\kappa_{10}^2 \equiv \frac{1}{2}(2\pi)^7 g_s^2(\alpha')^4$. The warped volume of the internal space is

$$V_6^w = \int {\rm d}^6 y \sqrt{g}\, h\,. \tag{8.17}$$

Formally this may be split into separate contributions from the bulk and the throat region

$$V_6^w \equiv (V_6^w)_{\rm bulk} + (V_6^w)_{\rm throat}\,. \tag{8.18}$$

The throat contribution is

$$\begin{aligned}(V_6^w)_{\rm throat} &\equiv {\rm Vol}(X_5)\int_0^{\rho_{\rm UV}} {\rm d}\rho\, \rho^5 h(\rho)\\ &= \frac{1}{2}{\rm Vol}(X_5) R^4 \rho_{\rm UV}^2\\ &= 2\pi^4 g_s N(\alpha')^2\, \rho_{\rm UV}^2\,.\end{aligned} \tag{8.19}$$

A key point is that the *warped* throat volume is independent of $\mathrm{Vol}(X_5)$.

The result (8.19) is rather robust. To confirm that (8.14) is a suitable approximation for the warp factor, we note that in the Klebanov-Tseytlin regime [106] of a Klebanov-Strassler throat, the warp factor may be written as

$$h(\rho) = \left(\frac{L}{\rho}\right)^4 \ln \frac{\rho}{\rho_s}\,, \tag{8.20}$$

where $L^4 \equiv \frac{3}{2\pi}\frac{g_s M^2}{N} R^4$, $\ln \frac{\rho_{\rm UV}}{\rho_s} \approx \frac{2\pi}{3}\frac{K}{g_s M}$ and $N \equiv MK$. Integrating (8.20) one finds

$$(V_6^w)_{\rm throat} = \frac{1}{2}\mathrm{Vol}(T^{1,1}) R^4 \rho_{\rm UV}^2\,, \tag{8.21}$$

in agreement with equation (8.19).

The bulk volume is model-dependent, but we can impose a very conservative lower bound on the total warped volume by omitting the bulk volume,

$$V_6^w > (V_6^w)_{\rm throat}\,. \tag{8.22}$$

This implies a lower limit on the four-dimensional Planck mass in string units

$$M_{\rm pl}^2 > \frac{(V_6^w)_{\rm throat}}{\kappa_{10}^2}\,. \tag{8.23}$$

**3.3. An Upper Bound on the Field Range.** Let us now consider inflation driven by the motion of a D3-brane in the background (8.12). The canonically-normalized inflaton field is

$$\varphi^2 = T_3 \rho^2\,, \qquad T_3 \equiv \frac{1}{(2\pi)^3}\frac{1}{g_s(\alpha')^2}\,. \tag{8.24}$$

The maximal radial displacement of the brane in the throat is the length of the throat, from the tip $\rho_{\rm IR} \approx 0$ to the ultraviolet end, $\rho_{\rm UV}$, so that $\Delta\rho \lesssim \rho_{\rm UV}$. Naively one could think that the range of the inflaton could be made arbitrarily large by increasing the length of the throat. However, what is relevant is the field range in

four-dimensional Planck units, which is

$$\left(\frac{\Delta\varphi}{M_{\rm pl}}\right)^2 < \frac{T_3\rho_{\rm UV}^2}{M_{\rm pl}^2} < \frac{T_3\kappa_{10}^2\rho_{\rm UV}^2}{(V_6^w)_{\rm throat}}\,. \tag{8.25}$$

Substituting equation (8.19) gives the following important constraint on the maximal field variation in four-dimensional Planck units:

$$\left(\frac{\Delta\varphi}{M_{\rm pl}}\right)^2 < \frac{4}{N}\,. \tag{8.26}$$

Two comments on this result are in order. First, the field range in Planck units only depends on the background charge $N$ and is manifestly independent of the choice of $X_5$, so our result is the same for any throat that is a warped cone over some $X_5$. Second, the size of the throat, and hence the validity of a supergravity description of the throat, increases with $N$. In the same limit, the field range in Planck units decreases, because the large throat volume causes the four-dimensional Planck mass to be large in string units. Because $N = 0$ corresponds to an unwarped throat, we require at the very least $N \geq 1$; in practice, $N \gg 1$ is required for a controllable supergravity description.

The bound (8.26) is extremely conservative, because we have neglected the bulk volume, which in many cases will actually be larger than the throat volume. Modifications of the geometry at the tip of the throat, where $\rho \ll R$, provide negligible additional field range. One might also try to evade this bound by considering a stack of $n$ D3-branes moving down the throat, which increases the effective tension. However, the backreaction from such a stack is important unless $n \ll N$, so this will not produce a bound weaker than (8.26) with $N = 1$.

## 4. Implications for Slow-Roll Brane Inflation

Via the Lyth relation (8.7), the bound (8.26) translates into a microscopic constraint on the maximal amount of gravitational waves produced during warped brane

inflation

$$\frac{r_{\rm CMB}}{0.009} \leq \frac{1}{N}\Big(\frac{60}{\mathcal{N}_{\rm eff}}\Big)^2 . \tag{8.27}$$

As explained in §2, for slow-roll inflation, recent observations [151, 156] imply

$$30 \lesssim \mathcal{N}_{\rm eff} \lesssim \mathcal{N}_{\rm end} \approx 60 . \tag{8.28}$$

Let us stress that the lower part of this range is occupied only by models with a large, positive scalar running or a blue scalar spectrum and a large tensor fraction.

This implies

$$\frac{r_{\rm CMB}}{0.009} \lesssim \frac{4}{N} . \tag{8.29}$$

Near-future CMB polarization experiments [37] will probe[6] $r_{\rm CMB} \gtrsim \mathcal{O}(10^{-2})$. Detection of gravitational waves in such an experiment would therefore imply that $N < 4$. This implies that the space is effectively unwarped, and that the supergravity description is uncontrolled. We therefore find that warped D-brane inflation can be falsifed by a detection of gravitational waves at the level $r_{\rm CMB} \gtrsim 0.01$.

One might have anticipated this result on the grounds that D-brane inflation models are usually considered to be of the 'small-field' type, and are typically thought to predict an unobservably small tensor fraction. Let us stress, however, that extracting precise predictions from D-brane inflation scenarios is rather involved, and requires careful consideration, and fine-tuning, of the potential introduced by moduli stabilization [18]. It is quite unlikely that the fully corrected potential will enjoy the same exceptional flatness as the uncorrected potential given in [95] (see Chapter 7). As moduli stabilization effects increase $\epsilon$, they increase $r$, and *a priori* this may be expected to lead to observable gravitational waves. Indeed, it has been argued in the context of more general single-field inflation that minimally tuned models correlate with maximal gravitational wave signals [41]. Nevertheless, our result implies that

[6]The ultimate detection limit is probably around $r \sim 10^{-3} - 10^{-4}$. Measuring even lower $r$ is prohibited by the expected magnitude of polarized dust foregrounds and by the lensing conversion of primordial E-modes to B-modes [150].

even the *maximal* signal in warped D-brane inflation is undetectably small. We have thus excluded the possibility of detectable tensors on purely kinematic grounds, *i.e.* by using only the size of the field space.

## 5. Implications for DBI Inflation

A very interesting alternative to standard slow-roll inflation arises when nontrivial kinetic terms drive inflationary expansion [12]. The DBI model [4, 147] is a string theory realization of this possibility in which a D3-brane moves rapidly in a warped background of the form (8.12). The resulting Dirac-Born-Infeld action is [147]

$$\mathcal{L}_{\rm DBI} = -f^{-1}(\varphi)\sqrt{1-2f(\varphi)X} + f^{-1}(\varphi) - V(\varphi)\,, \tag{8.30}$$

where $X \equiv -\frac{1}{2}g^{\mu\nu}\partial_\mu\varphi\partial_\nu\varphi$, $f^{-1}(\varphi) \equiv T_3 h^{-1}(\varphi)$ is the rescaled warp factor, and $\varphi^2 \equiv T_3\rho^2$. As was true in our earlier discussion, the warp factor is determined by solving the supergravity equations of motion in a given background. The potential for the brane motion, $V(\varphi)$, arises from more subtle interactions of the D3-brane with the rest of the compactification [18]. For the present discussion we will treat $V(\varphi)$ as a phenomenological potential, but ultimately it should of course be derived from an explicit string theory compactification [18].

We will now combine the Lyth bound with our field range bound (8.26) to constrain the tensor signal in DBI inflation.[7]

**5.1. A Generalized Lyth Bound.** We will first present the Lyth bound in a theory with a general kinetic term, then specialize to the DBI case. Consider the action [72]

$$S = \frac{1}{2}\int {\rm d}^4x\sqrt{-g}\Big[M_{\rm pl}^2\mathcal{R} + 2P(X,\varphi)\Big]\,, \tag{8.31}$$

[7]Further constraints on the reletivistic limit of brane inflation was obtained in interesting follow-up work by Lidsey and Huston [116]. We summarize their results in §7.

where $P(X,\varphi)$ is a general function of the inflaton $\varphi$ and of $X$. For slow-roll inflation with canonical kinetic term,

$$P(X,\varphi) \equiv X - V(\varphi)\,. \tag{8.32}$$

while DBI inflation may be parameterized by

$$P(X,\varphi) \equiv -f^{-1}(\varphi)\sqrt{1-2f(\varphi)X} + f^{-1}(\varphi) - V(\varphi)\,. \tag{8.33}$$

From (8.31) we find the energy density in the field to be $\rho = 2XP_{,X} - P$. We also define the speed of sound as

$$c_s^2 \equiv \frac{dP}{d\rho} = \frac{P_{,X}}{\rho_{,X}} = \frac{P_{,X}}{P_{,X} + 2XP_{,XX}}\,. \tag{8.34}$$

One can define slow-variation parameters in analogy with the standard slow-roll parameters

$$\epsilon \equiv -\frac{\dot{H}}{H^2} = \frac{XP_{,X}}{M_P^2 H^2}\,, \qquad \tilde{\eta} \equiv \frac{\dot{\epsilon}}{\epsilon H}\,, \qquad s \equiv \frac{\dot{c}_s}{c_s H}\,. \tag{8.35}$$

To first order in these parameters the basic cosmological observables are [72]

$$P_s = \frac{1}{8\pi^2 M_{\rm pl}^2}\frac{H^2}{c_s\epsilon}\,, \tag{8.36}$$

$$P_t = \frac{2}{\pi^2}\frac{H^2}{M_{\rm pl}^2}\,, \tag{8.37}$$

$$n_s - 1 = -2\epsilon - \tilde{\eta} - s\,, \tag{8.38}$$

$$n_t = -2\epsilon\,. \tag{8.39}$$

The tensor-to-scalar ratio in these generalized inflation models is

$$r = 16\,c_s\epsilon\,. \tag{8.40}$$

This nontrivial dependence on the speed of sound implies a modified consistency relation

$$r = -8\, c_s n_t \,. \tag{8.41}$$

As discussed recently by Lidsey and Seery [117], equation (8.41) provides an interesting possibility for testing DBI inflation (see also [149]). The standard slow-roll predictions are recovered in the limit $c_s = 1$.

Restricting to the homogeneous mode $\varphi(t)$ we find from (8.35) that

$$\frac{\mathrm{d}\varphi}{M_{\rm pl}} = \sqrt{\frac{2\epsilon}{P_{,X}}}\,\mathrm{d}\mathcal{N} \tag{8.42}$$

and hence

$$\frac{\Delta\varphi}{M_{\rm pl}} = \int_0^{\mathcal{N}_{\rm end}} \sqrt{\frac{r}{8}\frac{1}{c_s P_{,X}}}\,\mathrm{d}\mathcal{N}\,. \tag{8.43}$$

Notice the nontrivial generalization of the slow-roll result (8.4) through the factor $c_s P_{,X}$. For DBI inflation (8.33) this factor happens to be

$$c_s P_{,X} = 1\,, \tag{8.44}$$

where

$$c_s^2 = 1 - 2f(\varphi)X \equiv \frac{1}{\gamma^2(\varphi)}\,, \tag{8.45}$$

so that the Lyth bound remains the same as for slow-roll inflation.[8]

The variation of $r$ during inflation follows from (8.40)

$$\frac{d\ln r}{d\mathcal{N}} = \frac{d\ln\epsilon}{d\mathcal{N}} + \frac{d\ln c_s}{d\mathcal{N}} = \tilde{\eta} + s\,. \tag{8.46}$$

While the observed near scale-invariance of the density perturbations restricts the magnitude of $s = d\ln c_s/d\mathcal{N}$ in the range $0 \leq \mathcal{N} \lesssim 10$, outside that window $s$ can in principle become large and negative. By (8.46) this would source a rapid decrease in $r$. Note, however, that the results given in this section are first order in $s$ and

[8]This result has been obtained independently by S. Kachru and by H. Tye.

receive important corrections when $s$ is large. Furthermore, omission of terms in the DBI action involving two or more derivatives of $\varphi$ may not be consistent when $s$ is sufficiently large.

Constraints on the evolution of $r$ may also be understood by rewriting equation (8.46) as

$$\frac{d\ln r}{d\mathcal{N}} = n_t - (n_s - 1) = -\left[(n_s - 1) + \frac{r}{8c_s}\right] . \tag{8.47}$$

This implies that $r$ can decrease significantly only if the scalar spectrum becomes very blue ($n_s - 1 > 0$) and/or the speed of sound becomes very small, so that $r/c_s$ is large. During the time when observable scales exit the horizon this possibility is significantly constrained, but outside that window $r$ may decrease rapidly in some models.

**5.2. Constraints on Tensors.** Just as in slow-roll inflation we can write

$$\frac{r_{\rm CMB}}{0.009} \leq \frac{1}{N}\Big(\frac{60}{\mathcal{N}_{\rm eff}}\Big)^2 . \tag{8.48}$$

However, in DBI inflation we have to allow for the possibility that a nontrivial evolution of the speed of sound allows $\mathcal{N}_{\rm eff}$ to be considerably smaller than $\mathcal{N}_{\rm end}$, which weakens the Lyth bound. The precise value of $\mathcal{N}_{\rm eff}$ will be highly model-dependent.

In light of the constraint (8.48), constructing a successful DBI model with detectable tensors is highly nontrivial. First of all, such a model must produce a spectrum of scalar perturbations consistent with observations, *i.e.* with the appropriate amplitude and with a suitably small level of non-Gaussianity. Then, the model should include each of the following *additional* elements related to the large tensor signal:

(1) A consistent compactification in which

$$(V_6^w)_{\rm bulk} \ll (V_6^w)_{\rm throat} , \tag{8.49}$$

so that the inequality in (8.26) may be nearly saturated.

(2) A *small* five-form flux $N$, together with a demonstration that the supergravity corrections and brane backreaction are under control in this difficult limit.

(3) A decrease in $r$ that is rapid enough to ensure that $\mathcal{N}_{\rm eff} \ll 30$. In this situation the slow-variation parameters $\tilde{\eta}$, $s$ cannot both be small, substantially complicating the analysis.

It would be extremely interesting to find a system that satisfies all these constraints, especially because this would be a rare example of a complete string inflation model with detectable tensors.[9]

**5.3. Constraints on Quadratic DBI Inflation.** In this section we illustrate our considerations for one important class of DBI models,[10] those with a quadratic potential, *i.e.* we consider an action of the form (8.30), with

$$V(\varphi) = \frac{1}{2} m^2 \varphi^2 \,. \tag{8.50}$$

Such a potential might be generated by moduli-stabilization effects, which often drive D3-branes toward the tip of the throat. This particular example is a 'large-field' model, and so it should come as no surprise that it is strongly constrained by our upper limit (8.26) on the field range. At sufficiently late times, the Hubble parameter is [147]

$$H(\varphi) = c\,\varphi \,, \tag{8.51}$$

[9]We should mention one promising string inflation scenario, N-flation [61, 67], that does predict observable tensors. It would be very interesting to understand whether this model can indeed be realized in a string compactification [80].

[10]We consider the so-called 'UV model', *i.e.* with a D3-brane moving toward the tip of the throat; *cf.* [51] for an interesting alternative.

for some constant $c$. Using this in (8.35), one finds

$$\epsilon\,\gamma(\varphi) = 2M_{\rm pl}^2\Big(\frac{H_\varphi}{H}\Big)^2 = 2\left(\frac{M_{\rm pl}}{\varphi}\right)^2 . \tag{8.52}$$

This relates the DBI Lorentz factor $\gamma$ to the slow-roll parameter $\epsilon < 1$ and to the inflaton field value.

*Microscopic Constraint from Limits on Non-Gaussianity.* Observational tests of the non-Gaussianity of the primordial density perturbations are most sensitive to the three-point function of the comoving curvature perturbations. It is usually assumed that the three-point function has a form that would follow from the field redefinition

$$\zeta = \zeta_L + \frac{3}{5} f_{\rm NL}\zeta_L^2 , \tag{8.53}$$

where $\zeta_L$ is Gaussian. The scalar parameter $f_{\rm NL}$ quantifies the amount of non-Gaussianity. It is a function of three momenta which form a triangle in Fourier space. Here we cite results for the limit of an equilateral triangle. Slow-roll models predict $|f_{\rm NL}| \ll 1$ [125], which is far below the detection limit of present and future observations. For generalized inflation models represented by the action (8.31) one finds [52]

$$f_{\rm NL} = -\frac{35}{108}\Big(\frac{1}{c_s^2} - 1\Big) + \frac{5}{81}\Big(\frac{1}{c_s^2} - 1 - 2\Lambda\Big) , \tag{8.54}$$

where

$$\Lambda \equiv \frac{X^2 P_{,XX} + \frac{2}{3}X^3 P_{,XXX}}{X P_{,X} + 2X^2 P_{,XX}} . \tag{8.55}$$

For the case of DBI inflation (8.30), the second term in (8.54) is identically zero [52], so that the prediction for the level of non-Gaussianity (8.54) is[11]

$$f_{\rm NL} = -\frac{35}{108}\Big(\frac{1}{c_s^2} - 1\Big) \approx -\frac{35}{108}\gamma^2 , \tag{8.56}$$

[11]Notice that this result is generic to DBI inflation and is independent of the choice of the potential and the warp factor. This is in contrast to other observables like $n_s$, $P_s$, *etc.*

where the second relation holds when $c_s \ll 1$. This result leads to an upper bound on $\gamma$ from the observed limit on the non-Gaussianity of the primordial perturbations. The recent analysis of the WMAP 5-year data [111] gives $-151 < f_{\rm NL} < 253$ (95% confidence level), which implies

$$\gamma \lesssim 22\,. \tag{8.57}$$

Using the expressions (8.40) and (8.52), we have

$$N < 4\Big(\frac{M_{\rm pl}}{\varphi}\Big)^2 = \frac{r\gamma^2}{8} = \frac{27}{70} r|f_{\rm NL}|\,. \tag{8.58}$$

Combining the observational bound on gravitational waves [111], $r < 0.2$, with the bound on non-Gaussianity, we find

$$N \lesssim 12\,. \tag{8.59}$$

Quadratic DBI inflation with a larger amount of five-form flux is hence excluded by current observations. The Planck satellite may be sensitive enough to give the limits $|f_{\rm NL}| < 50$ and $r < 0.05$. Non-observation at these levels would give the bound $N < 1$, excluding quadratic DBI inflation.

*Microscopic Constraint from the Amplitude of Primordial Perturbations.* We can derive an additional constraint on this scenario by requiring the proper normalization of the scalar perturbation spectrum. Using the result (8.36) [72] for the scalar spectrum, along with the relation $c_s^{-1} = \gamma(\varphi) = \sqrt{1 + 4M_{\rm pl}^4 f(\varphi)(H_\varphi)^2}$ for DBI inflation, we find [4, 147]

$$P_s = \frac{16}{\pi^2}\frac{\gamma^2(\gamma^2-1)}{(r\gamma^2)^2}\frac{1}{M_{\rm pl}^4 f}\,. \tag{8.60}$$

For the $AdS_5$ warp factor (8.14)

$$M_{\rm pl}^4 f(\varphi) = \lambda\Big(\frac{M_{\rm pl}}{\varphi}\Big)^4 = \lambda\Big(\frac{r\gamma^2}{32}\Big)^2\,, \tag{8.61}$$

where

$$\lambda \equiv T_3 R^4 = \frac{\pi}{2}\frac{N}{\mathrm{Vol}(X_5)}\,, \tag{8.62}$$

we find

$$P_s = \left(\frac{32}{\pi}\right)^3 \times \frac{\gamma^2(\gamma^2-1)}{(r\gamma^2)^4}\frac{\mathrm{Vol}(X_5)}{N}\,. \tag{8.63}$$

In the relativistic limit we have $\gamma^2(\gamma^2-1) \sim \gamma^4 = 9 f_{\rm NL}^2$ and (8.63) becomes

$$P_s = \left(\frac{32}{3\pi}\right)^3 \frac{3}{r^4 f_{\rm NL}^2}\frac{\mathrm{Vol}(X_5)}{N} \gtrsim 3.2\,\frac{\mathrm{Vol}(X_5)}{N}\,, \tag{8.64}$$

where the last relation comes from the current observational bounds on $r$ and $f_{\rm NL}$ on CMB scales. COBE or WMAP give the normalization $P_s \approx 2.4 \times 10^{-9}$, so that we arrive at the condition

$$N \gtrsim 10^9\,\mathrm{Vol}(X_5)\,. \tag{8.65}$$

The requirements (8.59) and (8.65) are clearly inconsistent for the generic case, $\mathrm{Vol}(X_5) \sim \mathcal{O}(\pi^3)$. We conclude that quadratic DBI inflation in warped throats[12] cannot simultaneously satisfy the observational constraints on the amplitude and Gaussianity of the primordial perturbations unless $\mathrm{Vol}(X_5) \lesssim 10^{-8}$. In particular, this excludes realization of this scenario in a cut-off $AdS$ model or in a Klebanov-Strassler [105] throat. Cones with very small values of $\mathrm{Vol}(X_5)$ can be constructed by taking orbifolds or considering $Y^{p,q}$ spaces in the limit that $q$ is fixed and $p \to \infty$ [73]. However, it seems rather unlikely that one could embed these spaces into a string compactification.

## 6. Conclusions

We have established a firm upper bound on the canonical field range in Planck units for a D3-brane in a warped throat. This range can never be large, and can be of order one only in the limit of an unwarped throat attached to a bulk of negligible

[12]Throats that are not cones over Einstein manifolds could evade this constraint, and may be a more natural setting for realizing the DBI mechanism. We thank E. Silverstein for explaining this to us.

volume. Combined with the Lyth relationship [122] between the variation of the inflaton field during inflation and the gravitational wave signal, this implies a constraint on the tensor fraction in warped D-brane inflation. The tensor signal is undetectably small in slow-roll warped D-brane inflation, regardless of the form of the potential. In DBI inflation, detectable tensors may be possible only in a poorly-controlled limit of small warping, moderately low velocity, rapidly-changing speed of sound, and substantial backreaction. In this case, the scalar spectrum will typically have a strong blue tilt and/or become highly non-Gaussian shortly after observable scales exit the horizon.

We have also presented stronger constraints for the case of DBI inflation with a quadratic potential, finding that combined observational constraints on tensors and non-Gaussianity imply an upper bound $N \lesssim 12$ on the amount of five-form flux. Near-future improvements in the experimental limits could imply $N < 1$ and thus exclude the model. For models realized in a warped cone over a five-manifold $X_5$, current limits imply that the dimensionless volume of $X_5$, at unit radius, is smaller than $10^{-8}$. Manifolds of this sort do exist; extremely high-rank orbifolds and cones over special $Y^{p,q}$ manifolds are examples, but it is not clear that these can be embedded in a string compactification.

Although our result resonates with some well-known effective field theory objections (see *e.g.* [123]) to controllably flat inflaton potentials involving large field ranges, we stress that our analysis was entirely explicit and did not rely on notions of naturalness or of fine-tuning.

Our microscopic limit on the evolution of the inflaton implies that a detection of primordial gravitational waves would rule out most models of warped D-brane inflation, and place severe pressure on the remainder. We expect that compactification constraints on canonical field ranges imply similar bounds in many other string inflation models [54]. In this sense, current models of string inflation do not readily

provide detectable gravitational waves. However, this is not yet by any means a firm prediction of string theory, and it is more important than ever to search for a compelling model of large-field string inflation that overcomes this obstacle. Given the apparent difficulty of achieving super-Planckian field variations with controllably flat potentials for scalar fields in string theory, a detection of primordial gravitational waves would provide a powerful selection principle for string inflation models and give significant clues about the fundamental physics underlying inflation.

## 7. Epilogue

Our result for the maximal field range in brane inflation models [21] has inspired interesting subsequent work *e.g.* [28, 90, 97, 109, 112, 116, 136, 148]. In this section we briefly describe some of these recent developments.

**7.1. Bound in the Relativistic DBI Limit.** Lidsey and Huston [116] derived an interesting generalization of our field range bound [21] that is useful in the relativistic DBI limit ($|f_{\rm NL}| \gg 1$). First, one notes that for an arbitrary warp factor $h(\varphi) = T_3 f(\varphi)$ the geometric bound on the field range may be written as follows

$$\left(\frac{\Delta\varphi}{M_{\rm pl}}\right)^2 < \frac{4}{N_{\rm throat}}\,, \tag{8.66}$$

where

$$N_{\rm throat} \equiv \frac{4\,{\rm Vol}(X_5)}{\pi\,\varphi_{\rm UV}^2}\int_{\varphi_{\rm IR}}^{\varphi_{\rm UV}} {\rm d}\varphi\,\varphi^5 f(\varphi)\,. \tag{8.67}$$

If one defines $\Delta\varphi_\star$ to be the field variation when observable scales are generated dur-

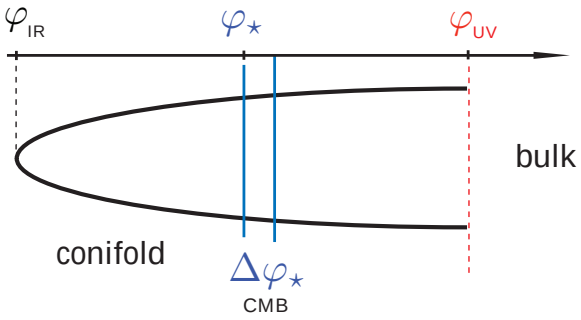


FIGURE 2. Conifold geometry. Lidsey and Huston [116] use a slice of the throat to bound the compactification volume.

ing inflation (this corresponds to $\Delta\mathcal{N}_\star \leq 4$ $e$-foldings of inflationary expansion or the CMB multipole range $2 \leq \ell < 100$), then the integral in (8.67) can be approximated as follows

$$\int_{\varphi_{\rm IR}}^{\varphi_{\rm UV}} {\rm d}\varphi\varphi^5 f(\varphi) > \Delta\varphi_\star\varphi_\star^5 f_\star > (\Delta\varphi_\star)^6 f_\star\,. \tag{8.68}$$

Here, we have bounded the integral by a small part of the Riemann sum, defined $f_\star \equiv f(\varphi_\star)$ and used $\Delta\varphi_\star < \varphi_\star$. Equation (8.66) then becomes

$$\left(\frac{\Delta\varphi_\star}{M_{\rm pl}}\right)^6 < \frac{\pi}{{\rm Vol}(X_5)}(f_\star M_{\rm pl}^4)^{-1}\,. \tag{8.69}$$

Next, we express the warped tension $f^{-1}$ in terms of the scalar power spectrum $P_s$, the tensor-to-scalar ratio $r$, and the non-Gaussianity parameter $f_{\rm NL}$. This relates $f_\star$ to observables

$$(f_\star M_{\rm pl}^4)^{-1} = \frac{\pi^2}{16}P_s^\star r_\star^2\left(1+\frac{1}{3|f_{\rm NL}|}\right)\,, \tag{8.70}$$

and hence gives

$$\left(\frac{\Delta\varphi_\star}{M_{\rm pl}}\right)^6 < \frac{\pi^3}{16{\rm Vol}(X_5)}P_s^\star r_\star^2\left(1+\frac{1}{3|f_{\rm NL}|}\right)\,. \tag{8.71}$$

For slow-roll models with $|f_{\rm NL}| \ll 1$ this is not a very useful constraint. However, for relativistic DBI models with $|f_{\rm NL}| \gg 1$ the bound (8.71) is independent of $f_{\rm NL}$. Since $P_s^\star \sim 2.4\times10^{-9}$, $r_\star < 0.4$ (from observations) and ${\rm Vol}(X_5) = \mathcal{O}(\pi^3)$ (from theory) we conclude that super-Planckian field variation is inconsistent with observations (unless ${\rm Vol}(X_5)$ is made unnaturally small). The Lyth bound (8.7) can now be written as

$$\left(\frac{\Delta\varphi_\star}{M_{\rm pl}}\right)^2 \approx \frac{r_\star}{8}(\Delta\mathcal{N}_\star)^2\,. \tag{8.72}$$

Substituting this into (8.71) we find [116]

$$r_\star < \frac{32P_s^\star}{(\Delta\mathcal{N}_\star)^6}\frac{\pi^3}{{\rm Vol}(X_5)} \sim \frac{10^{-10}}{{\rm Vol}(X_5)}\,. \tag{8.73}$$

We have used $P_s^\star = 2.4\times10^{-9}$ and $\Delta\mathcal{N}_\star \approx 4$. The tensor amplitude is therefore unobservably small for relativistic DBI models. We emphasize that the bound (8.73) does *not* apply to slow-roll models since $|f_{\rm NL}| > 1$ has been assumed in its derivation.

Interestingly, Lidsey and Huston also derived a lower limit on $r$ for models of UV DBI inflation with $|f_{\rm NL}| \gg 1$ and $n_s < 1$ [116]

$$r_\star > \frac{4(1-n_s)}{\sqrt{3|f_{\rm NL}|}}\,. \tag{8.74}$$

The limits (8.73) and (8.74) are clearly inconsistent unless $\mathrm{Vol}(X_5)$ is very small, *cf.* (8.59) and (8.65).

With the work of [21], [136], [24] and [116] there is now a growing body of evidence that the theoretically best-motivated models of relativistic (UV) DBI inflation are in tension with the data if microscopic constraints are applied consistently. In [136] and [24] it was shown numerically that these problems persist even if considerable freedom is allowed for the functional form of the brane potential $V(\varphi)$ and the background warp factor $f(\varphi)$.

### 7.2. Relaxing the Bound?

*Wrapped Branes.* Becker et al. [28] and independently Kobayashi et al. [109] suggested an interesting way to potentially relax the field range bound of [21]. Both papers showed that the bound weakens if the analysis of [21] is generalized to Dp-branes wrapping $(p-3)$-cycles in the throat. Recall that for D3-branes the maximal field range is bounded by $N^{-1/2}$

$$\Big(\frac{\Delta\varphi}{M_{\rm pl}}\Big)_{\rm D3} < 2N^{-1/2}\,. \tag{8.75}$$

For branes of higher dimensionality the relation between the radial coordinate $\rho$ and canonical field $\varphi$ changes and the field range bound scales only as $N^{-1/4}$ for D5-branes and is independent of $N$ for D7-branes,

$$\Big(\frac{\Delta\varphi}{M_{\rm pl}}\Big)_{\rm D5} < 2Cg_s^{-1/4}N^{-1/4} \tag{8.76}$$

$$\Big(\frac{\Delta\varphi}{M_{\rm pl}}\Big)_{\rm D7} < 2CN^0 \tag{8.77}$$

where

$$C \equiv \left(\frac{p g_s}{\mathrm{Vol}(X_5)}\right)^{1/2}. \tag{8.78}$$

Here, $p$ is the winding number of the wrapped brane. However, as Becker et al. [28] explain, inflationary models with wrapped branes suffer from significant backreaction (we discuss these problems and their generalizations in the next chapter).

*Multiple Coincident Branes.* Above we extended the Lyth bound to general $P(X, \phi)$ actions [21]

$$\frac{\Delta\varphi}{M_{\rm pl}} = \int_0^{\mathcal{N}_{\rm end}} \sqrt{\frac{r}{8}\frac{1}{c_s P_{,X}}}\, \mathrm{d}\mathcal{N}\,. \tag{8.79}$$

For both slow-roll inflation ($c_s = P_{,X} = 1$) and DBI inflation ($c_s = 1/\gamma$, $P_{,X} = \gamma$) we find that $c_s P_{,X} = 1$. For slow-roll inflation and DBI inflation there is therefore a one-to-one correspondence between $r$ and $\Delta\varphi$. However, from (8.79) one sees immediately that the Lyth bound is weakened for models with $c_s P_{,X} \gg 1$. Huston et al. [90] suggest that such an action can arise as the non-Abelian effective action of multiple coincident branes. However, their paper also exposes that models with observable gravitational wave amplitude can hardly be made consistent with non-Gaussianity constraints.

CHAPTER 9

# Comments on Field Ranges in String Theory

## 1. String Moduli and the Lyth Bound

It is a fascinating open question whether super-Planckian fields can be realized in a consistent microscopic theory of inflation. At the same time, the Lyth bound [122] and the advent of CMB polarization experiments makes the answer to this question timely. In Chapter 8 we proved the impossibility of super-Planckian field variation for D3-brane inflation in warped throats. In this chapter we broaden our scope and make some general remarks about the sizes of the moduli spaces for large classes of models of string inflation.

More concretely, we speculate about the following two constraints on moduli fields in string theory:

- **C1**: *Kinematical Constraints on the Field Range*: $(\Delta\varphi)_{\rm kin} < M_{\rm pl}$?
  Some fields in string theory are restricted by "pure geometry". In these cases very strong statements can be made about the impossibility of using those fields to construct inflationary models with observable tensors.
- **C2**: *Dynamical Constraints on the Field Range*: $(\Delta\varphi)_{\rm dyn} < M_{\rm pl}$?
  For the fields that violate the first condition (*i.e.* $(\Delta\varphi)_{\rm kin} > M_{\rm pl}$) we consider whether flat potentials can extend over super-Planckian distances. This requires careful study of backreaction effects and corrections to the inflaton potential.

In the following sections we describe simple examples for the constraints **C1** and **C2**. Elementary examples for **C1** are: branes on a torus, D3-branes in a warped throat and string axions. Wrapped higher-dimensional branes provide nice examples of **C2**. We also discuss possible counter-examples to **C2** [61, 148].

## 2. Branes

**2.1. Branes on $T^6$.** The first system we study is D-branes on a isotropic six-torus.[1] We compute a limit on the kinematical range of the brane coordinates.

*Field Range.* The Dp-branes are spacetime-filling and wrap a $(p-3)$–cycle on the torus. Let the volume of the torus and the volume of the cycle be $V_6 = (2\pi L)^6$ and $V_{p-3} = (2\pi L)^{p-3}$, respectively. Dimensional reduction of the ten-dimensional Einstein and Dirac-Born-Infeld actions defines the canonical field,

$$\varphi^2 = T_p V_{p-3} r^2 \,, \tag{9.1}$$

and the four-dimensional Planck mass,

$$M_{\rm pl}^2 = \kappa_{10}^{-2} V_6 \,, \qquad \kappa_{10}^2 \equiv \frac{1}{2}(2\pi)^7 g_s^2 (\alpha')^4 \,. \tag{9.2}$$

Generically, the brane coordinate is limited by the size of the torus $r < 2\pi L$. We then get the following result for the maximal field variation in Planck units

$$\left(\frac{\Delta\varphi}{M_{\rm pl}}\right)^2_{\rm Dp} < \frac{g_s}{2}\left(\frac{L}{l_s}\right)^{p-7} \ll 1 \,, \tag{9.3}$$

where $L \gg l_s \equiv \sqrt{\alpha'}$ and $g_s < 1$ in the controlled theoretical regime. Branes on an isotropic torus therefore provide a sharp example for the conjecture **C1**: the field range is kinematically limited to be sub-Planckian.

[1] For the case of an anisotropic torus some of the constraints presented here may be relaxed [127], [85].

**2.2. Branes on $AdS_5 \times X_5$.**

*Field Range.* String compactifications with a local throat region ($0 < r < r_{\rm max}$, $h(r) \sim \frac{R^4}{r^4}$) satisfy the following constraint on the compactification volume (see Chapter 8)

$$V_6 > (V_6)_{\rm throat} = {\rm Vol}(X_5) \int_0^{r_{\rm max}} {\rm d}r\, r^5 h(r) \tag{9.4}$$

$$= \frac{1}{2} r_{\rm max}^2 R^4 {\rm Vol}(X_5)\,. \tag{9.5}$$

As before, this implies a lower bound on the four-dimensional Planck mass. For a wrapped Dp-brane the maximal field range inside the throat is (see (9.1))

$$\Delta\varphi^2 < T_p V_{p-3} r_{\rm max}^2\,. \tag{9.6}$$

Using $V_{p-3} \sim R^{p-3}$ and $T_3 R^4 {\rm Vol}(X_5) = \frac{\pi}{2} N$ we therefore find

$$\left(\frac{\Delta\varphi}{M_{\rm pl}}\right)^2_{\rm Dp} < 4\,\frac{T_p R^{p-3}}{N T_3} \equiv \left(\frac{\Delta\varphi}{M_{\rm pl}}\right)^2_{\rm max}\,. \tag{9.7}$$

For the case of D3-branes we showed in Chapter 8 that $(\Delta\varphi)_{\rm kin} \leq (\Delta\varphi)_{\rm max} = \frac{2}{\sqrt{N}} M_{\rm pl} \ll M_{\rm pl}$. However, for higher-dimensional wrapped branes $(\Delta\varphi)_{\rm kin}$ can in principle be large [28, 109].

*Backreaction.* The above analysis leading to the bound (9.7) assumes that the wrapped branes can be treated as a probe of the background geometry. Quantitatively, this requires that the (local) curvature induced by the energy of the branes is much less than the curvature of the background space. This *backreaction constraint* takes the following form [28]

$$\gamma T_p R^{p-3} \ll N T_3\,. \tag{9.8}$$

Together with equation (9.7) this implies

$$\left(\frac{\Delta\varphi}{M_{\rm pl}}\right)^2_{\rm max} \ll \frac{1}{\gamma} \leq 1\,. \tag{9.9}$$

We therefore conclude that, although the kinematical range (9.7) can be large, the field range is bounded by dynamical considerations (9.9). This is an example where **C1** does not hold, but **C2** limits the field range to be sub-Planckian.

**2.3. D8-branes on $S^1/\mathbb{Z}_2 \times X^5$.** A very elegant example for a field that can have large kinematical range but sub-Planckian dynamical range was related to me by Maldacena[2] [126]. He considers a spacetime-filling D8-brane wrapping five dimensions of the compact space. The brane is pointlike in the sixth compact dimension (see Figure 1).

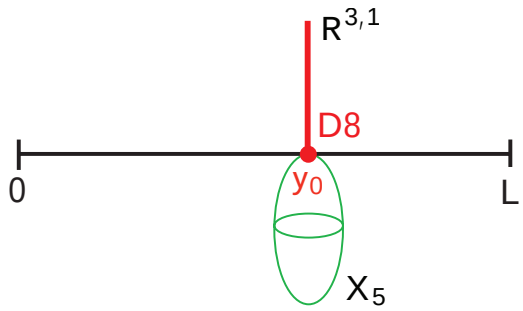


FIGURE 1. Wrapped D8-brane on $(\mathbb{R}^{3,1} \times S^1/\mathbb{Z}_2) \times X_5$.

*Field Range.* Using the above methods one easily finds the canonical range of the D8-brane in the sixth dimension (*cf.* equation (9.3))

$$\left(\frac{\Delta\varphi}{M_{\rm pl}}\right)^2_{\rm D8} = \frac{g_s}{2}\left(\frac{L}{l_s}\right). \tag{9.10}$$

This can be arbitrarily large for $L \gg l_s$. Notice that the field range for D8-branes (9.10) becomes parametrically larger in the controlled regime $L \gg l_s$. This is in contrast to the case for Dp-branes with $p < 7$ for which by (9.3) the field range decreases parametrically for $L \gg l_s$. This observation makes D8-branes moving along a long interval naively a promising system for super-Planckian field variation.

[2]I thank Juan Maldacena for the permission to reproduce his argument here.

*Backreaction.* Maldacena, however, argues that although the kinematical range (9.10) is unbounded, backreaction restricts the brane motion to be sub-Planckian.[3]

To see this, one considers backreaction of the D8-brane in the spacetime $\mathbb{R}^{3,1} \times S^1/\mathbb{Z}_2$. Orientifold planes at $y = 0, L$ bound the interval $S^1/\mathbb{Z}_2$. For a D8-brane at $y = y_0$ in the extra dimension the metric is

$$\mathrm{d}s^2 = h^{-1/2}\mathrm{d}x^2 + h^{1/2}\mathrm{d}y^2\,, \tag{9.11}$$

where the warp factor $h(y)$ obeys

$$\partial_y^2 h = -g\delta(y - y_0)\,. \tag{9.12}$$

Equation (9.12) has the following solution

$$h = 1 - (gL)\Theta(z - z_0)\cdot(z - z_0)\,, \qquad z \equiv \frac{y}{L}\,, \tag{9.13}$$

where $\Theta$ is the Heaviside function. Hence, the spacetime is flat for $z < z_0$ and curved AdS space for $z > z_0$. Notice that

$$h(z = 1) = 1 - (gL)(1 - z_0) \tag{9.14}$$

becomes singular at $(1 - z_0) = (gL)^{-1}$. The maximum value of $(1 - z_0)$ therefore is the minimum of 1 and $(gL)^{-1}$. For $(gL)^{-1} < 1$ the warped geometry becomes singular at $z = 1$ for $(1 - z_0) > (gL)^{-1}$. This singularity dynamically limits the range of controlled motion of the brane.

The four-dimensional Planck mass in the perturbed geometry is

$$M_{\rm pl}^2 = \frac{V_6}{g^2} = \frac{1}{g^2}V_5\int_0^L \mathrm{d}y\, h = \frac{V_5 L}{g^2}\left(1 - \frac{gL}{2}(1 - z_0)^2\right)\,. \tag{9.15}$$

[3]In this example we ignore factors of $\pi$ and focus our attention on the parametric dependence of the result.

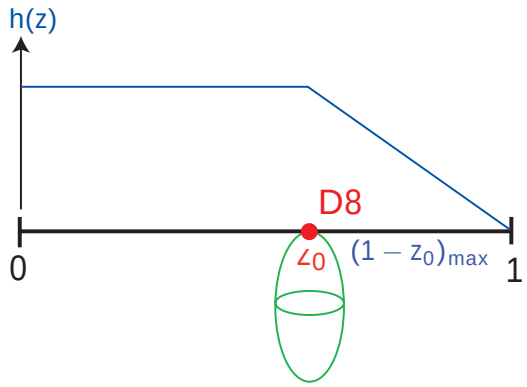


FIGURE 2. Warp factor induced by the D8-brane. For $(gL)^{-1} < 1$ a singularity appears at $z = 1$ for $(1 - z_0) > (gL)^{-1}$.

Given that the maximum of $(1 - z_0)$ is the minimum of 1 and $(gL)^{-1}$, we get the following constraints

$$\begin{aligned} M_{\rm pl}^2 &> \tfrac{V_5 L}{g^2}\Big(1 - \tfrac{1}{2}\tfrac{1}{gL}\Big) > \tfrac{V_5 L}{2g^2}\,, \qquad (gL)^{-1} < 1\,, \\ M_{\rm pl}^2 &> \tfrac{V_5 L}{g^2}\Big(1 - \tfrac{gL}{2}\Big) > \tfrac{V_5 L}{2g^2}\,, \qquad (gL) < 1\,. \end{aligned} \tag{9.16}$$

The canonical field range, $\varphi^2 = \frac{V_5 L^2}{g} z^2$, is limited by backreaction to

$$\begin{aligned} \Delta\varphi^2 &= \tfrac{V_5 L^2}{g} \cdot (gL)^{-2} = \tfrac{V_5}{g^3}\,, \qquad (gL)^{-1} < 1\,, \\ \Delta\varphi^2 &= \tfrac{V_5 L^2}{g} \cdot 1^2 = \tfrac{V_5 L^2}{g}\,, \qquad (gL) < 1\,. \end{aligned} \tag{9.17}$$

In Planck units we therefore find

$$\frac{\Delta\varphi^2}{M_{\rm pl}^2} < 2(gL)^{-1}\,, \qquad (gL)^{-1} < 1\,, \tag{9.18}$$

$$\frac{\Delta\varphi^2}{M_{\rm pl}^2} < 2(gL)\,, \qquad (gL) < 1\,. \tag{9.19}$$

This proves that although the kinematical range (9.10) can be parametrically large, backreaction of the D8-brane on the background geometry restricts its dynamical field range to be sub-Planckian, $(\Delta\varphi)_{\rm dyn} < M_{\rm pl}$.

**2.4. Monodromies.** Eva Silverstein and Alexander Westphal recently proposed a very interesting idea for realizing large-field inflation in string theory [148] using a *monodromy*[4] mechanism.

Their particular model considers a D4-brane wrapping a 1-cycle with monodromy in the Nil compactifications of Ref. [146]. The specific model is less important here than the general idea of using monodromy to extend the field range probed by the brane. We therefore focus on the general idea rather than the specific realization.

*Nil Geometry.* The Nil geometry

$$\frac{\mathrm{d}s^2_{\mathrm{Nil}}}{\alpha'} = L^2_{u_1}\mathrm{d}u_1^2 + \underbrace{L^2_{u_2}\mathrm{d}u_2^2 + L^2_x(\mathrm{d}x' + Mu_1\mathrm{d}u_2)^2}_{T^2} \tag{9.20}$$

compactified by the following projections

$$t_x \quad : \qquad (x', u_1, u_2) \to (x' + 1, u_1, u_2) \tag{9.21}$$

$$t_{u_1} \quad : \qquad (x', u_1, u_2) \to (x' - Mu_2, u_1 + 1, u_2) \tag{9.22}$$

$$t_{u_2} \quad : \qquad (x', u_1, u_2) \to (x', u_1, u_2 + 1) \tag{9.23}$$

gives the manifold $\mathcal{N}_3$. We consider type IIA string theory on an orientifold of the product space $\mathcal{N}_3 \times \tilde{\mathcal{N}}_3$. For the moment it suffices to consider a single $\mathcal{N}_3$. For each $u_1$ there is a 2-torus $T^2$ in $u_2$ and $x'$

$$\frac{\mathrm{d}s^2_{T^2}(u_1)}{\alpha'} = L^2_{u_2}\mathrm{d}u_2^2 + L^2_x(\mathrm{d}x' + Mu_1\mathrm{d}u_2)^2\,. \tag{9.24}$$

Going once around the circle $S^1$ defined by the $u_1$-direction the complex structure of the torus shift by $M$ units, *i.e.* $\tau \to \tau + M$ as $u_1 \to u_1 + 1$. The projection $t_{u_1}$ (9.22) identifies these equivalent tori. At $M$ special locations around the $u_1$-circle,

[4]In complex analysis, functions may fail to be single-valued as one goes around a path encircling a singularity, *e.g.* consider $f(z) = \ln z$ where $z = |z|e^{i\theta}$ – because $e^{z+2\pi in} = e^z$ one finds that $f(z) \to f(z) + 2\pi in$ as the origin is encircled $n$ times. In this example the covering space is a helicoid.

$Mu_1 = j \in \mathbb{Z}$, the tori are equivalent to rectangular tori

$$\frac{\mathrm{d}s^2_{T^2}}{\alpha'} = L_x^2 \mathrm{d}y_1^2 + L_{u_2}^2 \mathrm{d}y_2^2 \,, \tag{9.25}$$

where

$$y_1 \equiv x' + j u_2 \,, \quad y_2 \equiv u_2 \,. \tag{9.26}$$

*Wrapped Branes and Monodromy.* Silverstein and Westphal consider a D4-brane wrapped on the 1-cycle defined by $u_2 = \lambda$ or $(y_1, y_2) = (j\lambda, \lambda)$. It is proposed that transverse motion in the $u_1$-direction may be the source of inflation. The crucial point is the following: as the brane circles in the $u_1$-direction the fibred torus returns to an equivalent torus but the 1-cycle does *not*, *e.g.* at $u_1 = 0$, the brane wraps $(y_1, y_2) = (0, \lambda)$, while at $u_1 = 1$, the brane wraps $(y_1, y_2) = (M\lambda, \lambda)$. This monodromy is the key to extending the field range.

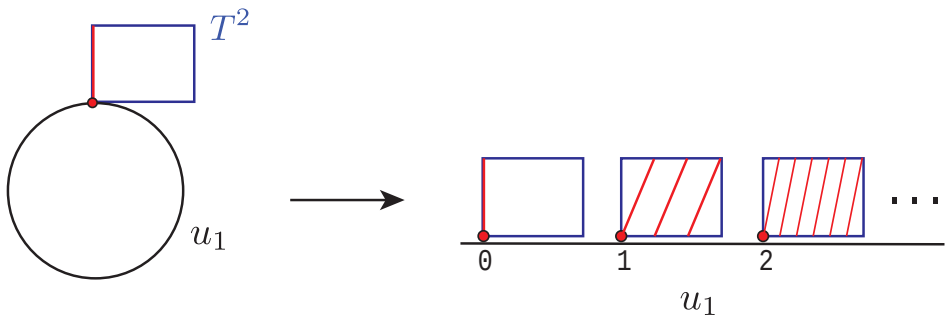


FIGURE 3. Wrapped D4-brane with Monodromy.

*Field Range.* As before, the four-dimensional Planck mass $M_{\rm pl}$ is fixed by the compactification volume $V_6 = (\alpha')^3 L^6$, where $L^3 \equiv L_{u_1} L_{u_2} L_x$, *i.e.*

$$M_{\rm pl}^2 = \frac{2}{(2\pi)^7} \frac{L^6}{g_s^2} \frac{1}{\alpha'} \,. \tag{9.27}$$

However, now, as a result of the monodromy, the brane field space is *not* constrained by the compactification volume. The monodromy effect implies that the D-brane moduli space lives on a subspace of the covering of the compactification, *i.e.* on the

space obtained by undoing the projection $t_{u_1}$. At fixed $M_{\rm pl}$, the field range in the $u_1$-direction can be large by moving around the $S^1$ many times (see Figure 3).

To quantify this one considers the DBI-action for the wrapped D4-brane

$$\begin{aligned} S_{\rm D4} &= \frac{-1}{(2\pi)^4(\alpha')^{5/2}}\int {\rm d}^5\xi\, e^{-\Phi}\sqrt{\det G(X)(\partial X)^2} && (9.28)\\ &= \frac{-1}{(2\pi)^4 g_s(\alpha')^{5/2}}\int_{\mathbb{R}^{3,1}\times u_2} {\rm d}^5\xi\,\sqrt{-g_4 g_{u_2u_2}(1-\alpha' g_{u_1u_1}\dot{u}_1^2)} && (9.29)\\ &\approx \frac{-1}{(2\pi)^4 g_s(\alpha')^2}\int {\rm d}^4x\sqrt{-g_4}\sqrt{L_{u_2}^2+L_x^2M^2u_1^2}\left(1-\frac{1}{2}\alpha' L_{u_1}^2\dot{u}_1^2\right). && (9.30)\end{aligned}$$

For large $u_1$ ($L_xMu_1 \gg L_{u_2}$), this gives

$$S_{\rm D4} = \int {\rm d}^4x\sqrt{-g_4}\left(\frac{1}{2}\dot{\varphi}^2-\mu^{10/3}\varphi^{2/3}\right), \tag{9.31}$$

where

$$\frac{\varphi^2}{M_{\rm pl}^2} = \alpha^2 u_1^3\,. \tag{9.32}$$

Here we have defined

$$\alpha^2 \equiv \frac{2}{9}(2\pi)^3 g_s\frac{M}{L^3}\frac{L_{u_1}}{L_{u_2}} \tag{9.33}$$

and

$$\frac{\mu^{10}}{M_{\rm pl}^{10}} \equiv \left(\frac{M_s}{M_{\rm pl}}\right)^{10}\cdot\frac{9}{4}\frac{M^2}{(2\pi)^8 g_s^2}\left(\frac{L_x}{L}\right)^3\frac{L_{u_2}}{L_{u_1}}\,. \tag{9.34}$$

For $\Delta u_1 = k \gg 1$, the field range

$$\frac{\Delta\varphi^2}{M_{\rm pl}^2} = \frac{2}{9}(2\pi)^3 g_s\frac{Mk^3}{L^3}\frac{L_{u_1}}{L_{u_2}} \tag{9.35}$$

can be super-Planckian for $Mk^3 > L^3$ and $L_{u_1} \gg L_{u_2}$.

*Backreaction.* Silverstein and Westphal [148] studied various backreaction effects and concluded that the field range can be super-Planckian even if dynamical constraints are taken into account. This makes their model very interesting and worthy of further investigation.

## 3. Axions

### 3.1. Field Ranges for String Theory Axions.

*Natural Inflation.* In the context of inflationary model building, axions have the attractive feature that their potential is protected by a shift symmetry $\varphi \to \varphi+\delta$. This symmetry guarantees that to first approximation the axion is massless. However, non-perturbative corrections break the shift symmetry and generically lead to a potential of the form

$$V(\varphi) = \Lambda^4\Big(1+\cos(\varphi/f_a)\Big)\,. \tag{9.36}$$

For $f_a > M_{\rm pl}$ this gives a successful and (technically) natural inflation model.

*Axions in String Theory.* String theory contains many axion fields (both model-independent and model-dependent). However, systematic studies by Banks et al. [16] and recently by Svrcek and Witten [155] suggest that string theory does not allow (parametrically) super-Planckian values for $f_a$ as required for inflation from a single axion field.

*Field Range.* We give a sketch of the argument in Ref. [16]. Consider the complex modulus field $\rho = \sigma + i\alpha$ (for concreteness the reader may imagine the dilaton or the overall volume). The associated Lagrangian is

$$\mathcal{L} = cM_{\rm pl}^2\frac{(\partial\sigma)^2+(\partial\alpha)^2}{4\sigma^2} - V(\sigma,\alpha)\,, \tag{9.37}$$

where $c=1$ for the dilaton and $c=3$ for the total volume. Instanton corrections induce a potential for the axion field $\alpha$

$$V \sim \Lambda^4\cos\alpha\,. \tag{9.38}$$

Let $\sigma$ be stabilized at $\sigma_\star$. The canonical axion field is then $\varphi^2 = \frac{c}{4}\frac{\alpha^2}{\sigma_\star^2}$ and

$$V \sim \Lambda^4\cos(\varphi/f_a)\,, \qquad \text{where} \quad \frac{f_a}{M_{\rm pl}} \equiv \frac{\sqrt{c/2}}{\sigma_\star}\,. \tag{9.39}$$

*Backreaction.* We notice that the axion decay constant $f_a$ can only be large if $\sigma_\star \ll 1$. However, the non-perturbative axion potential (generated *e.g.* from Euclidean branes wrapped over some cycle of size $\sigma_\star$) scales as $e^{-\sigma_\star}$. For $\sigma_\star \ll 1$, the factor $e^{-\sigma_\star}$ is not very small and therefore $n$-instanton corrections proportional to $e^{-n\sigma_\star}$ cannot be ignored. This presents a serious obstruction to the possibility of having parametrically large axion decay constants in string theory, since the multi-instanton corrections will destroy the desired large periodicity of the single instanton contribution, reducing the "effective" $f_a$ by a factor of $n$.

**3.2. N-flation: Assisted Axion Inflation.** As we have just seen, there seem to be fundamental obstructions to getting single axion fields with super-Planckian field range. However, as we reviewed in Chapter 4, the N-flation model of Dimopoulos et al. [61] (see also [67]) suggests that the effective field related to the Pythagorean sum of $N$ axions, $\Phi^2 \equiv \sum_i \varphi_i^2$, can have super-Planckian range, $(\Delta\Phi)_{\rm kin} > M_{\rm pl}$, even if all individual axions have sub-Planckians $f_a$'s, $\Delta\varphi_i < M_{\rm pl}$. However, this requires $N \geq 1000$ and it remains unclear whether the potential is radiatively stable or whether dynamical effects limit the effective field range $(\Delta\Phi)_{\rm dyn}$. N-flation remains an interesting candidate for large-field inflation that deserves further study.

## 4. Volume Modulus

So far we have considered the effective four-dimensional fields associated with localized energy densities (branes) moving through the compact extra dimensions. The moduli space was compact and it was natural to expect geometrical restrictions on the canonical field range.

In the search for super-Planckian field excursions it is therefore natural to look for fields with non-compact moduli spaces. An immediate example is the overall volume of the compactification manifold. The moduli space associated with the volume is non-compact with decompactification corresponding to infinite range.

*Single Field.* The volume (Kähler) modulus $\rho$ has a logarithmic Kähler potential

$$\mathcal{K} = -3M_{\rm pl}^2 \ln(\rho + \bar{\rho}) \equiv -3M_{\rm pl}^2 \ln \sigma \,. \tag{9.40}$$

Typical energy sources in string theory all scale as inverse powers of the volume $\sigma$

$$V = \sum_i \frac{a_i}{\sigma^{c_i}} \,, \tag{9.41}$$

where $c_i$ are constants of order unity. The canonical field associated with $\sigma$ is $\varphi = M_{\rm pl} \ln \sigma$. The potential for the canonical field is therefore a sum of steep potentials

$$V \sim \sum_i a_i e^{-c_i \phi / M_{\rm pl}} \,. \tag{9.42}$$

This can never be sufficiently flat for inflation over a super-Planckian range (at best the potential can be flat for a small field range near an inflection point in the potential [92, 119]).

*Multiple Fields.* One may wonder whether models with multiple Kähler moduli can enjoy flat potentials of super-Planckian range even though individually each field has a steep exponential potential. In the absence of a general no-go result for large-field inflation from multiple Kähler moduli, it is instructive to consider the explicit examples discussed in the literature. In Chapter 4 we reviewed Conlon and Quevedo's model for Kähler moduli inflation in the context of LARGE volume compactifications [15]. Elementary considerations [53] show that in this example the field range during inflation is always small. The same conclusion applies to any other realization of Kähler moduli inflation that we are aware of. No existing model has a flat potential over a super-Planckian range.

## 5. Implications

We caution the reader not to overinterpret the results of this chapter. We have given various examples for limits on the field range for moduli in string theory. Often we found that fields which naively have a large kinematical range, are dynamically limited to a sub-Planckian range by backreaction constraints. However, given that we have not identified a physical principle for why super-Planckian vevs should be censored by string theory, the examples we have given in this chapter can at best be viewed as illustrative for the challenges one faces when trying to embed large-field inflation in string theory.

# Part 4

# Conclusions

CHAPTER 10

# Inflationary UV Challenges/Opportunities

In this thesis we have discussed aspects of inflation that benefit most directly from the application of a UV-complete theory. In this chapter we summarize the main physics points that we learned from the analysis of D-brane inflation. We believe these conclusions to be more general than the particular example we studied.

## 1. The Inflaton Potential

The major challenge for a microphysical understanding of the inflationary era of the early universe is obtaining the requisite slow variation of the inflationary energy density. Typically, this is described in terms of an inflaton field with very flat potential $V(\phi)$ and quantified by the smallness of the slow-roll parameters $\epsilon$ and $\eta$. Many models suffer from an eta-problem, meaning that corrections to $V(\phi)$ shift the eta parameter by order unity

$$\Delta\eta \sim 1\,. \tag{10.1}$$

In this thesis, we have proposed a useful classification for corrections to the inflaton potential in terms of their contribution to the $\eta$–parameter. To establish a robust model and prove that slow-roll can occur requires theoretical control over all possible order one corrections to $\eta$. Corrections whose contributions to $\eta$ are parametrically suppressed can be ignored to first order (*i.e.* when treating the background evolution).

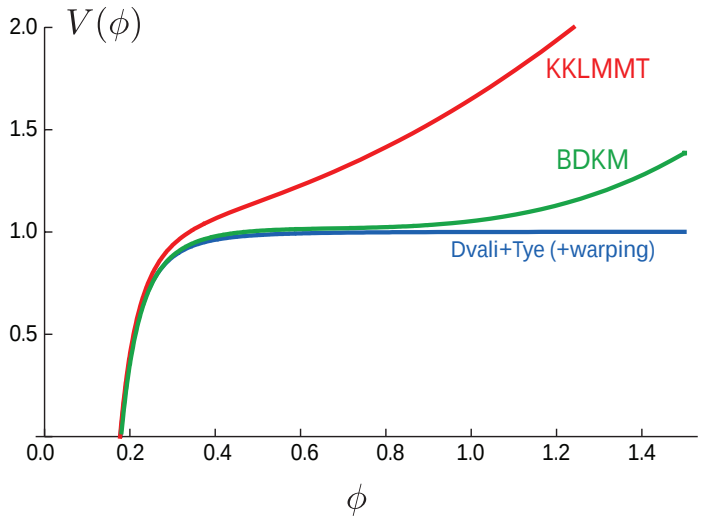


FIGURE 1. Computations of the brane potential.
a) Dvali+Tye (+warping) [64, 95]: $V_{\rm Coulomb}(\phi) = V_0(1 - c\phi^{-4})$.
b) KKLMMT [95]: $V_{\rm KKLMMT}(\phi) = V_{\rm Coulomb}(\phi) + \beta\phi^2$.
c) BDKM [19]: $V_{\rm BDKM}(\phi) = V_{\rm Coulomb}(\phi) + \lambda_1(\phi - \phi_0) + \lambda_3(\phi - \phi_0)^3$.

In Figure 1 we illustrate this scheme for the example of warped D-brane inflation. In a warped background the Coulomb attraction between a D3-brane and an anti-D3-brane is of the following form: $V_{\rm Coulomb}(\phi) = V_0(1 - c\phi^{-4})$. Warping suppression of the interaction makes the potential exponentially flat, $\epsilon, \eta \ll 1$. If this were the end of the story, this would be the perfect inflationary model. However, as we discussed in the bulk of this thesis, moduli stabilization effects give dangerous $\Delta\eta \sim 1$ corrections to $V_{\rm Coulomb}$. This is the origin of the eta-problem for these models. KKLMMT [95] showed that D3-brane backreaction on the compactification volume resulted in the following potential (see Chapter 4): $V_{\rm KKLMMT}(\phi) = V_{\rm Coulomb} + \beta\phi^2$. Generically, the potential is then too steep for inflation. In the first half of this thesis, we derived a crucial further correction to the potential arising from interaction of the D3-brane with D7-branes involved in the non-perturbative stabilization of the compactification volume. As we show in Figure 1 this allows a fine-tuned solution of the eta-problem close to a locally flat plateau around an inflection point. We also argued that all further corrections to the potential are parametrically suppressed ($\Delta\eta \ll 1$), so that we can claim a robust model. However, the model is very sensitive to the values of

the microscopic input parameters and the initial conditions (such as the initial brane position and velocity).

## 2. Gravitational Waves

One of the most exciting observational signatures of inflation is a spectrum of primordial gravitational waves. Interestingly, all inflationary models that predict an observable gravitational wave signal require that the inflaton field evolves over a super-Planckian range

$$\frac{r}{0.01} = \mathcal{O}(1) \left(\frac{\Delta\phi}{M_{\rm pl}}\right)^2 . \tag{10.2}$$

So far it has been challenging to derive such 'large-field' models from an explicit and controllable string compactification. For D-brane inflation Liam McAllister and I derived following bound on the field range

$$\frac{\Delta\phi}{M_{\rm pl}} < \frac{2}{\sqrt{N}} \ll 1 . \tag{10.3}$$

Similar field range bounds exist for most models of string inflation. However, a deeper physical principle behind these theoretical observations hasn't been established (although there have been some interesting proposals [11, 131, 132]). In particular, there is *no* general no-go result for gravitational waves from string inflation. Also, it should be noted that N-flation [61, 67] and the monodromy mechanism of Ref. [148] may be interesting exceptions that deserve further investigation.

## 3. Non-Gaussianity

In single-field slow-roll models of inflation the primordial density fluctuations are Gaussian to a very high degree [125]. Non-Gaussianity can only be large if higher-derivative terms, $X^n \equiv (\frac{1}{2}(\partial\phi)^2)^n$, play a crucial role during inflation. One is then faced with the problem of providing a plausible UV-completion of the theory. The relativistic limit of D-brane inflation (DBI inflation) is an interesting example where

higher-derivative terms are important and non-Gaussianities can be large in a controlled setting.

DBI inflation falls under the general category of higher-derivative theories first studied by Mukhanov and Garriaga [72]. The effective field theory action for these theories may be parameterized by an infinite series of higher-derivative terms $X^n$ suppressed by a cutoff scale $\Lambda^{2n}$

$$P(X,\phi) = P_0(\phi) + P_1(\phi)\frac{X}{\Lambda^2} + \frac{1}{2}P_2(\phi)\frac{X^2}{\Lambda^4} + \frac{1}{3!}P_3(\phi)\frac{X^3}{\Lambda^6} + \dots\,, \tag{10.4}$$

where $\frac{P_n}{\Lambda^{2n}} = \frac{d^nP}{dX^n}\big|_{X=0} \sim \mathcal{O}(1)$. Considering the special case of a $\frac{X^2}{\Lambda^4}$ correction to the slow-roll action, Creminelli [55] showed that the non-Gaussianity can only be large ($f_{\rm NL} > 1$) if $\frac{X}{\Lambda^2} > 1$. One then worries about the UV-convergence of (10.4).

DBI inflation is a special type of higher-derivative action

$$P_{\rm DBI}(X,\phi) = -f^{-1}\sqrt{1-2fX} + f^{-1} - V(\phi) \tag{10.5}$$

or

$$P_{\rm DBI} = -V(\phi) + f^{-1}\sum_{n=1}^{\infty}\lambda_n(fX)^n\,, \qquad \lambda_n \equiv (2n-3)!!\,. \tag{10.6}$$

In a generic effective field theory one would typically assume uncorrelated coefficients $\lambda_n$ in (10.6). In the relativistic limit $2fX \sim \mathcal{O}(1)$ one might then worry about the validity of (10.6). However, string theory does the sum! The coefficients $\lambda_n$ for the terms in (10.6) are not independent, but correlated by their string theoretic origin in the square-root DBI action (10.5). Any inflationary model with large non-Gaussianities arising from non-canonical kinetic effects requires a similiar degree of UV-completeness as DBI inflation.

"I have deep faith that the principle of the universe will be beautiful and simple."

*Albert Einstein*

"Of two equivalent theories or explanations, all other things being equal, the simpler one is to be preferred."

*Occam's Razor*

CHAPTER 11

# Epilogue

> "It doesn't matter how beautiful your theory is, it doesn't matter how smart you are or what your name is. If it doesn't agree with experiment, it's wrong."
> *Richard Feynman*

Cosmological observations are, for the first time, precise enough to allow detailed tests of theories of the early universe. This has established inflation [3, 83, 120] as the leading explanation for the origin of structure in the universe. In this thesis we described the search for the microphysical origin of inflation. The physics of inflation is in principle very simple – a universe dominated by the energy density of a uniform scalar field[1] that satisfies the slow-roll conditions leads to exponential expansion. The simplest scenario furthermore has the advantage that it is very predictive: canonical single-field inflation predicts a homogeneous and flat universe with small density perturbations that are nearly scale-invariant, adiabatic and Gaussian. These predictions are consistent with recent measurements of anisotropies in the cosmic microwave background temperature [151]. Inflation further predicts a stochastic background of gravitational waves which leaves subtle imprints in the polarization of the CMB and can therefore potentially be detected by future experiments. Involving two or more

[1]This can be a fundamental scalar or an effective scalar condensate.

scalar fields extends the possibilities, but also diminishes the predictive power of inflation. At present, the data does not require any extensions of the simplest models beyond single-field slow-roll.

The observational evidence for 'simple' inflation is strong and rapidly growing [111], and in the near future it will be possible to falsify a large fraction of existing models. This presents a remarkable opportunity for inflationary model-building, and it intensifies the need for a more fundamental description of inflation than current phenomenological models can provide. At the same time, theoretical advances in string theory (moduli stabilization, SUSY breaking, etc.) have led to the first reliable models of string inflation. This research is still in its infancy but it holds the promise to give an improved understanding of key UV-sensitive predictions of inflation (eta-problem, gravitational waves, non-Gaussianity). We have come to appreciate that understanding the universe on the largest scales depends crucially on insights about the physics of the very small. The future therefore holds much promise for cosmology and its connection to fundamental physics.

# Appendix

## Reading Guide for the Appendices

The following appendices are an integral part of this work and contain many original results and important theoretical additions to the main body of the thesis:

- Appendix A reviews the calculation of the two- and three-point functions for quantum fluctuations created during inflation. These classic results are used throughout the thesis as they form the basis for all modern comparisons of the inflationary predictions with the cosmological data.

- Appendices B, C and D complement the computations of Chapter 5.

- Appendices E, F, G, and H give important technical details of the arguments presented in Chapter 7.

- Finally, Appendix J collects frequently used results from early universe cosmology and string theory.

APPENDIX A

# Primordial Fluctuations from Inflation

In this appendix we review Maldacena's beautiful calculation of the two- and three-point functions for quantum fluctuations created during inflation [125]. The analysis shows that primordial non-Gaussianities are unobservably small for slow-roll models of inflation. Large non-Gaussianities, however, arise if inflation is driven by a scalar field with non-minimal kinetic term. We cite results for the two- and three-point functions for inflationary models with general speed of sound [52].

We use the classic results of this appendix throughout this thesis as they form the theoretical basis for comparing inflationary predictions to observational data.

## A.1. Slow-Roll Inflation

*Background.* Slow-roll models of inflation are described by a canonical scalar field $\phi$ minimally coupled to gravity

$$S = \frac{1}{2}\int \mathrm{d}^4x\sqrt{-g}\,\left[\mathcal{R} - (\nabla\phi)^2 - 2V(\phi)\right]\,, \qquad M_{\rm pl}^{-2} \equiv 8\pi G = 1\,. \tag{A.1}$$

We consider a flat background metric

$$\mathrm{d}s^2 = -\mathrm{d}t^2 + a(t)^2\delta_{ij}\mathrm{d}x^i\mathrm{d}x^j = a^2(\tau)(-\mathrm{d}\tau^2 + \delta_{ij}\mathrm{d}x^i\mathrm{d}x^j) \tag{A.2}$$

with scale factor $a(t)$ and Hubble parameter $H(t) \equiv \partial_t \ln a$ satisfying the Friedmann equations

$$3H^2 = \frac{1}{2}\dot{\phi}^2 + V(\phi)\,, \qquad \dot{H} = -\frac{1}{2}\dot{\phi}^2\,. \tag{A.3}$$

The scalar field satisfies the Klein-Gordon equation

$$\ddot{\phi} + 3H\dot{\phi} + V'(\phi) = 0\,. \tag{A.4}$$

The standard slow-roll parameters are

$$\epsilon = \frac{1}{2}\Big(\frac{V'}{V}\Big)^2 \approx \frac{1}{2}\frac{\dot{\phi}^2}{H^2}\,, \qquad \eta = \frac{V''}{V} \approx -\frac{\ddot{\phi}}{H\dot{\phi}} + \frac{1}{2}\frac{\dot{\phi}^2}{H^2}\,. \tag{A.5}$$

*ADM Formalism.* We treat fluctuations in the ADM formalism [13] where spacetime is sliced into three-dimensional hypersurfaces

$$\mathrm{d}s^2 = -N^2\mathrm{d}t^2 + g_{ij}(\mathrm{d}x^i + N^i\mathrm{d}t)(\mathrm{d}x^j + N^j\mathrm{d}t)\,. \tag{A.6}$$

Here, the lapse function $N(\mathbf{x})$ and the shift function $N_i(\mathbf{x})$ are non-dynamical Lagrange multipliers. The action (A.1) becomes

$$\begin{aligned} S \;=\; & \frac{1}{2}\int \mathrm{d}^4x\sqrt{-g}\Big[NR^{(3)} - 2NV + N^{-1}(E_{ij}E^{ij} - E^2) + \\ & N^{-1}(\dot{\phi} - N^i\partial_i\phi)^2 - Ng^{ij}\partial_i\phi\partial_j\phi - 2V\Big]\,, \end{aligned} \tag{A.7}$$

where

$$E_{ij} \equiv \frac{1}{2}(\dot{g}_{ij} - \nabla_i N_j - \nabla_j N_i)\,, \qquad E = E^i_i\,. \tag{A.8}$$

$E_{ij}$ is related to the extrinsic curvature of the three-dimensional spacetime slices $K_{ij} = N^{-1}E_{ij}$. To fix time and spatial reparameterizations we choose a gauge for the dynamical fields $g_{ij}$ and $\phi$ [125]

$$\delta\phi = 0\,, \qquad g_{ij} = a^2[(1+2\zeta)\delta_{ij} + h_{ij}]\,, \qquad \partial_i h_{ij} = h^i_i = 0\,. \tag{A.9}$$

In this gauge the inflaton field is unperturbed and all scalar degrees of freedom are parameterized by the metric fluctuation $\zeta(t,\mathbf{x})$. Geometrically, $\zeta$ measures the spatial curvature of constant-$\phi$ hypersurfaces, ${}^{(3)}\mathcal{R} = -4\nabla^2\zeta/a^2$. An important property of $\zeta$ is that it remains constant outside the horizon. We can therefore restrict our

computation to correlation functions at horizon crossing. The ADM action (A.7) implies the following constraint equations for the Lagrange multipliers $N$ and $N^i$

$$\nabla_i[N^{-1}(E^i_j - \delta^i_j E)] = 0\,, \tag{A.10}$$

$$R^{(3)} - 2V - N^{-2}(E_{ij}E^{ij} - E^2) - N^{-2}\dot{\phi}^2 = 0\,. \tag{A.11}$$

### A.1.1. Two-Point Function.

*Scalar Perturbations.* Maldacena solved for $N$ and $N^i$ in equations (A.10) and (A.11) and substituted the result back into the action. After integrations by parts and using the background equations of motion he finds [125]

$$S = \frac{1}{2}\int \mathrm{d}^4x\, a^3 \frac{\dot{\phi}^2}{H^2}\left[\dot{\zeta}^2 - a^{-2}(\partial_i\zeta)^2\right] \equiv \int \mathrm{d}^4x\, a^3\, \epsilon\, \Box\zeta\,. \tag{A.12}$$

For $H \sim$ const. this corresponds to the action for a massless field $\psi \equiv \frac{\dot{\phi}}{H}\zeta$ in de Sitter space

$$S = \frac{1}{2}\int \mathrm{d}^4x\, a^3\left[(\dot{\psi})^2 - a^{-2}(\partial_i\psi)^2\right] \tag{A.13}$$

$$= \frac{1}{2}\int \mathrm{d}^4x\, (H\tau)^{-2}\left[(\partial_\tau\psi)^2 - (\partial_i\psi)^2\right]\,. \tag{A.14}$$

We define the following Fourier expansion of the field $\psi$

$$\psi(\tau,\mathbf{x}) = \int \frac{\mathrm{d}^3k}{(2\pi)^3}\,\psi_{\mathbf{k}}(\tau)e^{i\mathbf{k}\cdot\mathbf{x}}\,. \tag{A.15}$$

The Fourier components $\psi_{\mathbf{k}}$ are promoted to operators and expressed via the following decomposition

$$\hat{\psi}_{\mathbf{k}} = v^*_k(\tau)\hat{a}^-_{\mathbf{k}} + v_{-k}(\tau)\hat{a}^+_{-\mathbf{k}}\,, \tag{A.16}$$

where the creation and annihilation operators $\hat{a}^+_{-\mathbf{k}}$ and $\hat{a}^-_{\mathbf{k}}$ satisfy the canonical commutation relation

$$[\hat{a}^-_{\mathbf{k}}, \hat{a}^+_{-\mathbf{k}'}] = (2\pi)^3\delta(\mathbf{k}+\mathbf{k}') \tag{A.17}$$

if and only if the mode functions are normalized as follows

$$\mathrm{Im}(v'_{-k}v^*_k) = 1\,, \qquad (...)' \equiv \partial_\tau(...)\,. \tag{A.18}$$

The Bunch-Davies vacuum, $\hat{a}^-_{\mathbf{k}}|0\rangle = 0$, corresponds to

$$v_k = \frac{H}{\sqrt{2k^3}}(1 - ik\tau)e^{ik\tau}\,. \tag{A.19}$$

On small scales, $k\tau \gg 1$, this reduces to the Minkowski vacuum. We then compute the power spectrum of $\psi$

$$\begin{aligned}\langle\psi_{\mathbf{k}}(\tau)\psi_{\mathbf{k}'}(\tau)\rangle &= (2\pi)^3\delta(\mathbf{k}+\mathbf{k}')|v_k(\tau)|^2 &\text{(A.20)}\\ &= (2\pi)^3\delta(\mathbf{k}+\mathbf{k}')\frac{H^2}{2k^3}(1+k^2\tau^2)\,. &\text{(A.21)}\end{aligned}$$

On super-horizon scales, $k\tau \ll 1$, this approaches a constant

$$\langle\psi_{\mathbf{k}}(\tau)\psi_{\mathbf{k}'}(\tau)\rangle \sim (2\pi)^3\delta(\mathbf{k}+\mathbf{k}')\frac{H^2}{2k^3}\,. \tag{A.22}$$

The de Sitter result for $\psi$ (A.22) allows us to compute the power spectrum of $\zeta = \frac{H}{\dot\phi}\psi$ at horizon crossing, $a(t_\star)H(t_\star) \sim k$,

$$\langle\zeta_{\mathbf{k}}(t)\zeta_{\mathbf{k}'}(t)\rangle = (2\pi)^3\delta(\mathbf{k}+\mathbf{k}')\frac{H^2_\star}{2k^3}\frac{H^2_\star}{\dot\phi^2_\star}\,. \tag{A.23}$$

We define the dimensional power spectrum $P_s(k)$ by

$$\langle\zeta_{\mathbf{k}}\zeta_{\mathbf{k}'}\rangle = (2\pi)^3\delta(\mathbf{k}+\mathbf{k}')\mathcal{P}_s(k)\,, \qquad P_s(k) \equiv \frac{k^3}{2\pi^2}\mathcal{P}_s(k)\,, \tag{A.24}$$

such that the real space variance of $\zeta$ is $\langle\zeta\zeta\rangle = \int_0^\infty P_s(k)\,\mathrm{d}\ln k$. This gives

$$P_s(k) = \frac{H^2_\star}{(2\pi)^2}\frac{H^2_\star}{\dot\phi^2_\star}\,. \tag{A.25}$$

Since $\zeta$ approaches a constant on super-horizon scales the spectrum at horizon crossing determines the future spectrum until a given fluctuation mode re-enters the horizon.

The scale dependence of the spectrum follows from the time-dependence of the Hubble parameter and is quantified by the spectral index

$$n_s - 1 \equiv \frac{d\ln P_s}{d\ln k} = \frac{1}{H_\star}\frac{d}{dt_\star}\ln\frac{H_\star^4}{\dot\phi_\star^2} = 2\eta_\star - 6\epsilon_\star\,. \tag{A.26}$$

*Tensor Perturbations.* The action for tensor fluctuations is

$$S = \frac{1}{8}\int \mathrm{d}x^4 a^3\left[(\dot h_{ij})^2 - a^{-2}(\partial_l h_{ij})^2\right]\,. \tag{A.27}$$

We define the following Fourier expansion

$$h_{ij} = \int \frac{\mathrm{d}^3k}{(2\pi)^3}\sum_{s=+,\times}\epsilon_{ij}^s(k)h_{\mathbf{k}}^s(t)e^{i\mathbf{k}\cdot\mathbf{x}}\,, \tag{A.28}$$

where $\epsilon_{ii} = k^i\epsilon_{ij} = 0$ and $\epsilon_{ij}^s(k)\epsilon_{ij}^{s'}(k) = 2\delta_{ss'}$. The two polarization modes of gravitational waves, $h_{\mathbf{k}}^s \equiv h_{\mathbf{k}}^{+,\times}$, correspond to massless scalars in de Sitter space for which the power spectrum is given by (A.22)

$$\langle h_{\mathbf{k}}h_{\mathbf{k}'}\rangle = (2\pi)^3\delta(\mathbf{k}+\mathbf{k}')\frac{1}{2k^3}\frac{H_\star^2}{M_{\rm pl}^2}\,. \tag{A.29}$$

The dimensionless power spectrum of tensor fluctuations therefore is

$$P_t(k) = \frac{2}{\pi^2}\frac{H_\star^2}{M_{\rm pl}^2}\,. \tag{A.30}$$

From (A.25) and (A.30) we get the tensor-to-scalar ratio

$$r \equiv \frac{P_t}{P_s} = 16\epsilon_\star\,. \tag{A.31}$$

The tensor spectral index is

$$n_t \equiv \frac{d\ln P_t}{d\ln k} = -2\epsilon_\star\,. \tag{A.32}$$

We see that single-field slow-roll models satisfy a consistency condition between the tensor-to-scalar ratio $r$ and the tensor tilt $n_t$

$$r = -8n_t\,. \tag{A.33}$$

**A.1.2. Three-Point Function and Non-Gaussianity.** Using the same formalism (but fighting with considerably more algebra) Maldacena also derived the bispectrum (three-point function) of scalar fluctuations [125]

$$\langle \zeta_{\mathbf{k}_1}\zeta_{\mathbf{k}_2}\zeta_{\mathbf{k}_3}\rangle = (2\pi)^3\delta\Big(\sum \mathbf{k}_i\Big)\frac{H_\star^4}{\dot\phi_\star^4}\frac{H_\star^4}{M_{\rm pl}^4}\frac{1}{\prod_i(2k_i^3)}\,\mathcal{A}_\star \tag{A.34}$$

where

$$\mathcal{A}_\star \equiv 2\frac{\ddot\phi_\star}{\dot\phi_\star H_\star}\sum_i k_i^3 + \frac{\dot\phi_\star^2}{H_\star^2}\underbrace{\left[\frac{1}{2}\sum_i k_i^3 + \frac{1}{2}\sum_{i\neq j} k_i k_j^2 + 4\frac{\sum_{i>j}k_i^2k_j^2}{\sum_i k_i}\right]}_{\equiv(\sum_i k_i^3)f(k)}\,. \tag{A.35}$$

*Shape of Non-Gaussianity.* A simple way to characterize the non-Gaussianity of $\zeta$ is to assume that it can be parameterized by a field redefinition of the form

$$\zeta = \zeta_L + \frac{3}{5}f_{\rm NL}\zeta_L^2\,, \tag{A.36}$$

where $\zeta_L$ is Gaussian and the constant $f_{\rm NL}$ measures the amount of non-Gaussianity of $\zeta$. Equation (A.36) is often called *local* non-Gaussianity. This leads to a momentum dependence of the three-point functions that is close to (but not exactly the same as) the momentum dependence found in (A.35). One may, however, define a weakly $k$-dependent $f_{\rm NL}$ parameter

$$f_{\rm NL} \sim \frac{5}{3}\frac{\mathcal{A}_\star}{(4\sum_i k_i^3)} = -\frac{5}{12}\left[(n_s-1) + f(k)n_t\right] \tag{A.37}$$

where $0 \leq f(k) \leq \frac{5}{6}$. This shows that $f_{\rm NL} \ll 1$ due to the near scale-invariance of the primordial spectra, $n_s - 1, n_t \ll 1$. Since it is generally believed that non-Gaussianity

is only observable if $f_{\rm NL} \gtrsim 1$, we conclude that primordial non-Gaussianities from slow-roll inflation are unobservable.

## A.2. Models with General Speed of Sound

While primordial fluctuations are highly Gaussian for slow-roll models of inflation, non-Gaussianities can be significant for models with non-canonical kinetic effects. Chen et al. [52] studied such models using the following parameterization for the inflaton action

$$S = \frac{1}{2}\int \mathrm{d}^4x\sqrt{-g}\,[\mathcal{R} + 2P(X,\phi)]\ , \tag{A.38}$$

where $X \equiv -\frac{1}{2}g^{\mu\nu}\partial_\mu\phi\partial_\nu\phi$. Examples of inflation models with actions of the type (A.38) are K-inflation [12], DBI inflation [147] and ghost inflation [10]. The function $P$ corresponds to the pressure of the scalar fluid, while its energy density is

$$\rho = 2XP_{,X} - P\,. \tag{A.39}$$

Furthermore, the models are characterized by a non-trivial speed of sound

$$c_s^2 \equiv \frac{dP}{d\rho} = \frac{P_{,X}}{P_{,X} + 2XP_{,XX}}\,. \tag{A.40}$$

Finally, it proves convenient to define parameters for the time-variation of the expansion rate $H(t)$ and the speed of sound $c_s(t)$

$$\epsilon = -\frac{\dot H}{H^2} = \frac{XP_{,X}}{H^2}\,, \qquad \tilde\eta = \frac{\dot\epsilon}{\epsilon H}\,, \tag{A.41}$$

$$s = \frac{\dot c_s}{c_s H}\,. \tag{A.42}$$

### A.2.1. Two-Point Function.

*Scalar Perturbations.* A calculation similar to that of the previous section gives the power spectrum of scalar fluctuations

$$P_s(k) = \frac{1}{8\pi^2 M_{\rm pl}^2}\frac{H_\star^2}{c_{s\star}\epsilon_\star}\,. \tag{A.43}$$

The r.h.s. of (A.43) is evaluated at the time of (sound) horizon exit at $a_\star H_\star = c_s k$. The scale-dependence of the spectrum is

$$n_s - 1 = -2\epsilon_\star - \tilde{\eta}_\star - s_\star \,. \tag{A.44}$$

*Tensor Perturbations.* The tensor fluctuation spectrum is the same as for slow-roll models

$$P_t(k) = \frac{2}{\pi^2}\frac{H_\star^2}{M_{\rm pl}^2} \tag{A.45}$$

$$n_t = -2\epsilon_\star \,. \tag{A.46}$$

The r.h.s. of (A.45) and (A.46) is evaluated at $a_\star H_\star = k$. We see that for models with $c_s \neq 1$ the consistency relation between $r$ and $n_t$, equation (A.33), is modified

$$r = -8 c_s n_t \,. \tag{A.47}$$

**A.2.2. Three-Point Function and Non-Gaussianity.** To present the results for the calculation of the three-point function it is useful to define two more parameters

$$\Sigma \equiv X P_{,X} + 2X^2 P_{,XX} = \frac{H^2\epsilon}{c_s^2} \,, \tag{A.48}$$

$$\lambda \equiv X^2 P_{,XX} + \frac{2}{3} X^3 P_{,XXX} \,. \tag{A.49}$$

Following Maldacena [125], Chen et al. [52] derived the three-point function of super-horizon curvature fluctuations

$$\langle \zeta_{\mathbf{k}_1} \zeta_{\mathbf{k}_2} \zeta_{\mathbf{k}_3} \rangle = (2\pi)^7 \delta(\mathbf{k}_1 + \mathbf{k}_2 + \mathbf{k}_3) \, (P_s)^2 \, \frac{1}{\prod_i k_i^3} \, \mathcal{A}_\star \,, \tag{A.50}$$

where

$$\begin{aligned}\mathcal{A}_\star \;\supset\; & \left(\frac{1}{c_s^2}-1-\frac{2\lambda}{\Sigma}\right)\frac{3k_1^2k_2^2k_3^2}{2K^3} \\ & + \left(\frac{1}{c_s^2}-1\right)\left(-\frac{1}{K}\sum_{i>j}k_i^2k_j^2+\frac{1}{2K^2}\sum_{i\neq j}k_i^2k_j^3+\frac{1}{8}\sum_i k_i^3\right). \end{aligned} \tag{A.51}$$

Here, we defined $K \equiv k_1 + k_2 + k_3$.

*Shape of Non-Gaussianity.* We notice that the momentum dependence of (A.51) is significantly different from the local shape of non-Gaussianity (A.35). While for (A.35) the signal is largest when one of the momenta is very small, $k_1 \ll k_2 \sim k_3$, (A.51) peaks when the magnitude of all momenta is the same, $k_1 \sim k_2 \sim k_3$. For obvious reasons this is called the *equilateral* shape [14]. One may define the parameter

$$f_{\rm NL}^{\rm equil} = \frac{5}{3}\frac{\mathcal{A}_\star}{(4\sum_i k_i^3)}\,, \tag{A.52}$$

where $\mathcal{A}_\star$ is now evaluated for equilateral triangles in momentum space. From (A.51) one then finds

$$f_{\rm NL}^{\rm equil} = -\frac{35}{108}\Big(\frac{1}{c_s^2}-1\Big)+\frac{5}{81}\Big(\frac{1}{c_s^2}-1-2\Lambda\Big)\,, \tag{A.53}$$

where

$$\Lambda \equiv \frac{\lambda}{\Sigma} = \frac{X^2P_{,XX}+\frac{2}{3}X^3P_{,XXX}}{XP_{,X}+2X^2P_{,XX}}\,. \tag{A.54}$$

*DBI Inflation.* For the Lagrangian of DBI inflation [147]

$$P_{\rm DBI}(X,\phi) = -f^{-1}(\phi)\sqrt{1-2f(\phi)X}+f^{-1}(\phi)-V(\phi)\,, \tag{A.55}$$

one finds that the second term in (A.53) is identically zero and

$$f_{\rm NL}^{\rm DBI} = -\frac{35}{108}\Big(\frac{1}{c_s^2}-1\Big)\,. \tag{A.56}$$

APPENDIX B

# Green's Functions on Conical Geometries

In this appendix we give mathematical details on the Green's functions used in Chapter 5. Further details may be found in Ref. [104].

## B.1. Green's Function on the Singular Conifold

The D3-branes that we consider throughout this thesis are point sources in the six-dimensional internal space. The backreaction they induce on the background geometry can therefore be related to the Green's functions for the Laplace problem on conical geometries (see Chapter 5)

$$-\nabla_X^2 G(X;X') = \frac{\delta^{(6)}(X-X')}{\sqrt{g(X)}}\,. \tag{B.1}$$

In the following we present explicit results for the Green's function on the singular conifold. In the large $r$ limit, far from the tip, the Green's functions for the resolved and deformed conifold reduce to those of the singular conifold [104].

In the singular conifold geometry (5.27), the defining equation (B.1) for the Green's function becomes

$$\frac{1}{r^5}\frac{\partial}{\partial r}\Big(r^5\frac{\partial}{\partial r}G\Big) + \frac{1}{r^2}\nabla_\Psi^2 G = -\frac{1}{r^5}\delta(r-r')\delta_{T^{1,1}}(\Psi-\Psi')\,, \tag{B.2}$$

where $\nabla_\Psi^2$ and $\delta_{T^{1,1}}(\Psi-\Psi')$ are the Laplacian and the normalized delta function on $T^{1,1}$, respectively. $\Psi$ stands collectively for the five angular coordinates of the base and $X \equiv (r,\Psi)$. An explicit solution for the Green's function is obtained by a series

expansion of the form

$$G(X;X') = \sum_L Y_L^*(\Psi')Y_L(\Psi)H_L(r;r')\,. \tag{B.3}$$

The $Y_L$'s are eigenfunctions of the angular Laplacian,

$$\nabla_\Psi^2 Y_L(\Psi) = -\Lambda_L Y_L(\Psi)\,, \tag{B.4}$$

where the multi-index $L$ represents a set of discrete quantum numbers related to the symmetries of the base of the cone. The angular eigenproblem is worked out in detail in §B.2. If the angular wavefunctions are normalized as

$$\int \mathrm{d}^5\Psi\,\sqrt{g_{T^{1,1}}}\,Y_L^*(\Psi)Y_{L'}(\Psi) = \delta_{LL'}\,, \tag{B.5}$$

then

$$\sum_L Y_L^*(\Psi')Y_L(\Psi) = \delta_{T^{1,1}}(\Psi-\Psi')\,, \tag{B.6}$$

and equation (B.2) reduces to the radial equation

$$\frac{1}{r^5}\frac{\partial}{\partial r}\Big(r^5\frac{\partial}{\partial r}H_L\Big) - \frac{\Lambda_L}{r^2}H_L = -\frac{1}{r^5}\delta(r-r')\,, \tag{B.7}$$

whose solution away from $r=r'$ is

$$H_L(r;r') = A_\pm(r')r^{c_L^\pm}\,, \qquad c_L^\pm \equiv -2 \pm \sqrt{\Lambda_L+4}\,. \tag{B.8}$$

The constants $A_\pm$ are uniquely determined by integrating equation (B.7) across $r=r'$. The Green's function on the singular conifold is

$$G(X;X') = \sum_L \frac{1}{2\sqrt{\Lambda_L+4}} \times Y_L^*(\Psi')Y_L(\Psi) \times \begin{cases} \frac{1}{r'^4}\Big(\frac{r}{r'}\Big)^{c_L^+} & r \le r'\,, \\ \frac{1}{r^4}\Big(\frac{r'}{r}\Big)^{c_L^+} & r \ge r'\,, \end{cases} \tag{B.9}$$

where the angular eigenfunctions $Y_L(\Psi)$ are given explicitly in §B.2.

### B.2. Eigenfunctions of the Laplacian on $T^{1,1}$

In this section we complete the Green's function on the singular conifold (B.9) by solving for the eigenfunctions of the Laplacian on $T^{1,1}$

$$\begin{aligned}\nabla^2_\Psi Y_L &= \frac{1}{\sqrt{g}}\partial_m(g^{mn}\sqrt{g}\partial_n Y_L) = (6\nabla^2_1 + 6\nabla^2_2 + 9\nabla^2_R)Y_L \\ &= -\Lambda_L Y_L\,,\end{aligned} \tag{B.10}$$

where

$$\nabla^2_i Y_L \equiv \frac{1}{\sin\theta_i}\partial_{\theta_i}(\sin\theta_i\partial_{\theta_i}Y_L) + \Big(\frac{1}{\sin\theta_i}\partial_{\phi_i} - \cot\theta_i\partial_\psi\Big)^2 Y_L\,, \tag{B.11}$$

$$\nabla^2_R Y_L \equiv \partial^2_\psi Y_L\,. \tag{B.12}$$

The solution to equation (B.10) is obtained through separation of variables

$$Y_L(\Psi) = J_{l_1,m_1,R}(\theta_1)J_{l_2,m_2,R}(\theta_2)\,e^{im_1\phi_1+im_2\phi_2}\,e^{\frac{i}{2}R\psi}\,, \tag{B.13}$$

where

$$\frac{1}{\sin\theta_i}\partial_{\theta_i}(\sin\theta_i\partial_{\theta_i}J_{l_i,m_i,R}(\theta_i)) - \Big(\frac{m_i}{\sin\theta_i} - \frac{R}{2}\cot\theta_i\Big)^2 J_{l_i,m_i,R}(\theta_i) = -\Lambda_{l_i,R}J_{l_i,m_i,R}(\theta_i)\,. \tag{B.14}$$

The eigenvalues are $\Lambda_{l_i,R} \equiv l_i(l_i+1) - \frac{R^2}{4}$. Explicit solutions for equation (B.14) are given in terms of hypergeometric functions ${}_2F_1(a,b,c;x)$

$$\begin{aligned}J^\Upsilon_{l_i,m_i,R}(\theta_i) &= N^\Upsilon_L\,(\sin\theta_i)^{m_i}\Big(\cot\frac{\theta_i}{2}\Big)^{R/2}\times \\ &\quad {}_2F_1\Big(-l_i+m_i, 1+l_i+m_i, 1+m_i-\frac{R}{2}; \sin^2\frac{\theta_i}{2}\Big)\,,\end{aligned} \tag{B.15}$$

$$\begin{aligned}J^\Omega_{l_i,m_i,R}(\theta_i) &= N^\Omega_L\,(\sin\theta_i)^{R/2}\Big(\cot\frac{\theta_i}{2}\Big)^{m_i}\times \\ &\quad {}_2F_1\Big(-l_i+\frac{R}{2}, 1+l_i+\frac{R}{2}, 1-m_i+\frac{R}{2}; \sin^2\frac{\theta_i}{2}\Big)\,,\end{aligned} \tag{B.16}$$

where $N_L^{\Upsilon}$ and $N_L^{\Omega}$ are determined by the normalization condition (B.5). If $m_i \geq R/2$, solution $\Upsilon$ is non-singular. If $m_i \leq R/2$, solution $\Omega$ is non-singular. When $m_i = R/2$, the solutions coincide. The full wavefunction corresponds to the spectrum

$$\Lambda_L = 6\Big(l_1(l_1+1) + l_2(l_2+1) - \frac{R^2}{8}\Big)\,. \tag{B.17}$$

The eigenfunctions transform under $SU(2)_1 \times SU(2)_2$ as the spin $(l_1, l_2)$ representation and under the $U(1)_R$ with charge $R$. The multi-index $L$ has the data:

$$L \equiv (l_1, l_2), (m_1, m_2), R\,.$$

The following restrictions on the quantum numbers correspond to the existence of single-valued regular solutions:

- $l_1$ and $l_2$ are both integers or both half-integers.
- $m_1 \in \{-l_1, \cdots, l_1\}$ and $m_2 \in \{-l_2, \cdots, l_2\}$.
- $R \in \mathbb{Z}$ with $\frac{R}{2} \in \{-l_1, \cdots, l_1\}$ and $\frac{R}{2} \in \{-l_2, \cdots, l_2\}$.

As discussed in §5.2, chiral operators in the dual gauge theory correspond to $l_1 = \frac{R}{2} = l_2$.

APPENDIX C

# Computation of Backreaction in the Singular Conifold

This appendix computes the gravitational backreaction of a D3-brane on the volume of a four-cycle in the singular conifold.

## C.1. Correction to the Four-Cycle Volume

Recall from Chapter 5 the definition (5.14) of the (holomorphic) correction to the warped volume of a four-cycle $\Sigma_4$

$$\delta V^w_{\Sigma_4} = \mathrm{Re}(\zeta(X')) = \int_{\Sigma_4} \mathrm{d}^4X \sqrt{g^{ind}(X)}\, \delta h(X;X')\,, \tag{C.1}$$

where $\delta h(X;X') = \mathcal{C}G(X;X')$ and $T_3\mathcal{C} = 2\pi$.

**Embedding, Induced Metric and a Selection Rule.** The induced metric on the four-cycle, $g^{ind}$, is determined from the background metric and the embedding constraint. In §5 of Chapter 5 we introduced the class of supersymmetric embeddings (5.36). Equation (5.37) and the form of the angular eigenfunctions of the Green's function (see §B.2 of Appendix B) imply that (C.1) is proportional to

$$\frac{e^{\frac{i}{2}R\psi_s}}{(2\pi)^2}\int_0^{2\pi}\mathrm{d}\phi_1\, e^{i(m_1+\frac{R}{2}n_1)\phi_1}\int_0^{2\pi}\mathrm{d}\phi_2\, e^{i(m_2+\frac{R}{2}n_2)\phi_2} = e^{\frac{i}{2}R\psi_s}\,\delta_{m_1,-\frac{R}{2}n_1}\,\delta_{m_2,-\frac{R}{2}n_2}\,. \tag{C.2}$$

We may therefore restrict the computation to values of the $R$-charge that satisfy

$$m_1 = -\frac{R}{2}n_1\,, \quad m_2 = -\frac{R}{2}n_2\,. \tag{C.3}$$

The winding numbers $n_i$ (5.42) are rational numbers of the form

$$n_i \equiv \frac{\tilde{n}_i}{q}\,, \qquad \tilde{n}_i \in \mathbb{Z}\,, \tag{C.4}$$

where $\tilde{n}_i$ and $q$ do not have a common divisor. Therefore the requirement that the magnetic quantum numbers $m_i$ be integer or half-integer leads to the following selection rule for the $R$-charge

$$R = q \cdot k\,, \quad k \in \mathbb{Z}\,. \tag{C.5}$$

**Green's Function and Reduced Angular Eigenfunctions.** The Green's function on the conifold (§B.1) is

$$G(X;X') = \sum_L Y_L^*(\Psi')Y_L(\Psi)H_L(r;r')\,, \tag{C.6}$$

where it is important that the angular eigenfunctions (§B.2) are normalized correctly on $T^{1,1}$

$$\int \mathrm{d}^5\Psi\sqrt{g_{T^{1,1}}}|Y_L(\Psi)|^2 = 1\,, \tag{C.7}$$

or

$$V_{T^{1,1}}\int_0^1 \mathrm{d}x\,[J_{l_1,m_1,R}(x)]^2\int_0^1 \mathrm{d}y\,[J_{l_2,m_2,R}(y)]^2 = 1\,. \tag{C.8}$$

The coordinates $x$ and $y$ are defined in (5.41). Next, we show that the hypergeometric angular eigenfunctions reduce to Jacobi polynomials if we define

$$l_1 \equiv \frac{R}{2} + L_1\,, \quad l_2 \equiv \frac{R}{2} + L_2\,, \qquad L_1, L_2 \in \mathbb{Z}\,. \tag{C.9}$$

This parameterization is convenient because chiral terms are easily identified by $L_1 = 0 = L_2$. Non-chiral terms correspond to non-zero $L_1$ and/or $L_2$. Without loss of generality we define chiral terms to have $R > 0$ and anti-chiral terms to have $R < 0$.

With these restrictions the angular eigenfunctions of §B.2 simplify to

$$J_{\frac{R}{2}+L_1,-\frac{R}{2}n_1,R}(x) = x^{\frac{R}{4}(1+n_1)}(1-x)^{\frac{R}{4}(1-n_1)}\,P_{L_1,R,n_1}(x)\,, \tag{C.10}$$

$$J_{\frac{R}{2}+L_2,-\frac{R}{2}n_2,R}(y) = y^{\frac{R}{4}(1+n_2)}(1-y)^{\frac{R}{4}(1-n_2)}\,P_{L_2,R,n_2}(y)\,, \tag{C.11}$$

where

$$P_{L_1,R,n_1}(x) \equiv N_{L_1,R,n_1}P_{L_1}^{\frac{R}{2}(1+n_1),\frac{R}{2}(1-n_1)}(1-2x)\,, \tag{C.12}$$

$$P_{L_2,R,n_2}(y) \equiv N_{L_2,R,n_2}P_{L_2}^{\frac{R}{2}(1+n_2),\frac{R}{2}(1-n_2)}(1-2y)\,. \tag{C.13}$$

The $P_N^{\alpha,\beta}$ are Jacobi polynomials and the normalization constants $N_{L_1,R,n_1}$ and $N_{L_2,R,n_2}$ can be determined from (C.8).

**Main Integral.** Assembling the ingredients of the previous subsections (induced metric, embedding constraint, Green's function) we find that (C.1) may be expressed as

$$\begin{aligned} T_3\,\delta V_{\Sigma_4}^w &= (2\pi)^3\int_0^1 \mathrm{d}x\mathrm{d}y\,\sqrt{g^{ind}(x,y)}\sum_{L,\psi_s} Y_L^*(x',y')Y_L(x,y)H_L(r;r') \\ &= \frac{V_{T^{1,1}}}{2}\sum_{L,\psi_s} Y_L^*\,(r')^{c_L^+}\times e^{\frac{i}{2}R\psi_s'}\,r_{\min}^{-c_L^+}\times\frac{I_K^n(Q_L^+)}{\sqrt{\Lambda_L+4}}\,, \end{aligned} \tag{C.14}$$

where

$$I_K^n(Q_L^+)\equiv\int_0^1 \mathrm{d}x\mathrm{d}y\,\mathcal{G}(x,y)\left(\frac{r(x,y)}{r_{\min}}\right)^{-6Q_L^+}P_{L_1,R,n_1}(x)P_{L_2,R,n_2}(y)\,. \tag{C.15}$$

Here $K\equiv(L_1,L_2,R)$, $n\equiv(n_1,n_2)$ and

$$Q_L^\pm\equiv\frac{c_L^\pm}{6}+\frac{R}{4}\,,\qquad c_L^\pm\equiv-2\pm\sqrt{\Lambda_L+4}\,. \tag{C.16}$$

The sum in equation (C.14) is restricted by the selection rules (C.3) and (C.5). Equation (C.15) is the main result of this section.

In the following we will show that the integral (C.15) vanishes for all non-chiral terms and reduces to a simple expression for (anti)chiral terms.

### C.2. Non-Chiral Contributions

In this section we prove that

$$\begin{aligned} I_K^n(Q) \;\equiv\; & \int_0^1 \mathrm{d}x\mathrm{d}y\; P_{L_1,R,n_1}(x) P_{L_2,R,n_2}(y) \times \\ & \times x^{Q(1+n_1)}(1-x)^{Q(1-n_1)} y^{Q(1+n_2)}(1-y)^{Q(1-n_2)} \times \\ & \times \left[ \frac{(1+n_1)^2}{2} \frac{1}{x(1-x)} - 2n_1 \frac{1}{1-x} \right. \\ & \left. + \frac{(1+n_2)^2}{2} \frac{1}{y(1-y)} - 2n_2 \frac{1}{1-y} - 1 \right] \end{aligned} \tag{C.17}$$

vanishes for $Q \to Q_L^+$ iff $L_1 \neq 0$ or $L_2 \neq 0$. This proves that non-chiral terms do not contribute to the perturbation $\delta V_{\Sigma_4}^w$ to the warped four-cycle volume.

The Jacobi polynomial $P_N^{\alpha,\beta}(x)$ satisfies the following differential equation

$$\begin{aligned} & -N(N+\alpha+\beta+1) P_N^{\alpha,\beta}(1-2x) = \\ & \quad = x^{-\alpha}(1-x)^{-\beta} \frac{d}{dx} \left( x^{1+\alpha}(1-x)^{1+\beta} \frac{d}{dx} P_N^{\alpha,\beta}(1-2x) \right) . \end{aligned} \tag{C.18}$$

Multiplying both sides by $x^{q_\alpha}(1-x)^{q_\beta}$ and integrating over $x$ gives

$$\begin{aligned} & -N(N+\alpha+\beta+1) \int_0^1 \mathrm{d}x\, P_N^{\alpha,\beta}(1-2x)\, x^{q_\alpha}(1-x)^{q_\beta} = \\ & \quad = \int_0^1 \mathrm{d}x\, P_N^{\alpha,\beta}(1-2x)\, x^{q_\alpha}(1-x)^{q_\beta} \times \\ & \quad \times \left[ (q_\alpha+q_\beta+1)(\alpha+\beta-q_\alpha-q_\beta) + \frac{q_\alpha(\alpha-q_\alpha) - q_\beta(\beta-q_\beta)}{(1-x)} + \frac{q_\alpha(q_\alpha-\alpha)}{x(1-x)} \right] , \end{aligned} \tag{C.19}$$

where we have used integration by parts.

In the case of interest, (C.17), we make the following identifications: $N \equiv L_1,\ \alpha \equiv \frac{R}{2}(1+n_1),\ \beta \equiv \frac{R}{2}(1-n_1),\ q_\alpha \equiv Q(1+n_1),\ q_\beta \equiv Q(1-n_1)$. This gives

$$\int_0^1 \mathrm{d}x\, P_{L_1}^{\frac{R}{2}(1+n_1),\frac{R}{2}(1-n_1)}(1-2x)\, x^{Q(1+n_1)}(1-x)^{Q(1-n_1)} \times \left(\frac{(1+n_1)^2}{2x(1-x)} - \frac{2n_1}{(1-x)}\right) =$$
$$= X_{L_1,R,Q} \int_0^1 \mathrm{d}x\, P_{L_1}^{\frac{R}{2}(1+n_1),\frac{R}{2}(1-n_1)}(1-2x)\ x^{Q(1+n_1)}(1-x)^{Q(1-n_1)}\,, \qquad \text{(C.20)}$$

where

$$X_{L_1,R,Q} \equiv \frac{(2Q + 4Q^2 - L_1^2 - L_1 R - R - 2L_1 - 2RQ)}{Q(2Q-R)}\,. \qquad \text{(C.21)}$$

The corresponding identity for the $y$-integral follows from the above expression and the replacements $L_1 \to L_2$ and $n_1 \to n_2$. We then notice that the integral (C.17) is

$$\begin{aligned} I_K^n(Q) &= (X_{L_1,R,Q} + Y_{L_2,R,Q} - 1) \times \Lambda_{L_1,R,n_1,Q}\, \Lambda_{L_2,R,n_2,Q} \\ &= \frac{6(Q-Q_L^+)(Q-Q_L^-)}{Q(2Q-R)} \times \Lambda_{L_1,R,n_1,Q}\, \Lambda_{L_2,R,n_2,Q}\,, \end{aligned} \qquad \text{(C.22)}$$

where

$$\Lambda_{L_1,R,n_1,Q} \equiv \int_0^1 \mathrm{d}x\, P_{L_1,R,n_1}(x)\ x^{Q(1+n_1)}(1-x)^{Q(1-n_1)}\,, \qquad \text{(C.23)}$$

$$\Lambda_{L_2,R,n_2,Q} \equiv \int_0^1 \mathrm{d}y\, P_{L_2,R,n_2}(y)\ y^{Q(1+n_2)}(1-y)^{Q(1-n_2)}\,. \qquad \text{(C.24)}$$

Since $I_K^n(Q) \propto (Q - Q_L^+)$ it just remains to observe that the integrals (C.23) and (C.24) are finite to conclude that

$$\lim_{Q \to Q_L^+} I_K^n = 0 \quad \text{iff} \quad Q_L^+ \neq \frac{R}{2}\,. \qquad \text{(C.25)}$$

This proves that non-chiral terms do not contribute corrections to the warped volume of any holomorphic four-cycle of the form (5.36).

### C.3. Chiral Contributions

Finally, let us consider the special case $Q_L^+ = \frac{R}{2}$ which corresponds to chiral operators ($L_1 = L_2 = 0$) in the dual gauge theory. In this case,

$$I_R^{\text{chiral}} \equiv \lim_{Q \to \frac{R}{2}} I_K^n = \frac{3R+4}{2}\frac{1}{R} \times \Lambda_{0,R,n_1,\frac{R}{2}} \times \Lambda_{0,R,n_2,\frac{R}{2}}\,, \tag{C.26}$$

where

$$\Lambda_{0,R,n_1,\frac{R}{2}} \equiv \int_0^1 \mathrm{d}x\, P_{0,R,n_1}(x)\; x^{\frac{R}{2}(1+n_1)}(1-x)^{\frac{R}{2}(1-n_1)}\,, \tag{C.27}$$

$$\Lambda_{0,R,n_2,\frac{R}{2}} \equiv \int_0^1 \mathrm{d}y\, P_{0,R,n_2}(y)\; y^{\frac{R}{2}(1+n_2)}(1-y)^{\frac{R}{2}(1-n_2)}\,. \tag{C.28}$$

Notice that $P_{0,R,n_i} = N_{0,R,n_i} = (N_{0,R,n_i})^{-1}(P_{0,R,n_i})^2$. Hence,

$$\Lambda_{0,R,n_1,\frac{R}{2}} \equiv (N_{0,R,n_1})^{-1} \int_0^1 \mathrm{d}x \left(P_{0,R,n_1}(x)\left[x^{(1+n_1)}(1-x)^{(1-n_1)}\right]^{R/4}\right)^2 \tag{C.29}$$

$$\Lambda_{0,R,n_2,\frac{R}{2}} \equiv (N_{0,R,n_2})^{-1} \int_0^1 \mathrm{d}y \left(P_{0,R,n_2}(y)\left[y^{(1+n_2)}(1-y)^{(1-n_2)}\right]^{R/4}\right)^2 \tag{C.30}$$

and

$$\Lambda_{0,R,n_1,\frac{R}{2}} \times \Lambda_{0,R,n_2,\frac{R}{2}} = \frac{1}{V_{T^{1,1}} N_{0,R,n_1} N_{0,R,n_2}} \tag{C.31}$$

by the normalization condition (C.8) on the angular wave function. Therefore, we get the simple result

$$\frac{I_R^{\text{chiral}}}{\sqrt{\Lambda_R^{\text{chiral}}+4}} = \frac{1}{V_{T^{1,1}} N_{0,R,n_1} N_{0,R,n_2}} \times \frac{1}{R}\,. \tag{C.32}$$

We substitute this into equation (C.14) and get

$$T_3\,(\delta V^w_{\Sigma_4})_{\text{chiral}} = \frac{1}{2}\sum_s \sum_{R=q\cdot k} \frac{1}{R} \times \Big(\prod_i (\bar{w}_i')^{p_i}\Big)^{R/P} \times \frac{1}{\bar{\mu}^R} \times e^{i\frac{R}{P}2\pi s}\,, \tag{C.33}$$

where we used

$$(r')^{3R/2}\frac{Y_R^*(\Psi')}{N_{0,R,n_1}N_{0,R,n_2}} = \Big(\prod_i (\bar{w}_i')^{p_i}\Big)^{R/P} \tag{C.34}$$

and

$$e^{i\arg(\mu)R}\, r_{\rm min}^{-3R/2} = \frac{1}{\bar\mu^R}\,. \tag{C.35}$$

The sum over $s$ in (C.33) counts the $P$ different roots of equation (5.36):

$$\sum_{s=0}^{P-1} e^{\frac{q\cdot k}{P}2\pi s} = P\,\delta_{\frac{q\cdot k}{P},j}\,, \quad j\in\mathbb{Z}\,. \tag{C.36}$$

Dropping primes, we therefore arrive at the following sum

$$T_3\,(\delta V^w_{\Sigma_4})_{\rm chiral} = \frac{1}{2}\sum_{j=1}^{\infty}\frac{1}{j}\times\Big(\prod_i \bar w_i^{p_i}\Big)^j\times\frac{1}{\bar\mu^{P\cdot j}}\,, \tag{C.37}$$

which gives

$$T_3\,(\delta V^w_{\Sigma_4})_{\rm chiral} = -\frac{1}{2}\,\ln\left[1-\frac{\prod_i \bar w_i^{p_i}}{\bar\mu^P}\right]\,. \tag{C.38}$$

For the anti-chiral terms ($R<0$) an equivalent computation gives the complex conjugate of this result.

The $R=0$ term formally gives a divergent contribution that needs to be regularized by introducing a UV cutoff at the end of the throat. Alternatively, as discussed in §5.2, this term does not appear if we define $\delta h$ as the solution of (5.18) with $\sqrt{g}\,\rho_{bg}(Y)=\delta^{(6)}(Y-X_0)$. This choice amounts to evaluating the change in the warp factor, $\delta h$, created by moving the D3-brane from some reference point $X_0$ to $X$. We may choose the reference point $X_0$ to be at the tip of the cone, $r=0$, and thereby remove the divergent zero mode.

The total change in the warped volume of the four-cycle is therefore

$$\delta V^w_{\Sigma_4} = (\delta V^w_{\Sigma_4})_{\rm chiral} + (\delta V^w_{\Sigma_4})_{\rm anti-chiral} \tag{C.39}$$

and

$$T_3\,{\rm Re}(\zeta) = T_3\,\delta V^w_{\Sigma_4} = -{\rm Re}\left(\ln\left[\frac{\mu^P-\prod_i w_i^{p_i}}{\mu^P}\right]\right)\,. \tag{C.40}$$

Finally, the prefactor of the nonperturbative superpotential is

$$A(w_i) = A_0\, e^{-T_3\zeta/n} = A_0 \left(\frac{\mu^P - \prod_i w_i^{p_i}}{\mu^P}\right)^{1/n}. \tag{C.41}$$

APPENDIX D

# Computation of Backreaction in $Y^{p,q}$ Cones

This appendix computes the gravitational backreaction of a D3-brane on the volume of four-cycles in $Y^{p,q}$ cones.

## D.1. Setup

**Metric and Coordinates on $Y^{p,q}$.** Cones over $Y^{p,q}$ manifolds have the following metric

$$\mathrm{d}s^2 = \mathrm{d}r^2 + r^2 \mathrm{d}s^2_{Y^{p,q}}\,, \tag{D.1}$$

where the Sasaki-Einstein metric on the $Y^{p,q}$ base is given by [73, 74]

$$\begin{aligned} \mathrm{d}s^2_{Y^{p,q}} &= \frac{1-y}{6}\left(\mathrm{d}\theta^2 + \sin^2\theta\,\mathrm{d}\phi^2\right) + \frac{1}{v(y)w(y)}\mathrm{d}y^2 + \frac{v(y)}{9}(\mathrm{d}\psi + \cos\theta\,\mathrm{d}\phi)^2 \\ &\quad + w(y)\big[\mathrm{d}\alpha + f(y)\left(\mathrm{d}\psi + \cos\theta\,\mathrm{d}\phi\right)\big]^2\,. \end{aligned} \tag{D.2}$$

The following functions have been defined

$$v(y) \equiv \frac{b - 3y^2 + 2y^3}{b - y^2}\,, \quad w(y) \equiv \frac{2(b-y^2)}{1-y}\,, \quad f(y) \equiv \frac{b - 2y + y^2}{6(b-y^2)}\,, \tag{D.3}$$

with

$$b \equiv \frac{1}{2} - \frac{p^2 - 3q^2}{4p^3}\,\sqrt{4p^2 - 3q^2}\,. \tag{D.4}$$

The parameters $p$ and $q$ are two coprime positive integers. The zeros of $v(y)$ are

$$y_{1,2} = \frac{1}{4p}\left(2p \mp 3q - \sqrt{4p^2 - 3q^2}\right), \qquad y_3 = \frac{3}{2} - (y_1 + y_2)\,. \tag{D.5}$$

It is convenient to introduce

$$x \equiv \frac{y - y_1}{y_2 - y_1} \,. \tag{D.6}$$

The angular coordinates $\theta$, $\phi$, $\psi$, $x$, and $\alpha$ span the ranges

$$\begin{aligned} &0 \le \theta \le \pi \,, \quad 0 < \phi \le 2\pi \,, \quad 0 < \psi \le 2\pi \,, \\ &0 \le x \le 1 \,, \quad 0 < \alpha \le 2\pi\ell \,, \end{aligned} \tag{D.7}$$

where $\ell \equiv -\frac{q}{4p^2 y_1 y_2}$.

**Green's Function.** The Green's function on the $Y^{p,q}$ cone is

$$G(X;X') = \sum_L \frac{1}{4(\lambda+1)} \times Y_L^*(\Psi') Y_L(\Psi) \times \begin{cases} \frac{1}{r'^4}\left(\frac{r}{r'}\right)^{2\lambda} & r \le r' \,, \\ \frac{1}{r^4}\left(\frac{r'}{r}\right)^{2\lambda} & r \ge r' \,. \end{cases} \tag{D.8}$$

Here $L$ is again a complete set of quantum numbers and $\Psi$ represents the set of angular coordinates $(\theta, \phi, \psi, x, \alpha)$. The eigenvalue of the angular Laplacian is $\Lambda_L \equiv 4\lambda(\lambda+2)$. The spectrum of the scalar Laplacian on $Y^{p,q}$, as well as the eigenfunctions $Y_L(\Psi)$, were calculated in [31, 101]. We do not review this treatment here, but simply present an explicit form of $Y_L(\Psi)$

$$Y_L(\Psi) = N_L \, e^{i(m\phi + n_\psi \psi + \frac{n_\alpha}{\ell}\alpha)} J_{l,m,2n_\psi}(\theta) R_{n_\alpha, n_\psi, l, \lambda}(x) \,, \tag{D.9}$$

where

$$R_{n_\alpha, n_\psi, l, \lambda}(x) = x^{\alpha_1}(1-x)^{\alpha_2}(a-x)^{\alpha_3} h(x) \,, \qquad a \equiv \frac{y_1 - y_3}{y_1 - y_2} \,. \tag{D.10}$$

The parameters $\alpha_i$ depend on $n_\psi$ and $n_\alpha$ (see [101]), and the function $h(x)$ satisfies the following differential equation

$$\left[\frac{d^2}{dx^2} + \left(\frac{\gamma}{x} + \frac{\delta}{x-1} + \frac{\epsilon}{x-a}\right)\frac{d}{dx} + \frac{\alpha\beta x - k}{x(1-x)(a-x)}\right] h(x) = 0 \,. \tag{D.11}$$

The parameters $\alpha$, $\beta$, $\gamma$, $\delta$, $\epsilon$, $k$ depend on $p, q$ and on the quantum numbers of the $Y^{p,q}$ base. Explicit expressions may be found in [101].

Finally, we introduce the normalization condition that fixes $N_L$ in (D.9). If we define $z \equiv \sin^2 \frac{\theta}{2}$ then the normalization condition

$$\int \mathrm{d}^5\Psi \sqrt{g_{Y^{p,q}}} |Y_L(\Psi)|^2 = 1 \tag{D.12}$$

becomes

$$N_L^2 \int_0^1 \mathrm{d}z\, \mathrm{d}x\, \sqrt{g(x,z)}\, J^2 R^2 = \frac{1}{(2\pi)^3 \ell}\,, \tag{D.13}$$

where

$$\sqrt{g(x,z)} = \sqrt{g(x)} = \frac{q(2p+3q+\sqrt{4p^2-3q^2}-6qx)}{24p^2}\ . \tag{D.14}$$

**Embedding, Induced Metric and a Selection Rule.** The holomorphic embedding of four-cycles in $Y^{p,q}$ cones is described by the algebraic equation [50]

$$\prod_{i=1}^{3} w_i^{p_i} = \mu^{2p_3}\,, \tag{D.15}$$

where

$$w_1 \equiv \tan\frac{\theta}{2}\, e^{-i\phi}\,, \tag{D.16}$$

$$w_2 \equiv \frac{1}{2}\sin\theta\, x^{\frac{1}{2y_1}} (1-x)^{\frac{1}{2y_2}} (a-x)^{\frac{1}{2y_3}} e^{i(\psi+6\alpha)}\,, \tag{D.17}$$

$$w_3 \equiv \frac{1}{2} r^3 \sin\theta\, [x(1-x)(a-x)]^{1/2} e^{i\psi}\,. \tag{D.18}$$

This results in the following embedding equations in terms of the real coordinates

$$\psi = \frac{1}{1+n_2}(n_1\phi - 6n_2\alpha) - \psi_s\,, \tag{D.19}$$

$$\begin{aligned} r &= r_{\min}\left[z^{1+n_1+n_2}(1-z)^{1-n_1+n_2}\right]^{-1/6}\left[x^{2e_1}(1-x)^{2e_2}(a-x)^{2e_3}\right]^{-1/6} \\ &\equiv r_{\min} r_z r_x\,, \end{aligned} \tag{D.20}$$

where

$$\psi_s \equiv \arg(\mu) + \frac{2\pi s}{p_2+p_3}\,, \qquad s \in \{0,1,\ldots,(p_2+p_3)-1\} \tag{D.21}$$

$$r_{\min}^{3/2} \equiv |\mu|\,, \tag{D.22}$$

and

$$e_i \equiv \frac{1}{2}\Big(1+\frac{n_2}{y_i}\Big)\,, \tag{D.23}$$

$$n_1 \equiv \frac{p_1}{p_3}\,, \tag{D.24}$$

$$n_2 \equiv \frac{p_2}{p_3}\,. \tag{D.25}$$

Integration over $\phi$ and $\alpha$ together with the embedding equation (D.19) dictates the following selection rules for the quantum numbers of the angular eigenfunctions (D.9),

$$m = -\frac{n_1}{2}Q_R\,, \quad n_\alpha = 3\ell n_2 Q_R\,, \quad n_\psi = \frac{1+n_2}{2}Q_R\,, \tag{D.26}$$

where $Q_R$ is the $R$-charge defined as $Q_R \equiv 2n_\psi - \frac{1}{3\ell}n_\alpha$. In this case $\alpha_i = e_i\frac{Q_R}{2}$.

Finally, we need the determinant of the induced metric on the four-cycle

$$\mathrm{d}\theta\mathrm{d}x\,\sqrt{g^{ind}} = \frac{r^4}{z(1-z)x(1-x)(a-x)}\,\mathcal{G}(x,z)\,\mathrm{d}z\mathrm{d}x\,. \tag{D.27}$$

$\mathcal{G}(x,z)$ is a polynomial of order 3 in $x$ and of order 2 in $z$.

**Main Integral.** The main integral (the analog of (C.15)) is therefore given by

$$I_L = \int \frac{\mathrm{d}x\mathrm{d}z\,\mathcal{G}(x,z)\,N_L^2}{z(1-z)x(1-x)(a-x)}\left(\frac{r}{r_{\min}}\right)^{-6Q_L^+} P^{a,b}_{A=l-n_\psi}(1-2z)\,h_L(x)\,, \tag{D.28}$$

with $a \equiv (1+n_1+n_2)\frac{Q_R}{2}$, $b \equiv (1-n_1+n_2)\frac{Q_R}{2}$ and $6Q_L^+ \equiv 2\lambda+\frac{3}{2}Q_R$. We will calculate this integral for a general $6Q_L^+ = 2w+\frac{3}{2}Q_R$ and then take the limit $w \to \lambda$.

First we compute the integral over $z$ in complete analogy to the treatment of Appendix C. The Jacobi polynomial satisfies

$$r_z^{3Q_R}\frac{d}{dz}\Big(r_z^{-3Q_R}z(1-z)\frac{d}{dz}P_A^{a,b}(1-2z)\Big)+A(A+1+a+b)P_A^{a,b}(1-2z)=0\,. \quad \text{(D.29)}$$

Let us multiply this equation by $r_z^{-(2w+\frac{3}{2}Q_R)}$ and integrate over $z$. It can be shown that there is a third order polynomial $\mathbb{G}(x)$ which is implicitly defined by the following relation

$$\frac{\mathcal{G}(x,z)}{z(1-z)}-\mathbb{G}(x)=\frac{\mathcal{G}(x,z=0)}{(1+n_1+n_2)^2\left(\frac{w^2}{9^2}-\frac{Q_R^2}{16}\right)}\times$$
$$\times\left[r_z^{2w+\frac{3}{2}Q_r}\frac{d}{dz}\left(z(1-z)r_z^{-3Q_R}\frac{d}{dz}\left(r_z^{\frac{3}{2}Q_R-2w}\right)\right)+A(A+1+a+b)\right]\,. \quad \text{(D.30)}$$

The right-hand side vanishes after multiplying by $r_z^{-6Q_L^+}P_A^{a,b}(1-2z)$ and integrating, and we get

$$I_L=\int\frac{\mathrm{d}x\,\mathbb{G}(x)\,N_L^2}{x(1-x)(a-x)}\,r_x^{-6Q_L^+}h_L(x)\int\mathrm{d}z\,r_z^{-6Q_L^+}P_A^{a,b}(1-2z)\,. \quad \text{(D.31)}$$

## D.2. Non-Chiral Contributions

To evaluate (D.31) we make use of the differential equation (D.11). We multiply (D.11) by $r_x^{-2w-\frac{3}{2}Q_R}$ and integrate over $x$. There exists a first order polynomial $M\sqrt{g(x)}$ such that

$$\frac{\mathbb{G}(x)}{x(1-x)(a-x)}-M\sqrt{g(x)}=$$
$$=\frac{144\,\mathbb{G}(x=0)}{(1-n_2)(3Q_R+4\lambda)(18Q_Rn_2+8\lambda n_2-9Q_R-4\lambda-24)}\times\Big[(\alpha\beta x-k)-$$
$$-r_x^{2w+\frac{3}{2}Q_R}\frac{d}{dx}\Big(r_x^{-2w-\frac{3}{2}Q_R}(\gamma(1-x)(a-x)+\delta x(x-a)+\epsilon x(x-1))\Big)$$
$$+r_x^{2w+\frac{3}{2}Q_R}\frac{d^2}{dx^2}\Big(x(1-x)(a-x)r_x^{-2w-\frac{3}{2}Q_R}\Big)\Big]\,, \quad \text{(D.32)}$$

where we defined

$$M \equiv \frac{48(\lambda - w)(\lambda + w + 2)}{(1 + n_2)(16w^2 - 9Q_R^2)} \,. \tag{D.33}$$

After multiplying by $r_x^{-6Q_L^+} h(x)$ and integrating over $x$, the right-hand side vanishes and we have

$$\begin{aligned} I_L &= MN_L^2 \int \mathrm{d}x\mathrm{d}z \, \sqrt{g(x,z)} \left(\frac{r}{r_{\min}}\right)^{-6Q_L^+} P_A^{a,b}(1-2z)\, h(x) && \text{(D.34)} \\ &= MN_L \int \mathrm{d}z\mathrm{d}x \, \sqrt{g} \, \left(\frac{r}{r_{\min}}\right)^{-2\lambda} J(z) R(x) \,. && \text{(D.35)} \end{aligned}$$

Since $\lim_{w\to\lambda} M = 0$, this immediately implies that $\lim_{w\to\lambda} I_L = 0$ 'on-shell', *i.e.* for all operators except for the chiral ones. Just as for the singular conifold case, we have therefore proven that non-chiral terms do not contribute to the perturbation to the warped four-cycle volume.

### D.3. Chiral Contributions

For the chiral operators one finds

$$\lambda = \frac{3}{4} Q_R \,, \tag{D.36}$$

and both the numerator and the denominator of $M$ (D.33) vanish. Chiral operators also require $A = l - n_\psi$ to be equal to zero. Taking the chiral limit we therefore find

$$\begin{aligned} I_L &= \frac{(3Q_R + 4)}{(1 + n_2)Q_R} N_L^2 \int \frac{\mathrm{d}x \, q(2p + 3q + \sqrt{4p^2 - 3q^2} - 6qx)}{24p^2} \left(\frac{r}{r_{\min}}\right)^{-3Q_R} && \text{(D.37)} \\ &= \frac{(3Q_R + 4)}{(1 + n_2)Q_R} \frac{1}{(2\pi)^3 \ell} \,, && \text{(D.38)} \end{aligned}$$

since $A = 0$ implies $P_A^{a,b}(1 - 2z) = 1$ and $h(x) = 1$. The integral in (D.37) reduces to the normalization condition (D.13). Finally, we use the identity for chiral wavefunctions $r^{\frac{3}{2}Q_R} Y_L(\Psi) = (w_1^{n_1} w_2^{n_2} w_3)^{\frac{Q_R}{2}}$ and the relation between $T_3 \, (\delta V_{\Sigma_4}^w)_{\text{chiral}}$ and $I_L$ (an analog of (C.14)). Note that the $(2\pi)^3$ in (C.14) should be changed to $(2\pi)^3 \ell$ as

$\alpha$ runs from 0 to $2\pi\ell$. We hence arrive at the analog of (C.33)

$$T_3\,(\delta V^w_{\Sigma_4})_{\rm chiral} = \frac{1}{2}\sum_{Q_R,s}\frac{2}{(1+n_2)Q_R}\,(\bar w_1^{n_1}\bar w_2^{n_2}\bar w_3)^{\frac{Q_R}{2}}\;e^{i\frac{(1+n_2)}{2}Q_R\psi_s}\,, \tag{D.39}$$

where we recall that $\psi_s = \frac{2\pi s}{p_2+p_3}$. The summation over $s$ effectively picks out $n_\psi = \frac{(1+n_2)}{2}Q_R$ to be of the form $(p_2+p_3)s'$ with natural $s'$, or $Q_R = 2p_3 s'$. After summation over $s'$ we have

$$T_3\,(\delta V^w_{\Sigma_4})_{\rm chiral} = -\frac{1}{2}\ln\left[\frac{\bar\mu^{2p_3}-\prod_i \bar w_i^{p_i}}{\bar\mu^{2p_3}}\right]\,. \tag{D.40}$$

A similar calculation for the anti-chiral contributions gives the complex conjugate of (D.40).

The final result for the perturbation of the warped volume of four-cycles in cones over $Y^{p,q}$ manifolds is then

$$T_3\,\delta V^w_{\Sigma_4} = -{\rm Re}\left(\ln\left[\frac{\mu^{2p_3}-\prod_i w_i^{p_i}}{\mu^{2p_3}}\right]\right)\,, \tag{D.41}$$

so that

$$A(w_i) = A_0\left(\frac{\mu^{2p_3}-\prod_i w_i^{p_i}}{\mu^{2p_3}}\right)^{1/n}. \tag{D.42}$$

APPENDIX E

# The F-term Potential

In this appendix we derive the F-term potential for D3-branes and wrapped D7-branes in the conifold.

## E.1. The Singular Conifold

The conifold constraint, $\sum_{i=1}^{4} z_i^2 = 0$, for complex coordinates $\{z_i; i = 1, 2, 3, 4\}$ may be written as $\det(W) = 0$ where

$$W = \frac{1}{\sqrt{2}} \begin{pmatrix} z_3 + iz_4 & z_1 - iz_2 \\ z_1 + iz_2 & -z_3 + iz_4 \end{pmatrix} \equiv \begin{pmatrix} w_3 & w_2 \\ w_1 & w_4 \end{pmatrix} . \tag{E.1}$$

The Kähler potential (7.3) is chosen such that the Kähler metric on the conifold, $k_{\alpha\overline{\beta}} \equiv \partial_\alpha \partial_{\overline{\beta}} k$, is Calabi-Yau (Ricci-flat)

$$\begin{aligned} \mathrm{d}s^2 &= \partial_\alpha \partial_{\overline{\beta}} k \, \mathrm{d}u^\alpha \mathrm{d}\overline{u^\beta} \\ &= k'' \, |\mathrm{Tr}(W^\dagger \mathrm{d}W)|^2 + k' \, \mathrm{Tr}(\mathrm{d}W \mathrm{d}W^\dagger) \, , \end{aligned} \tag{E.2}$$

where $(\dots)' \equiv \frac{d(\dots)}{dr^3}$ and $\{u_\alpha; \alpha = 1, 2, 3\}$ are three complex coordinates on the conifold, *e.g.* $u_\alpha = z_\alpha$. The metric on the conifold (E.2) may be cast in the form (7.2) where

$$\mathrm{d}s^2_{T^{1,1}} = \frac{1}{9}\Big(\mathrm{d}\psi + \sum_{i=1}^{2} \cos\theta_i \mathrm{d}\phi_i\Big)^2 + \frac{1}{6}\sum_{i=1}^{2} (\mathrm{d}\theta_i^2 + \sin^2\theta_i \mathrm{d}\phi_i^2) \, , \tag{E.3}$$

is the metric on the Einstein space $T^{1,1}$.

The complex coordinates $z_i$ are related to the real coordinates $\{r \in [0,\infty], \theta_i \in [0,\pi], \phi_i \in [0,2\pi], \psi \in [0,4\pi]\}$ via

$$z_1 = \frac{r^{3/2}}{\sqrt{2}} e^{\frac{i}{2}\psi}\left[\cos\left(\frac{\theta_1+\theta_2}{2}\right)\cos\left(\frac{\phi_1+\phi_2}{2}\right) + i\cos\left(\frac{\theta_1-\theta_2}{2}\right)\sin\left(\frac{\phi_1+\phi_2}{2}\right)\right], \quad \text{(E.4)}$$

$$z_2 = \frac{r^{3/2}}{\sqrt{2}} e^{\frac{i}{2}\psi}\left[-\cos\left(\frac{\theta_1+\theta_2}{2}\right)\sin\left(\frac{\phi_1+\phi_2}{2}\right) + i\cos\left(\frac{\theta_1-\theta_2}{2}\right)\cos\left(\frac{\phi_1+\phi_2}{2}\right)\right], \quad \text{(E.5)}$$

$$z_3 = \frac{r^{3/2}}{\sqrt{2}} e^{\frac{i}{2}\psi}\left[-\sin\left(\frac{\theta_1+\theta_2}{2}\right)\cos\left(\frac{\phi_1-\phi_2}{2}\right) + i\sin\left(\frac{\theta_1-\theta_2}{2}\right)\sin\left(\frac{\phi_1-\phi_2}{2}\right)\right], \quad \text{(E.6)}$$

$$z_4 = \frac{r^{3/2}}{\sqrt{2}} e^{\frac{i}{2}\psi}\left[-\sin\left(\frac{\theta_1+\theta_2}{2}\right)\sin\left(\frac{\phi_1-\phi_2}{2}\right) - i\sin\left(\frac{\theta_1-\theta_2}{2}\right)\cos\left(\frac{\phi_1-\phi_2}{2}\right)\right]. \quad \text{(E.7)}$$

The complex coordinates $w_i$ are related to the real coordinates $\{r, \theta_i, \phi_i, \psi\}$ via

$$w_1 = r^{3/2} e^{\frac{i}{2}(\psi-\phi_1-\phi_2)} \sin\frac{\theta_1}{2}\sin\frac{\theta_2}{2}, \quad \text{(E.8)}$$

$$w_2 = r^{3/2} e^{\frac{i}{2}(\psi+\phi_1+\phi_2)} \cos\frac{\theta_1}{2}\cos\frac{\theta_2}{2}, \quad \text{(E.9)}$$

$$w_3 = r^{3/2} e^{\frac{i}{2}(\psi+\phi_1-\phi_2)} \cos\frac{\theta_1}{2}\sin\frac{\theta_2}{2}, \quad \text{(E.10)}$$

$$w_4 = r^{3/2} e^{\frac{i}{2}(\psi-\phi_1+\phi_2)} \sin\frac{\theta_1}{2}\cos\frac{\theta_2}{2}. \quad \text{(E.11)}$$

### E.2. Making $SO(4)$ Symmetry Manifest

It is sometimes convenient to write the F-term potential (7.13) in terms of the four homogeneous coordinates $z_i$ of the embedding space $\mathbb{C}^4$ which makes the $SO(4)$ symmetry of the conifold transparent. For that reason we define a new metric $\widehat{\mathcal{K}}^{A\overline{B}}$ which depends on $z_i$ in such a way that for any function $W(z_i)$ the following identity is satisfied

$$D_A W \widehat{\mathcal{K}}^{A\overline{B}} \overline{D_B W} \equiv D_\Sigma W \mathcal{K}^{\Sigma\overline{\Omega}} \overline{D_\Omega W}, \quad \text{(E.12)}$$

where $\{Z^A\} \equiv \{\rho, z_i; i = 1,2,3,4\}$ and $\{Z^\Sigma\} \equiv \{\rho, z_\alpha; \alpha = 1,2,3\}$. In this equation the conifold constraint, $z_4^2 = z_4^2(z_\alpha) = -\sum_{\alpha=1}^3 z_\alpha^2$, is substituted *after* differentiation on the left-hand side and *before* differentiation on the right-hand side. The metric $\widehat{\mathcal{K}}^{A\overline{B}}(z_i)$ defined through (E.12) is not unique and the choice of one over another is a

matter of convenience. We construct $\widehat{\mathcal{K}}^{A\overline{B}}$ with the help of the auxiliary matrix $J^A{}_\Sigma$

$$\widehat{\mathcal{K}}^{A\overline{B}} = J^A{}_\Sigma \, \mathcal{K}^{\Sigma\overline{\Omega}} \, J^{\overline{B}}{}_{\overline{\Omega}} \,, \tag{E.13}$$

where $J^A{}_\Sigma$ is defined as follows

$$D_\Sigma W = \frac{\partial Z^A}{\partial Z^\Sigma} D_A W \equiv J^A{}_\Sigma \, D_A W \,, \qquad J^A{}_\Sigma = \left(\begin{array}{c|c} 1 & 0 \\ \hline 0 & \delta_{i\alpha} \\ \hline 0 & \frac{-z_\alpha}{\sqrt{-\sum_{\gamma=1}^3 z_\gamma^2}} \end{array}\right). \tag{E.14}$$

This gives $\widehat{\mathcal{K}}^{A\overline{B}}$ as a function of $z_\alpha$. To find it as a function of $z_i$ guess a $\widehat{\mathcal{K}}^{A\overline{B}}(z_i)$ such that it reduces to $\widehat{\mathcal{K}}^{A\overline{B}}(z_\alpha)$ after substituting the conifold constraint. This step and hence $\widehat{\mathcal{K}}^{A\overline{B}}(z_i)$ is not unique. Nevertheless finding an $SO(4)$–invariant $\widehat{\mathcal{K}}^{A\overline{B}}(z_i)$ is not difficult, *e.g.* replacing $\left(-\sum_{\gamma=1}^3 z_\gamma^2\right)^{1/2}$ by $z_4$ everywhere in $\widehat{\mathcal{K}}^{A\overline{B}}(z_\alpha)$ and $J^A{}_\Sigma$ we find

$$\widehat{\mathcal{K}}^{A\overline{B}} = \frac{\kappa^2 U}{3} \left(\begin{array}{c|c} U + \gamma k_l \hat{k}^{l\overline{m}} k_{\overline{m}} & k_l \hat{k}^{l\overline{\jmath}} \\ \hline \hat{k}^{i\overline{m}} k_{\overline{m}} & \frac{1}{\gamma} \hat{k}^{i\overline{\jmath}} \end{array}\right), \tag{E.15}$$

where

$$k_i = \frac{\overline{z_i}}{r} \,, \tag{E.16}$$

and

$$\hat{k}^{i\overline{\jmath}} = J^i{}_\alpha \, k^{\alpha\overline{\beta}} \, J^{\overline{\jmath}}{}_{\overline{\beta}} = r \left[\delta^{i\overline{\jmath}} + \frac{1}{2} \frac{z_i \overline{z_j}}{r^3} - \frac{\overline{z_i} z_j}{r^3}\right]. \tag{E.17}$$

Notice that $\hat{k}^{i\overline{\jmath}}$ is *not* the inverse of $k_{i\overline{\jmath}} = \frac{1}{r}\left[\delta_{i\overline{\jmath}} - \frac{1}{3}\frac{\overline{z_i} z_j}{r^3}\right]$, which is $k^{i\overline{\jmath}} = r\left[\delta^{i\overline{\jmath}} + \frac{1}{2}\frac{z_i \overline{z_j}}{r^3}\right]$. From (E.16) and (E.17) one then finds

$$k_l \hat{k}^{l\overline{\jmath}} = \frac{3}{2} \overline{z^j} \,, \qquad k_l \hat{k}^{l\overline{m}} k_{\overline{m}} = \frac{3}{2} r^2 = \hat{r}^2 = k \,, \tag{E.18}$$

and hence,

$$\widehat{\mathcal{K}}^{A\overline{B}} = \frac{\kappa^2 U}{3} \left(\begin{array}{c|c} \rho + \overline{\rho} & \frac{3}{2}\overline{z_j} \\ \hline \frac{3}{2} z_i & \frac{r}{\gamma}\left[\delta^{i\overline{\jmath}} + \frac{1}{2}\frac{z_i \overline{z_j}}{r^3} - \frac{\overline{z_i} z_j}{r^3}\right] \end{array}\right). \tag{E.19}$$

Using the above results we arrive at the F-term potential

$$V_F = \frac{\kappa^2}{3U^2}\left[(\rho+\overline{\rho})|W_{,\rho}|^2 - 3(\overline{W}W_{,\rho}+c.c.) + \frac{3}{2}(\overline{W_{,\rho}}z^i W_{,i}+c.c.) + \frac{1}{\gamma}\hat{k}^{i\overline{j}}W_{,i}\overline{W_{,j}}\right]. \tag{E.20}$$

The result (E.20) is essential for the main analysis presented in Chapter 7. In terms of the $w_i$-coordinates the F-term potential (E.20) is

$$V_F = \frac{\kappa^2}{3U^2}\left[(\rho+\overline{\rho})|W_{,\rho}|^2 - 3(\overline{W}W_{,\rho}+c.c.) + \frac{3}{2}(\overline{W_{,\rho}}w^i W_{,i}+c.c.) + \frac{1}{\gamma}\hat{k}^{i\overline{j}}W_{,i}\overline{W_{,j}}\right], \tag{E.21}$$

where

$$\hat{k}^{i\overline{j}} = r\left[\delta^{i\overline{j}} + \frac{1}{2}\frac{w_i\overline{w_j}}{r^3} - \frac{c_i^{i'}c_j^{j'}\overline{w_{i'}}w_{j'}}{r^3}\right]. \tag{E.22}$$

The matrix $c_j^{i'}$ has only four non-zero elements $c_2^1 = c_1^2 = 1$ and $c_4^3 = c_3^4 = -1$.

APPENDIX F

# Dimensional Reduction

As explained in detail in Chapters 5 and 7, D7-branes wrapping certain four-cycles in the compactification source nonperturbative effects that stabilize the volume modulus. In §F.1 we identify the real part of the Kähler modulus with the warped volume of the four-cycle and give a detailed derivation of the DeWolfe-Giddings Kähler potential. These results are well known, but our goal here is to fix notation with enough care to permit precise discussions in Chapter 7. §F.2 computes the throat contribution to the warped four-cycle volume for our setup and relates it to microscopic compactification data. We also explain how this relates microscopic input to the energy scale of inflation. Finally, in §F.3, we present an improved derivation of the field range bound of [21] that includes a non-trivial breathing mode of the compactification.

## F.1. Kähler Modulus and Kähler Potential

We consider the line element

$$\mathrm{d}s^2 = h^{-1/2}(y)e^{-6u}g_{\mu\nu}\mathrm{d}x^\mu\mathrm{d}x^\nu + h^{1/2}(y)e^{2u}g_{\alpha\bar{\beta}}\mathrm{d}y^\alpha\mathrm{d}\overline{y^\beta}\,, \tag{F.1}$$

where $g_{\mu\nu}$ is the four-dimensional Einstein frame metric, $h$ is the warp factor, $g_{\alpha\bar{\beta}}$ is a fiducial metric on the internal space, and the factor $e^u$ extracts the breathing mode.

Before proceeding, let us explain the division of the metric $\tilde{g}_{\alpha\bar{\beta}} \equiv e^{2u}g_{\alpha\bar{\beta}}$ into a fiducial metric $g$ and a breathing mode $e^{2u}$. These two objects do play different roles:

note in particular that although $g$ affects the four-dimensional Planck mass

$$M_{\rm pl}^2 = \frac{1}{\pi}(T_3)^2 \int {\rm d}^6 y \sqrt{g}\, h \equiv \frac{1}{\pi}(T_3)^2 V_6^w \,, \tag{F.2}$$

the breathing mode does not, because of the factor $e^{-6u}$ in the spacetime term of (F.1).

For any fixed location $Y \equiv Y_\alpha$ of the D3-brane, there is a minimum $\rho_\star(Y)$ of the nonperturbatively-generated potential for the Kähler modulus $\rho$. (We will soon come to a precise definition of $\rho$ in terms of the fields in (F.1).) We argued in §3 for an adiabatic approximation in which, as the D3-brane moves and hence the location $\rho_\star(Y)$ of the instantaneous minimum changes, $\rho$ moves to remain in this instantaneous minimum $\rho_\star(Y)$. In terms of the fields in (F.1), this is most conveniently represented[1] by fixing the fiducial metric once and for all, but allowing the breathing mode $e^{u(Y,\bar{Y})}$ to keep track of the change in the volume that is due to the displacement of the D3-brane.

To this end, we normalize the fiducial metric $g$ to correspond to $\rho_\star(0)$, *i.e.* so that the volume computed with $g$ is precisely the physical volume of the internal space when the D3-brane sits at the tip of the throat, $Y \approx 0$. Then, $e^{u(Y,\bar{Y})}$ represents the change in the volume that is due to the displacement of the D3-brane away from the tip, and by this definition, $u(0) = 0$. In the throat region, the fiducial metric takes the form

$$g_{\alpha\bar{\beta}} {\rm d}y^\alpha {\rm d}\overline{y^\beta} = {\rm d}\hat{r}^2 + \hat{r}^2 {\rm d}s^2_{T^{1,1}} \,. \tag{F.3}$$

The non-perturbative superpotential arising from strong gauge dynamics on $n$ D7-branes (or Euclidean D3-instantons) wrapping a four-cycle $\Sigma_4$ in the background (F.1) is [18]

$$|W_{\rm np}|^2 \propto \exp\left[-\frac{2T_3 V^w_{\Sigma_4} e^{4u}}{n}\right] , \tag{F.4}$$

[1]At the end of this section we will verify that choosing a different normalization of the fiducial metric does not affect any physical quantities.

where $V^w_{\Sigma_4} \equiv \int \mathrm{d}^4\xi \sqrt{g^{ind}}\, h$. Before the mobile D3-brane enters the throat region, the (warped) four-cycle volume is $(V^w_{\Sigma_4})_0$. When the D3-brane is in the throat, it induces a perturbation in the warp factor, $\delta h$, which sources a change in the warped four-cycle volume, $\delta V^w_{\Sigma_4}(Y)$. (This change in the warped volume is logically distinct from the shift in the stabilized value of the Kähler modulus studied in Appendix H.) Hence,

$$|W_{\rm np}|^2 \;\propto\; \exp\left[-\frac{2T_3\delta V^w_{\Sigma_4}(Y)e^{4u(Y,\bar{Y})}}{n}\right]\exp\left[-\frac{2T_3(V^w_{\Sigma_4})_0 e^{4u(Y,\bar{Y})}}{n}\right] \tag{F.5}$$

$$\equiv\; |A(Y)|^2 e^{-a(\rho+\bar{\rho})}\,. \tag{F.6}$$

We now define $a \equiv \frac{2\pi}{n}$ and identify the Kähler modulus [18]

$$\rho + \bar{\rho} \equiv \Gamma e^{4u(Y,\bar{Y})} + \gamma k(Y,\bar{Y})\,, \qquad \Gamma \equiv \frac{T_3(V^w_{\Sigma_4})_0}{\pi}\,. \tag{F.7}$$

Here $k$ is the little Kähler potential for the fiducial metric on the conifold, $\partial_\alpha\partial_{\bar{\beta}}k \equiv g_{\alpha\bar{\beta}}$. The term proportional to $k$ in (F.7) has to be added to make $\rho$ holomorphic; see [18, 77] for extensive discussions of this issue. Because $u(0) = k(0) = 0$, we may relate the parameter $\Gamma$ to the value of the stabilized Kähler modulus $\rho$ when the D3-brane is at the tip of the throat,

$$\Gamma \equiv \rho_\star(0) + \bar{\rho}_\star(0) = 2\sigma_\star(0) \equiv 2\sigma_0\,. \tag{F.8}$$

The range of allowed values for $\sigma_0$ is constrained by the throat contribution to the warped four-cycle volume, which we will compute in the next section.

With these definitions the DeWolfe-Giddings Kähler potential is

$$\mathcal{K} = -3M_{\rm pl}^2 \ln\left[\rho + \bar{\rho} - \gamma k(Y,\bar{Y})\right] = -3M_{\rm pl}^2 \ln\left[\Gamma e^{4u(Y,\bar{Y})}\right]\,. \tag{F.9}$$

To determine the constant $\gamma$, we compare the kinetic terms derived from the DBI action,

$$\mathcal{L}^{\rm DBI}_{\rm kin} = -\frac{1}{2}T_3 e^{-4u} g_{\alpha\bar{\beta}}\partial_\mu Y^\alpha \partial^\mu \overline{Y^\beta}\,, \tag{F.10}$$

with the kinetic terms[2] derived from (F.9),

$$\begin{aligned}\mathcal{L}^{\mathcal{K}}_{\rm kin} &= -\mathcal{K}_{\alpha\bar\beta}\partial_\mu Y^\alpha \partial^\mu \overline{Y^\beta} \\ &\approx 3M_{\rm pl}^2 e^{-4u}\partial_\alpha\partial_{\bar\beta}e^{4u}\partial_\mu Y^\alpha\partial^\mu\overline{Y^\beta}\,, \end{aligned} \tag{F.11}$$

where

$$\partial_\alpha\partial_{\bar\beta}e^{4u} = -\frac{\gamma}{\Gamma}\partial_\alpha\partial_{\bar\beta}k = -\frac{\gamma}{\Gamma}g_{\alpha\bar\beta}\,. \tag{F.12}$$

Equations (F.10) and (F.11) are consistent if we define

$$\gamma \equiv \frac{\Gamma}{6}\frac{T_3}{M_{\rm pl}^2} = \frac{1}{6}\frac{(V_{\Sigma_4}^w)_0}{V_6^w}\,. \tag{F.13}$$

Using equation (F.8) this may be written in the useful form

$$\gamma = \frac{\sigma_0}{3}\frac{T_3}{M_{\rm pl}^2}\,. \tag{F.14}$$

We now notice that the physical quantities of interest, such as $\rho$ and $\gamma k$, are independent of the split into breathing mode $e^{u(0)}$ and fiducial metric $g$ in (F.1). For

[2]Of course, the complete kinetic terms for the D3-brane coordinates and the volume modulus are

$$\begin{aligned}\mathcal{L}_{\rm kin} &\equiv -\mathcal{K}_{\rho\bar\rho}\partial_\mu\rho\partial^\mu\overline{\rho} - \mathcal{K}_{Y_\alpha\overline{Y_\beta}}\partial_\mu Y^\alpha\partial^\mu\overline{Y^\beta} - \left(\mathcal{K}_{\rho\overline{Y_\beta}}\partial_\mu\rho\partial^\mu\overline{Y^\beta} + c.c.\right) \\ &= 3M_{\rm pl}^2\frac{\gamma k_{\alpha\bar\beta}\partial_\mu Y^\alpha\partial^\mu\overline{Y^\beta}}{U} \\ &\quad -3M_{\rm pl}^2\left|\frac{\partial_\mu\rho}{U}\right|^2 + 3M_{\rm pl}^2\left|\frac{\gamma k_\alpha\partial_\mu\overline{Y^\alpha}}{U}\right|^2 + 3M_{\rm pl}^2\left(\frac{\partial_\mu\rho}{U}\frac{\gamma k_{\bar\beta}\partial^\mu\overline{Y^\beta}}{U} + c.c.\right) \\ &\approx \frac{3M_{\rm pl}^2\gamma k_{\alpha\bar\beta}\partial_\mu Y^\alpha\partial^\mu\overline{Y^\beta}}{U}\,, \end{aligned}$$

In the final relation we have focused attention on a subset of the kinetic terms for the D3-brane coordinates. This is justified for several reasons. First, in Chapter 7 we are specifically searching for (fine-tuned) configurations in which the D3-brane potential is unusually flat. In such a case, it is consistent to use an adiabatic approximation for the motion of the volume modulus, and omit the kinetic terms for $\rho$. Next, the term involving $|k_\alpha\partial_\mu\overline{Y^\alpha}|^2$ is suppressed, relative to the term we have retained, by $U^{-1} \ll 1$. Furthermore, $k_\alpha$ vanishes at the tip of a singular conifold, and is correspondingly very small at the tip of the deformed conifold we are considering. Finally, from the explicit form of $k$ we learn that the term $|k_\alpha\partial_\mu\overline{Y^\alpha}|^2$ is suppressed by the small quantity $(\phi/M_{\rm pl})^2$ relative to the term we have retained.

example,

$$\gamma k = \frac{1}{6}\frac{T_3}{[M_{\rm pl}^2 e^{6u}]}\frac{T_3[(V_{\Sigma_4}^w)_0 e^{4u}]}{\pi}[e^{2u}k] = \frac{1}{6}\frac{(\tilde{V}_{\Sigma_4}^w)_0}{\tilde{V}_6^w}\tilde{k} \equiv \tilde{\gamma}\tilde{k}\,, \tag{F.15}$$

where we have defined

$$\tilde{k} \equiv e^{2u}k = e^{2u}r^2 = \tilde{r}^2\,, \tag{F.16}$$

and

$$\tilde{\gamma} \equiv e^{-2u}\gamma = \frac{\tilde{\Gamma}}{6}\frac{T_3}{[M_{\rm pl}^2 e^{6u}]} = \frac{1}{6}\frac{(\tilde{V}_{\Sigma_4}^w)_0}{\tilde{V}_6^w}\,, \tag{F.17}$$

where

$$\tilde{\Gamma} \equiv \Gamma e^{4u} = 2\sigma_0 e^{4u}\,. \tag{F.18}$$

This shows that $\tilde{\gamma}\tilde{k}$ is invariant under the change of conventions

$$e^{2u(0)} \to \lambda e^{2u(0)}\,, \qquad g_{\alpha\bar{\beta}} \to \lambda^{-1} g_{\alpha\bar{\beta}}\,. \tag{F.19}$$

One easily sees that $\rho + \bar{\rho}$ is likewise invariant. We have therefore justified our original choice of the convenient value $u(0) = 0$.

### F.2. Warped Four-Cycle Volume

The four-cycle $\Sigma_4$ wrapped by the D7-branes is, in principle, compact. The volume of the four-cycle receives contributions both from the throat region and the bulk, $(V_{\Sigma_4}^w)_0 = (V_{\Sigma_4}^w)_{0,\rm throat} + (V_{\Sigma_4}^w)_{0,\rm bulk}$. Since we have access to explicit metric information only in the throat region we cannot evaluate $(V_{\Sigma_4}^w)_{0,\rm bulk}$. However, we can still make progress by deriving results that are largely independent of the unknown bulk region. In the remainder of this section we compute $(V_{\Sigma_4}^w)_{0,\rm throat}$ for various embeddings and use $(V_{\Sigma_4}^w)_0 \equiv B_4 (V_{\Sigma_4}^w)_{0,\rm throat}$, with $B_4 > 1$, to parameterize the unknown bulk contribution. In the non-compact limit, $(V_{\Sigma_4}^w)_{0,\rm throat}$ diverges. Here we identify the leading order divergence and regularize the throat volume by introducing the UV cutoff $\hat{r}_{\rm UV}$, where the throat attaches to the bulk and $h(\hat{r}_{\rm UV}) \approx 1$.

We use the following approximation to the warp factor [87, 106],

$$h \approx \frac{L^4}{\hat{r}^4} \ln \frac{\hat{r}}{\varepsilon^{2/3}} \,, \tag{F.20}$$

where

$$2T_3 L^4 = \frac{27}{16\pi^2} \left( \frac{3g_s M}{2\pi K} \right) N \,, \qquad \ln Q_0 \equiv \ln \frac{\hat{r}_{\rm UV}}{\varepsilon^{2/3}} \approx \frac{2\pi K}{3g_s M} \,. \tag{F.21}$$

At large radius $\hat{r}$ the D7-brane wraps an $S^3$ and the metric on the four-cycle is

$$\mathrm{d}s^2_{\Sigma_4} \to \mathrm{d}\hat{r}^2 + \hat{r}^2 \mathrm{d}s^2_{S^3} \,. \tag{F.22}$$

The warped four-cycle volume then becomes

$$(V^w_{\Sigma_4})_0 \equiv \int \mathrm{d}^4\xi \sqrt{g^{ind}} h \;\; = \;\; B_4 L^4 \mathrm{Vol}(S^3) \int_{\hat{r}_\mu}^{\hat{r}_{\rm UV}} \frac{\mathrm{d}\hat{r}}{\hat{r}} \ln \frac{\hat{r}}{\varepsilon^{2/3}} \tag{F.23}$$

$$= \;\; B_4 L^4 \mathrm{Vol}(S^3) \ln Q_\mu \left[ \ln Q_0 - \frac{1}{2} \ln Q_\mu \right] \,, \tag{F.24}$$

where $Q_\mu \equiv \frac{\hat{r}_{\rm UV}}{\hat{r}_\mu} > 1$. The numerical value of $\mathrm{Vol}(S^3)$ depends on the specific embedding. For the Kuperstein embedding we have [114]

$$\mathrm{Vol}(S^3) = \frac{16\pi^2}{9} \,, \tag{F.25}$$

and hence, by (F.7),

$$\Gamma = \frac{3}{2\pi} B_4 N \ln Q_\mu \left[ 1 - \frac{1}{2} \frac{\ln Q_\mu}{\ln Q_0} \right] \,. \tag{F.26}$$

This implies

$$\omega_0 \equiv a\sigma_0 \;\; = \;\; \frac{3}{2} B_4 \left( \frac{N}{n} \right) \ln Q_\mu \left[ 1 - \frac{1}{2} \frac{\ln Q_\mu}{\ln Q_0} \right] \,, \tag{F.27}$$

$$\approx \;\; \frac{3}{2} B_4 \left( \frac{N}{n} \right) \ln Q_\mu \,. \tag{F.28}$$

Since, $B_4 > 1$, $N/n > 1$ and $Q_\mu > 1$, this can assume a range of values, with $\omega_0 = \mathcal{O}(10)$ being easily achievable. The value of $\omega_0$ is important as it determines

the scale of inflation

$$\frac{V_{dS}}{M_{\rm pl}^4} \sim \frac{e^{-2\omega_0}}{2\omega_0}\,. \tag{F.29}$$

In particular, for $B_4 = \mathcal{O}(1)$ and $\ln Q_\mu = \mathcal{O}(1)$, constraints on the minimal phenomenologically viable inflation scale, $V_{dS} > \mathcal{O}(\text{TeV}^4) \sim 10^{-60} M_{\rm pl}^4$ or $\omega_0 \lesssim 150$, translate into an upper limit on the background five form flux

$$\frac{N}{n} < \mathcal{O}(10^2)\,. \tag{F.30}$$

This can be a serious constraint on nonperturbative volume stabilization by the KKLT mechanism.

Finally, the ACR [9] embeddings, $\prod_{i=1}^4 w_i^{p_i} = \mu^P$, satisfy

$$\text{Vol}(S^3) = \frac{16\pi^2}{9} P\,, \tag{F.31}$$

and hence

$$\omega_0 \approx \frac{3}{2} P B_4 \left(\frac{N}{n}\right) \ln Q_\mu\,. \tag{F.32}$$

## F.3. Canonical Field Range

**F.3.1. Canonical Inflaton.** The inflaton action includes the kinetic term

$$\mathcal{L}_{\rm kin} = -\frac{1}{2} T_3 e^{-4u(\hat{r})} (\partial_\mu \hat{r})^2 \equiv -\frac{1}{2} (\partial_\mu \varphi)^2\,, \tag{F.33}$$

so the canonical inflaton field is

$$\varphi = \int \left(T_3 \frac{\Gamma}{\tilde{\Gamma}(\hat{r})}\right)^{1/2} \mathrm{d}\hat{r}\,. \tag{F.34}$$

For analytical considerations the following approximation is often sufficient (see Appendix H for more accurate analytical results)

$$\varphi^2 \approx \frac{\Gamma}{\tilde{\Gamma}(\hat{r})} T_3 \hat{r}^2 \approx \frac{2\sigma_0}{\rho + \bar{\rho}} T_3 \hat{r}^2 \approx T_3 \hat{r}^2 \equiv \phi^2\,. \tag{F.35}$$

This is independent of the split into breathing mode and fiducial metric in (F.1):

$$\frac{\varphi^2}{M_{\rm pl}^2} = \frac{[\Gamma e^{4u}]}{\tilde{\Gamma}} \frac{T_3[e^{2u}\hat{r}^2]}{[M_{\rm pl}^2 e^{6u}]} = \frac{\tilde{r}^2}{\frac{1}{\pi}T_3 \widetilde{V}_6^w} \,. \tag{F.36}$$

This implies

$$\frac{\gamma k}{\rho + \bar{\rho}} = \frac{\Gamma}{\rho + \bar{\rho}} \frac{T_3 \hat{r}^2}{6 M_{\rm pl}^2} \approx \frac{\Gamma}{\tilde{\Gamma}} \frac{T_3 \hat{r}^2}{6 M_{\rm pl}^2} = \frac{1}{6} \frac{\varphi^2}{M_{\rm pl}^2} \tag{F.37}$$

and the DeWolfe-Giddings Kähler potential becomes separable

$$\kappa^2 \mathcal{K} \approx -3 \ln(\rho + \bar{\rho}) - 3 \ln u \,, \qquad u \equiv 1 - \frac{1}{6} \frac{\varphi^2}{M_{\rm pl}^2} \,. \tag{F.38}$$

**F.3.2. Bound on the Field Range.** We now derive the microscopic bound on the inflaton field range in four-dimensional Planck units [21]. Recall that the Planck mass depends on the warped volume of the internal space as

$$M_{\rm pl}^2 = \frac{1}{\pi} (T_3)^2 V_6^w \,, \tag{F.39}$$

where $V_6^w$ is computed from the fiducial metric excluding the breathing mode. The warped volume of the internal space receives contributions both from the throat and from the bulk, $V_6^w = (V_6^w)_{\rm throat} + (V_6^w)_{\rm bulk}$. Since the bulk metric is not known we use the parametrization $V_6^w \equiv B_6 (V_6^w)_{\rm throat}$, with $B_6 > 1$, to characterize the unknown bulk contribution. Using the warp factor (F.20), we find that the leading contribution to the throat volume is

$$(V_6^w)_{\rm throat} = \frac{\pi}{T_3} \frac{N}{4} \hat{r}_{\rm UV}^2 \,. \tag{F.40}$$

This implies that the range of the inflaton is bounded by [21]

$$\frac{\varphi^2}{M_{\rm pl}^2} \leq \frac{\varphi_{\rm UV}^2}{M_{\rm pl}^2} = \frac{4}{e^{4u(r_{\rm UV})} N B_6} \,, \tag{F.41}$$

where

$$e^{4u(r_{\rm UV})} = \frac{\sigma(r_{\rm UV})}{\sigma(0)} \,. \tag{F.42}$$

In Chapter 8 we explained that this relation sharply limits the amount of gravitational waves that can be expected in D-brane inflation models. One of the main results of the present paper is that the bound (F.41) also provides a surprisingly strong constraint on the possibility of fine-tuning the inflaton potential, even in cases where the energy scale of inflation is too low for gravitational waves to be relevant.

The bound (F.41) is written in a slightly stronger and more general form than the bound given in Chapter 8,

$$\frac{\varphi^2}{M_{\rm pl}^2} \leq \frac{4}{N}\,. \tag{F.43}$$

The factor $B_6 > 1$ is simply an explicit representation of the unknown bulk contribution to $V_6^w$ and hence to $M_{\rm pl}^2$. The breathing mode factor requires further explanation. Recall that we have used the convention $e^{u(0)} = 1$, so that the breathing mode factor is unity when the D3-brane is at the tip of the throat. We will now argue that in the configurations of interest, the variation of the breathing mode as the D3-brane is displaced from the tip is characterized by the condition $e^{4u(r)} = \frac{\sigma(r)}{\sigma(0)} \geq 1$. The D3-brane potential from moduli stabilization is minimized when the D3-brane is at the tip of the throat, in all the configurations studied in this paper (see also [59]). Displacing the D3-brane from the tip increases the potential, and so tends to increase the compactification volume, because positive energy causes a runaway potential for the volume. (We have confirmed this expectation by explicit numerical analysis in §4.3, and by analytical arguments in Appendix H.) Thus, moving the D3-brane up the throat dilates the space, and leads to $e^{4u(r)} = \frac{\sigma(r)}{\sigma(0)} > 1$ for $r > 0$. This effect goes in the direction of making the bound (F.41) *stronger* than (F.43), but the effect is very small in practice: in the cases we considered, $1 < \frac{\sigma(r_{\rm UV})}{\sigma(0)} < 1.1$. Such a factor is a negligible correction in comparison to the uncertainties in $B_6$, so it is very reasonable to omit it, as in Chapter 8.

APPENDIX G

# Stability in the Angular Directions

In this appendix we study the angular stability of the radial inflationary trajectory proposed in Chapter 7.

## G.1. Kuperstein Embedding

The following analysis complements our Kuperstein case study of §3 and §4 in Chapter 7. In §G.1.1 we derive the condition for extremal trajectories $z_1 = \pm\frac{r^{3/2}}{\sqrt{2}}$ whose angular stability we investigate in §G.1.2.

**G.1.1. Extremal Trajectories.** Recall that the Kuperstein potential (7.26) depends only on the following dynamical fields: $|z_1|^2$, $z_1 + \overline{z_1}$, $r$, and $\sigma = \mathrm{Re}(\rho)$. Along a trajectory that extremizes the potential in the angular directions we must have $\frac{\partial V}{\partial \Psi_i} = 0$ for all $r$, so we aim to find points in $T^{1,1}$ that satisfy

$$\frac{\partial |z_1|^2}{\partial \Psi_i} = 0 = \frac{\partial (z_1 + \overline{z_1})}{\partial \Psi_i}\,. \tag{G.1}$$

We examine (G.1) by introducing local coordinates in the vicinity of a fiducial point $\mathbf{z}_0 \equiv (z_1', z_2', z_3', z_4')$. The coordinates around this point are given by the five generators of $SO(4)$ acting nontrivially on $\mathbf{z}_0$

$$\mathbf{z}(r, \Psi_i) = \exp(\mathsf{T})\, \mathbf{z}_0\,. \tag{G.2}$$

The Kuperstein embedding, $z_1 = \mu$, breaks the global $SO(4)$ symmetry of the conifold down to $SO(3)$, and the D3-brane potential preserves this $SO(3)$ symmetry. We will

find that the actual trajectory breaks this $SO(3)$ down to $SO(2)$ which we take to act on $z_3$ and $z_4$. The coordinates that make this $SO(2)$ stability group manifest are given by

$$\mathsf{T} \equiv \left(\begin{array}{cc|cc} 0 & \alpha_2 & \alpha_3 & \alpha_4 \\ -\alpha_2 & 0 & \beta_3 & \beta_4 \\ \hline -\alpha_3 & -\beta_3 & 0 & 0 \\ -\alpha_4 & -\beta_4 & 0 & 0 \end{array}\right), \tag{G.3}$$

where $\Psi_i \equiv \{\alpha_i, \beta_i\} \in \mathbb{R}$ are the local coordinates of the base of the cone. We aim to find $\mathbf{z}_0$ such that the potential $V(z_1 + \overline{z_1}, |z_1|^2)$ is extremal along $\mathbf{z}_0$. We here find trajectories along which the linear variation of $z_1 + \overline{z_1}$ and $|z_1|^2$ vanishes. First, we observe from (G.2) and (G.3) that for arbitrary $\mathbf{z}_0$ we have

$$\delta z_1 = \sum_{i=2}^{4} \alpha_i z_i' , \qquad \alpha_i \in \mathbb{R} . \tag{G.4}$$

and, hence,

$$\delta|z_1|^2 = \sum_{i=2}^{4} \alpha_i (z_i' \bar{z}_1' + z_1' \bar{z}_i') \equiv 0 . \tag{G.5}$$

To satisfy (G.5) for all $\alpha_i$ one requires

$$z_i' = i\rho_i z_1' , \qquad \rho_i \in \mathbb{R} . \tag{G.6}$$

We may use $SO(3)$ to set $\rho_3 = \rho_4 = 0$, while keeping $\rho_2$ finite. The conifold constraint, $z_1^2 + z_2^2 = 0$ then implies $\rho_2 = \pm 1$, while the requirement

$$\delta(z_1' + \bar{z}_1') = a_2(z_2' + \bar{z}_2') = 0 , \tag{G.7}$$

makes $z_2'$ purely imaginary and $z_1'$ real. This proves that the following is an extremal trajectory of the brane potential for the Kuperstein potential

$$z_1' = \pm \frac{1}{\sqrt{2}} r^{3/2} , \qquad z_2' = \pm i z_1' . \tag{G.8}$$

**G.1.2. Stability.** Let us now study the stability of the potential along the path (G.8). From (G.2) one finds

$$z_1 = z_1' \left[ 1 - \frac{1}{2}(\alpha_2^2 + \alpha_3^2 + \alpha_4^2) + \frac{i}{2}\rho_2(2\alpha_2 - \alpha_3\beta_3 - \alpha_4\beta_4) + \cdots \right] , \tag{G.9}$$

and

$$\begin{aligned} z_1 + \bar{z}_1 &= 2z_1' \left[ 1 - \frac{1}{2}(\alpha_2^2 + \alpha_3^2 + \alpha_4^2) + \cdots \right] , & \text{(G.10)} \\ |z_1|^2 &= (z_1')^2 \left[ 1 - (\alpha_3^2 + \alpha_4^2) + \cdots \right] . & \text{(G.11)} \end{aligned}$$

Since the Kuperstein potential (7.26) depends only on $r$, $z_1 + \overline{z_1}$, and $z_1\overline{z_1}$, and

$$\left. \frac{\partial |z_1|^2}{\partial \Psi_i} \right|_0 = \left. \frac{\partial (z_1 + \overline{z_1})}{\partial \Psi_i} \right|_0 = 0 \tag{G.12}$$

where $\big(\dots\big)\big|_0$ denotes evaluation at $\mathbf{z}_0$, we find

$$\left. \frac{\partial V}{\partial \Psi_i} \right|_0 = 0 \,, \tag{G.13}$$

and

$$\left. \frac{\partial^2 V}{\partial \Psi_i \partial \Psi_j} \right|_0 = \left. \left[ \frac{\partial V}{\partial |z_1|^2} \frac{\partial^2 |z_1|^2}{\partial \Psi_i \partial \Psi_j} + \frac{\partial V}{\partial (z_1 + \overline{z_1})} \frac{\partial^2 (z_1 + \overline{z_1})}{\partial \Psi_i \partial \Psi_j} \right] \right|_0 , \tag{G.14}$$

where

$$\partial_i \partial_j |z_1|^2 \big|_0 = \pm \frac{r^{3/2}}{\sqrt{2}} \, \partial_i \partial_j (z_1 + \overline{z_1})|_0 + r^3 \delta_{i2}\delta_{j2} = -r^3 \delta_{i3}\delta_{j3} - r^3 \delta_{i4}\delta_{j4} \,. \tag{G.15}$$

Hence, the angular mass matrix at $\mathbf{z}_0$ has the form

$$\left. \frac{\partial^2 V}{\partial \Psi_i \partial \Psi_j} \right|_0 = \left( \begin{array}{ccccc} X & 0 & 0 & 0 & 0 \\ 0 & X+Y & 0 & 0 & 0 \\ 0 & 0 & X+Y & 0 & 0 \\ 0 & 0 & 0 & 0 & 0 \\ 0 & 0 & 0 & 0 & 0 \end{array} \right) \begin{array}{l} \alpha_2 \\ \alpha_3 \\ \alpha_4 \\ \beta_3 \\ \beta_4 \end{array} \tag{G.16}$$

where

$$X \equiv \mp\sqrt{2}r^{3/2}\frac{\partial V}{\partial(z_1+\overline{z_1})}\bigg|_0 , \tag{G.17}$$

$$Y \equiv -r^3\frac{\partial V}{\partial|z_1|^2}\bigg|_0 . \tag{G.18}$$

The flat-directions in the $\beta$–angles parameterize the symmetry group $SO(3)/SO(2)$ that leaves the Kuperstein embedding $z_1 = \mu$ invariant. The $\alpha_3$ and $\alpha_4$–angles have degenerate eigenvalues.

To calculate the eigenvalues $X$ and $Y$ we note that the F-term potential (7.26) may be written as

$$V_F = \mathcal{C}(r,\sigma)\mathcal{G}^{1/n}\bigg[(2a\sigma+6) - \frac{6\,e^{a\sigma}|W_0|}{|A_0|}\mathcal{G}^{-1/2n} + \frac{3}{2n}\Big(\frac{1}{\mu}(z_1+\overline{z_1}) - \frac{2}{\mu^2}|z_1|^2\Big)\mathcal{G}^{-1} + \frac{4c}{n}\frac{r}{r_\mu}\Big(1-\frac{|z_1|^2}{2r^3}\Big)\mathcal{G}^{-1}\bigg], \tag{G.19}$$

and the D-term potential (7.20) depends only on $r$ and is independent of the angles (at least far from the tip [59]). In (G.19) we have defined the functions

$$\mathcal{C}(r,\sigma) \equiv \frac{\kappa^2 a|A_0|^2 e^{-2a\sigma}}{3U^2} > 0\,, \qquad \partial_{z_1+\overline{z_1}}\mathcal{C} = \partial_{|z_1|^2}\mathcal{C} = 0\,, \tag{G.20}$$

$$\mathcal{G} \equiv \frac{|A|}{|A_0|} = \left|1-\frac{z_1}{\mu}\right|^2 , \qquad \partial_{z_1+\overline{z_1}}\mathcal{G} = \frac{-1}{\mu}\,, \quad \partial_{|z_1|^2}\mathcal{G} = \frac{1}{\mu^2}\,, \tag{G.21}$$

$$\mathcal{G}_0 \equiv \mathcal{G}|_0 = |1\mp x^{3/2}|^2 = g(x)^2\,, \tag{G.22}$$

and the variable

$$x \equiv \mathrm{sign}(z_1)\frac{r}{r_\mu} = \frac{\phi}{\phi_\mu}\,. \tag{G.23}$$

After a lengthy but straightforward computation we find

$$X = \pm\frac{2\mathcal{C}}{n}\frac{x^{3/2}}{|1\mp x^{3/2}|^{2(1-1/n)}}\Bigg[2a\sigma+\frac{9}{2}-\frac{3\,e^{a\sigma}|W_0|}{|A_0|}\frac{1}{|1\mp x^{3/2}|^{1/n}} \mp 3\Big(1-\frac{1}{n}\Big)\frac{x^{3/2}(1\mp x^{3/2})}{|1\mp x^{3/2}|^2}-3c\Big(1-\frac{1}{n}\Big)\frac{x}{|1\mp x^{3/2}|^2}\Bigg], \quad \text{(G.24)}$$

and

$$X+Y=\big(1\mp x^{3/2}\big)\,X+\frac{2\mathcal{C}c}{n}\,\frac{x}{|1\mp x^{3/2}|^{2(1-1/n)}}\left(1+\frac{3}{2c}x^2\right), \quad \text{(G.25)}$$

where

$$c\equiv\frac{9}{4n\,a\sigma_0\frac{\phi_\mu^2}{M_{\rm pl}^2}}\,. \quad \text{(G.26)}$$

Notice that stability of the trajectory $z_1=\pm\frac{1}{\sqrt{2}}r^{3/2}$ for both positive and negative real $z_1$ only requires that $X>0$ (from (G.25) this automatically implies $X+Y>0$; at least for the regime of interest: $r<r_\mu$). Hence, from equation (G.24) a simple numerical check can decide whether a specific scenario is stable in the angular directions. For all potential inflationary trajectories we have performed this stability test.

*Analytical approximation.* In Appendix H we explain how the position of the Kähler modulus in the AdS vacuum, $\sigma_F$, shifts to $\sigma_0$ when the minimum gets uplifted to de Sitter

$$a\sigma_0\approx a\sigma_F+\frac{s}{a\sigma_F}\,,\qquad s\equiv\frac{V_D(0,\sigma_F)}{|V_F(0,\sigma_F)|}\,, \quad \text{(G.27)}$$

where $\frac{3|W_0|}{|A_0|}e^{a\sigma_F}=2a\sigma_F+3$ and $\frac{3|W_0|}{|A_0|}e^{a\sigma_0}\approx 2a\sigma_0+3+2s$. Substituting this into (G.24) we find

$$X = \pm\frac{2\mathcal{C}}{n}\frac{x^{3/2}}{|1\mp x^{3/2}|^{2(1-1/n)}}\Bigg[\frac{3}{2}-\frac{2s}{|1\mp x^{3/2}|^{1/n}}+2a\sigma_0\Big(1-\frac{1}{|1\mp x^{3/2}|^{1/n}}\Big) + 3\Big(1-\frac{1}{|1\mp x^{3/2}|^{1/n}}\Big)\mp 3\Big(1-\frac{1}{n}\Big)\frac{x^{3/2}(1\mp x^{3/2})}{|1\mp x^{3/2}|^2} -3c\Big(1-\frac{1}{n}\Big)\frac{x}{|1\mp x^{3/2}|^2}\Bigg]. \quad \text{(G.28)}$$

In the limit $x \to 0$ this becomes

$$\lim_{x\to 0} X = \mp \frac{\mathcal{C}}{n} x^{3/2} \left[4s - 3\right] . \tag{G.29}$$

Hence, the near tip region is stable on the negative axis and unstable on the positive axis. Notice that it was essential to include the shift from uplifting to realize this.

## G.2. Ouyang Embedding

**G.2.1. Extremal Trajectories.** For the Ouyang embedding, $w_1 = \mu$, the brane potential depends on $w_1 + \overline{w_1}$, $|w_1|^2$ and $|w_2|^2$. To find extremal trajectories of the potential we therefore require

$$\frac{\partial |w_1|^2}{\partial \Psi_i} = \frac{\partial |w_2|^2}{\partial \Psi_i} = \frac{\partial (w_1 + \overline{w_1})}{\partial \Psi_i} = 0 \, . \tag{G.30}$$

We introduce local coordinates by applying generators of $SU(2)$ to the generic point $W_0$

$$W = e^{i\mathsf{T}_1} W_0 e^{-i\mathsf{T}_2} \, , \qquad W_0 \equiv \begin{pmatrix} w_3' & w_2' \\ w_1' & w_4' \end{pmatrix} , \tag{G.31}$$

where

$$\mathsf{T}_i \equiv \begin{pmatrix} \alpha_i & \beta_i + i\gamma_i \\ \beta_i - i\gamma_i & -\alpha_i \end{pmatrix} . \tag{G.32}$$

This implies

$$\delta w_1 = -i(\alpha_1 + \alpha_2) w_1' + (-\beta_1 + i\gamma_1) w_3' + (\beta_2 - i\gamma_2) w_4' + \cdots \tag{G.33}$$

and $\delta(w_1 + \bar{w}_1) = 0$ gives $w_1' \in \mathbb{R}$, $w_3' = w_4' = 0$. We find that $\delta |w_1|^2 = 0$ and $\delta |w_2|^2 = 0$ if $w_2' \in \mathbb{R}$. The conifold constraint $w_1' w_2' = 0$ then restricts the solution to the following two options:

$$w_1' = 0 \, , \qquad |w_2'| = r^{3/2} \, , \qquad \Leftrightarrow \qquad \theta_1 = \theta_2 = 0 \, , \tag{G.34}$$

or

$$w_1' = \pm r^{3/2}\,, \qquad w_2' = 0\,, \qquad \Leftrightarrow \qquad \theta_1 = \theta_2 = \pi\,. \tag{G.35}$$

*Delta-flat direction.* For $w_1' = 0$ the superpotential correction to the potential vanishes and inflation is impossible, as noted in [45] and reviewed in §5 of Chapter 7.

*Non-delta-flat direction.* For $w_2' = 0$ the superpotential correction to the potential does not vanishes. In fact, along this extremal trajectory the potential can be shown to be identical to the potential for the Kuperstein case. Stability for Ouyang and Kuperstein however is different as we discuss next.

### G.2.2. Stability.

*Delta-flat direction.* Near $w_1' = 0$, $w_2' \neq 0$ we have

$$w_1 = w_2' \left[\beta_1\beta_2 - \gamma_1\gamma_2 - i(\beta_1\gamma_2 + \beta_2\gamma_1)\right] \tag{G.36}$$

$$w_2 = w_2' \left[1 + i(\alpha_1 + \alpha_2) - \frac{1}{2}(\alpha_1 + \alpha_2)^2 - \frac{1}{2}(\beta_1^2 + \beta_2^2 + \gamma_1^2 + \gamma_2^2)\right] \tag{G.37}$$

and (to second order)

$$w_1 + \overline{w_1} = 2w_2' \left[\beta_1\beta_2 - \gamma_1\gamma_2\right] \tag{G.38}$$

$$|w_1|^2 = 0 \tag{G.39}$$

$$|w_2|^2 = (w_2')^2 \left[1 - (\beta_1^2 + \beta_2^2 + \gamma_1^2 + \gamma_2^2)\right]\,. \tag{G.40}$$

The mass matrix in these coordinates is non-diagonal, but may easily be diagonalized by the transformation

$$\beta_{1,2} = \frac{u_1 \pm v_1}{\sqrt{2}}\,, \quad \gamma_{1,2} = \frac{v_2 \pm u_2}{\sqrt{2}}\,, \quad U^2 \equiv u_1^2 + u_2^2\,, \quad V^2 \equiv v_1^2 + v_2^2\,. \tag{G.41}$$

This gives

$$w_1 + \overline{w_1} = w_2' \left[U^2 - V^2\right]\,, \qquad |w_2|^2 = (w_2')^2 \left[1 - (U^2 + V^2)\right]\,. \tag{G.42}$$

A lengthy but straightforward computation gives the eigenvalues of the angular mass matrix of the potential along the delta-flat direction

$$X_U = \frac{2\mathcal{C}c}{n}\, x \left[1 \mp \frac{1}{4c}\, x^{1/2} \left(4a\sigma + 9 - \frac{6e^{a\sigma}|W_0|}{|A_0|}\right)\right], \tag{G.43}$$

$$X_V = \frac{2\mathcal{C}c}{n}\, x \left[1 \pm \frac{1}{4c}\, x^{1/2} \left(4a\sigma + 9 - \frac{6e^{a\sigma}|W_0|}{|A_0|}\right)\right]. \tag{G.44}$$

We confirmed that these stability criteria are precisely what was found for the delta-flat direction in Burgess *et al.* [45] (*cf.* their equation (3.15)). Equation (G.43) and (G.44) show that the delta-flat direction is angularly stable if $x < x_c$ and unstable if $x > x_c$, where

$$x_c \equiv \left(\frac{4c}{4s-3}\right)^2 = \frac{1}{(4s-3)^2}\left(\frac{9}{a\sigma_0}\right)^2 \frac{1}{n^2}\frac{M_{\rm pl}^4}{\phi_\mu^4}\,. \tag{G.45}$$

Equation (G.45) is the generalization of (7.92) to general $n$. Applying the field range bound in the form $\frac{\phi_\mu^2}{M_{\rm pl}^2} < \frac{4}{N}$ one finds

$$x_c > \frac{1}{(4s-3)^2}\left(\frac{9}{a\sigma_0}\right)^2 \frac{N^2}{(4n)^2} \geq 1\,. \tag{G.46}$$

For typical parameters the delta-flat direction is hence stable from the tip to at least the location of the D7-branes.

*Non-delta-flat direction.* The non-delta-flat trajectory of the Ouyang embedding is very closely related to the extremal trajectories of the Kuperstein embedding. In fact, the shape of the potential is identical for the two cases. However, the stability analysis reveals subtle, but important differences.

Near $w_2' = 0$, $w_1' \neq 0$ we have

$$w_1 + \bar{w}_1 = 2w_1'\left[1 - \frac{1}{2}(U^2 + V^2)\right], \qquad |w_1|^2 = (w_1')^2\left[1 - V^2\right], \tag{G.47}$$

where we have defined

$$U^2 \equiv (\alpha_1 + \alpha_2)^2\,, \qquad V^2 \equiv \beta_1^2 + \beta_2^2 + \gamma_1^2 + \gamma_2^2\,. \tag{G.48}$$

Computing the eigenvalues of the angular mass matrix we find results that are almost identical to the Kuperstein results (G.24) and (G.25) except for one crucial sign difference:

$$X_U = X\,, \tag{G.49}$$

$$X_V = \left(1 \mp x^{3/2}\right) X + \frac{2\mathcal{C}c}{n} \frac{x}{|1 \mp x^{3/2}|^{2(1-1/n)}} \left( \boxed{-}\, 1 + \frac{3}{2c} x^2 \right), \tag{G.50}$$

where $X$ is the Kuperstein result (G.24). Since the leading term in (G.50) now comes with the opposite sign (*cf.* (G.25)), the non-delta-flat trajectory for Ouyang is typically unstable for small $x$ whereas the corresponding trajectory for Kuperstein is stable

$$X_V \approx -\frac{2\mathcal{C}c}{n} \frac{x}{|1 \mp x^{3/2}|^{2(1-1/n)}} < 0\,. \tag{G.51}$$

This is consistent with the results of [45].

### G.3. Stability for small $r$

To summarize our discussion of stability for the Kuperstein scenario and the Ouyang scenario we now give an intuitive explanation of angular stability in the limit of small $r$.

For either the Kuperstein or the Ouyang embedding, stability near the tip $r \to 0$ is controlled by the term in the potential proportional to $k^{1\bar{1}}$. We first focus on the Kuperstein embedding. Since $k^{1\bar{1}}$ contains a term proportional to $r^{-3}$, its contribution to the second derivative of the potential with respect to an angular variable $\Psi_i$, $\frac{\partial^2 V}{\partial \Psi_i^2}$, grows as $r$. All other terms grow at least as $r^{3/2}$ (this follows from $\frac{\partial}{\partial \Psi} = \frac{\partial z_i}{\partial \Psi} \frac{\partial}{\partial z_i} + c.c.$ and $\frac{\partial z_i}{\partial \Psi} \sim r^{3/2}$). A parallel consideration confirms that $k^{1\bar{1}}$ is responsible for the leading contribution to the stability analysis in the case of the Ouyang embedding as well.

Now, the trajectories $z_1 = \pm \frac{r^{3/2}}{\sqrt{2}}$ maximize $|z_1|^2$ for a given $r$, and any variation of angles may only increase $k^{1\bar{1}} = r\left(1 - \frac{|z_1|^2}{2r^3}\right)$. Hence the trajectories in question

are stable at small $r$ under fluctuations of any angles that affect $|z_1|^2$. So far, this analysis does not include the phase of $z_1$, which of course leaves $|z_1|^2$ invariant. The leading correction to the potential from fluctuations of this phase comes not through $k^{1\bar{1}}$ but through terms in $V$ proportional to $z_1 + \overline{z_1}$. These terms change sign when $z_1$ does; thus, one of the signs in $z_1 = \pm\frac{r^{3/2}}{\sqrt{2}}$ corresponds to the stable trajectory, while the other sign corresponds to an unstable trajectory. We showed above that the stable trajectory in fact corresponds to $z_1 < 0$ (careful consideration of the shift of the volume, *cf.* Appendix H, is required for that argument.)

The analysis for the Ouyang embedding is very similar. The delta-flat trajectory $|w_2|^2 = r^3$ ($\theta_1 = \theta_2 = 0$) maximizes the ratio $\frac{|w_2|^2}{r^3}$. Thus, any angular fluctuation can only decrease the ratio $\frac{|w_2|^2}{r^3}$, without affecting $\frac{|w_1|^2}{r^3}$ (*cf.* (G.39)). This is easily checked with the help of the angular coordinates $\theta_i$ (E.8). On the other hand, the trajectory $|w_1|^2 = r^3$ ($\theta_1 = \theta_2 = \pi$) maximizes $\frac{|w_1|^2}{r^3}$, and angular fluctuations away from this trajectory decrease the ratio $\frac{|w_1|^2}{r^3}$, without affecting $\frac{|w_2|^2}{r^3}$. As a result, $k^{1\bar{1}} = r\left(1 + \frac{|w_1|^2}{2r^3} - \frac{|w_2|^2}{r^3}\right)$ cannot decrease in the case of the delta-flat trajectory $|w_2|^2 = r^3$, but necessarily has a negative mode along the non-delta-flat trajectory $|w_2|^2 = r^3$. Hence, the non-delta-flat trajectory is unstable for small $r$. No further consideration is needed to show that the delta-flat trajectory $|w_2|^2 = r^3$ is stable. Since angular fluctuations around $w_1 = 0$ can not affect $w_1 + \overline{w_1}$ term the leading contribution always comes from $k^{1\bar{1}}$.

We have therefore demonstrated that near the tip, the trajectory $|z_1|^2 = 2r^3$ is stable for the Kuperstein embedding, whereas the trajectory $|w_1|^2 = r^3$ in the Ouyang embedding is unstable.

### G.4. Higher-degree ACR Embeddings

We conclude this appendix with a derivation of the non-delta flat trajectory for higher degree ACR embeddings. As before, to find an extremal radial direction we need to satisfy the equations $\frac{\partial V}{\partial \Psi_i} = 0$ for any $r$. Since the potential for a general ACR

embedding depends only on $|\Phi|^{2P}$, $\mathrm{Re}(\Phi^P)$ and

$$\begin{aligned} Z \;\equiv\; & \left|p_1\frac{w_4}{w_1}+p_3\frac{w_2}{w_3}\right|^2+\left|p_1\frac{w_3}{w_1}+p_4\frac{w_2}{w_4}\right|^2 \\ & +\left|p_2\frac{w_3}{w_2}+p_4\frac{w_1}{w_4}\right|^2+\left|p_2\frac{w_4}{w_2}+p_3\frac{w_1}{w_3}\right|^2 , \end{aligned} \tag{G.52}$$

we will consider these terms separately. Extremizing $\mathrm{Re}(\Phi^P)$ with respect to the phase of $\Phi$ selects real $\Phi^P$. For any *non-zero* $\Phi$ we can use equations (G.31) and (G.32) to show that

$$\mathrm{Re}\left[\frac{\delta\Phi^P}{\Phi^P}\right]=\mathrm{Re}\left[\sum_i p_i\frac{\delta w_i}{w_i}\right]=0 \tag{G.53}$$

for

$$\left|\frac{w_1}{w_3}\right|^2 \;=\; \tan^2\frac{\theta_1}{2}=\frac{p_1+p_4}{p_2+p_3}\,, \tag{G.54}$$

$$\left|\frac{w_1}{w_4}\right|^2 \;=\; \tan^2\frac{\theta_2}{2}=\frac{p_1+p_3}{p_2+p_4}\,, \tag{G.55}$$

and

$$\Phi^P=\pm\lambda^P r^{3P/2}\,, \tag{G.56}$$

where

$$\lambda^P\equiv\frac{(p_1+p_3)^{\frac{1}{2}(p_1+p_3)}(p_1+p_4)^{\frac{1}{2}(p_1+p_4)}(p_2+p_3)^{\frac{1}{2}(p_2+p_3)}(p_2+p_4)^{\frac{1}{2}(p_2+p_4)}}{P^P}\,. \tag{G.57}$$

Notice that this point trivially extremizes $|\Phi|^{2P}$ since

$$\delta|\Phi|^{2P}=|\Phi|^{2P}\mathrm{Re}\left[\frac{\delta\Phi^P}{\Phi^P}\right]=0\,. \tag{G.58}$$

In addition, since $\Phi^P$ is real, equation (G.53) also implies $\delta\mathrm{Re}(\Phi^P)=0$. Finally, surprisingly enough, (G.54, G.55) also extremize (G.52) with respect to the angular directions. Therefore (G.56) is an extremal radial trajectory which exists for a generic case in addition to the delta-flat direction, $\Phi=0$. For $P=1$ this reproduces the non-delta-flat direction for the Ouyang embedding, *cf.* §G.2. For $P=2$, $p_1=p_2=1$

we find that the Karch-Katz embedding has a non-delta-flat direction given by $\Phi^2 = w_1 w_2 = w_3 w_4 = \pm\frac{1}{4} r^3$.

Although every ACR embedding contains non-delta flat directions (G.56), we now argue that these higher degree embeddings ($P > 1$) are *not* promising settings for flat potentials. Recall that for the $P = 1$ Kuperstein an inflection point could be arranged on the negative $z_1$–axis (modulo consistency with microscopic constraints) basically because a $x^{3/2}$-term in the potential led to a negative divergence of $\eta$ for small $x$, which could be balanced against the $x^2$–term from the $\eta$-problem for intermediate $x$ (see §4.1). For $P > 1$ embeddings this possibility disappears since there are then no terms of lower order in $x$ than the $x^2$–term. Hence,

$$\lim_{x \to 0} \eta = \frac{2}{3} \,. \tag{G.59}$$

This is suggestive evidence that fine tuning in higher degree ACR embeddings cannot give inflation, at least not at $x < 1$ (*cf.* [113]).

APPENDIX H

# Stabilization of the Volume

In this appendix we discuss subtleties in the stabilization of the compactification volume.

In the AdS minimum of a KKLT compactification, the stabilized value of the Kähler modulus $\omega_F \equiv a\sigma_F$ is given by the SUSY condition

$$D_\rho W|_{r=0,\,\omega_F} = 0 \qquad \Rightarrow \qquad \left.\frac{\partial V_F}{\partial \omega}\right|_{\omega_F} = 0\,, \tag{H.1}$$

which in terms of the flux superpotential is [93]

$$3\frac{|W_0|}{|A_0|}e^{\omega_F} = 2\omega_F + 3\,. \tag{H.2}$$

Adding an antibrane to lift the KKLT AdS minimum to a dS minimum induces a small shift in the stabilized volume, $\omega_0 = \omega_F + \delta\omega$. We compute this shift in §H.1. This gives the value of the Kähler modulus in the absence of a mobile D3-brane (or when the brane is near the tip of the throat). The presence of a D3-brane away from the tip induces a further shift of the volume that depends on the brane position, which we denote $\omega_\star(r)$. We compute this dependence of the Kähler modulus on the D3-brane position in §H.2. (See also [113].)

### H.1. Shift Induced by Uplifting

The stabilized value of the Kähler after uplifting, $\omega_0 = \omega_F + \delta\omega$, is determined from

$$\left.\frac{\partial V}{\partial \omega}\right|_{\omega_0} = 0 \approx \left.\frac{\partial^2 V_F}{\partial \omega^2}\right|_{\omega_F} \delta\omega + \left.\frac{\partial V_D}{\partial \omega}\right|_{\omega_0} , \tag{H.3}$$

where, from (7.20),

$$\left.\frac{\partial V_D}{\partial \omega}\right|_{\omega_0} = \left.\frac{-2V_D}{\omega}\right|_{\omega_0} \approx \left.\frac{-2V_D}{\omega_F}\right|_{\omega_F} \left[1 - 3\frac{\delta\omega}{\omega_F}\right] . \tag{H.4}$$

Solving (H.3) and (H.4) for $\delta\omega$ we find

$$\delta\omega = \frac{\omega_F}{3 + \frac{\omega^2}{2V_D}\left.\frac{\partial^2 V_F}{\partial \omega^2}\right|_{\omega_F}} . \tag{H.5}$$

From equation (7.34) we have

$$V_F(0,\omega) = C\frac{e^{-2\omega}}{(2\omega)^2}\left[(2\omega+6) - 6e^{\omega}\frac{|W_0|}{|A_0|}\right] \tag{H.6}$$

$$V_D(0,\omega) = D\frac{1}{(2\omega)^2} \tag{H.7}$$

and

$$\frac{\partial V_F}{\partial \omega} = -\frac{\omega+2}{\omega}\left[V_F + C\frac{e^{-2\omega}}{2\omega}\right] . \tag{H.8}$$

Since

$$V_F(0,\omega_F) = -C\frac{e^{-2\omega_F}}{2\omega_F} , \tag{H.9}$$

equation (H.8) vanishes at $\omega_F$, confirming equation (H.1). The second derivative of the F-term potential at $\omega_F$ is

$$\begin{aligned}\left.\frac{\partial^2 V_F}{\partial \omega^2}\right|_{\omega_F} &= -\frac{2}{(\omega_F)^2}\left[(\omega_F)^2 + \frac{5}{2}\omega_F + 1\right] V_F(0,\omega_F) \\ &\approx +2\left|V_F(0,\omega_F)\right| ,\end{aligned} \tag{H.10}$$

where $\omega_F \gg 1$. It proves convenient to define the ratio of the antibrane energy to the F-term energy *before* uplifting,

$$s \equiv \frac{V_D(0,\omega_F)}{|V_F(0,\omega_F)|}\,, \tag{H.11}$$

where stability of the volume modulus in a metastable de Sitter vacuum typically requires $1 \lesssim s \lesssim \mathcal{O}(3)$. Using $\frac{(\omega_F)^2}{s} \gg 1$ in equation (H.5), we find

$$\omega_0 \approx \omega_F + \frac{s}{\omega_F}\,. \tag{H.12}$$

Although $\delta\omega$ is small, it appears in an exponent in the potential (7.34), so that its effect there has to be considered:

$$\begin{aligned} 3\frac{|W_0|}{|A_0|}e^{\omega_0} = 3\frac{|W_0|}{|A_0|}e^{\omega_F}e^{\delta\omega} &\approx (2\omega_F+3)\left(1+\frac{s}{\omega_F}\right) \\ &\approx 2\omega_F + 3 + 2s\,, \\ &\approx 2\omega_0 + 3 + 2s\,. \end{aligned} \tag{H.13}$$

## H.2. Shift Induced by Brane Motion

Adding a mobile D3-brane to the compactification induces a further shift of the Kähler modulus that depends on the radial position of the brane, $\omega_\star(r)$. The function $\omega_\star(r)$ is determined by the solution of a transcendental equation,

$$\partial_\omega V|_{\omega_\star(r)} = 0\,. \tag{H.14}$$

Although equation (H.14) does not have an exact analytic solution, here we derive a simple, but very accurate approximate solution. (See also [113].) The precise form of the solution we give here is only valid for the trajectory $z_1 = -\frac{r^{3/2}}{\sqrt{2}}$ of the Kuperstein potential (see Chapter 7). While these results can easily be generalized to the trajectory $z_1 = \frac{r^{3/2}}{\sqrt{2}}$ and to more general embeddings, we have argued in the

main body of the paper that the trajectory $z_1 = -\frac{r^{3/2}}{\sqrt{2}}$ in the Kuperstein embedding is of primary interest as far as the possibility of inflationary solutions is concerned.

First, we notice that $\omega_\star$ appears both in polynomial terms and exponential terms in (H.14). Letting $\omega_\star \to \omega_0 = \omega_F + \frac{s}{\omega_F}$ (see equation (H.12)) in all polynomial terms, but *not* in the exponentials, we transform the transcendental equation (H.14) into a quadratic equation for $e^{\omega_\star(r)}$. Solving this we obtain the dependence of the Kähler modulus on the brane position as an expansion in $x$

$$\omega_\star(r) = \omega_0 \left[1 + c_1 x + c_{3/2} x^{3/2} + c_2 x^2 + \dots\right] , \tag{H.15}$$

where

$$\omega_0 = \omega_F + \frac{s}{\omega_F} + \frac{s(3s-5)}{2\omega_F^2} + \mathcal{O}(\omega_F^{-3}) , \tag{H.16}$$

and

$$c_1 = \left(\frac{27}{8n^2}\frac{M_{\rm pl}^2}{\phi_\mu^2}\right)\frac{1}{\omega_F^3} + \mathcal{O}(\omega_F^{-4}) , \tag{H.17}$$

$$c_{3/2} = \frac{1}{n}\frac{1}{\omega_F}\left[1 - \frac{1}{2\omega_F}\right] + \mathcal{O}(\omega_F^{-3}) , \tag{H.18}$$

$$c_2 = \left(\frac{s-1}{6}\frac{\phi_\mu^2}{M_{\rm pl}^2}\right)\frac{1}{\omega_F^2} + \mathcal{O}(\omega_F^{-3}) . \tag{H.19}$$

As we can see from this, typically $c_{3/2} \gg c_1, c_2$, so that the following expression is a good approximation

$$\omega_\star(r) \approx \omega_0 \left[1 + c_{3/2} x^{3/2}\right] . \tag{H.20}$$

In fact, in the cases we studied numerically this proved to be a remarkably accurate approximation to the exact result. Notice also that $c_1$, $c_{3/2}$, $c_2$ are all positive – the volume shrinks as the D3-brane moves towards the tip.

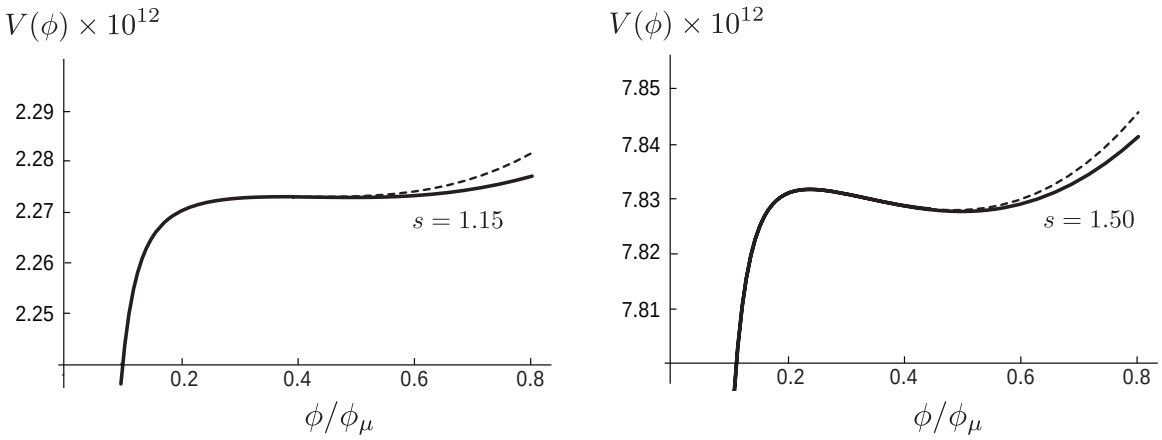


FIGURE 1. **D3-brane potential $\mathbb{V}(\phi)$.**
Shown are the analytic potential derived from (H.20)(dashed line) and the exact numerical result (solid line).

### H.3. Canonical Inflaton Revisited

Equipped with (H.20) for the evolution of the volume modulus, we may obtain a more accurate analytical result for the canonical inflaton field (F.34),

$$\varphi(r) = \int \Big( \frac{3\sigma_0 T_3}{U(r, \sigma_\star(r))} \Big)^{1/2} \mathrm{d}r \,, \tag{H.21}$$

where

$$\frac{3\sigma_0 T_3}{U(r, \sigma_\star(r))} = \frac{3}{2} T_3 \left( \frac{\omega_\star(r)}{\omega_\star(0)} - \frac{\frac{3}{2} T_3 r^2}{6 M_{\rm pl}^2} \right)^{-1} \,. \tag{H.22}$$

This implies

$$\begin{aligned} \varphi(r) &= \int \left[ 1 + c_{3/2} \left( \frac{\phi}{\phi_\mu} \right)^{3/2} - \frac{\phi^2}{6 M_{\rm pl}^2} \right]^{-1/2} \mathrm{d}\phi & \text{(H.23)} \\ &\approx \phi \left[ 1 - \frac{c_{3/2}}{5} \left( \frac{\phi}{\phi_\mu} \right)^{3/2} + \frac{\phi^2}{36 M_{\rm pl}^2} \right] , & \text{(H.24)} \\ &\approx \phi \,. & \text{(H.25)} \end{aligned}$$

APPENDIX J

# Collection of Useful Results

In this appendix we cite key results of early universe cosmology and string theory. As these results are used throughout the thesis, we collect them here for easy reference.

## J.1. Early Universe Cosmology

### J.1.1. Primordial Fluctuations.

*Scalar Fluctuations.* We define scalar metric perturbations $\zeta(t, \mathbf{x})$ by the following line element

$$\mathrm{d}s^2 = -\mathrm{d}t^2 + e^{2\zeta(t,\mathbf{x})} a^2(t) \delta_{ij} \mathrm{d}x^i \mathrm{d}x^j \,. \tag{J.1}$$

The power spectrum of $\zeta$ is

$$\langle \zeta_{\mathbf{k}} \zeta_{\mathbf{k}'} \rangle = (2\pi)^3 \delta(\mathbf{k} + \mathbf{k}') \mathcal{P}_s(k) \,, \tag{J.2}$$

where $\zeta_{\mathbf{k}}(t) = \int \mathrm{d}^3x \zeta(t, \mathbf{x}) e^{-i\mathbf{k}\cdot\mathbf{x}}$. By convention we define the following dimensionless power spectrum

$$P_s(k) \equiv \frac{k^3}{2\pi^2} \mathcal{P}_s(k) \,. \tag{J.3}$$

This is normalized such that the variance of $\zeta$ is $\langle \zeta\zeta \rangle = \int_0^\infty P_s(k) \, \mathrm{d}\ln k$. The scale-dependence of the power spectrum is defined by the scalar spectral index

$$n_s - 1 \equiv \frac{d \ln P_s}{d \ln k} \,. \tag{J.4}$$

Scale-invariance corresponds to $n_s = 1$.

We may also define the running of the spectral index by

$$\alpha_s \equiv \frac{dn_s}{d\ln k}\,. \tag{J.5}$$

If $\zeta$ is Gaussian then the power spectrum contains all the statistical information. Non-Gaussianity is encoded in higher-order correlation functions of $\zeta$. *Local* non-Gaussianity is parameterized by the following field redefinition

$$\zeta = \zeta_L + \frac{3}{5} f_{\rm NL} \zeta_L^2\,, \tag{J.6}$$

where $\zeta_L$ is Gaussian.

*Tensor Fluctuations.* We define tensor metric perturbations $h_{ij}(t,\mathbf{x})$ by the following line element

$$\mathrm{d}s^2 = -\mathrm{d}t^2 + a^2(t)(\delta_{ij} + h_{ij}(t,\mathbf{x}))\mathrm{d}x^i\mathrm{d}x^j\,, \qquad \partial_i h_{ij} = h^i_i = 0\,. \tag{J.7}$$

The power spectrum of $h$ is

$$\langle h_{\mathbf{k}} h_{\mathbf{k}'}\rangle = (2\pi)^3\delta(\mathbf{k}+\mathbf{k}')\mathcal{P}_t(k)\,, \tag{J.8}$$

where $h_{\mathbf{k}}$ is the Fourier transform of the two polarization modes of $h_{ij}$ (see Appendix A). The dimensionless power spectrum is

$$P_t(k) \equiv \frac{k^3}{2\pi^2}\mathcal{P}_t(k)\,. \tag{J.9}$$

Its scale-dependence is encoded in the tensor spectral index

$$n_t \equiv \frac{d\ln P_t}{d\ln k}\,. \tag{J.10}$$

Scale-invariance corresponds to $n_t = 0$. We define the tensor-to-scale ratio

$$r \equiv \frac{P_t}{P_s}\,. \tag{J.11}$$

### J.1.2. Inflationary Predictions.

*Slow-roll Models.* We use the standard slow-roll parameters

$$\epsilon = -\frac{\dot{H}}{H^2} \approx \frac{M_{\rm pl}^2}{2}\Big(\frac{V'}{V}\Big)^2\,, \qquad \eta \approx M_{\rm pl}^2\frac{V''}{V}\,, \qquad \xi^{(2)} = M_{\rm pl}^4\frac{V'V'''}{V^2}\,. \tag{J.12}$$

Inflation predicts a nearly scale-invariant spectrum of scalar perturbations

$$P_s(k) = \frac{1}{8\pi^2 M_{\rm pl}^2}\frac{H^2}{\epsilon}\bigg|_{k=aH} \approx \frac{1}{24\pi^2 M_{\rm pl}^4}\frac{V}{\epsilon}\bigg|_{k=aH}\,. \tag{J.13}$$

At first-order in slow-roll there is a small scale-dependence

$$n_s - 1 = 2\eta - 6\epsilon\,. \tag{J.14}$$

The spectrum is very nearly Gaussian, with

$$f_{\rm NL} \approx -\frac{5}{12}(n_s - 1)\,. \tag{J.15}$$

Running of the spectral index is second-order in slow-roll

$$\alpha_s \approx 16\epsilon\eta - 24\epsilon^2 - 2\xi^{(2)}\,. \tag{J.16}$$

Inflation also predicts a nearly scale-invariant spectrum of tensor perturbations

$$P_t(k) = \frac{2}{\pi^2}\frac{H^2}{M_{\rm pl}^2}\bigg|_{k=aH}\,. \tag{J.17}$$

At first-order in slow-roll there is a small scale-dependence

$$n_t = -2\epsilon\,. \tag{J.18}$$

The tensor-to-scalar ratio is

$$r = 16\epsilon\,, \tag{J.19}$$

and the single-field slow-roll consistency relation is

$$r = -8n_t\,. \tag{J.20}$$

*Models with General Speed of Sound.* The action

$$S = \int \mathrm{d}^4x\sqrt{-g}\left[\frac{M_{\rm pl}^2}{2}\mathcal{R} + P(X,\phi)\right], \qquad X \equiv -\frac{1}{2}g^{\mu\nu}\partial_\mu\phi\partial_\nu\phi\,, \tag{J.21}$$

describes a fluid with pressure $P$, energy density $\rho = 2XP_{,X} - P$, and speed of sound

$$c_s^2 \equiv \frac{dP}{d\rho} = \frac{P_{,X}}{P_{,X} + 2XP_{,XX}}\,. \tag{J.22}$$

Such a fluid can source inflation if the following slow-variation parameters

$$\epsilon = -\frac{\dot H}{H^2}\,, \qquad \tilde\eta = \frac{\dot\epsilon}{\epsilon H}\,, \qquad s = \frac{\dot c_s}{c_s H} \tag{J.23}$$

are small. The non-trivial speed of sound modifies the scalar spectrum

$$P_s(k) = \left.\frac{1}{8\pi^2 M_{\rm pl}^2}\frac{H^2}{c_s\epsilon}\right|_{c_sk=aH}\,. \tag{J.24}$$

Its scale-dependence becomes

$$n_s - 1 = -2\epsilon - \tilde\eta - s\,. \tag{J.25}$$

For $c_s \ll 1$ the spectrum can be highly non-Gaussian

$$f_{\rm NL}^{\rm equil} = -\frac{35}{108}\Big(\frac{1}{c_s^2} - 1\Big) + \frac{5}{81}\Big(\frac{1}{c_s^2} - 1 - 2\Lambda\Big)\,, \tag{J.26}$$

where

$$\Lambda \equiv \frac{X^2P_{,XX} + \frac{2}{3}X^3P_{,XXX}}{XP_{,X} + 2X^2P_{,XX}}\,. \tag{J.27}$$

The tensor spectrum is the same as for slow-roll models (J.17).

## J.2. String Theory

In the following we find it convenient to define the fundamental string scale and the string length as follows

$$M_s^2 = \frac{1}{\alpha'} = l_s^{-2} \,. \tag{J.28}$$

We used the reduced four-dimensional Planck scale

$$M_{\rm pl}^2 = \frac{1}{8\pi G} = (2.43 \times 10^{18}\,{\rm GeV})^2 \,. \tag{J.29}$$

**J.2.1. Dimensional Reduction.** The ten-dimensional Einstein action dimensionally reduced to four dimensions leads to the following correspondence

$$\frac{M_{10}^8}{2}\int {\rm d}^{10}X\sqrt{-G}\,\mathcal{R}_{10} \to \frac{M_{\rm pl}^2}{2}\int {\rm d}^4x\sqrt{-g}\,\mathcal{R}_4 + \dots \,, \tag{J.30}$$

where $M_{10}^8 = \frac{2}{(2\pi)^7 g_s^2} M_s^8$ and

$$\frac{M_{\rm pl}^2}{M_s^2} = \frac{2}{(2\pi)^7 g_s^2}\frac{V_6}{l_s^6} \,. \tag{J.31}$$

**J.2.2. Warped Compactification.** A warped compactification has the following generic line element

$${\rm d}s^2 = h^{-1/2}(y) g_{\mu\nu}{\rm d}x^\mu {\rm d}x^\nu + h^{1/2}(y)\tilde{g}_{ij}{\rm d}y^i{\rm d}y^j \,. \tag{J.32}$$

The compactification volume that enters the dimensional reduction (J.31) then is

$$V_6 = \int {\rm d}^6 y \sqrt{\tilde{g}}\, h(y) \,. \tag{J.33}$$

Locally, the internal metric is often taken to be a cone, $\tilde{g}_{ij}{\rm d}y^i{\rm d}y^j = {\rm d}r^2 + r^2{\rm d}s^2_{X_5}$, with radial coordinate $r$ and base manifold $X_5$.

*$AdS_5 \times X_5$.* The warp factor for $AdS_5 \times X_5$ on the interval $r_{\rm IR} < r < r_{\rm UV}$ is

$$h(r) = \frac{R^4}{r^4} \,, \qquad \frac{R^4}{l_s^4} \equiv 4\pi g_s N \frac{\pi^3}{{\rm Vol}(X_5)} \,, \tag{J.34}$$

where *e.g.* ${\rm Vol}(S_5) = \pi^3$, ${\rm Vol}(T^{1,1}) = \frac{16\pi^3}{27}$.

*Conifold.* The warp factor in the large radius limit of the Klebanov-Strassler solution is

$$h(r) = \frac{R^4}{r^4}\left[1 + c\ln\Big(\frac{r}{r_0}\Big) + \frac{c}{4}\right], \qquad c \equiv \frac{3}{2\pi}\frac{g_s M^2}{N}. \tag{J.35}$$

### J.2.3. D-branes.

*Dp-brane Tension.* The tension of a Dp-brane is

$$T_p = \frac{M_s^{p+1}}{(2\pi)^p g_s}. \tag{J.36}$$

*Dp-brane Action in Warped Background.* Dimensional reduction in the background (J.32) leads to the following effective action for a Dp-brane

$$S_{Dp} = \int \mathrm{d}^4\xi\sqrt{-g}\,\mathcal{L}_{Dp}, \qquad \mathcal{L}_{Dp} = -f^{-1}(\phi)\sqrt{1-2f(\phi)X} - f^{-1}(\phi), \tag{J.37}$$

where $X \equiv -\frac{1}{2}g^{\mu\nu}\partial_\mu\phi\partial_\nu\phi$ and

$$\phi^2 = (T_p V_{p-3})r^2, \qquad f^{-1}(\phi) = (T_p V_{p-3})h^{-1}, \qquad V_{p-3} = \int \mathrm{d}^{p-3}\xi\sqrt{g}. \tag{J.38}$$

### J.2.4. Supergravity.

*F-term Potential.* The potential for complex superfields $\Phi_i$ is

$$V_F = e^{\mathcal{K}/M_{\rm pl}^2}\Big[\mathcal{K}^{A\bar{B}} D_A W \overline{D_B W} - \frac{3}{M_{\rm pl}^2}|W|^2\Big]. \tag{J.39}$$

Here, $\mathcal{K}(\Phi_i, \bar{\Phi}_i)$ and $W(\Phi_i)$ are the Kähler potential and the superpotential, respectively. We defined the covariant derivative, $D_A W = \partial_A W + \frac{1}{M_{\rm pl}^2}(\partial_A \mathcal{K})W$, and the Kähler metric, $\mathcal{K}_{A\bar{B}} = \partial_A\partial_{\bar{B}}\mathcal{K}$.

*D3s and D7s in the Conifold.* In this thesis we consider D3-branes on the (singular) conifold. The D3-brane position is given by the complex coordinates $z_i$ which satisfy

$$\sum z_i^2 = 0 \quad \text{and} \quad \sum |z_i|^2 = r^3. \tag{J.40}$$

Moduli stabilization requires a stack of $n$ D7-branes that wrap a four-cycle in the compact space. This four-cycle is defined by the embedding condition $f(z_i) = 0$. The volume of the four-cycle relates to the Kähler modulus $\rho$.

The system of D3-branes and wrapped D7-branes corresponds to the following superpotential

$$W = W_0 + A(z_i)e^{-a\rho}\,, \qquad A(z_i) = f(z_i)^{1/n}\,. \tag{J.41}$$

The Kähler potential is

$$\mathcal{K} = -3M_{\rm pl}^2 \ln\left[\rho + \bar{\rho} - \gamma k(z_i, \bar{z}_i)\right] \equiv -3M_{\rm pl}^2 \ln U\,, \tag{J.42}$$

where $\gamma$ is a constant and $k$ is the Kähler potential of the conifold

$$k(z_i, \bar{z}_i) = \frac{3}{2}\Big(\sum_i |z_i|^2\Big)^{2/3}. \tag{J.43}$$

Equations (J.41) and (J.42) lead to the following potential (J.39)

$$V_F = \frac{1}{3M_{\rm pl}^2 U^2}\left[(\rho+\overline{\rho})|W_{,\rho}|^2 - 3(\overline{W}W_{,\rho} + c.c.) + \frac{3}{2}(\overline{W_{,\rho}}z^i W_{,i} + c.c.) + \frac{1}{\gamma}\hat{k}^{i\bar{j}}W_{,i}\overline{W_{,j}}\right], \tag{J.44}$$

where

$$\hat{k}^{i\bar{j}} \equiv r\left[\delta^{i\bar{j}} + \frac{1}{2}\frac{z_i\overline{z_j}}{r^3} - \frac{\overline{z_i}z_j}{r^3}\right]. \tag{J.45}$$

# Bibliography


[1] O. Aharony, Y. E. Antebi and M. Berkooz, Open String Moduli in KKLT Compactifications, *Phys. Rev.* **D72**, 106009 (2005), [hep-th/0508080].

[2] O. Aharony, S. S. Gubser, J. M. Maldacena, H. Ooguri and Y. Oz, Large $N$ Field Theories, String Theory and Gravity, *Phys. Rept.* **323**, 183 (2000), [hep-th/9905111].

[3] A. Albrecht and P. J. Steinhardt, Cosmology for Grand Unified Theories with Radiatively Induced Symmetry Breaking, *Phys. Rev. Lett.* **48**, 1220 (1982).

[4] M. Alishahiha, E. Silverstein and D. Tong, DBI in the Sky, *Phys. Rev.* **D70**, 123505 (2004), [hep-th/0404084].

[5] R. Allahverdi, K. Enqvist, J. Garcia-Bellido and A. Mazumdar, Gauge-invariant MSSM Inflaton, *Phys. Rev. Lett.* **97**, 191304 (2006), [hep-ph/0605035].

[6] R. A. Alpher, H. Bethe and G. Gamow, The Origin of Chemical Elements, *Phys. Rev.* **73**, 803 (1948).

[7] D. Amati, K. Konishi, Y. Meurice, G. C. Rossi and G. Veneziano, Nonperturbative Aspects in Supersymmetric Gauge Theories, *Phys. Rept.* **162**, 169 (1988).

[8] K. N. Ananda, C. Clarkson and D. Wands, The Cosmological Gravitational Wave Background from Primordial Density Perturbations, *Phys. Rev.* **D75**, 123518 (2007), [gr-qc/0612013].

[9] D. Arean, D. E. Crooks and A. V. Ramallo, Supersymmetric Probes on the Conifold, *JHEP* **11**, 035 (2004), [hep-th/0408210].

[10] N. Arkani-Hamed, P. Creminelli, S. Mukohyama and M. Zaldarriaga, Ghost Inflation, *JCAP* **0404**, 001 (2004), [hep-th/0312100].

[11] N. Arkani-Hamed, L. Motl, A. Nicolis and C. Vafa, The String Landscape, Black Holes and Gravity as the Weakest Force, *JHEP* **06**, 060 (2007), [hep-th/0601001].

[12] C. Armendariz-Picon, T. Damour and V. F. Mukhanov, k-Inflation, *Phys. Lett.* **B458**, 209 (1999), [hep-th/9904075].

[13] R. Arnowitt, S. Deser and C. W. Misner, The Dynamics of General Relativity, gr-qc/0405109.

[14] D. Babich, P. Creminelli and M. Zaldarriaga, The Shape of Non-Gaussianities, *JCAP* **0408**, 009 (2004), [astro-ph/0405356].

[15] V. Balasubramanian, P. Berglund, J. P. Conlon and F. Quevedo, Systematics of Moduli Stabilisation in Calabi-Yau Flux Compactifications, *JHEP* **03**, 007 (2005), [hep-th/0502058].

[16] T. Banks, M. Dine, P. J. Fox and E. Gorbatov, On the Possibility of Large Axion Decay Constants, *JCAP* **0306**, 001 (2003), [hep-th/0303252].

[17] T. Banks, M. R. Douglas and N. Seiberg, Probing F-theory with Branes, *Phys. Lett.* **B387**, 278 (1996), [hep-th/9605199].
[18] D. Baumann, A. Dymarsky, I. R. Klebanov, J. Maldacena, L. McAllister and A. Murugan, On D3-brane Potentials in Compactifications with Fluxes and Wrapped D-branes, *JHEP* **11**, 031 (2006), [hep-th/0607050].
[19] D. Baumann, A. Dymarsky, I. R. Klebanov and L. McAllister, Towards an Explicit Model of D-brane Inflation, *JCAP* **0801**, 024 (0600), [arXiv:0706.0360 [hep-th]].
[20] D. Baumann, A. Dymarsky, I. R. Klebanov, L. McAllister and P. J. Steinhardt, A Delicate Universe: Compactification Obstacles to D-brane Inflation, *Phys. Rev. Lett.* **99**, 141601 (0500), [arXiv:0705.3837 [hep-th]].
[21] D. Baumann and L. McAllister, A Microscopic Limit on Gravitational Waves from D-brane Inflation, *Phys. Rev.* **D75**, 123508 (2007), [hep-th/0610285].
[22] D. Baumann and L. McAllister, Inflation in String Theory, *Ann. Rev. Nucl. Part. Sci.* (2009).
[23] D. Baumann, P. J. Steinhardt, K. Takahashi and K. Ichiki, Gravitational Wave Spectrum Induced by Primordial Scalar Perturbations, *Phys. Rev.* **D76**, 084019 (0300), [hep-th/0703290].
[24] R. Bean, S. E. Shandera, S. H. Henry Tye and J. Xu, Comparing Brane Inflation to WMAP, *JCAP* **0705**, 004 (2007), [hep-th/0702107].
[25] K. Becker, M. Becker, M. Haack and J. Louis, Supersymmetry Breaking and $\alpha'$-Corrections to Flux-induced Potentials, *JHEP* **06**, 060 (2002), [hep-th/0204254].
[26] K. Becker, M. Becker and A. Krause, M-theory Inflation from Multi M5-brane Dynamics, *Nucl. Phys.* **B715**, 349 (2005), [hep-th/0501130].
[27] K. Becker, M. Becker and J. H. Schwarz, *String Theory and M-theory: A Modern Introduction* (Cambridge University Press, 2007).
[28] M. Becker, L. Leblond and S. E. Shandera, Inflation from Wrapped Branes, *Phys. Rev.* **D76**, 123516 (2007), [arXiv:0709.1170 [hep-th]].
[29] M. K. Benna and I. R. Klebanov, Gauge-String Dualities and Some Applications, arXiv:0803.1315 [hep-th].
[30] S. Benvenuti, S. Franco, A. Hanany, D. Martelli and J. Sparks, An Infinite Family of Superconformal Quiver Gauge Theories with Sasaki-Einstein Duals, *JHEP* **06**, 064 (2005), [hep-th/0411264].
[31] D. Berenstein, C. P. Herzog, P. Ouyang and S. Pinansky, Supersymmetry Breaking from a Calabi-Yau Singularity, *JHEP* **09**, 084 (2005), [hep-th/0505029].
[32] M. Berg, M. Haack and B. Körs, Loop Corrections to Volume Moduli and Inflation in String Theory, *Phys. Rev.* **D71**, 026005 (2005), [hep-th/0404087].
[33] M. Berg, M. Haack and B. Körs, String Loop Corrections to Kähler Potentials in Orientifolds, *JHEP* **11**, 030 (2005), [hep-th/0508043].
[34] M. Berg, M. Haack and B. Körs, On Volume Stabilization by Quantum Corrections, *Phys. Rev. Lett.* **96**, 021601 (2006), [hep-th/0508171].
[35] J. J. Blanco-Pillado *et al.*, Racetrack Inflation, *JHEP* **11**, 063 (2004), [hep-th/0406230].

[36] J. J. Blanco-Pillado *et al.*, Inflating in a Better Racetrack, *JHEP* **09**, 002 (2006), [hep-th/0603129].
[37] J. Bock *et al.*, Task Force on Cosmic Microwave Background Research, astro-ph/0604101.
[38] J. R. Bond, L. Kofman, S. Prokushkin and P. M. Vaudrevange, Roulette Inflation with Kähler Moduli and their Axions, *Phys. Rev.* **D75**, 123511 (2007), [hep-th/0612197].
[39] R. Bousso and J. Polchinski, Quantization of Four-Form Fluxes and Dynamical Neutralization of the Cosmological Constant, *JHEP* **06**, 006 (2000), [hep-th/0004134].
[40] L. A. Boyle, *Probing the Early Universe with Gravtiational Waves*, PhD thesis, Princeton University (2006).
[41] L. A. Boyle, P. J. Steinhardt and N. Turok, Inflationary Predictions Reconsidered, *Phys. Rev. Lett.* **96**, 111301 (2006), [astro-ph/0507455].
[42] R. H. Brandenberger and C. Vafa, Superstrings in the Early Universe, *Nucl. Phys.* **B316**, 391 (1989).
[43] E. I. Buchbinder, J. Khoury and B. A. Ovrut, New Ekpyrotic Cosmology, *Phys. Rev.* **D76**, 123503 (2007), [hep-th/0702154].
[44] A. Buchel, Inflation on the Resolved Warped Deformed Conifold, *Phys. Rev.* **D74**, 046009 (2006), [hep-th/0601013].
[45] C. P. Burgess, J. M. Cline, K. Dasgupta and H. Firouzjahi, Uplifting and Inflation with D3 branes, *JHEP* **03**, 027 (2007), [hep-th/0610320].
[46] C. P. Burgess *et al.*, Warped Supersymmetry Breaking, *JHEP* **04**, 053 (2006), [hep-th/0610255].
[47] S. Burles, K. M. Nollett and M. S. Turner, Big-Bang Nucleosynthesis Predictions for Precision Cosmology, *Astrophys. J.* **552**, L1 (2001), [astro-ph/0010171].
[48] A. Butti, M. Grana, R. Minasian, M. Petrini and A. Zaffaroni, The Baryonic Branch of Klebanov-Strassler Solution: A Supersymmetric Family of $SU(3)$ Structure Backgrounds, *JHEP* **03**, 069 (2005), [hep-th/0412187].
[49] P. Candelas and X. C. de la Ossa, Comments on Conifolds, *Nucl. Phys.* **B342**, 246 (1990).
[50] F. Canoura, J. D. Edelstein, L. A. P. Zayas, A. V. Ramallo and D. Vaman, Supersymmetric Branes on $AdS_5 \times Y^{p,q}$ and their Field Theory Duals, *JHEP* **03**, 101 (2006), [hep-th/0512087].
[51] X. Chen, Inflation from Warped Space, *JHEP* **08**, 045 (2005), [hep-th/0501184].
[52] X. Chen, M.-x. Huang, S. Kachru and G. Shiu, Observational Signatures and Non-Gaussianities of General Single Field Inflation, *JCAP* **0701**, 002 (2007), [hep-th/0605045].
[53] J. Conlon and L. McAllister, private communication (2007).
[54] J. P. Conlon and F. Quevedo, Kähler Moduli Inflation, *JHEP* **01**, 146 (2006), [hep-th/0509012].
[55] P. Creminelli, On Non-Gaussianities in Single-Field Inflation, *JCAP* **0310**, 003 (2003), [astro-ph/0306122].
[56] K. Dasgupta, C. Herdeiro, S. Hirano and R. Kallosh, D3/D7 Inflationary Model and M-theory, *Phys. Rev.* **D65**, 126002 (2002), [hep-th/0203019].

[57] F. Denef, Les Houches Lectures on Constructing String Vacua, arXiv:0803.1194 [hep-th].
[58] O. DeWolfe and S. B. Giddings, Scales and Hierarchies in Warped Compactifications and Brane Worlds, *Phys. Rev.* **D67**, 066008 (2003), [hep-th/0208123].
[59] O. DeWolfe, L. McAllister, G. Shiu and B. Underwood, D3-brane Vacua in Stabilized Compactifications, *JHEP* **09**, 121 (2007), [hep-th/0703088].
[60] R. Dicke, P. J. E. Peebles, P. Roll and D. Wilkinson, Cosmic Black-Body Radiation, *Astrophys. J.* **142**, 414 (1965).
[61] S. Dimopoulos, S. Kachru, J. McGreevy and J. G. Wacker, N-flation, hep-th/0507205.
[62] S. Dodelson, *Modern Cosmology* (Amsterdam, Netherlands: Academic Press, 2003).
[63] M. R. Douglas and S. Kachru, Flux Compactification, *Rev. Mod. Phys.* **79**, 733 (2007), [hep-th/0610102].
[64] G. R. Dvali and S. H. H. Tye, Brane Inflation, *Phys. Lett.* **B450**, 72 (1999), [hep-ph/9812483].
[65] A. Dymarsky, I. R. Klebanov and N. Seiberg, On the Moduli Space of the Cascading $SU(M+p) \times SU(p)$ Gauge Theory, *JHEP* **01**, 155 (2006), [hep-th/0511254].
[66] R. Easther, W. H. Kinney and B. A. Powell, The Lyth Bound and the End of Inflation, *JCAP* **0608**, 004 (2006), [astro-ph/0601276].
[67] R. Easther and L. McAllister, Random Matrices and the Spectrum of N-flation, *JCAP* **0605**, 018 (2006), [hep-th/0512102].
[68] H. Firouzjahi and S. H. H. Tye, Closer towards Inflation in String Theory, *Phys. Lett.* **B584**, 147 (2004), [hep-th/0312020].
[69] H. Firouzjahi and S. H. H. Tye, Brane Inflation and Cosmic String Tension in Superstring Theory, *JCAP* **0503**, 009 (2005), [hep-th/0501099].
[70] S. Frolov, I. R. Klebanov and A. A. Tseytlin, String Corrections to the Holographic RG Flow of Supersymmetric $SU(N) \times SU(N+M)$ Gauge Theory, *Nucl. Phys.* **B620**, 84 (2002), [hep-th/0108106].
[71] O. J. Ganor, On Zeroes of Superpotentials in F-theory, *Nucl. Phys. Proc. Suppl.* **67**, 25 (1998).
[72] J. Garriga and V. F. Mukhanov, Perturbations in k-Inflation, *Phys. Lett.* **B458**, 219 (1999), [hep-th/9904176].
[73] J. P. Gauntlett, D. Martelli, J. Sparks and D. Waldram, Sasaki-Einstein Metrics on $S_2 \times S_3$, *Adv. Theor. Math. Phys.* **8**, 711 (2004), [hep-th/0403002].
[74] J. P. Gauntlett, D. Martelli, J. Sparks and D. Waldram, Supersymmetric $AdS_5$ Solutions of M-theory, *Class. Quant. Grav.* **21**, 4335 (2004), [hep-th/0402153].
[75] G. von Gersdorff and A. Hebecker, Kähler Corrections for the Volume Modulus of Flux Compactifications, *Phys. Lett.* **B624**, 270 (2005), [hep-th/0507131].
[76] S. B. Giddings, S. Kachru and J. Polchinski, Hierarchies from Fluxes in String Compactifications, *Phys. Rev.* **D66**, 106006 (2002), [hep-th/0105097].
[77] S. B. Giddings and A. Maharana, Dynamics of Warped Compactifications and the Shape of the Warped Landscape, *Phys. Rev.* **D73**, 126003 (2006), [hep-th/0507158].

[78] L. Görlich, S. Kachru, P. K. Tripathy and S. P. Trivedi, Gaugino Condensation and Nonperturbative Superpotentials in Flux Compactifications, *JHEP* **12**, 074 (2004), [hep-th/0407130].
[79] M. B. Green, J. H. Schwarz and E. Witten, *Superstring Theory. Vol. 1: Introduction* (Cambridge University Press, 1987).
[80] T. W. Grimm, Axion Inflation in Type II String Theory, arXiv:0710.3883 [hep-th].
[81] S. S. Gubser, Einstein Manifolds and Conformal Field Theories, *Phys. Rev.* **D59**, 025006 (1999), [hep-th/9807164].
[82] S. Gukov, C. Vafa and E. Witten, CFT's from Calabi-Yau Four-Folds, *Nucl. Phys.* **B584**, 69 (2000), [hep-th/9906070].
[83] A. H. Guth, The Inflationary Universe: A Possible Solution to the Horizon and Flatness Problems, *Phys. Rev.* **D23**, 347 (1981).
[84] A. H. Guth and S. Y. Pi, Fluctuations in the New Inflationary Universe, *Phys. Rev. Lett.* **49**, 1110 (1982).
[85] M. Haack *et al.*, Update of D3/D7-Brane Inflation on $K3 \times T^2/Z_2$, 0804.3961.
[86] C. P. Herzog, Q. J. Ejaz and I. R. Klebanov, Cascading RG Flows from New Sasaki-Einstein Manifolds, *JHEP* **02**, 009 (2005), [hep-th/0412193].
[87] C. P. Herzog, I. R. Klebanov and P. Ouyang, Remarks on the Warped Deformed Conifold, hep-th/0108101.
[88] R. Holman, P. Ramond and G. G. Ross, Supersymmetric Inflationary Cosmology, *Phys. Lett.* **B137**, 343 (1984).
[89] E. Hubble, A Relation between Distance and Radial Velocity among Extra–galactic Nebulae, *Proc. Nat. Acad. Sci.* **15**, 168 (1929).
[90] I. Huston, J. E. Lidsey, S. Thomas and J. Ward, Gravitational Wave Constraints on Multi-Brane Inflation, arXiv:0802.0398 [hep-th].
[91] K. A. Intriligator and N. Seiberg, Lectures on Supersymmetric Gauge Theories and Electric-Magnetic Duality, *Nucl. Phys. Proc. Suppl.* **45BC**, 1 (1996), [hep-th/9509066].
[92] N. Itzhaki and E. D. Kovetz, Inflection Point Inflation and Time Dependent Potentials in String Theory, *JHEP* **10**, 054 (2007), [arXiv:0708.2798 [hep-th]].
[93] S. Kachru, R. Kallosh, A. Linde and S. P. Trivedi, de Sitter Vacua in String Theory, *Phys. Rev.* **D68**, 046005 (2003), [hep-th/0301240].
[94] S. Kachru, J. McGreevy and P. Svrcek, Bounds on Masses of Bulk Fields in String Compactifications, *JHEP* **04**, 023 (2006), [hep-th/0601111].
[95] S. Kachru *et al.*, Towards Inflation in String Theory, *JCAP* **0310**, 013 (2003), [hep-th/0308055].
[96] R. Kallosh, On Inflation in String Theory, hep-th/0702059.
[97] R. Kallosh and A. Linde, Testing String Theory with CMB, *JCAP* **0704**, 017 (2007), [arXiv:0704.0647 [hep-th]].
[98] R. Kallosh, N. Sivanandam and M. Soroush, Axion Inflation and Gravity Waves in String Theory, *Phys. Rev.* **D77**, 043501 (2007), [arXiv:0710.3429 [hep-th]].
[99] A. Karch and E. Katz, Adding Flavor to AdS/CFT, *JHEP* **06**, 043 (2002), [hep-th/0205236].

[100] J. Khoury, B. A. Ovrut, P. J. Steinhardt and N. Turok, The Ekpyrotic Universe: Colliding Branes and the Origin of the Hot Big Bang, *Phys. Rev.* **D64**, 123522 (2001), [hep-th/0103239].

[101] H. Kihara, M. Sakaguchi and Y. Yasui, Scalar Laplacian on Sasaki-Einstein manifolds $Y^{p,q}$, *Phys. Lett.* **B621**, 288 (2005), [hep-th/0505259].

[102] S. A. Kim and A. R. Liddle, N-flation: Multi-field Inflationary Dynamics and Perturbations, *Phys. Rev.* **D74**, 023513 (2006), [astro-ph/0605604].

[103] I. R. Klebanov, TASI Lectures: Introduction to the AdS/CFT Correspondence, hep-th/0009139.

[104] I. R. Klebanov and A. Murugan, Gauge / Gravity Duality and Warped Resolved Conifold, *JHEP* **03**, 042 (2007), [hep-th/0701064].

[105] I. R. Klebanov and M. J. Strassler, Supergravity and a Confining Gauge Theory: Duality Cascades and chiSB-Resolution of Naked Singularities, *JHEP* **08**, 052 (2000), [hep-th/0007191].

[106] I. R. Klebanov and A. A. Tseytlin, Gravity Duals of Supersymmetric $SU(N) \times SU(N+M)$ Gauge Theories, *Nucl. Phys.* **B578**, 123 (2000), [hep-th/0002159].

[107] I. R. Klebanov and E. Witten, Superconformal Field Theory on Threebranes at a Calabi-Yau Singularity, *Nucl. Phys.* **B536**, 199 (1998), [hep-th/9807080].

[108] I. R. Klebanov and E. Witten, AdS/CFT Correspondence and Symmetry Breaking, *Nucl. Phys.* **B556**, 89 (1999), [hep-th/9905104].

[109] T. Kobayashi, S. Mukohyama and S. Kinoshita, Constraints on Wrapped DBI Inflation in a Warped Throat, *JCAP* **JCAP01**, 028 (2007), [arXiv:0708.4285 [hep-th]].

[110] E. W. Kolb and M. S. Turner, *The Early Universe* (Reading, MA: Addison-Wesley, 1990).

[111] E. Komatsu *et al.*, Five-Year Wilkinson Microwave Anisotropy Probe Observations: Cosmological Interpretation, 0803.0547.

[112] A. Krause, Large Gravitational Waves and Lyth Bound in Multi Brane Inflation, arXiv:0708.4414 [hep-th].

[113] A. Krause and E. Pajer, Chasing Brane Inflation in String-Theory, arXiv:0705.4682 [hep-th].

[114] S. Kuperstein, Meson Spectroscopy from Holomorphic Probes on the Warped Deformed Conifold, *JHEP* **03**, 014 (2005), [hep-th/0411097].

[115] A. R. Liddle, A. Mazumdar and F. E. Schunck, Assisted Inflation, *Phys. Rev.* **D58**, 061301 (1998), [astro-ph/9804177].

[116] J. E. Lidsey and I. Huston, Gravitational Wave Constraints on Dirac-Born-Infeld Inflation, *JCAP* **0707**, 002 (2007), [arXiv:0705.0240 [hep-th]].

[117] J. E. Lidsey and D. Seery, Primordial Non-Gaussianity and Gravitational Waves: Observational Tests of Brane Inflation in String Theory, *Phys. Rev.* **D75**, 043505 (2007), [astro-ph/0610398].

[118] A. Linde, Inflationary Cosmology, *Lect. Notes Phys.* **738**, 1 (2008), [arXiv:0705.0164 [hep-th]].

[119] A. Linde and A. Westphal, Accidental Inflation in String Theory, *JCAP* **0803**, 005 (2008), [arXiv:0712.1610 [hep-th]].

[120] A. D. Linde, A New Inflationary Universe Scenario: A Possible Solution of the Horizon, Flatness, Homogeneity, Isotropy and Primordial Monopole Problems, *Phys. Lett.* **B108**, 389 (1982).
[121] D. Lüst, P. Mayr, S. Reffert and S. Stieberger, F-theory Flux, Destabilization of Orientifolds and Soft Terms on D7-branes, *Nucl. Phys.* **B732**, 243 (2006), [hep-th/0501139].
[122] D. H. Lyth, What would we learn by detecting a gravitational wave signal in the cosmic microwave background anisotropy?, *Phys. Rev. Lett.* **78**, 1861 (1997), [hep-ph/9606387].
[123] D. H. Lyth and A. Riotto, Particle Physics Models of Inflation and the Cosmological Density Perturbation, *Phys. Rept.* **314**, 1 (1999), [hep-ph/9807278].
[124] J. M. Maldacena, The Large $N$ Limit of Superconformal Field Theories and Supergravity, *Adv. Theor. Math. Phys.* **2**, 231 (1998), [hep-th/9711200].
[125] J. M. Maldacena, Non-Gaussian Features of Primordial Fluctuations in Single Field Inflationary Models, *JHEP* **05**, 013 (2003), [astro-ph/0210603].
[126] J. M. Maldacena, private communication (2007).
[127] L. McAllister, private communication (2007).
[128] L. McAllister and E. Silverstein, String Cosmology: A Review, *Gen. Rel. Grav.* **40**, 565 (2007), [arXiv:0710.2951 [hep-th]].
[129] S. Mollerach, D. Harari and S. Matarrese, CMB Polarization from Secondary Vector and Tensor Modes, *Phys. Rev.* **D69**, 063002 (2004), [astro-ph/0310711].
[130] V. Mukhanov, *Physical Foundations of Cosmology* (Cambridge University Press, 2005).
[131] A. Nicolis, On Super-Planckian Fields, arXiv:0802.3923 [hep-th].
[132] H. Ooguri and C. Vafa, On the Geometry of the String Landscape and the Swampland, *Nucl. Phys.* **B766**, 21 (2007), [hep-th/0605264].
[133] P. Ouyang, Holomorphic D7-branes and Flavored $N = 1$ Gauge Theories, *Nucl. Phys.* **B699**, 207 (2004), [hep-th/0311084].
[134] D. Overbye, *Lonely Hearts of the Cosmos* (Back Bay Books, 1999).
[135] S. Panda, M. Sami and S. Tsujikawa, Prospects of Inflation in Delicate D-brane Cosmology, *Phys. Rev.* **D76**, 103512 (2007), [arXiv:0707.2848 [hep-th]].
[136] H. V. Peiris, D. Baumann, B. Friedman and A. Cooray, Phenomenology of D-Brane Inflation with General Speed of Sound, *Phys. Rev.* **D76**, 103517 (0600), [arXiv:0706.1240 [astro-ph]].
[137] S. Perlmutter *et al.* (Supernova Cosmology Project), Measurements of Omega and Lambda from 42 High-Redshift Supernovae, *Astrophys. J.* **517**, 565 (1999), [astro-ph/9812133].
[138] J. Polchinski, *String Theory. Vol. 1: An Introduction to the Bosonic String* (Cambridge University Press, 1998).
[139] J. Polchinski, *String Theory. Vol. 2: Superstring Theory and Beyond* (Cambridge University Press, 1998).
[140] L. Randall and R. Sundrum, An Alternative to Compactification, *Phys. Rev. Lett.* **83**, 4690 (1999), [hep-th/9906064].
[141] L. Randall and R. Sundrum, A Large Mass Hierarchy from a Small Extra Dimension, *Phys. Rev. Lett.* **83**, 3370 (1999), [hep-ph/9905221].

[142] A. G. Riess *et al.* (Supernova Search Team), Type Ia Supernova Discoveries at $z > 1$ From the Hubble Space Telescope: Evidence for Past Deceleration and Constraints on Dark Energy Evolution, *Astrophys. J.* **607**, 665 (2004), [astro-ph/0402512].
[143] N. Seiberg, Naturalness versus Supersymmetric Nonrenormalization Theorems, *Phys. Lett.* **B318**, 469 (1993), [hep-ph/9309335].
[144] M. A. Shifman and A. I. Vainshtein, On Gluino Condensation in Supersymmetric Gauge Theories. $SU(N)$ and $O(N)$ Groups, *Nucl. Phys.* **B296**, 445 (1988).
[145] M. A. Shifman and A. I. Vainshtein, On Holomorphic Dependence and Infrared Effects in Supersymmetric Gauge Theories, *Nucl. Phys.* **B359**, 571 (1991).
[146] E. Silverstein, Simple de Sitter Solutions, 0712.1196.
[147] E. Silverstein and D. Tong, Scalar Speed Limits and Cosmology: Acceleration from D-cceleration, *Phys. Rev.* **D70**, 103505 (2004), [hep-th/0310221].
[148] E. Silverstein and A. Westphal, Monodromy in the CMB: Gravity Waves and String Inflation, arXiv:0803.3085 [hep-th].
[149] Y.-S. Song and L. Knox, The Detectability of Departures from the Inflationary Consistency Equation, *Phys. Rev.* **D68**, 043518 (2003), [astro-ph/0305411].
[150] D. Spergel and L. Page, private communication (2007).
[151] D. N. Spergel *et al.* (WMAP), Wilkinson Microwave Anisotropy Probe (WMAP) three year results: Implications for Cosmology, *Astrophys. J. Suppl.* **170**, 377 (2007), [astro-ph/0603449].
[152] P. J. Steinhardt, A Quintessential Introduction to Dark Energy, *Phil. Trans. Roy. Soc. Lond.* **A361**, 2497 (2003).
[153] P. J. Steinhardt and M. S. Turner, A Prescription for Successful New Inflation, *Phys. Rev.* **D29**, 2162 (1984).
[154] P. J. Steinhardt and N. Turok, A Cyclic Model of the Universe, *Science* **296**, 1436 (2002).
[155] P. Svrcek and E. Witten, Axions in String Theory, *JHEP* **06**, 051 (2006), [hep-th/0605206].
[156] M. Tegmark *et al.*, Cosmological Constraints from the SDSS Luminous Red Galaxies, *Phys. Rev.* **D74**, 123507 (2006), [astro-ph/0608632].
[157] B. Underwood, Brane Inflation is Attractive, arXiv:0802.2117 [hep-th].
[158] L.-M. Wang, V. F. Mukhanov and P. J. Steinhardt, On the problem of predicting inflationary perturbations, *Phys. Lett.* **B414**, 18 (1997), [astro-ph/9709032].
[159] S. Weinberg, The Cosmological Constant Problem, *Rev. Mod. Phys.* **61**, 1 (1989).
[160] S. Weinberg, *Cosmology* (Oxford University Press, 2008).
[161] J. A. Wheeler and K. Ford, *Geons, Black Holes, and Quantum Foam: A Life in Physics* (Norton, 1998).
[162] E. Witten, Dimensional Reduction of Superstring Models, *Phys. Lett.* **B155**, 151 (1985).
[163] E. Witten, Non-Perturbative Superpotentials In String Theory, *Nucl. Phys.* **B474**, 343 (1996), [hep-th/9604030].
[164] B. Zwiebach, *A First Course in String Theory* (Cambridge, UK: Univ. Pr., 2004).